The role of the LHCX light-harvesting complex protein family in diatom photoprotection

Lucilla Taddei

Université Pierre et Marie Curie

Ecole Doctorale Complexité du Vivant

Laboratoire de Biologie Computationnelle et Quantitative

Equipe : Génomique fonctionnelle des diatomées

The Role of the LHCX Light-Harvesting Complex Protein Family in Diatom Photoprotection

Par Lucilla Taddei

Thèse de doctorat de Biologie

Dirigée par Dr. Angela Falciatore

Présentée et soutenue publiquement le 25 Juillet 2016

Devant un jury composé de :

CARDOL Pierre	Chercheur FRS-FNRS	Rapporteur
MOROSINOTTO Tomas	Professeur d'Université, Padova	Rapporteur
DE VITRY Catherine	Directrice de Recherche CNRS	Examinateur
TIRICHINE Leila	Ingénieur de Recherche ENS	Examinateur
LEPETIT Bernard	Chercheur associé, Université, Kostanz	Examinateur
CARBONE Alessandra	Professeur d'Université UPMC	Examinateur
FALCIATORE Angela	Directrice de Recherche CNRS	Directrice de thèse
JAUBERT Marianne	Maître de Conférences UPMC	Co-Directrice de thèse

"An idea like this can possibly be realized only in a new world, where the spirit must have the courage to look for new means to respond to new essential needs, because the traditional means are not available there. Then, the spirit of invention will wake up, since there the audacity and perseverance combine with necessity."

Johann Wolfgang von Goethe, Wilhelm Meister's Journeyman Years, Book III

Acknowledgements

This thesis offered me the considerable opportunity to learn how to study photosynthesis and photoprotection, which I consider a precious and personal tool for my future that I will preserve, develop and extend with enthusiasm to others, as I was learned.

For both the scientific and human apprenticeships that I had in these years of researches and travels it is now time to thank the persons that contributed to the accomplishment of my Thesis.

I want to express my gratefulness to all the members of the jury for having accepted to examine my thesis.

Dr. Angela Falciatore is my Thesis Director and I foremost thank her for giving to me the possibility and the time to make science a part of my life, where it became pleasure, edification and critical exchange, enjoying it all the PhD long. I also foremost admire her steady determination, scientific curiosity and intelligence.

I warmly thank Prof. Alessandra Carbone, chief of the laboratory that hosted me: she did not inherit it but conceived it with awakened voyance. I thank her for hosting me in this lab where I did experiment working in an exciting multidisciplinary environment at the edge between experimental and theoretical biology.

Dr. Marianne Jaubert, my thesis co-director, has my most sincere gratitude for her patient and wise guidance and for disclosing to me the scientific method in the laboratory experiments and in the data analysis.

I want to thank Dr. Jean-Pierre Bouly for his critical and pointed suggestions which were pivotal in my research progress. My gratitude goes to Dr. Giovanni Finazzi for his excellent expertise and crystalline way to explain to me photosynthesis and photoprotection as well as its scientific orientation in the path of discoveries all my PhD long. My sincere thanks go to Dr. Bernard Lepetit, for its excellent supervision in the biochemical and spectroscopic characterization of photosynthetic complexes. Especially its expertise in the knowledge of biochemistry and spectroscopy, that he taught to me are an invaluable cultural baggage for me. My sincere thanks also go to Prof. Van Amerongen and Dr. Volha Chukhutsina for their professionalism in the collaboration on the III chapter of this thesis. Their expertise in the ultrafast spectroscopy always struck me and this admiration open my eyes on the state of understanding in the process of photosynthesis. Prof. Peter Kroth merits all my thankfulness for having hosted me in its lab at Kostanz to perform the separation of the photosynthetic complexes in an excellent research environment. My heartfelt thanks go to Prof. Michel Goldschmidt-Clermont for his attentive and constructive advices during my Comitées de Thèse. I want to thank the collaborators of the Chapter II Dr. Johan Lavaud, Dr. Benjamin Bailleul, Dr. Alessandra Rogato and Dr. Remo Sanges for their contribution in realizing my first scientific paper.

My colleagues and co-workers in the laboratory deserve all my dearest appretiation: the wondrous vitality and foresight of Rossella, the dear intelligence of Antonio, the calm and secure wisdom of Giulio, the lively enthusiasm of Michael. I thank Soizic, Gilles, Nicolas, Ingrid, Nikolaos, Aubin, Stéphane, Matteo, Guido, Frederic, Thierry, Mathilde,

Antonin, Yasaman and Francesco, the members of the other teams in the lab, for having always shared good moments in the common spaces.

I was involved in the Initial Training Network AccliPhot project, and thanks to the financial support of the European Commission, these have also been for me intense years of travels and visiting: I was driven by my research project to other destinantions like Grenoble, Bordeaux, Kostanz, Dusseldorf, Cork and many other, where I enriched my scientific project and my vision of the world by exchanging and learning from wondrous people. In the AccliPhot consortium I met Dr. Oliver Ebenhöh, the coordinator of the AccliPhot, able of precise management but also capable of overflowing energy, curiosity during the meetings and workshops.

I would like to thank my AccliPhot friends Serena, Valeria, Anja, Antonella, Fiona, Kailash, Dipali, Giulio, Martina, Brieuc, Ioannis, Federica, Jessica, with whom I spent gorgeous moments everywhere we went.

Table of contents

List of Figures and Tables

Chapter I: Introduction

Chapter III: Role of LHCX proteins in short- and long-term high light acclimation in the marine diatom Phaeodactylum tricornutum

Chapter I

Introduction

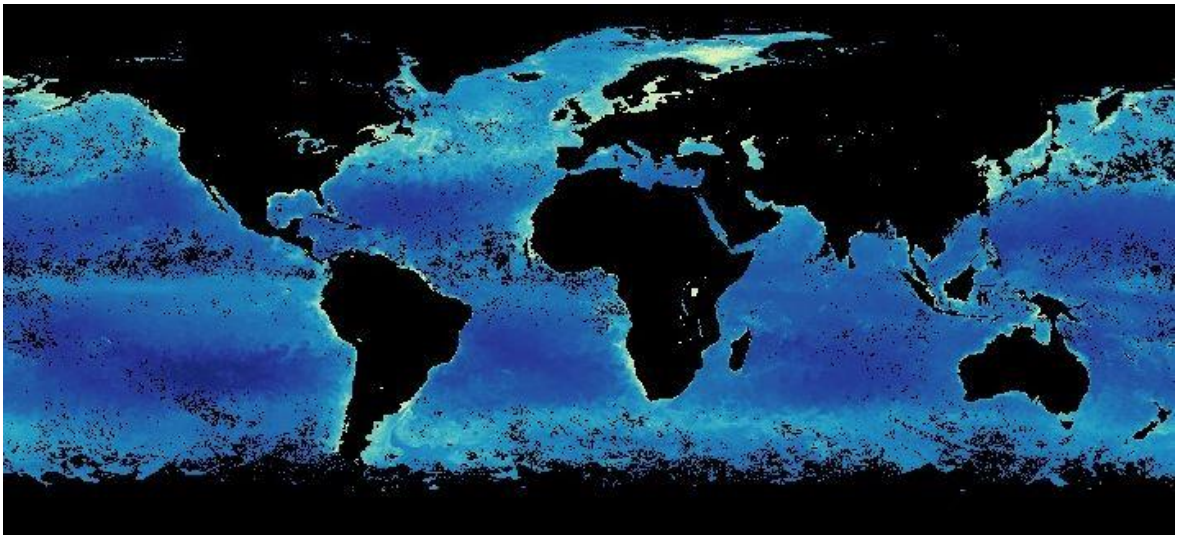

A satellite's view on the surface of the Earth. The color refers to chlorophyll concentration in Earth waters. NASA Earth Observations.

Introduction

Phytoplankton are a very diverse group of mostly single-celled photosynthetic organisms, that drift within the marine and freshwaters currents. Although these microorganisms represent less than 1% of the Earth's photosynthetic biomass, they synthetize more than 45% of our planet's annual primary productivity (Field et al. 1998).

Many different divisions can be distinguished in the phytoplankton community as compared to the terrestrial photosynthetic organisms, since the majority of these latter all belong to the same subkingdom, the Embryophyta (Figure 1). This impressive diversification of the phytoplankton community is reflected for instance in the light spectral signature that these organisms are able to capture for photosynthesis (Grossman et al. 1995), and also in their photoprotective capacity (Ruban et al. 2004; Finazzi & Minagawa 2015), since the pigments and proteins used for light harvesting and protection differ significantly within the phytoplankton.

A possible reason for that might resides in the fact that the aquatic environment differs from the terrestrial one in many aspects and impose different constraints on photosynthetic organisms (Depauw et al. 2012). Light intensity and nutrient concentrations are more diluted in aquatic as compared to the terrestrial environments and the spectrum of the light, is comparable only between the land and the surface layers of the water body. The underwater light field varies with the incident solar radiation and the time of the day, and also because of the absorptive properties of water and the scattering processes caused by the presence of coloured dissolved organic matter, to which photosynthetic organisms themselves contribute (Kirk 1994). Water selectively absorbs light in the red and infrared wavebands which causes a progressive dominance of the remaining blue-green (400-500 nm) spectral components with depth. In addition, movements in aquatic environments (caused by mixing in the upper layers, tides, streams), have no equivalent in the terrestrial ones (Mann & Lazier 2006), and marine phytoplankton can experience dramatic changes in the perceived light conditions. Therefore, aquatic organisms must be able to sense and rapidly respond to these changes.

Important examples of such acclimation abilities are the capacity of phytoplankton to adjust their pigmentation to the spectral composition of light of their habitat (Scanlan et al. 2009) and to quickly activate photoprotection responses, to rapid changes in light quantity (MacIntyre et al. 2000). Other responses include vertical migration (Villareal & Carpenter 2003), phototaxis (Sineshchekov et al. 2002), as well as chloroplast movement and reorientation (Wada et al. 2003).

To a remarkable extent, marine diatoms produce 40% of the organic carbon production in the sea (Nelson et al. 1995) and represent one of the most successful groups of algae in the phytoplankton community. The secret of their ecological success is thought to resides in their capacity to maintain a photosynthetic activity despite highly variable environmental conditions (MacIntyre et al. 2000; Strzepek & Harrison 2004; Wagner et al. 2006). This flexibility possibly helped diatoms to access and adapt to new ecological niches inducing the diversification of this group into well over 10^5 species (Kooistra et al. 2007), finally making of them the major photoautotrophic protistan lineage.

Despite diatom ecological importance, today the knowledge of their photobiology is still largely based on physiological and *in situ* studies, with less information available at the molecular level, in contrast to other aquatic model systems such as cyanobacteria (Grossman et al. 2001) or *Chlamydomonas* (Rochaix 2002). To fill this gap in our knowledge, my research has focused on the characterization of the mechanisms regulating diatom flexible chloroplast activity. For these studies, I have integrated multiple knowledges and tools from different disciplines, e.g., genetic and genomic, biochemistry, physiology, as well as kinetics of fluorescence yields at room temperature and time-resolved spectroscopy, using as paradigm the model specie *Phaeodactylum tricornutum.*

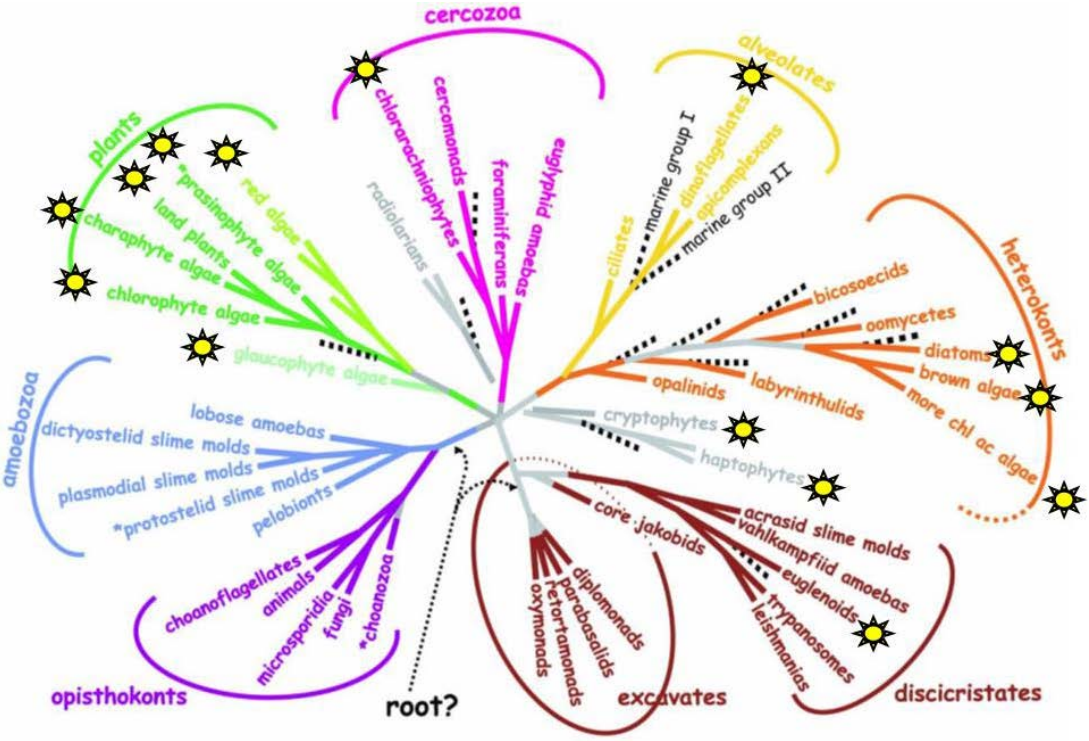

Figure 1 A consensus phylogenetic tree of the eight major characterized eukaryotes. The majority of characterized eukaryotes can be associated to one of the eight major groups. This result has been obtained studying the genetic sequences, the morphological and the physiological characteristics of these organisms, such as the presence and the peculiarities of flagella and mitochondria. Eukaryotic oxygenic photosynthesis originated in the group of Plants which contains all primary photosynthetic endosymbionts. The use of oxygenic photosynthesis (indicated by a yellow sun) was diffused to four other eukaryotic groups by means of secondary and tertiary endosymbiosis. The illustrated figure is adapted from Baldauf (2003).

1. General characteristics of diatoms

Diatoms are Bacillariophyceae within the division of the Heterokontophyta (also known as Stramenopiles). These microalgae dominate the phytoplankton community, whenever light and inorganic nitrogen, phosphorous, silicon and trace elements are sufficient to support their growth (Morel & Price 2003). Generating as much organic carbon per year as all the terrestrial rainforests combined do (Field et al. 1998), they are at the base of aquatic food webs (Armbrust 2009). They are almost equally abundant in marine and limnic environments (Falkowski et al. 2004) and are considered the group that show the highest fitness in turbulent environments (Margalef 1978).

In a relatively short evolutionary time period (<240 millions of years) diatoms diversified into hundreds of genera and 10^5 species showing today a remarkable variety of shapes and sizes (Kooistra et al. 2007; Vanormelingen et al. 2007). The main lineages of diatoms are the centrics (Figure 2 A) and the pennate (Figure 2 B), which have a radial and a longitudinal symmetry

respectively, and diverged from a common ancestor about 90 million years ago (Kooistra et al. 2007). Planktonic diatoms live in open oceans whereas the benthic forms are found in tidal regions (Kooistra et al. 2007). However, since some species are able to alternate between the two life forms, namely the 'tychoplanctonic', the distinction between plankton and benthos is not absolute. As a general rule, centric diatoms are planktonic, whereas pennates are rather benthic and live on sediments or other surfaces.

Diatoms are not able to perform active movements and, as a consequence, they are subjected to passive movements determined by their sinking rate and water movements. However, some pennate species are capable of limited movements, along a substrate, by secreting a mucilaginous material along a slit-like channel called ‘raphe’, (Figure 2 C). Moreover, in the oceans, some large diatom species, such as *Ditylum brightwellii*, can also move up and down in the water column by changing the ionic composition of their vacuole (Fisher et al. 1996), whereas other species, as *Skeletonema costatum* and *Thalassiosira nordenskioldii*, can also control their buoyancy by making colonies (Karp-Boss & Jumars 1998).

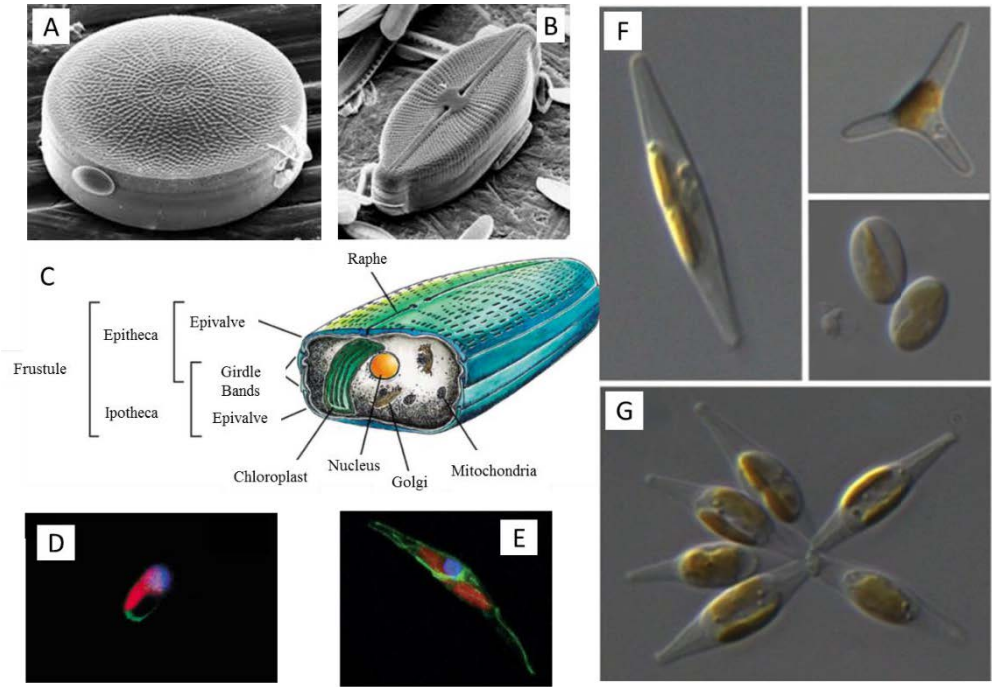

Figure 2 Pictures of diatoms. (A) Scanning Electron Microscopy image of the centric diatom *Actinocyclus octonarius* and (B) of the pennate diatom *Cosmioneis pusilla*. Both images are from © 2008 David G. Mann. (C) Graphic representation of the internal and external organization of a pennate diatom. Image from (Falciatore & Bowler 2002). Fluorescence microscopy images of the pennate diatom *P. tricornutum* in the oval (Falciatore & Bowler 2002) (D) and in the fusiform (De Martino et al. 2009) (E) morphological types. In red is the chlorophyll autofluorescence originating

from the chloroplast. The DNA is labelled with the DAPI stainer, therefore, the blue autofluorescence indicates the position of the nucleus. Moreover, thses cells are genetically transformed with a vector bearing the Green Fluorescent Protein attached to a cytosolic protein, which produces the green signal. (F) Light micrographs showing the three morphotypes of *P. tricornutum*: left, fusiform; top right, triradiate; bottom right, oval. (G) Light micrographs of a small cluster of cells of *P. tricornutum*. Each cell is approximately 15 μm in length. Images courtesy of Alessandra De Martino.

Given the ecological importance of diatoms, knowing their biology, evolution, and acclimation strategy can impact our understanding of contemporary oceans.

1.1 Diatom cellular features

1.1.1 The cell wall of diatoms

Diatoms have a beautifully chiseled cell wall impregnated of silica, called the frustule (Figure 2 A and B). Because of this feature, they participate to the regulation of the silicon cycle on Earth. The frustule is made of two halves, one half is smaller as compared to the other one and fits inside the larger one like a Petri dish (Figure 2 C). The larger half of the frustule is called the epitheca, and the smaller one is known as the hypotheca. Each theca is composed of two parts: the valve (which forms the larger outer surface) and the girdle (circular bands of silica attached to the edge of the valve) (Figure 2 C).

Cell growth is precluded by the frustule, therefore, during mitosis, a new valve is synthesized within the pre-existing valve. Consequently, after each mitotic event, one of the two daughter cells heritages the smaller theca and over successive divisions, the cells become progressively smaller and diatoms of dramatically different sizes can be found within a population (Pickett-Heaps et al. 1990). However, once a critical size threshold is reached, which is approximately a 30% decrease in the size relative to the initial size, a sexual reproduction cycle is necessary to return to the maximum size (detail of the process in paragraph 2.2). In addition to silica, the cell wall also contains organic materials which form a thin coat around valves made of secreted extracellular polymeric substances (EPS).

1.1.2 Diatom cell cycle

During their life, diatoms divide principally asexually, through mitosis. The different phases of diatom mitosis have been well documented by elegant electron microscopy and cell biology study, which also revealed interesting diatom specific features (De Martino et al. 2009).

As for other eukaryotes, vegetative cell cycle comprises the coordinated succession of a phase of DNA replication or synthesis (S phase), a phase of physical separation of both copies of the genomes (mitosis or M phase), and cell division itself (cytokinesis). The S and M phases are separated by two gap phases, one before the S phase (gap 1 phase or G1) and the other before the M phase (gap 2 phase, or G2). The phases between two cycles, is called interphase. During G1 phase, the cell duplicates its cellular content, whereas in G2 phase, chromosomes that are duplicated in S phase, are checked for mutations. The segregation of chloroplasts is performed before nucleus division and the two chloroplasts localize each in one side of the cell that will be separated by the future division plane.

After the chloroplast division, the nuclear membrane is partially broken and the organization of a microtubule organizing center (MTOC) takes place. The MTOC defines the structures from which the microtubules propagate, it plays a crucial role in eukaryotic cell division and it is composed of the microtubule of the polar complex. The chromosomes attached to the microtubules in a single ring can segregate and after the cytokinesis the two daughter cells are finally separated by a plasmatic mebrane.

After mitosis and cytokinesis, a peculiar vesicle, known as the silica deposition vesicle (SDV), is formed between the nucleus and the plasma membrane, in a position where the two new hypovalves will be generated. The SDV extends itself into a tube and then diffuses to eventually form a huge vesicle along one side of the cell. A new valve is formed within the SDV by the transport and the deposition of silica, proteins, and polysaccharides into the SDV. Once the two hypovalves are complete, the two daughter cells can then separate and grow separately.

However, one daughter cell is always smaller than the other, owing to the different sizes of the parental thecae from which they are derived. The renovation of the original size occurs via sexual

reproduction. After the 'gametogenesis' phase, the resulting male and female gametes combine to create a diploid auxospore that is surrounded by a special organic or inorganic silica wall which allows expansion. Auxospore expansion is a finely controlled process (Mann 1993), during which the enlarged size of the new cell is restored. Generally, centric diatoms form diverse gametes: the egg cells are large and the sperm cells are motile and flagellated (oogamy). Several evidences indicated that in these diatoms, the sexual reproduction is influenced by external species-specific factors such as light irradiance, day length and temperature (Chepurnov et al. 2002). Although auxosporulation in pennate diatoms is also dependent on environmental factors, the primary event inducing gametogenesis onset seems to be cell-cell interactions between vegetative cells from different sexually compatible clones (mating types). The gametes produced by most pennates are, in contrast to those produced by centric diatoms, non-flagellated and morphologically identical (isogamy) (Chepurnov et al. 2004).

The mechanisms controlling sexual reproduction in diatoms are still largely unknown and the meiotic process is controlled under laboratory conditions only in a few species, like *Seminavis robusta* (Chepurnov et al. 2002) and *Pseudo-nitzschia delicatissima* (D'Alelio et al. 2009).

1.1.3 The model specie *P. tricornutum*

The model system used in this thesis work is the pennate diatom *P. tricornutum* (Figure 2 D-G). This is the second diatom for which a whole genome sequence has been generated (Bowler et al. 2008) after the centric diatom *Thalassiosira pseudonana* (Armbrust & et al. 2004). This pennate diatom was principally selected because of its relatively small genome size (27,4 Mb), the highly accessible genetic resources and also because it has been adopted in laboratory-based researches of diatom physiology for numerous years.

Despite it is not considered to have a big ecological importance, various ecotypes have been isolated in various locations worldwide (De Martino et al. 2007), typically in coastal areas with deep variations in salinity. In contrast to other diatoms, *P. tricornutum* can exist in three diverse morphotypes (see Figure 2 F) and the transition into a different shape can be stimulated by environmental circumstances (De Martino et al. 2007). This characteristic is useful for the understanding of the molecular basis that control cell shape and morphogenesis. The plastic behavior

to change its shape likely relies on the unusual nature of its cell wall, which is principally organic and poorly silicified in the fusiform and triradiate cell shapes (Borowitzka & Volcani 1978). Indeed, *P. tricornutum* does not have an obligate necessity for silica during growth (Brzezinski et al. 1990) and a silicified cell wall is found only in the oval morphotype.

In *P. tricornutum*, a reduction of the cell size has not been observed during mitosis and evidences of sexual reproduction events have not been yet reported. Several *P. tricornutum* accessions have been collected from different sites worldwide and have been characterized and described, allowing the study of natural modulation in cellular responses or gene expression (De Martino et al. 2007; Bowler et al. 2008). During my research activity I have worked on the ecotype called Pt1 that has been also used in the genome sequencing project (Bowler et al. 2008) and the Pt4 ecotype, because its peculiar chloroplast physiology features (Bailleul et al. 2010).

Besides the cell wall, diatoms also possess a range of other peculiar features that diverge from the classical cellular structures of land plants and animals (Bowler et al. 2010). The diatom chloroplast is of particular interest for my research. This organelle is significantly different from the chlorophyte one, because it has an envelope surrounded by four membranes instead of two (Pyszniak & Gibbs 1992), thylakoids arranged in stacks of three, no spatial segregation of the photosystems, and a peculiar protein and pigment organization (Wilhelm et al. 2006; Finazzi et al. 2010; Goss & Lepetit 2014). Because these peculiar features are likely the results of the complex evolutionary history of diatoms, in the following paragraph I summarize the main steps that contributed to the evolution of diatoms and their particular genetic and cellular features so far mentioned.

1.1.4 The diatom evolution

Oxygenic photosynthesis appears to have evolved only once in the prokaryotic cyanobacteria, but spread to all over a variety of eukaryotic kingdoms through several endosymbiotic events. The initial, primary, endosymbiosis occurred about 1.5 billion years ago, when an ancestral cyanobacterium was engulfed by a phagocytic cell which failed to digest it (Douglas 1998). The cyanobacterium became subsequently a non-autonomous organelle, the chloroplast, specialized in the capture and fixation of CO_2 (Archibald & Keeling 2002). This endosymbiosis event led to three

primary plastid lineages: the green algae (Chlorophyta), the red algae (Rhodophyta) and the Glaucophyta which all belong to the kingdom of Plants (Figure 1 and 3).

All primary plastids are enclosed in a double membrane which coincides to the inner and outer membranes of the ancestral cyanobacterial Gram-negative envelope (Archibald & Keeling 2002). Subsequently, the capacity to perform oxygenic photosynthesis diffused throughout the eukaryotic crown groups by subsequent secondary, and sometimes even tertiary, endosymbiotic events (Figure 3 (Keeling 2010)). These latter events implied the internalisation of algal endosymbionts by non-photosynthetic cells (Archibald & Keeling 2002), and the resulting secondary or tertiary plastids are confined into either three or four membranes. In the four-membrane plastids, the third membrane is derived from the plasma membrane of the endosymbiont and the fourth membrane is derived from the endoplasmatic reticulum (ER) of the secondary host cell.

Diatoms probably arose 280 million years ago from a secondary endosymbiosis event, when a non photosynthetic eukaryote acquired a chloroplast by engulfing a photosynthetic eukaryote, probably a red algal endosymbiont (Falkowski et al. 2004). More recent studies derived by the analysis of diatom genomes and phylogenomic investigations (Moustafa et al. 2009) revealed that two serial secondary endosymbiotic events occurred, with a green and then a red alga engulfed by the heterotrophic eukaryotes. Each endosymbiotic event led to new combination of genes from the hosts and the endosymbionts. Plastid genomes have retained genes related to the chloroplast function, but other genes have been either lost or transferred to the nuclear genome (Oudot-Le Secq et al. 2007). The fact that some genes have both a chloroplast- and a nucleus-encoded copy might indicate that gene transfer to the nucleus could be still ongoing (Green 2011) .

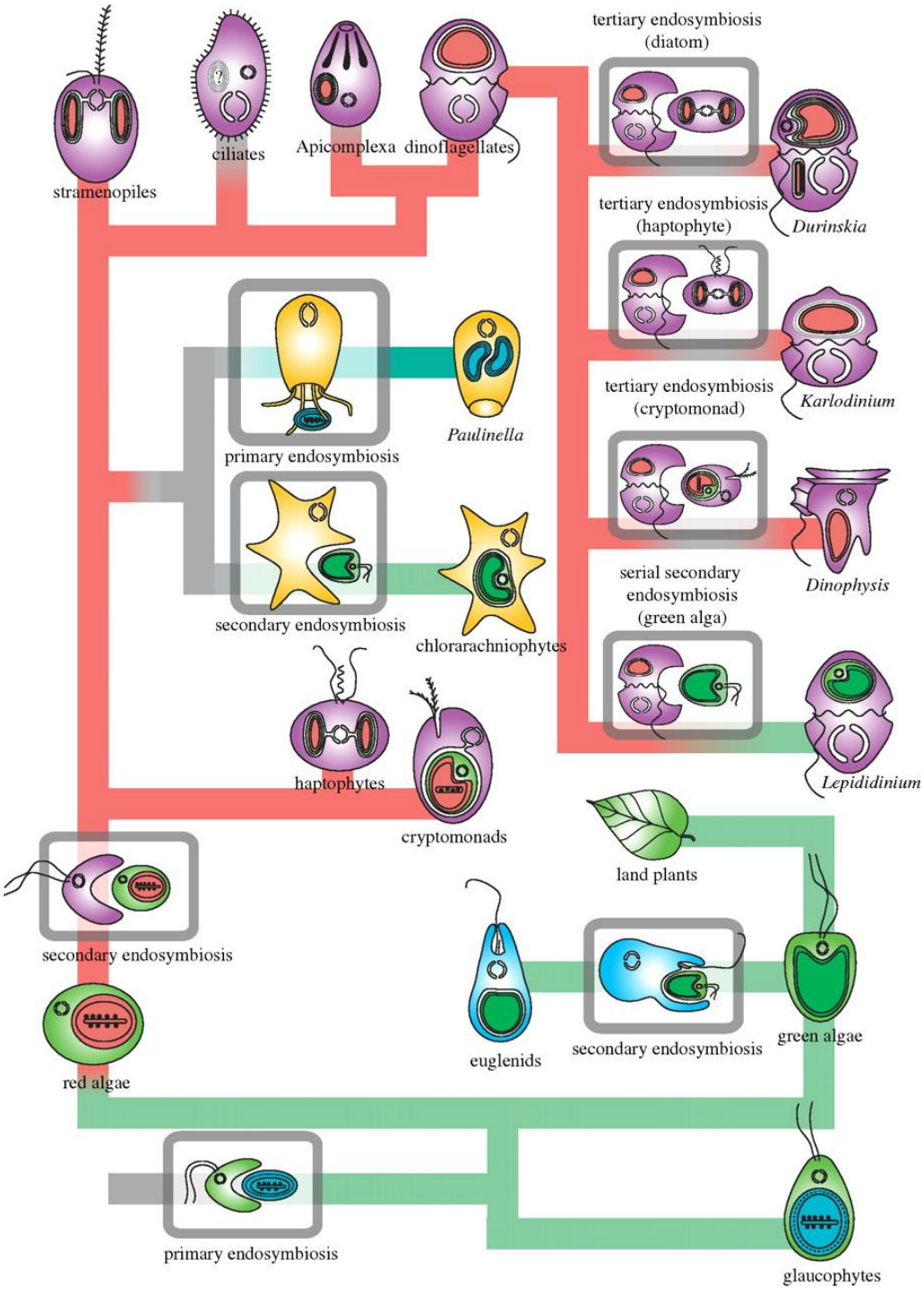

Figure 3 Hypothetical evolution pathway of plastid inheritance in eukaryotic phytoplankton. The primary endosymbiont generated the green algae, red algae, and glaucophytes (here followed by a green line), while all other groups of algae result from secondary endosymbiosis of a primary eukaryotic alga (followed by a red line), among which we find the Stramenopiles. Two serial secondary endosymbiotic events, with a green and then a red alga engulfed by the heterotrophic eukaryotes generated diatoms. Figure from (Keeling 2010)

Although originating from diverse endosymbiotic events, all chloroplasts conserved membranes made of lipoprotein – the thylakoid membranes – in which the photosynthetic apparatus is embedded (Falkowski & Raven 2007). These membranes form closed vesicles called thylakoids

and divide the inner space of the chloroplast into the intrathylakoidal space (lumen) and the phase surrounding the thylakoids, the stroma (Falkowski & Raven 2007) (Figure 4).

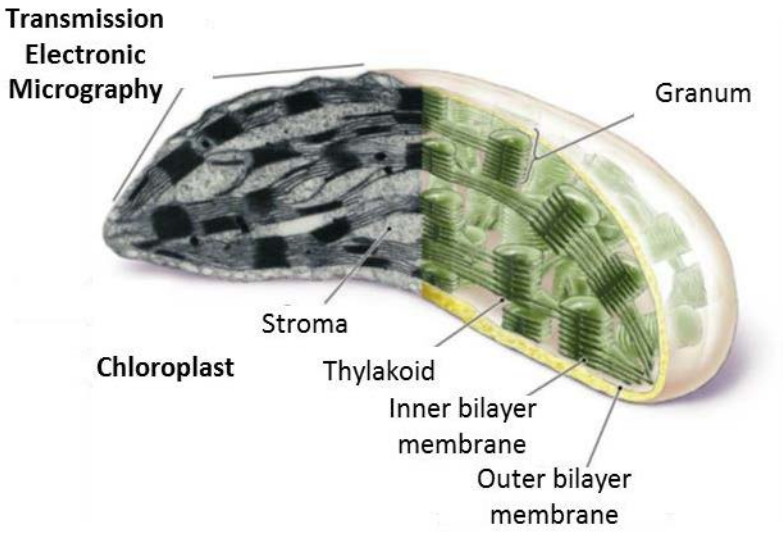

Figure 4 The chloroplast. Merged image of a Transmission Electron Micrography and a schematic representation of a plant chloroplast. Image adapted from Pearson Education, Inc., publishing as Benjamin Cummings.

Apart the similarities in the thylakoid-stroma organization, primary and secondary plastids have a substantial difference: the thylakoids of the green lineage can form tight stacks that are frequently related each other by a single thylakoid (Figure 5 A), whereas diatoms thylakoids are appressed in stacks of three (Figure 5 B). Cyanobacteria, red algae and glaucophytes thylakoids do not form stacks at all (Falkowski & Raven 2007).

The thylakoids of algal plastids are organized around a pyrenoid body which is enriched in high concentrations of Calvin-cycle enzymes and takes also part to the carbon concentrating mechanism (CCM) of algae (Thoms et al. 2008) (Figure 5 C). The shape of plastids and their numbers vary greatly in diatoms, but remain constant in a group. Pennate diatoms generally have a low number of plastids per cell, sometimes only one.

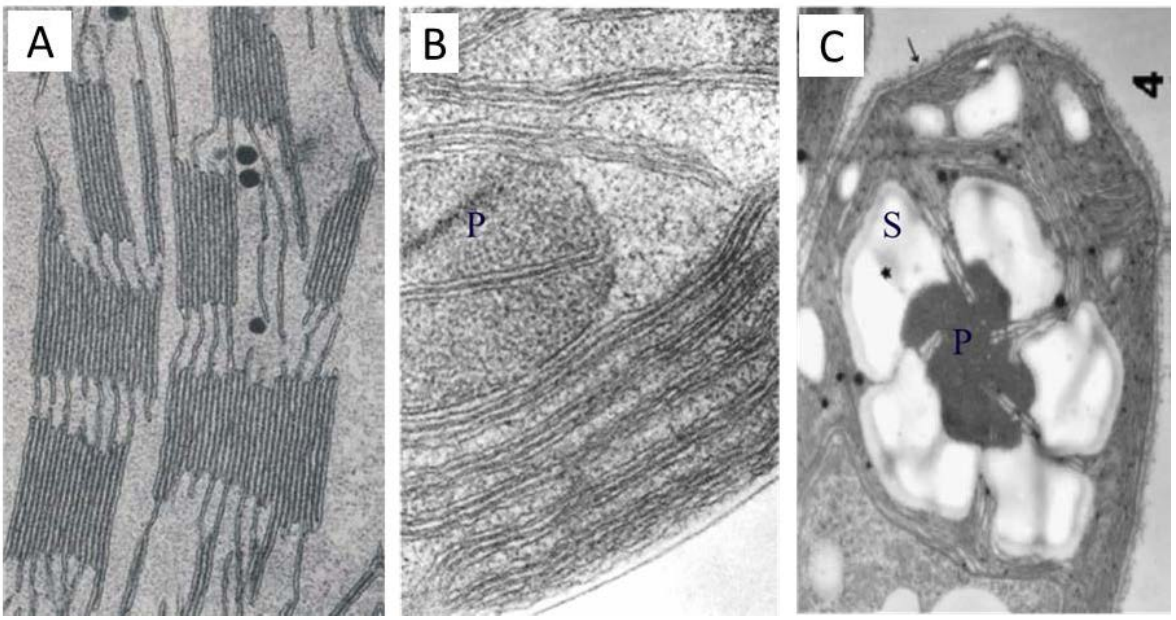

Figure 5 The diverse structures of chloroplastic thylakoids by electron micrographs. Spinach-leaf chloroplasts (A) show the stacking of thylakoid vesicles into grana and the interconnection of the grana by single thylakoids. The dark round spots in the stroma are the plastoglobuli (lipid droplets). Image source: (Stryer 1995). The plastid of the diatom *P. tricornutum* (B) shows the characteristic arrangement of diatom thylakoids in bands of three loosely appressed thylakoids. One pair of thylakoids membranes penetrates the pyrenoid body (P). Source: (Pyszniak & Gibbs 1992). The chlorophyte *Dunaliella viridis* plastid (C) shows an almost random stacking of the thylakoids, and pairs of thylakoids partially penetrate the pyrenoid body (P) which is surrounded by large starch grains (S). Image source: (Borowitzka & Siva 2007).

1.1.5 Novel informations on diatom biology revealed by genome-enabled investigations

In the last decade, the completed genome sequences from various diatom species offered the opportunity to explore evolution, biology and metabolism of these microalgae and have provided a deeper comprehension of the mechanisms behind their ecological success in the contemporary oceans.

The first genomes available for analysis have been those of the centric diatom *T. pseudonana* (Armbrust & et al. 2004) and of the pennate diatom *P. tricornutum* (Bowler et al. 2008). Since then, additional genomes from representative diatom species have been sequenced or are under the sequencing process (Tirichine & Bowler 2011) (e.g., the toxic species *Pseudo-nitzschia multiseries*, and the polar species *Fragilariopsis cylindrus* (by the Joint Genome Institute). At the same time, the Marine Microbial Eukaryote Transcriptome Sequencing Project, generated 178 transcriptomes from 92 different strains, allowing the identification of diatom genome distinct properties and the diatom

core genes, which are conserved in all (or most) species and are exclusive of these organisms (Keeling et al. 2014).

The comparative analysis of several diatom genomes also indicated that diatoms contain a unique combination of genes and pathways acquired through multiple endosymbiotic events. The integration of these genes generated novel metabolic combinations never seen before, possibly concurring to create diatom specific features. For instance, in the diatom genomes exist genes originating from the ancestral heterotrophic host and the photosynthetic symbiont (Armbrust & et al. 2004). These animal/plant-like roots have been confirmed in both species *P. tricornutum* and *T. pseudonana*, by the co-existence of metabolic features typically found in plants (such as photosynthesis) and in metazoans (such as a complete and functional urea cycle and a mitochondrial fatty acid oxidation pathways) (Armbrust & et al. 2004; Bowler et al. 2008).

The presence of a complete urea cycle was formerly thought to be enclosed to organisms that assimilate complex organic nitrogen compounds and excrete nitrogenous waste products. However, large-scale gene expression studies and functional characterization of several urea cycle genes (Maheswari et al. 2009; Allen et al. 2011) revealed that the urea cycle in diatoms is used for the biosynthesis of organic nitrogenous compounds rather than for their catabolism, as is the case of animals (Esteban-Pretel et al. 2010). In conclusion, this cycle possibly enables diatoms to efficiently use carbon and nitrogen from their environment when nitrogen concentration is limiting by recycling intracellular nitrogen compounds (Allen et al. 2011).

From the analysis of *P. tricornutum* genome, it also emerged that hundreds of bacterial genes were dispersed all over the diatom genomes (Bowler et al. 2008) likely by horizontal gene transfers between diatoms and bacteria. Seemingly, diatoms are often found in associations with bacteria (Carpenter & Janson 2000). These genetic transmissions likely provided novel possibilities for metabolite use and perception of environmental signals (for example in diatom genomes there is an expansion of the bacterial two-component regulatory systems).

On a different note, diatoms have developed sophisticated strategies to cope with nutrient limitation such as iron, which is often limited in open-ocean regions. *T. oceanica*, for example, seems to have adjusted its photosynthetic apparatus to use less iron (Strzepek & Harrison 2004). This specie

has even substitute iron-requiring electron-transport proteins with equivalent proteins that necessitate copper (Peers & Price 2006). By contrast, *P. tricornutum* responds to iron limited conditions down-regulating the reactions that require huge amount of iron, while up-regulating alternative pathways to contrast the oxidative stress and to enhance auxiliary iron-acquisition pathways (Allen et al. 2008). Thus, raphid pennate and centric diatoms developed different strategies to deal with a shortage of iron. In addition, centric and pennate diatoms also differ in their capacity to store this element. A study has indicated the existence of a peculiar iron-storage molecule such as ferretin, in several pennate genera (*Pseudo-nitzschia*, *Fragilariopsis* and *Phaeodactylum*) (Marchetti et al. 2009). Ferretin is also known to defend the cells against oxidative stress. Interestingly, *T. pseudonana* does not encode ferretin. So it appears that this gene was probably inherited by lateral gene transfer from other species after the division between pennates and centrics or that it was present in both lineages but was subsequently lost by centric diatoms. Another recent study revealed that diatoms use the protein ISIP2a to concentrate iron at the cell surface as part of a novel copper-independent system (Morrissey et al. 2014).

Concerning the CO_2 metabolism, for a long time diatoms have been considered as C3 photosynthetic organisms. However, some studies suggested that the diatom *T. weissflogii* might concentrate CO_2 in the pyrenoid body, with a C4-like biochemical reaction (Roberts et al. 2007). This form of photosynthesis could permit a more efficient usage of CO_2 as shown in a few land plants, such as sugar cane and maize. Only C3 photosynthesis has been reported in *T. pseudonana* and, although various genes potentially involved in a C4-like photosynthesis have been identified in *P. tricornutum* (Kroth et al. 2008), it has been proposed that they might have alternative roles in excess energy dissipation and pH homeostasis (Haimovich-Dayan et al. 2012). Therefore, to date, the existence of a C4-like photosynthesis is still controversial in diatoms.

In addition to the information from the sequencing projects, the last years have also seen an expansion of marine environmental genomic studies that provided new information on the physiology and the molecular biology of these organisms in their natural habitat, as well as their relationships with other organisms occupying the same ecological niche. Recently, analyses of the Tara Oceans expedition data have provided new estimations on diatom global diversity and

community composition. In particular, it has been shown that diatoms are the 6th most abundant organismal group and the most abundant phytoplankton group in the contemporary ocean (Vargas et al. 2015; Malviya et al. 2015).

1.2 A suite of new molecular resources to understand diatom biology

Beside the genomic information, a set of molecular-based tools has been set up in selected diatom model species, allowing functional genomic studies in these microalgae. Genetic transformation systems are available for *P. tricornutum* (Apt et al. 1996; Siaut et al. 2007; Karas et al. 2015), *T. pseudonana* (Poulsen et al. 2006), *Pseudo-nitzschia multistriata* and *Pseudo-nitzschia arenysensis* (Sabatino et al. 2015), as well for other diatom species whose genomes have not been sequenced, like *Cyclotella Cryptica*, *Navicula Saprophila* (Dunahay & Jarvis 1995) and *Cylindrotheca fusiformis* (Fischer et al. 1999).

A set of reporter genes have been used, particularly in *P. tricornutum*, including the *Escherichia coli UIDA* (β-glucuronidase) gene, the *CAT* (chloramphenicol acetyl transferase) gene, the firefly luciferase, different variants of the green fluorescent protein, GFP, and the jellyfish aequorin gene (Falciatore et al. 1999; Falciatore et al. 2000). A serie of Gateway-based vectors for diatoms has been also created to boost functional analysis in a high-throughput mode (Siaut et al. 2007).

Attempts have been made in recent years to explore diatom gene function via the comprehensive analysis of EST libraries (http://www.biologie.ens.fr/diatomics/EST3/) (Maheswari et al. 2005). More recently, massive transcriptomic information derived by microarray analyses and next generation RNA sequencing data from different diatom species exposed to diverse stimuli and stresses (Keeling et al. 2014; Mock et al. 2008; Nymark et al. 2009; Nymark et al. 2013; Thamatrakoln et al. 2013; Valle et al. 2014; Alipanah et al. 2015) have highlighted the existence of some diatom-specific adaptive strategies, pinpointing molecular regulators of environmental change responses.

The sexual cycle in most diatom model species such as *P. tricornutum* and *T. pseudonana* cannot be controlled in the laboratory, hampering the development of classical genetic studies. (Even

though meiosis is uncertain in *P. tricornutum*, I observed a structure 'pilus-like' relying two *P. tricornutum* cells once (Figure 6) that made me think that some exchanges were in course between the two cells.)

Figure 6 Two *P. tricornutum* cells possibly connected by a wire.

Genetic manipulation on diatoms mostly relied on the modulation of gene expression by gene over-expression (Siaut et al. 2007) and gene silencing (De Riso et al. 2009). These approaches have been extensively used in this work and additional information on these techniques will be provided in the introduction of Chapter IV. However, in the last years, the first evidences of stable targeted gene editing via the TALEN (Daboussi et al. 2014) and the CRISPR/Cas9 (Nymark et al. 2016) technologies have been provided. Although these tools are still in their infancy regarding their routinely application in diatoms, they open completely new possibilities for the diatom gene functional characterization and their exploitation in biotechnology.

Differently from the nuclear genetic engineering, we are still unable to routinely modify chloroplast genes and, as consequence, the diatom chloroplast still contains many secrets. The first targeted plastid mutagenesis has been achieved by homologous recombination in the *PSBA* gene, which encodes the D1 protein (Materna et al. 2009), but the mechanisms leading to the mutation have not been completely established. However, this work provided the first evidence that diatom plastid transformation is feasible and that the engineering of chloroplast genes could become a common tool.

Likely because of the peculiar chloroplast structures, many difficulties still persist in purifying intact chloroplast from the diatom model species such as *P. tricornutum*. However, a significant progress has also been made in recent years in the understanding of the components of the diatom photosystems and the molecular organization of the light-harvesting complexes (Buchel

2003; Beer et al. 2006; Lepetit et al. 2007; Schaller-Laudel et al. 2015; Muhseen et al. 2015), due to the use of novel biochemical approaches allowing to isolate the photosynthetic complexes in pennate and centrics diatoms. Proteomic approaches have also been used to provide initial information on the thylakoid protein complexes of *T. pseudonana* and *P. tricornutum*, revealing the existence of diatom-specific photosystem I (PSI) associated proteins and providing a new information on the assembly and dynamics of the diatom photosynthetic complexes (Grouneva et al. 2011).

2. The photosynthetic process

Nearly all life on Earth is supported, directly or indirectly, by the energy produced by photosynthesis, the biological process that converts light to chemical bond energy. The electrons used for the enzymatic reduction of CO_2 are removed from H_2O, which results in the release of O_2. The slow production of O_2 from oxygenic photoautotrophs during millennia, first within the oceans, then on the land, induced the oxidation of the Earth's atmosphere determining the biology and the geochemistry of Earth (Falkowski et al. 2004).

The photosynthetic process involves a series of light-dependent and light-independent reactions that in eukaryotic phototrophs take place in the chloroplast. The main components of the photosynthetic apparatus consist of protein complexes, pigments and pigment-binding proteins, embedded in the thylakoid membranes. Whereas the general mechanism of oxygenic photosynthesis has been conserved throughout different photosynthetic organisms, the pigments and proteins of the light-harvesting complexes have diversified. Here, I first summarize the main photosynthic reactions, and after I provide additional information on the functional complexes in photosynthesis (paragraph 2.4), with a particular focus on the diatom components, if characterized.

2.1 The photosynthetic electron transfer reactions

The initial reaction of photosynthesis involves the capturing of light by the light-harvesting complexes, which consist of pigments and pigment-binding proteins (Grossman et al., 1995). Oxygenic photoautotrophs constitutively express two photosystems, the PSI and the PSII (Jordan et al. 2001; Kamiya & Shen 2003) which work in series and are co

nnected by electron carriers. Both photosystems consist in a Reaction enter (RC), which contains several molecule of chlorophyll *a* (Ferreira et al. 2004), and two peripheral pigment-proteins complexes: the core, or inner antenna and the light harvesting pigment binding complexes (LHC), or outer antenna (Grossman et al. 1995).

Light is directly absorbed by the chlorophyll *a* in the PSII RC or by the pigments in the core and in the antenna. In this latter case, the energy is funneled from the periphery of the photosystem to a pair of chlorophyll *a* in the RC via excitation energy transfer (EET). These two chlorophylls have a maximal absorption of light at 680 nm and are therefore called P_{680} (Falkowski and Raven, 1997). After light absorption, the primary electron donor chlorophyll *a* becomes a good reducer and passes its electrons to a molecule of pheophytin. The oxidized PSII generates an electrochemical potential of +1.1 volts, enough to remove two electrons each from two water molecules, used to neutralize the chlorophyll *a* cation (P680+) that remained after the charge separation. This reaction creates a molecule of O_2 at a cost of four photons – one for each electron moved. Thereby, the transformation of four photons into four electrons takes place in the RC (Duysens et al. 1961). These reactions result also in the release of protons (H+) in the lumen (Falkowski & Raven 2007) generating a transmembrane proton gradient and an associated electric field.

Each released electron from P680 is transferred through a chain of electron carriers, known as the Hill and Bendall Z scheme (Hill & Bendall 1960): first to pheophytin and then from reduced pheophytin to a non-mobile plastoquinone present in a site inside the PSII called QA-binding site. The plastoquinone subsequently donates the electron to a mobile plastoquinone bound at the QB-site in the PSII. This plastoquinone is released from QB site only after becoming fully reduced (PQH_2) by the acquisition of a second electron. Even though the quinone in QB site is localized entirely within the hydrophobic part of the membrane, the protons are taken up from the stromal side of the membrane and not from the luminal pool released from the water lysis.

The cytochrome b_6f catalyses the transfer of electrons from PQH_2 to the copper-protein plastocyanin (PC) placed in the lumen and it concomitantly releases the protons attached to the QH_2 across the thylakoid membrane which enforces the proton gradient inside the lumen (Figure 7). The reduced PC subsequently delivers the electrons to the PSI RC.

Similar to PSII, four photons are funnelled from the LHC of PSI (LHCI) to a pair of chlorophyll *a* molecules with a maximal absorption at 700 nm (P700) located at the reaction center site. The excited P700* releases an electron to an acceptor chlorophyll molecule (A0) and is thereupon transferred to ferredoxin on the stromal side of the thylakoids through a series of electron acceptors, including several iron-sulfur clusters. The PSI RC is constantly oxidized by light-driven charge separation in P700*, and the four electrons delivered by PC are used to re-reduce the excited PS700* and to return to its ground state.

The electron transfer ends with the deposition of the four electrons in two pairs on two molecules of Nicotinamide Adenine Dinucleotide Phosphate (NADP) through an enzymatic reduction of NADP+ by Ferrodoxin/NADP Reductase (FNR) using ferrodoxin (Fd) as electron donor (Figure 7). Overall, this process is known as the linear electron flow (LEF). The proton motive force that is generated across the thylakoid membrane with the linear electron flow from PSII to PSI is used for the synthesis of adenosine triphosphate (ATP) by the ATP synthase. ATP and NADPH drive the 'dark reactions' that transfer the electrons to CO_2, but these molecules are also involved in other metabolic pathways in particular that of nitrogen, silica and phosphates.

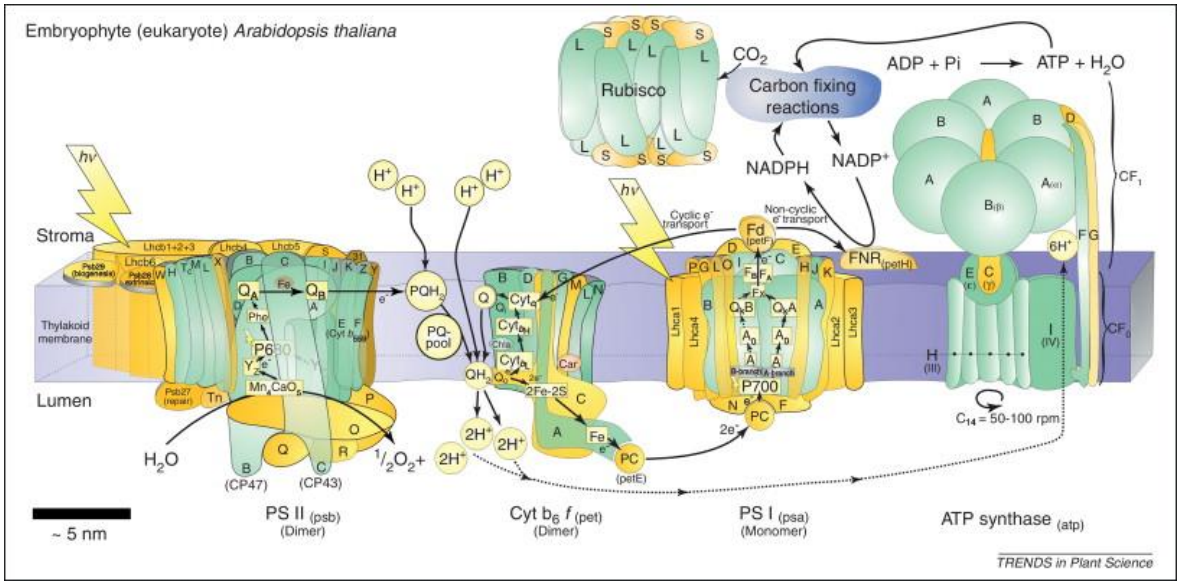

Figure 7 The linear electron flow in photosynthesis. Simplified view of the major proteins and protein complexes of the chloroplast photosynthetic apparatus in a generic photosynthetic organism. Figure from (Allen et al. 2011)

2.2 The carbon-fixation reactions

In the carbon-fixation reactions, the ATP and the NADPH produced by the photosynthetic electron-transfer reactions serve as the source of energy and reducing power, respectively, to drive the conversion of CO_2 to carbohydrate. Once the carbon accumulates in the cell (in the plastid or in the cytoplasm as CO_2 or HCO_3-), it is routed to pyrenoid where its assimilation is performed via the RuBisCo enzyme. In algae, this enzyme is very densely packed into chloroplast complexes called pyrenoid bodies. These bodies are almost crystalline RuBisCO and also contain carbonic anhydrase. This latter enzyme catalyzes the hydration of CO_2 to form HCO_3 to hamper the efflux of CO_2 from the chloroplast and to actively concentrate the CO_2 in the chloroplast. The same enzyme converts the HCO_3 to CO_2 which is immediately used by the RuBisCo enzyme.

The CO_2 is assimilated into organic compounds through the Calvin cycle, which takes place in the chloroplast stroma. A molecule of CO_2 is combined to a five-carbon sugar (ribulose 1,5 diphosphate) to form two molecules of a three-carbon product (3-phosphoglycerate, PGA). The PGA is then reduced in a molecule with three carbons, the glyceraldehyde 3-phosphate (PGAL). A carbon enters the Calvin cycle in each cycle and three rounds produce one molecule of PGAL which is converted into sucrose or starch. The overall cycle can be broken down into three phases: carboxylation, reduction, and regeneration (Nelson & Cox 2013). The three phases are schematically illustrated in Figure 8.

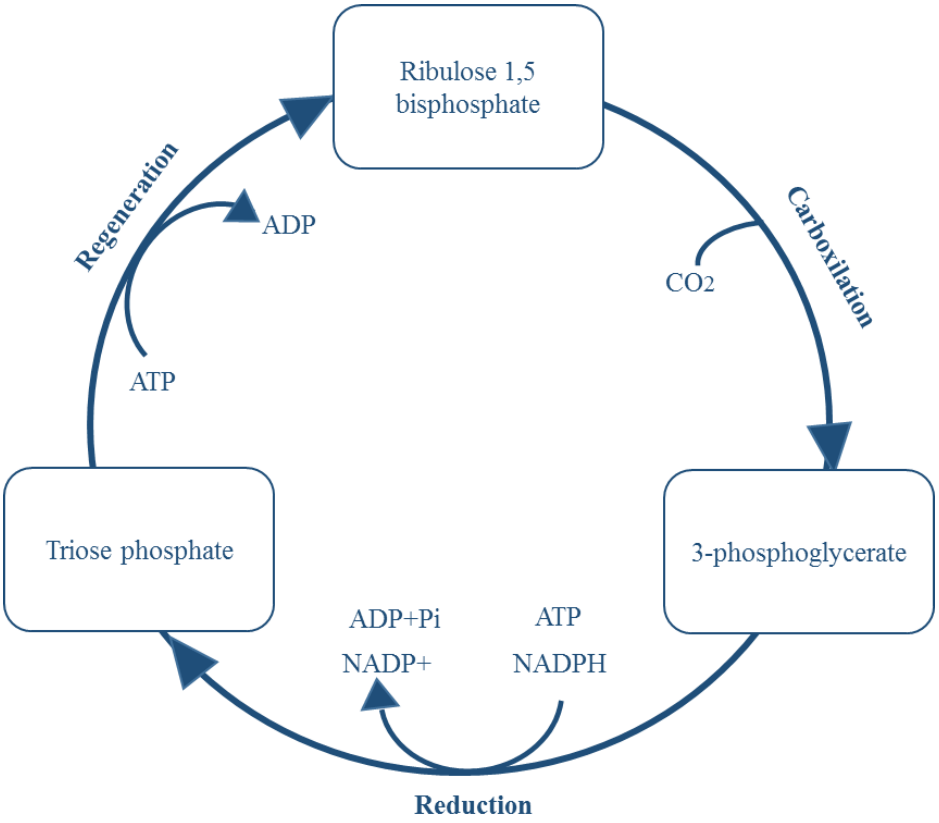

Figure 8 The three stages of the Calvin-Benson cycle: carboxylation, reduction, and generation. Most of the ATP and all the NADPH are used in the reduction phase, and some ATP is used in the regeneration phase. The triose phosphate is a collective name for glyceraldehyde 3-phosphate and dihydroxyacetone phosphate.

The overall stoichiometry of the Calvin-Benson cycle from CO_2 to triose phosphate is:

$$3CO_2 + 9ATP + 6NADPH + 5H_2O \rightarrow PGAL + 9ADP + 8Pi + 6NADP + 3H^+$$

Suggesting that 6 NADPH and 9 ATP from photosynthesis are used to produce glyceraldehyde 3-phosphate and the needed ratio of ATP/NADPH is 1.5.

2.3 The alternative electron transfers

In the linear electron flow, four electrons produce one oxygen molecule and 2 NADPH molecules. The same 4 electrons pump a total of 12 protons into the thylakoid lumen from the stroma. However, protons do not drive a complete rotation of the chloroplastic ATPase and only 2.57 ATP molecules are produced by linear electron flow transport. Therefore, the true ATP/NADPH ratio by linear electron transport is not 1.5 but 1.29. This mechanism generates a shortfall of ATP from linear electron flow and something else must account for the additional ATP required for CO_2 fixation in the Calvin-Benson pathway (Allen 2002).

Thereby, the ATP/NADPH ratio in some organisms is adjusted by some plastid-localized ATP generating processes, which are alternative to the linear electron flux and are: the malate valve, the Mehler peroxidase reactions, also known as water to water cycle, the action of the Plastide Terminal Oxidase and the Cyclic Electron Flow (CEF) (Eberhard et al. 2008). With all these processes, the regulation of linear and alternative electron transport allows some flexibility in the ratio of ATP and NAPDH production.

Differently from green algae and plants, that use extensively the alternative processes, diatoms regulate the ATP/NADPH ratio shortfall by performing metabolic exchanges between the chloroplast and the mitochondria. In particular, NADPH from the chloroplast, is exported to the mitochondria in exchange of ATP, finally balancing the shortfall (Bailleul et al. 2015).

2.4 The photosynthetic apparatus

PSI and PSII are the complexes responsible for light energy capture and conversion into chemical energy. PSII is a light dependent water-plastoquinone oxido-reductase, and PSI is a light-dependent plastocyanin-ferrodoxin oxido-reductase. Both photosystems are characterized by the presence of antenna complexes involved in the light harvesting and the transfer of the excitation energy to the core complex and the RC, responsible for charge separation. Here I will briefly describe the components of the photosynthetic apparatus: the light harvesting pigments (chlorophylls, carotenoids), the antenna proteins, the PSII and PSI, the cytochrome b_6f and the ATPase.

2.4.1 The light harvesting pigments

Pigments have multiple important functions in photosynthetic membrane, such as absorption of light, efficient energy transfer to the RC, stabilization of the photosynthetic apparatus as well as the protection against excessive light. In diatoms, the two main classes of photosynthetic pigments are the chlorophylls and carotenoids.

2.4.1.1 Chlorophylls

The chlorophylls belong to the family of the cyclic tetrapyrrole molecules, having four pyrrole residues that coordinate a magnesium atom and an anhydrophobic phytol chain (Figure 9).

These pigments can absorb light because their electrons can switch to a higher excited energy levels storing the energy of the photon absorbed.

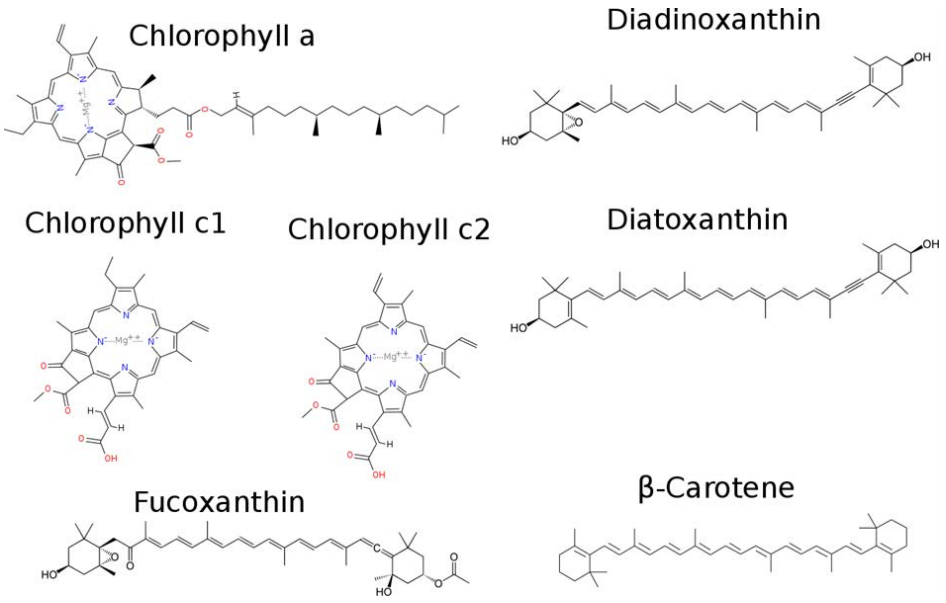

Figure 9. Molecular structure of the main pigments of *P. tricornutum*.

The absorption spectrum of chlorophylls shows two main absorption bands one in the blue (B peak), and one in the red region (Q peak) of the spectrum, representing two different excited states of the molecule (Figure 10).

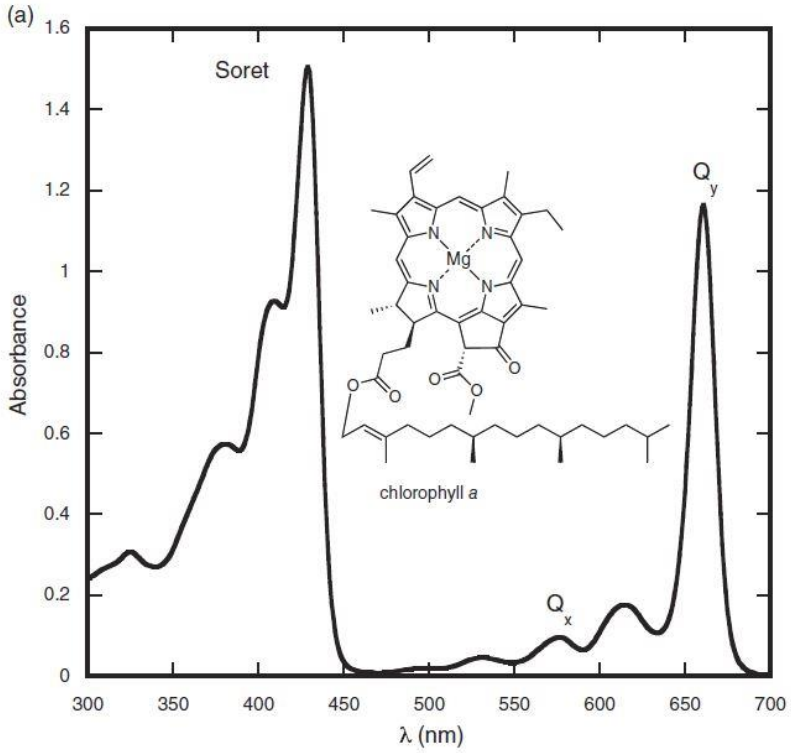

Figure 10. Absorption spectrum of chlorophyll *a*. The two main absorption bands are the Qy and the Soret band.

The lowest excited state of chlorophyll *a* can be populated by electrons that absorb a red photon, or by electrons decaying from higher excited states because they absorbed the more energetic blue photons. Based on the organization of the electrons in the energetic levels, the molecules of chlorophyll in the lowest excited state are called singlet excited state (^{1}Chl*), whereas the other having the electron in a higher excited state are called triplet excited state of the chlorophyll (^{3}Chl*). This latter specie is very reactive and can reduce the O_2 present in the lumen, creating radical oxygen species (ROS) that can react with the lipids and the proteins of the photosynthetic apparatus or even worst with the nuclear genome, finally damaging the cell.

Excited chlorophyll can decay from a triplet to a singlet excited state following alternative pathways that I will describe more in detail in the paragraph 3.

Diatoms and other brown-colored algae possess the chlorophyll *a*, but use chlorophyll *c* instead of chlorophyll *b* (Figure 9). Chlorophyll *c* is the most unusual of all the chlorophylls since it lacks the phytol chain. There are several structural variations of chlorophyll *c,* such as chlorophyll *c1* and chlorophyll *c2*. The chlorophyll *c* absorption spectrum is shifted as compared to that of chlorophyll *a*, which increases diatom light absorption capacity in the 450-470 nm region of which the marine environment is enriched. In Figure 11 are shown the absorption spectra of the pigments present in the diatom *Cyclotella meneghiniana*.

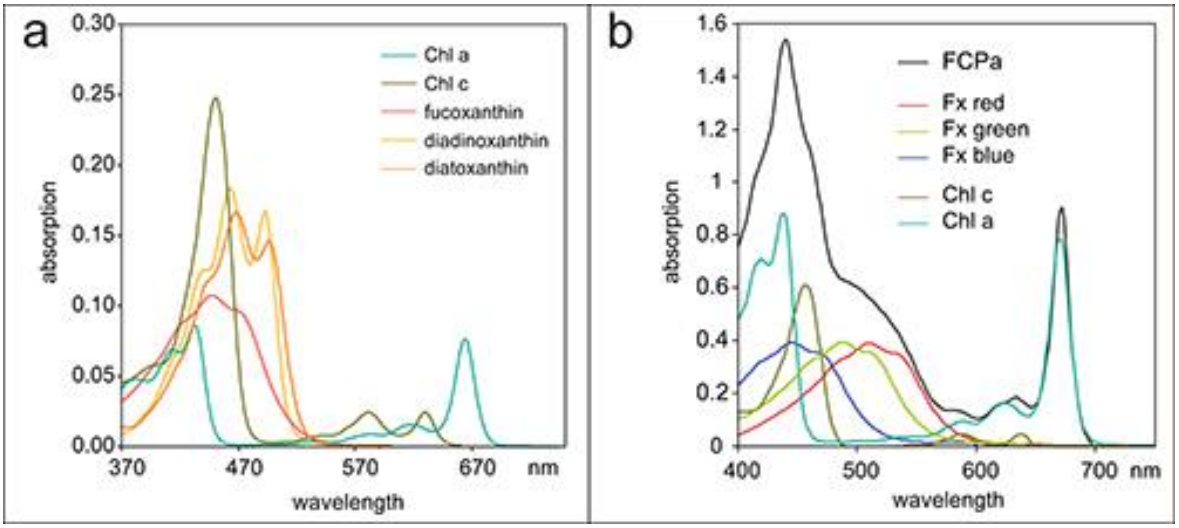

Figure 11 Absorbance spectra of diatom pigments (a); and (b) of one of the light harvesting complexes (FCPa) of *C. meneghiniana*. Chl: chlorophylle; Fx: fucoxanthin. From http://www.goethe-university-frankfurt.de/60243915/research

2.4.1.2 Carotenoids

Carotenoids are accessory pigments that consist of long hydrocarbons chains and are divided into two classes: the carotenes (e.g. ß-carotene) and the oxygenated derivative of carotenes (e.g. xanthophyll cycle pigments diadinoxanthin and diatoxanthin) (Figure 9). These pigments can be attached to the antenna proteins or dissolved in the lipid layer shields around the phtotosynthetic complexes.

In non stressfull environmental conditions, carotenoids mostly serve as accessory light-harvesting pigments and transfer their energy to chlorophyll *a* allowing to extend the absorption spectrum of photosynthetic organisms (Figure 11) (Croce et al. 2003). Indeed, these molecules contain a series of conjugated bonds, which are responsible for the absorption of light in the blue-

green part of the light spectrum (Figure 11) thanks to the highest excitation state, which gives them colours ranging from yellow to orange-red and in some cases even brown (Armstrong & Hearst 1996). In addition, they stabilize the structure and the assembly of protein complexes in the thylakoid membrane (Plumley & Schmidt 1987).

Carotenoids also protect against photo-oxidative damages (Havaux & Niyogi 1999) because they can directly scavenge the oxygen radicals (Demmig-Adams & Adams 1996; Lepetit et al. 2012). In addition, they can safely de-excite the triplet (Ballottari et al. 2013) and singlet (Frank et al. 1996) of chlorophyll excited states. This role in the photoprotection is possible because the first excited state of carotenoids, as compared to that of chlorophyll, has an ultrafast relaxation time (Polivka & Sundström 2004). This efficient thermal relaxation to the ground state makes carotenoids efficient quenchers of excited electronic states and devoils their possible involvement in photoprotection (Frank et al. 1994).

In diatoms, beside ß-carotenes, the major carotenoids are the xanthophylls fucoxanthin (fx), diadinoxanthin (Dd) and diatoxanthin (Dt). Fucoxanthin, a light harvesting xanthophyll, it is not present in plants and it is responsible for diatoms brown colour.

2.4.2 The photosynthetic complexes

2.4.2.1 The PSII complex

The PSII is an intrinsic complex of proteins in the thylakoid membranes of oxygenic photoautotrophs (Fig. 1.8). It is composed by a RC, a core complex or inner antenna and an additional outer antenna which has the function to amplify the spectrum of absorbance of the core (Dekker & Boekema 2005). This structure is highly conserved in all oxygenic organisms (Umena et al. 2011; Nield et al. 2000; Büchel & Kühlbrandt 2005) and the information on PSII are mostly derived from the high-resolution structure of the PSII oxygen evolving centre from the cyanobacterium *Thermosynechoccus elongates* at 3.5 Å resolution (Ferreira et al. 2004).

In its functional form the PSII core complex is a dimer (Kouřil et al. 2013), where each monomer is composed of a RC and a core antenna. The RC is composed of the proteins D1 and D2 and cytochrome b_{559}, this latter being probably active in the photoprotection (Shinopoulos & Brudvig

2012). These proteins are entoured by two core antenna proteins CP43, CP47 and several proteins and inorganic cofactors involved in oxygen evolution. On the lumenal side of the core there are extrinsic proteins forming the Oxygen Evolving Complex (OEC) that are PsbO, PsbQ, PsbP and PsbR. In total, PSII complex has 19 subunits in each monomer and coordinates between 250 and 300 chlorophyll molecules depending on the environmental conditions and the species (Anderson & Andersson 1988). Diatoms PSII shows specific features: it contains a novel extrinsic PSII protein on the luminal side that directly associates to PSII core (Nagao et al. 2007). This protein is called Psb31 and serves as a substitute for PsbO in supporting oxygen evolution (Nagao et al. 2013).

In the eukaryote kingdom the genes encoding D1, D2, CP43 and CP47 are located in the chloroplast genome, whereas the genes for the OEC are nuclear encoded (Allen et al. 2011). This is the case also for diatoms (Oudot-Le Secq et al. 2007).

As it will be described in the paragraph 3.1.2, PSII is also the target of the photoxidative damage that occurs under strong light, determining inhibition of its activity.

2.4.2.2 The cytochrome b_6f complex

The cytochrome b_6f complex is a membrane-intrinsic light independent oxidoreductase, that oxidizes the plastoquinol and reduces the plastocyanin while translocating protons (Stroebel et al. 2003). Cytochrome b_6f is a close structural and functional homologue of respiratory complex III, in which each pair of electrons moves four protons from the the stroma to the the thylakoid lumen (Figure 7). The cytochrome b_6f is composed by eight subunits. In *P. tricornutum* seven genes are located in the chloroplast, with the exception of the gene encoding the Rieske Fe-S subunit, which is located in the nucleus. In plants, not only the Rieske Fe-S subunit gene is located in the nucleus, but also the gene encoding the subunit M.

Cyanobacteria and most unicellular green algae contain both the copper-protein plastocyanin and the iron-containing cytochrome c_6, as soluble electron carriers between cytochrome b_6f and PSI. At difference, most algae containing chlorophyll *c* lack plastocyanin and contain cytochrome c_6 (Raven et al. 1999), with the excpetion of the diatom *T. oceanica* where plastocyanin has been found

(Peers & Price 2006). The cytochrome c_6 gene in *P. tricornutum* is located in the chloroplast, at difference with *A. thaliana*.

2.4.2.3 The PSI complex

The PSI is a membrane-intrinsic complex of proteins composed by the proteins of the RC PsaA and PsaB and other ten proteins (Figure 7). Of the 18 genes that encode PSI proteins only *PsaA*, *PsaB*, *PsaC*, *PsaI* and *PsaJ* genes are located in the chloroplast genome in plants. In the diatom *P. tricornutum*, the same genes are found in the chloroplast genome as well, in addition to the *PsaD*, *PsaE*, *PsaF*, *PsaL* and *PsaM*. The PsaK gene is lacking in diatoms. The division between chloroplast- and nuclear-located genes in *P. tricornutum* is the same than in the red alga *Cyanidioschyzon merolae*, confirming the red alga origin of the diatom chloroplast. The model of PSI structure derived from a variety of biochemical and biophysical studies as well as from the X-ray structure at 2.5 Å (Fromme et al. 2001; Grotjohann & Fromme 2005; Jordan et al. 2001).

The primary donor in PSI is named P700 after chlorophyll absorption maximum (700 nm) of the primary donor. PSI of algae and plants also binds an outer light-harvesting antenna (LHCI). About 100 chlorophylls and 20 ß-carotenes in plants are bound to the core, the rest of the approximately 170 chlorophylls is bound to LHCI or located between LHCI and the core.

In green algae, LHCI-PSI complexes bind a larger number of antennas, which contain approximately 280 chlorophylls in total (Bassi et al. 1992). Also here, all 15 assigned ß-carotenes are found in the core of PSI, (Amunts et al. 2010; Ben-Shem et al. 2003). In diatoms, studies on isolated FCP-PSI complexes show that they bind around 200 Chls in total, where around half should be assigned to the core and half to FCP complexes (Ikeda et al. 2008; Veith & Büchel 2007).

Also the PSI can undergo a photoinhibition process caused by ROS (Sonoike & Terashima 1994; Sonoike 1996). Even though the PSII photoinhibition has been more investigated, it has been recently proposed that PSI photoinhibition might be more dangerous than that of PSII one because of the very slow recovery rate of PSI (Sonoike 2011). Therefore, it has been proposed that in fluctuating light regimes it might be more important to photoprotect PSI as compared to PSII (Tikkanen & Aro 2012).

The fractions enriched of PSI from diatoms presented a composition similar to PSI core complex from green plants (Berkaloff et al. 1990). In diatoms PSI and PSII are not segregated like in plants (Pyszniak & Gibbs 1992), however PSI seems to possess a specific and different light harvesting antenna from PSII (Veith & Büchel 2007).

2.4.2.4 The ATP synthase

The ATP synthase (ATPse) is a complex that generates ATP while transporting a proton, therefore it is a defined as proton-translocating ATP hydrolase (Watt et al. 2010). The photosynthetic electron transport establishes a transmembrane proton gradient, a proton-motive force that serves to drive the ATPase reaction in the direction of ATP synthesis. The ATPase activity itself resides in a water-soluble domain called CF1, that is anchored to the membrane. The proton translocation is performed by the hydrophobic, membrane- intrinsic CF0 domain. The genes encoding the subunit of ATPse are nine. In *A. thaliana,* six out of nine genes are located in the nucleus, at difference with *P. tricornutum*, where only one gene, encoding the γ-subunit, is located in the nucleus. Also in this case the position of these genes is identical to the red algae one.

2.4.2.5 The light harvesting complex

In photosynthetic eukaryotes, the light harvesting proteins (LHC) are encoded by genes localised in the nucleus (Allen et al. 2011). These proteins are classified in two groups depending on the position that they occupy in the thylakoid membranes: the water soluble antenna that are extrinsic to the thylakoidal membranes are called phycobilisomes, whereas the hydrophobic antenna containing chlorophyll and carotenoid are inside the membranes (Grossman et al. 1995; Falkowski & Raven 2007). The hydrophobic antenna are present in green algae and land plants, heterokontophytes, haptophytes, cryptophytes and dinoflagellates (Figure 1), whereas phycobilisomes are used by rhodophytes, glaucophytes and also cryptophytes (Figure 1) and cyanobacteria (Green & Durnford 1996; Delwiche 1999).

While the structure of the RC is well conserved among the photosynthetic organisms, the antenna systems differentiated in the diverse groups. Today the X-ray christallography structures of PSII LHC (LHCII) (Liu et al. 2004) and the supercomplex LHC-PSI are available (Ben-Shem et al.

2003) for pea plant. The LHCII consist of three transmembrane helices that coordinate eight molecules of chlorophyll *a* and six chlorophyll *b*. Two lutein carotenoids molecules arranged in an 'X' structure help to keep the complex together and the structure contains also one neoxanthin and one violaxanthin. The study of the crystal of PSI LHC (LHCI) showed that each LHCI binds 11 molecules of chlorophyll *a* and 3 molecules of chlorophyll *b*, indicating a lower affinity for chlorophyll *b* as compared to the LHCII. LHCI also binds five carotenoids, mainly lutein, violaxanthin and ß-carotene, while neoxanthin is not present at variance with the LHCII (Wientjes & Croce 2011). Similar proteins have been found in the membrane of algae as well (Grossman et al. 1995; Green et al. 2003).

The lhc suffix followed by "a" indicates that the protein is associated to the Photosystem I, whereas if it is followed by "b" it means that it is associated to PSII. The nomenclature is complicated by the fact that LHC proteins are also often identified by the nomenclature CP (Chlorophyll Protein).

Because of their high content in fucoxanthin, the LHC of diatoms are called fucoxanthin chlorophyll a/c-binding proteins (FCP), and each monomer binds chlorophylls (*a* and *c*), fucoxanthin molecules, Dd, Dt and ß-carotene (Lepetit et al. 2010). In low light conditions, the chlorophyll to carotenoid stoichiometry of the light-harvesting antenna of diatoms differs from that of higher plants, with the chlorophyll *a*: carotenoid ratio being 1:1 (Lepetit et al. 2010) lower than that of plants (Liu et al. 2004). This ratio varies with the culture conditions, for instance when the carotenoid concentration increases with high light (Lepetit et al. 2010).

The model of the FCP structure is based on the sequence homology with LHC proteins in pea (Wilhelm et al. 2006). The sequence of the FCP is similar to the LHCII, mainly in the helices 1 and 3, even though, diatoms antenna are smaller in size because the loop termini are shorter as compared to LHCII (Bhaya & Grossman 1993) (19 kDa for FCP and 25 kDa for LHCII) (Buchel 2003).

In centric diatoms the FCP aggregate in trimers, called FCPa and into higher oligomeric states, possibly hexameric, called FCPb (Buchel 2003). In the pennate diatom *P. tricornutum* only the trimeric subpopulation has been clearly identified (Lepetit et al. 2010). In centric diatoms, these supercomplexes contain different polypetides: the FCPa contains mainly 18 kDa proteins and a small

amount of 19 kDa among which the LHCX (called FCP6 in centric diatoms) proteins. The LHCX proteins belong to the LHC family but have a photoprotecting role rather than a light harvesting one (Ghazaryan et al. 2016). The FCPb supercomplexes contain 19 kDa sized polyptetides that belong to the LHCF family, the major light harvesting proteins in diatoms (Buchel 2003). These subpopulations have different absorption properties: the FCPb absorb less in the region around 490 nm and more in the region around 540 nm as compared to FCPa trimers (Beer et al. 2006), suggesting that the trimers in *C. meneghiniana* might bind more blue shifted absorbing fucoxanthin as compared to FCPb. Biochemical studies and spectroscopic analysis based on these evidences propose that the FCPb binds to PSII in a greater amount than to PSI (Szabó et al. 2010; Chukhutsina et al. 2013).

The genes encoding the diatom FCP polypeptides belong to one of these four classes: the LHCF (Lepetit et al. 2010; Grouneva et al. 2011); the LHCR, resembling to the light harvesting proteins of red alga associated to PSI which might be the specific antenna of PSI also in diatoms (Lepetit et al. 2010; Grouneva et al. 2011); the LHCX, involved in photoprotection rather than light-harvesting (Beer et al. 2006; Lepetit et al. 2010; Grouneva et al. 2011; Nagao et al. 2013); and the RedCAPs antenna, whose function is still unknown (Sturm et al. 2013).

3. The photoprotection mechanisms

Photosynthetic rates are controlled by many factors, among them irradiance is one of the major regulator. The dependence of photosynthesis on light intensity can be figured out with the photosynthesis-irradiance (P-E) relationship (Figure 12).

The light saturation curve is linear at low light intensitities when all the light absorbed is used for photochemistry. However, when the light absorbed exceeds the photosynthetic capacity a saturation of the photosynthesis is observed.

Exposure to environmental stress (e.g., excessive light absorbed, nutrient deficiencies, extreme temperatures, etc.) generally lowers the photosynthetic assimilation of CO_2 (Adams et al. 2014) and decreases the threshold of the light intensity perceived as saturating (Figure 13), since the level of excess light is a function of both irradiance and photosynthetic light utilization. Therefore, a saturation of the photosynthetic capacity can occur not only at high light intensities but also also at low irradiance under nutrient starvation or low CO_2 conditions.

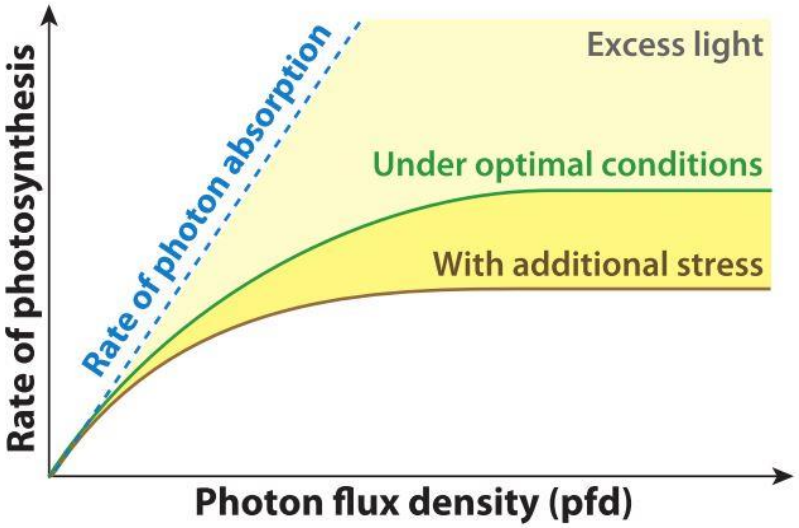

Figure 12. The rates of photosynthesis and light absorption versus incident light intensity. The point of saturation is dependent on whether the plant is shade- or sun-acclimated, nutrient starved or repleted. Figure from (Li et al. 2009)

When light is absorbed by chlorophyll *a*, it has three main ways to be dissipated: it can be (1) re-emitted as fluorescence, (2) transferred to the reaction center of PSII and used for photochemistry, or (3) thermally dissipated through a process called Non Photochemical Quenching of Chlorophyll fluorescence (NPQ) (Figure 13). In case of excessive light, and therefore photosynthesis saturation, the singlet excited state of chlorophyll can form the triplet state (4) which often reacts with molecular oxygen producing the ROS (Figure 13). All these routes of energy dissipation are in competition and the quickest mechanism will de-excite the ^{1}Chl*. The chlorophyll *a* fluorescence is predominantly emitted by the antenna of PSII at room temperature and the modulation of its yield (called quenching of chlorophyll fluorescence) can be used as a measure of photosynthetic activity (Krause and Weis, 1991) (see paragraph 4).

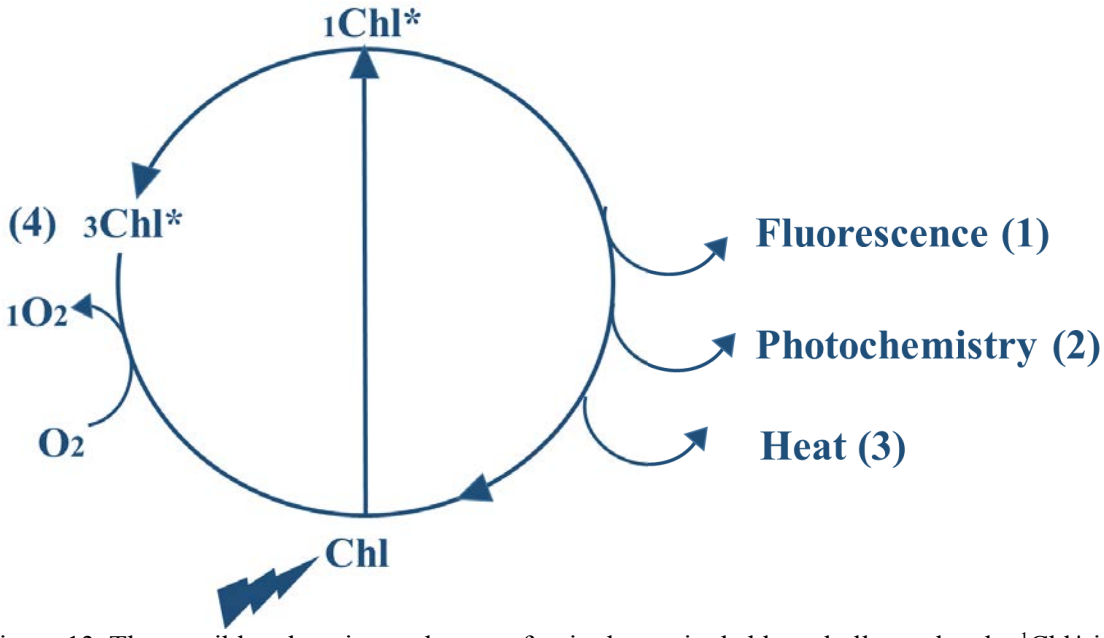

Figure 13. The possible relaxation pathways of a singlet excited chlorophyll *a* molecule. ^{1}Chl* is the singlet chlorophyll a molecule, ^{3}Chl* is the triplet chlorophyll a molecule, Chl is the chlorophyll in the ground energetic state.

Photosynthetic organisms developed various mechanisms to rapidly acclimate to metabolic and light fluctuations. On the basis of the responses time-scales, it is possible to distinguish: the short-term responses such as NPQ (Non Photochemical Quenching of chlorophyll fluorescence), that are active in a few seconds after the change in the light irradiations and de-excite the ^{1}Chl* decreasing the yields of photochemistry; and the long-term responses, which are active over time-scales of hours to seasons, and that normally require a modulation of gene expression and the protein content (Eberhard et al. 2008).

3.1 The various components of the NPQ

NPQ has various components: the fast energy-dependent (qE), the state transition (qT), the slow photoinhibitory (qI), and the zeaxanthin dependent quenching (qZ) (Dall'Osto 2005), each of which has peculiar relaxation kinetics (Krause & Weis 1991).

Diatoms exhibit a large capacity of NPQ depending on growth conditions, largely relaying on the qE component, with levels up to 5 times higher than are found in higher plants (Lavaud et al. 2002; Lavaud et al. 2003; Ruban et al. 2004). Therefore, in the next paragraphs, I provide a synthetic description of the qT and the qI processes, while describing in more details the qE components.

3.1.1 The state transition component, qT

The main role of state transition is to balance the absorbtion capacity of the two photosystems in low light (Finazzi 2005) or in the first seconds of exposure to high light intensity (Finazzi & Minagawa 2015). In this process, that is reversible and light quality dependent, LHCII proteins move from PSII to PSI in order to lessen the excitation pressure on PSII or viceversa.

In plants and green algae, PSII is mostly localized in the grana stacks of the chloroplast and PSI is found in the unstacked membranes of the stroma. Phosphorylation of LHCII by a membrane-bound kinase leads to the migration of part of the LHCII away from the the grana (Finazzi 2005). The LHCII kinase is activated by the reduction of the plastoquinone (PQ) pool, and is de-activated when the excitation pressure on PSII decreases and PQ becomes oxidized. The dephosphorylation of LHCII on PSI marks the return of LHCII to Photosystem II.

In diatoms there are no evidence of state transitions presence (Owens 1986). In addition, the diatom thylakoids do not form grana stacks and PSI and PSII are not segregated (Pyszniak & Gibbs 1992). However, results from *Arabidopsis thaliana stn7,* which is blocked in state transitions, showed no change in the qT component (Bellafiore et al. 2005), thus challenging the interpretation that this NPQ component is due to state transitions. qT would be rather due to the accumulation of zeaxanthin (Dall'Osto 2005) and should be called qZ (Nilkens et al. 2010).

3.1.2 The zeaxanthin dependent component, qZ

This photoprotective state of the photocomplexes dependent on zeaxanthin concentration and independent of the proton gradient, in nature,has been found to be activeactive for months in open fields even with higher temperatures(Demmig-Adams & Adams 2006; Demmig-Adams et al. 2012). Therefore, qZ seems to have a big impact on biomass yields in evergreen plants during the winter or water stress, or low light-grown plants exposed to excess light.

3.1.3 The slow photoinhibitory component, qI

A slow relaxing quenching mechanism is known as the photoinhibitory component qI. qI is commonly associated with the damage of the D1 protein that leads to photoinhibition and lower the

photosynthetic capacity. In the eukaryote kingdom the D1, D2, CP43 and CP47 proteins of the PSII are targets of ROS (Aro et al. 1993). The effect of the photoxidative damage is a loss of function of these proteins, in particular the D1, that are inactivated and degradated by action by the proteases located in the chloroplast. In this occasion, the entire PSII complex is deplaced from the grana stacks and repaired in the stroma lamella, to finally return to the grana margins when the newly encoded proteins are inserted in the RC (Aro et al. 1993). In diatoms, where grana are not present, the information on the localization of the repair site is missing. The high rate of these proteins turn-over might explain the presence of these genes in the chloroplast.

3.1.4 The energy dependent component, qE

qE is the fastest quenching mechanism and works by dissipating the excess absorbed light energy as heat. There are three essential factors for the activation of qE: 1) a high pH gradient across the thylakoid membrane, 2) the de-epoxidized xanthophylls synthesized by the xanthophyll cycle enzyme, and 3) some members of the light-harvesting complex (LHC) protein superfamily involved in photoprotection (Figure 14).

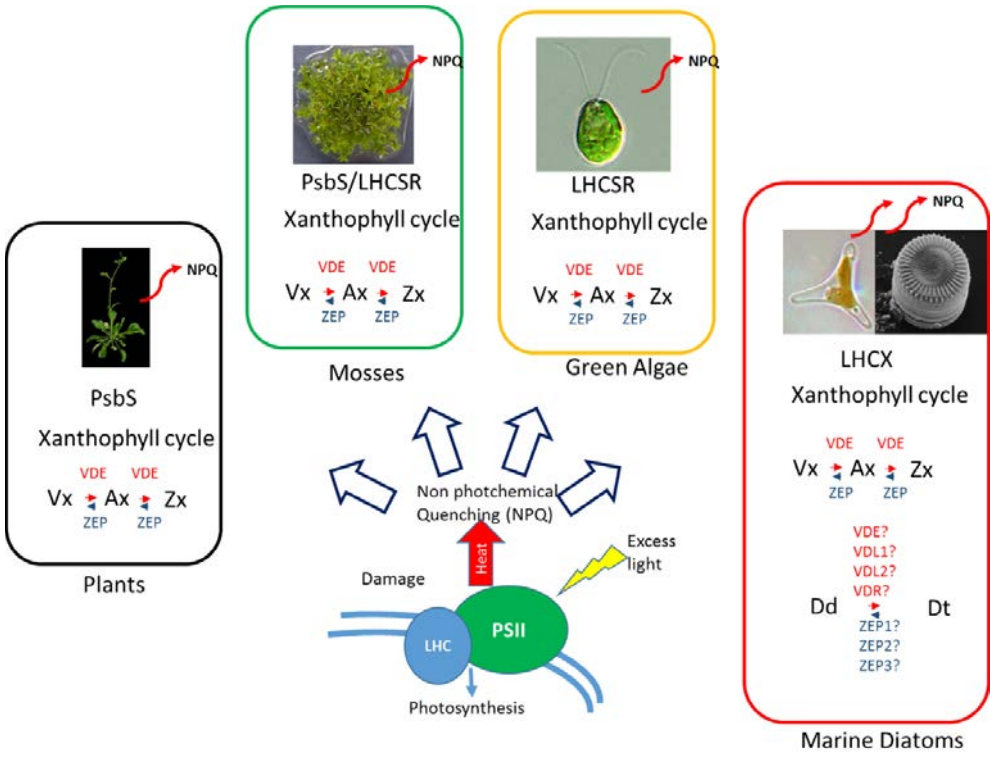

Figure 14. Scheme representing the molecular regulators of responses to excessive light of plants (*Arabidopsis thaliana*), mosses (*Physcomitrella patens*), green algae (*Chlamydomonas reinhardtii*), and marine diatoms [*Phaeodactylum tricornutum* and *Thalassiosira pseudonana*]. Adapted from (Depauw et al. 2012).

3.1.4.1 The proton gradient

Excessive light absorbed occurs with a decrease in the pH in the thylakoid lumen because the light driven proton translocation across the thylakoid membrane exceeds the dissipation rate of proton gradient by the ATPase. There are physiological evidences and functional studies on mutants that demonstrate that qE is regulated by the proton gradient. When the gradient is caused to collapse with the uncoupler dicyclohexylcarbodiimide (DCCD) (Jahns & Heyde 1999) qE is unable to build up and mutants that are defective in generating the proton gradient show a lower qE than the wild type (Munekage et al. 2001; Okegawa et al. 2007).

The roles of the proton gradient in qE are two fold. Firstly, it activates the xanthophyll cycle (paragraph 3.1.4.2). Second, antenna protonated by the acidic conditions of the lumen, undergo reorganization in the structure that passes from a light harvesting to a dissipative state.

In diatoms, although the low lumen pH is needed to activate the enzymes of the xanthophyll cycle, the continual presence of the proton gradient itself is not needed for quenching (Goss et al. 1995).

It has also been observed that the uncoupling of the proton gradient led to the concomitant decrease of NPQ capacity and Dt content, but the decrease of the quenching was not linearly correlated with the decrease of Dt (Lavaud & Kroth 2006). Consequently, the role of the proton gradient might go beyond the activation of the xanthophyll cycle, suggesting that the proton gradient in diatoms might also induce LHC conformational change in a dissipative state, through protonation, as it happens in higher plants.

3.1.4.2 The xanthophyll cycle

The intimate relationship between NPQ and the xanthophyll cycle (XC) has been known for decades (Demmig-Adams 1990). In plants and green algae, the xanthophyll cycle refers to the light-dependent reversible interconversion of the xanthophyll violaxanthin into its de-epoxidized forms: antheraxanthin and zeaxanthin (VAZ cycle) (Latowski et al. 2004) (Figure 15).

In the VAZ cycle the de-epoxidation reactions are catalyzed by violaxanthin deepoxidase (VDE) (Yamamoto & Kamite 1972) and the reducing power for the reaction is provided by ascorbate (Hager 1969). During normal light conditions, the inactive and monomeric VDE enzyme is in the thylakoid lumen (Hager & Holocher 1994). However, when the pH decreases below a threshold level (5.2, (Hager 1969)), the enzyme is activated, it becomes a dimer (Arnoux et al. 2009) and associates with the thylakoid membrane (Hager & Holocher 1994) where its substrate violaxanthin is located (Morosinotto et al. 2002). There, it can convert violaxanthin into antheraxathin and after in zeaxanthin (Rockholm & Yamamoto 1996). The return to light-limiting conditions for photosynthesis or darkness induces the conversion of zeaxanthin to violaxanthin by the stromal enzyme zeaxanthin epoxidase (ZEP) (Bugos et al. 1998; Jahns et al. 2009) which is active at neutral or basic pH values (Hager 1975). ZEP requires NADPH and O_2 as cosubstrates to reintroduce the epoxy group into zeaxanthin and antheraxanthin (Büch et al. 1995).

In diatoms, beside the violaxanthin-antheraxanthin-zeaxanthin cycle, an additional reversible xanthophyll cycle is also present, converting diadinoxanthin (Dd) to diatoxanthin (Dt) under high-light, in a single de-epoxidation step ((Lohr & Wilhelm 2001; Lohr & Wilhelm 1999) Fig 1.16). The model diatom *P. tricornutum* presents seven genes putatively involved in the two xanthophyll cycles, three for the epoxidase reactions (the zeaxanthin epoxidases *zep1, 2* and *3*) to convert zeaxanthin to violaxanthin or Dt to Dd, and four for the opposite reactions (violaxanthin de-epoxidase, *VDE*-like *VDL 1* and *2,* and the *VDE*-related *VDR*). The expansion of these gene families is in sharp contrast with what happens in plants, where only one *VDE* and one *ZEP* are present. Nowadays the precise role of these seven diatom genes in the xanthophyll cycle is not known.

Because of the enzyme characteristics, the epoxidation reaction in diatoms is strongly inactivated when the proton gradient is established, favouring a very high rate of production of Dt (Goss et al. 2006). Indeed, in algae that contain the diadino- and diatoxanthin cycle, even if the ΔpH is abolished, NPQ is positively correlated with Dt accumulation (Goss et al. 2006). This slow relaxation of the NPQ is due either to a strong inactivation and a slow activity of the enzyme involved in the cycle of the xanthophylls by the proton gradient. The enzyme catalyzing the de-epoxidation reaction in diatoms has a lower Km value for ascorbate compared to VDE (Grouneva et al. 2006),

and also the pH dependence of this putative enzyme is linked to the ascorbate concentrations suggesting that the rate of this reaction is finely regulated by multiple factors *in vivo*.

As in plants an efficient de-epoxidation reaction depends on the presence of a lipid in the thylakoid membrane, the MGDG (Goss et al. 2005; Goss et al. 2007). This lipid allows a solubilisation of the hydrophobic xanthophyll pigments and a better accessibility for the enzyme to the substrates. Interestingly, the concentration of MGDG needed in diatoms to obtain a complete solubilization of the xanthophyll pigments, is lower as compared to the green lineage (Goss et al. 2005) possibly because the pool size of the xanthophyll pigments is higher in diatoms (Lavaud et al. 2003; Lepetit et al. 2010).

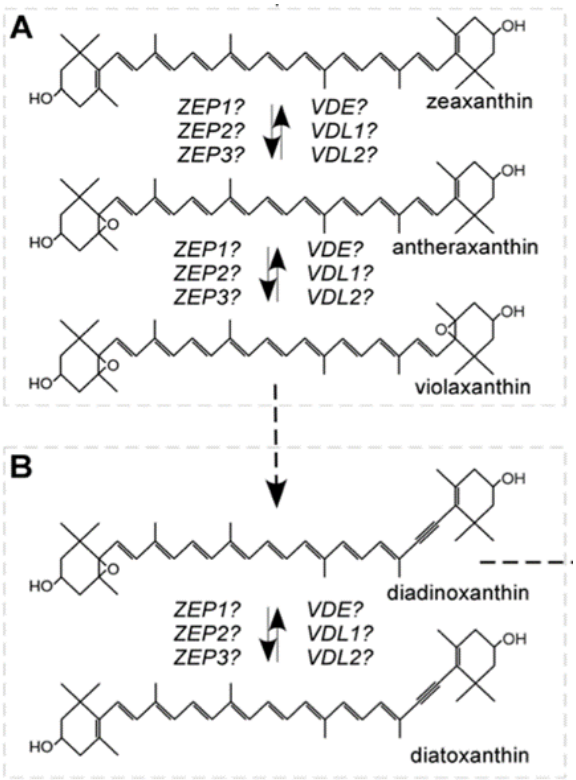

Figure 15: Scheme of the reactions of the two xanthophyll cycles present in diatoms. A: the violaxanthin-zeaxanthin cycle. B: the diadinoxanthin-diatoxanthin cycle. (Coesel et al. 2008 PloS one).

3.1.4.3 The light harvesting antenna involved in photoprotection

In different phototrophs, several LHC proteins have been found to be implicated in the qE regulation (Figure 14).

3.1.4.3.1 PsbS

Proteins involved in qE have been first discovered in the plant *A. thaliana*, by identifing mutants that were defective in qE, but had normal xanthophyll levels (Li et al. 2000; Peterson & Havir 2000). The characterization of one of these mutants, *npq4-1*, revealed that a PSII protein, PsbS, is essential for qE (Li et al. 2000). Structure analysis of PsbS revealed two luminal glutamate residues in the luminal loops that are required for its function and that are responsible for sensing the lumen pH (Li et al. 2002).

The current model of NPQ in plants considers that upon high light exposure, a decrease in lumen pH activates NPQ (Demmig et al. 1987) and induces the formation of two sites (quenching sites) where the excessive energy absorbed is dissipated. The first one, Q1, is located in detached LHCII trimeric antenna (Holzwarth et al. 2009) and it is activated after the protonation of proteins in the antenna - one of which is PsbS (Li et al. 2004; Fan et al. 2015). The protonation of the acidic residues leads to a conformational change and activation of PsbS which dimerizes (Fan et al. 2015) and this conformational change cascades to other LHCII proteins allowing the detachment of LHCII from the PSII supercomplexes and resulting in quenching (Holzwarth et al. 2009). However, a high NPQ has also been observed in absence of PsbS. This event was observed when the pH in the lumen attained very low pH values (Johnson & Ruban 2011). This suggests that PsbS role might be to increase the pH sensitivity of antenna lumenal residues and that the reorganization of the LHC antenna is still possible without PsbS presence but the reorganization process is very slow. This site of quenching requires PsbS and is independent of zeaxanthin (Holzwarth et al. 2009).

The second proposed quenching is called Q2 and it is a slower zeaxanthin-dependent mechanism (Demmig et al. 1987; Niyogi et al. 1998; Holzwarth et al. 2009) located within the monomeric antenna attached to the reaction centers (Ahn et al. 2008; Avenson et al. 2008). This quenching is independent of PsbS presence (Holzwarth et al. 2009).

3.1.4.3.2 LHCSR3

The antenna proteins responsible for photoprotection in *C. reinhardtii* are called LHCSR, (Light Harvesting Complex Stress-Related). One protein, called LHCSR1, is constitutively present although at low light levels but can induce only little qE (Peers et al. 2009; Mou et al. 2012; Truong

2011), whereas another one LHCSR3 strongly accumulates in excess light and is responsible for most of the qE activity in *C. reinhardtii* (Peers et al. 2009). LHCSR3 is encoded by two genes, *LHCSR3.1* and *LHCSR3.2* (Peers et al. 2009), whereas LHCSR1 is encoded by one gene *LHCSR1,* and their aminoacidic sequences are identical by 87% (Bonente et al. 2011).

Biochemical characterization of LHCSR showed some similarities but also some interesting differences with respect to PsbS (Bonente et al. 2011). As PsbS, LHCSR binds dicychlohexylcarbodiimide, (DCCD, a protein- modifying agent that covalently binds to acidic residues involved in reversible protonation events) and senses pH changes with three residues lumen exposed, as demonstrated in a recent work (Ballottari et al. 2015). However, differently from PsbS, LHCSR binds Chlorophyll *a*, Chlorophyll *b* and xanthophylls similar to LHC antenna complexes (Bonente et al. 2008). In addition, spectroscopic analysis showed that LHCSR3 in detergent solution has a very short fluorescence lifetime (<100 ps) compared to other members of the LHC family. This implies that LHCSR3 quenches Chlorophyll *a* fluorescence (Bonente et al. 2011). Interestingly, LHCSR3 binds zeaxanthin even though zeaxanthin has a minor effect on the NPQ in *C. reinhardtii* (Bonente et al. 2011). *C. reinhardtii* has also two *PSBS* genes, but the protein is not present in normal or in high light conditions (Peers et al. 2009; Bonente et al. 2008) and have been detected only after UV-B treatment (Guillaume Allorent and Michel Goldschmidt-Clermont, personal communication).

Also for *C. reihardtii* a model for NPQ regulation has been suggested. The sites of quenching of the excessive energy in *C. reinhardtii* have been proposed to be located in the antenna of PSII (Elrad et al. 2002; Tokutsu & Minagawa 2013) and in the core (Pocock et al. 2007). After high light exposure, the expression of LHCSR3 is induced. The protein then reversibly associates with the PSII-LHCII supercomplex forming the PSII-LHCII-LHCSR3 supercomplex. It is only after the protonation of LHCSR3, induced by low lumenal pH through protonatable DCCD-binding sites, that the supercomplex can switch from a light harvesting state to a photoprotective state and dissipate the excessive energy (Tokutsu & Minagawa 2013). Thus, LHCSR has the properties of both an energy quencher, a function catalysed by LHCB proteins in vascular plants (Ahn et al. 2008; Avenson et al. 2008; Ruban et al. 2007), and a sensor for lumenal pH, which is a function covered by PsbS in plants (Li et al. 2004; Betterle et al. 2009; Bonente et al. 2008).

Interstingly, both *PsbS* and *LHCSR* genes are present in the genome of *Physcomitrella patens,* a bryophyte that diverged from vascular plants around 400 million years ago, early after land colonization (Rensing et al. 2008). NPQ in *P. patens* depends on both PsbS and LHCSR (Alboresi et al. 2010; Gerotto et al. 2011) which are expressed toghether, and presents an active xanthophyll cycle (Alboresi et al. 2008). This was confirmed by the generation of specific *P. patens* knock out (KO) mutants for *LHCSR1*, *LHCSR2* and *PsbS* genes (Alboresi et al. 2010), showing that these proteins are active in promoting NPQ and contribute to photoprotection under excess light conditions. However LHCSR1 is responsible for most NPQ activity and it is constitutively expressed (Alboresi et al. 2010).

Further studies demonstrated that high light acclimated *P. patens* plants show an increase of NPQ which is positively correlated to overexpression of both LHCSR1 and PsbS proteins. On the other hand, *P. patens* acclimated to low temperature increase the expression of *PsbS* and *LHCSR2* (Gerotto et al. 2011). These data suggest that the two functional *LHCSR* genes are differentially regulated by environmental factors (Gerotto et al. 2011).

A recent study allowed estimating the dependence of *P. patens* NPQ reactions on zeaxanthin content. By characterizing the phenotype of multiple mutants, it was shown that zeaxanthin has an important role on LHCSR-dependent NPQ (Pinnola et al. 2013), in contrast to *C. reinhardtii* (Bonente et al. 2011). On the other hand, the PSBS-dependent NPQ component is less affected by the lack of zeaxanthin (Pinnola et al. 2013). This observation possibly suggests that zeaxanthin acquired a major role in photoprotecting terrestirial photosynthetic organisms as compared to the aquatic one.

3.1.4.3.3 LHCX

For a long time, it was believed that the extraordinarily NPQ capacity of diatoms was due to the presence of a peculiar xanthophyll cycle (see paragraph 3.1.3.2). However, recent studies clearly demonstrated the existence of a LHCSR-dependent NPQ mechanisms in these algae as well (Zhu & Green 2010; Bailleul et al. 2010; Ghazaryan et al. 2016).

In the genome of the model diatom *P. tricornutum* four LHCSR-like proteins, called LHCX in diatoms, have been found. Several members (five) have been identified also in *T. pseudonana*

genome (Armbrust & et al. 2004), suggesting that the expansion of this gene family is a common trait in diatoms. Initial information on their involvement in the NPQ has been provided by the characterization of the LHCX1 isoform (Bailleul et al. 2010). This gene is highly expressed in low light acclimated cells and it is not further induced by high light stress (Bailleul et al. 2010; Lepetit et al. 2013; Nymark et al. 2013). A constitutive expression for some LHCX genes has also been observed in other species, such as in *T. pseudonana* (Zhu & Green 2010; Grouneva et al. 2011; Wu et al. 2012), in *C. cryptica* (Westermann & Rhiel 2005) and in *C. meneghiniana* (Beer et al. 2006).

Functional characterization in *P. tricornutum* indicated that LHCX1 is required for efficient light responses (Bailleul et al. 2010). In particular, knock down lines grown in low light conditions showed a reduced NPQ content, but an unchanged de-epoxidation state (DES). Therefore, it has been proposed that this constitutively expressed protein provides diatoms with a machinery capable of anticipating sudden changes in the underwater light field, giving a selective growth advantage (Figure 16).

Moreover, the *LHCX1* gene has been targeted during adaptive evolution, as revealed by a comparative analysis of several *P. tricornutum* ecotypes isolated from different latitudes, displaying different *LHCX1* expression and NPQ levels (Bailleul et al. 2010).

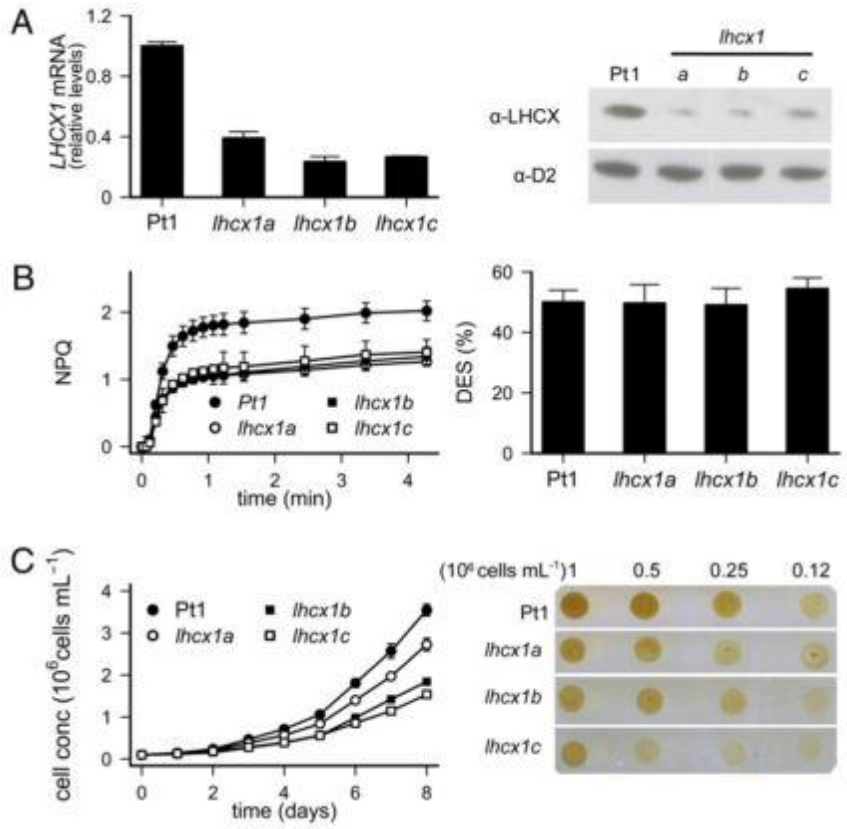

Figure 16 Characterisation of *P. tricornutum* NPQ regulation by LHCX1 in non stressfull light conditions. (A) Analyses of LHCX1 mRNA by qRT-PCR (Left) and protein levels (Right), and (B) NPQ (Left) and DES (Right) values, in wild-type (Pt1) and three RNAi silenced lines (*lhcx1a, b, c*), sampled 8 h after the onset of illumination. Relative transcript levels were determined using RPS as a reference gene and values normalized to gene expression levels of the wild type (Pt1). (C) Growth curve of the Pt1 and *lhcx1* cells (Left) under 12 h:12 h light:dark regime at 30 µmol photons $m^{-2} \cdot s^{-1}$ (SE refers to duplicate measurements from three biological samples), and growth tests on cells spotted on solid media (Right). A total of 5 µL of different cell dilutions (1, 0.5, 0.25, and $0.12 \cdot 10^6 \cdot$mL cells) were spotted and pictures were taken after 5 days. Image source: (Bailleul et al. 2010).

LHCX are three helix transmembrane proteins and apart the high similarity with LHC proteins, especially in the helix regions (Gundermann & Büchel 2012) their pigmentation is still under debate. It has been proposed that at least in centric diatoms they might be pigmented because LHCX proteins content correlate with diatoxanthin content (Beer et al. 2006). However, the knock down mutant for LHCX in *P. tricornutum* (Bailleul et al. 2010) and *C. meneghiniana* (Ghazaryan et al. 2016) do not show an altered pigment content and a direct proof for pigment binding of any LHCX is still missing.

3.2 New insights into diatom NPQ capacity and unsolved questions

The molecular mechanisms controlling NPQ in diatoms are not as well advanced as in higher plants and new studies are just emerging.

In centric diatoms, a positive correlation between the content of LHCX in FCPa and Dt content has been found. In addition, the Dt content is inversely correlated with the fluorescence yield in the FCP by in vitro analysis, indicating a higher quenching capacity. On the other hand, in FCPb, the FCP supercomplex without LHCX, the fluorescence yield was independent on the amount of Dt bound (Gundermann & Büchel 2008). However, using a knock-down approache on *C. meneghiniana*, it has been shown that pigment interactions inside FCPa were not influenced by the presence or absence of LHCX. LHCX modulated content rather alters pigment-pigment interactions inside the FCPa aggregates (Ghazaryan et al. 2016). In this latter case, the role of these proteins in diatoms might be to induce a structural change in the FCP antenna, having a similar role to the plant PSBS (Goss & Lepetit 2014).

Some recent time-resolved optical spectroscopy studies proposed that NPQ in diatoms has two quenching sites (Figure 17): Q1 and Q2 (Miloslavina et al. 2009; Chukhutsina et al. 2014). Q1 is quickly induced after excess light exposure and rapidly relaxes in darkness. Since it reminds of the LHCII aggregation quenching proposed by Ruban and Horton (Horton et al. 1991) in higher plants and the Q1 site quenching by Holzwarth et al. in 2009 (Holzwarth et al. 2009), it has been attributed to some antenna aggregation induced by the pH gradient formation. Q2 quenching site is located in PSII core and it is induced after the pH gradient formation, it remains active also in darkness and relaxes only in presence of dim light, following the dynamic of the xanthophyll cycle pigments. This model also suggests that FCPb remain unquenched during both Q1 and Q2 (Miloslavina et al. 2009).

In summary, after the high light, some FCPa in PSII core become quenched and then detach from the PS. Then the formation of Dt leads to the formation of the new quenching Q2 in the PSII cores. After the exposure to darkness the quenching in the antenna disappears, whereas the quenching in the PSII RC persists and relaxes only with some light.

Recent studies using ultracentrifugation of sucrose gradients allowed to separate the diatom photosynthetic complexes (Buchel 2003; Beer et al. 2006; Lepetit et al. 2010). The photosynthetic extracts so obtained can be analysed to identify the molecular components and their quenching capacities. In the centric diatom *C. meneghiniana*, LHCX proteins have been detected by western blot associated to FCPa, which are a sub-population of FCP obtained after the centrifugation process (Beer et al. 2006). After ultracentrifugation sucrose gradient and mass spectrometry analysis, LHCX1, LHCX2 and LHCX4 were found in FCPa of the centric diatom *T. pseudonana,* whereas in the pennate diatom *P. tricornutum* LHCX1 and LHCX2 were found in PSI, in the free protein band (Grouneva et al. 2011) and in FCP with the same technique (Lepetit et al. 2010).

However, the role of the extended LHCX family in the formation of these sites and the information of their localization in the photosynthetic complexes, like PSII and PSI, is still missing. In addition, the role of LHCX1 in NPQ regulation has been studied only in the non-stressfull light condition in *P. tricornutum* and not in sustained high light, when its functional ortholog LHCSR3 is induced. These are some of the topics that I studied during my thesis that are summarized in the section "Aim of the thesis".

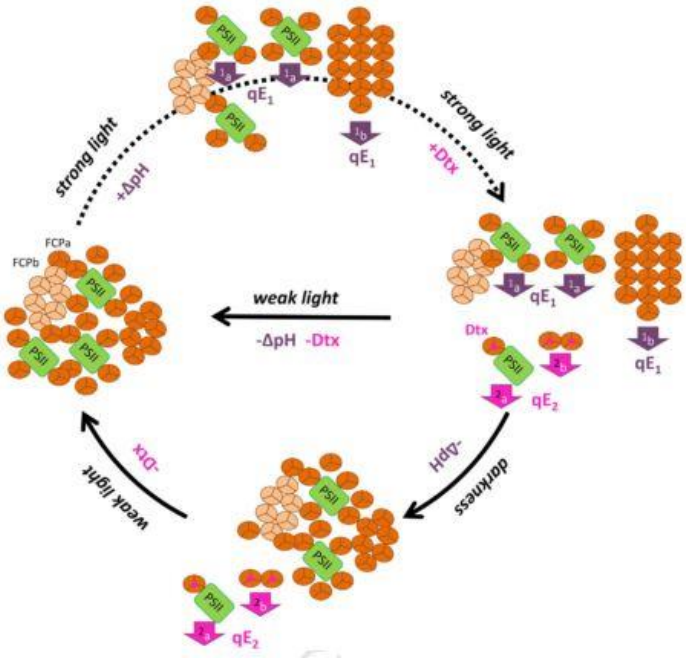

Figure 17 Model of NPQ in diatoms. In saturating light conditions two quenching mechanisms independent of diatoxanthin (Dtx) are present. The first (upper part of the figure) (qE1) represents the quenching of the whole PSII complex (1a), the second quenching is in FCPa antenna that aggregate due to ΔpH formation (1b). With the rapid accumulation of a Dt pool (middle right), Dt-related quenching appears (qE2). It is manifested by quenching of PSII that almost lacks FCPs (2a). Very probably the quenching site is located at an FCPa antenna attached to the core, although direct

quenching of PSII cores cannot be excluded. This effect is accompanied with Dt-dependent quenching of FCPa that has been disconnected from PSII complexes (2b). All qE2 quenching is persistent in the darkness (lower part of the figure), but disappears after weak light treatment.

4. The measure of the kinetics of chlorophyll fluorescence at room temperature

Because in this work I used different approaches to measure photosynthetic activity based on chlorophyll fluorescence, here I briefly summarize the principle of these techniques. Chl fluorescence analysis has become an indispensable method for photosynthetic studies because it is a non-intrusive tool and it can give useful and rapid information on the photosynthetic activity (Krause and Weis, 1991).

Chlorophyll fluorescence emission at room temperature represents the light energy that photosystem II has no capacity to convert into chemical energy and it is reemitted, slightly red-shifted. The kinetics of fluorescence yields can be monitored using fluorometers, which use the pulse saturation method (Figure 18).

The rapid decrease of fluorescence (quenching) due to the use of light energy for photochemistry is the photochemical quenching (qP). However, as soon as photosynthetic organisms are exposed to saturating light conditions a slower decrease in fluorescence yield (from seconds to minutes) can generally be observed. This quenching that it is not due to photochemistry corresponds to the non photochemical quenching of chlorophyll fluorescence (NPQ), and allows the dissipation of excess absorbed light as heat (Muller et al. 2001).

The photoprotection through heat dissipation can be determined by measuring the chlorophyll fluorescence during brief ($\leq$ 1s) pulses of light that saturates photochemistry so that there is no more quenching due to qP.

Different phases can be distinguished during the measurement of the fluorescence yield. In a first phase, samples are dark or low light adapted at least 15 min before measurement to oxidate the electron transporters and open all RC to photochemistry. The parameter called minimal fluorescence level (F_0) is a proxy for all the open RC and it is measured during darkness using a low

intensity modulated light (0.1 μmol photons $m^{-2}s^{-1}$) which ensures that QA remains maximally oxidized.

A saturating pulse of light is then applied, simultaneously reducing all PSII reaction centers and allowing the measurement of the maximal fluorescence (Fm). The intensity of the saturation pulse is such that it reduces and closes to further reactions all QA sites, thereby removing the photochemical quenching (qP) component. Comparison of Fm with the minimal fluorescence measured in darkness (Fo) yields the range across which fluorescence can vary (thus called variable fluorescence, Fv, which is equal to Fm − Fo) and it is used to calculate the efficiency (Fv/Fm) of PS II to absorb light and use it for photochemistry. Given the fact that cells were acclimated to obtain all the RC to be open, NPQ is expected to be zero during Fm measurement.

After a short period of dark adaptation to allow re-oxidation of electron transporters, actinic light is switched on. Actinic light is the light absorbed by the photosynthetic apparatus to drive electron transport. To analyze NPQ, actinic light intensity is adjusted to saturate photochemical capacity of the sample, to achieve also the maximal NPQ induction.

During the application of actinic light, at intervals, further brief (<1s) saturating pulses are applied. Since there is no quenching anymore due to qP the quenching due solely to NPQ can be determined (Baker 2008). These latter allow to measure the maximal fluorescence during exposure to actinic light (Fm').

The overall NPQ of Chl fluorescence can be determined as

$$NPQ = (Fm - Fm')/Fm' \qquad \text{(Bilger and Bjorgman 1990)} \qquad \text{(Eq. 1)}$$

Since any difference between Fm and Fm' has to be interpreted as due to non photochemical quenching processes, the degree to which Fm' is lower than Fm reflects the magnitude of the NPQ process in act in the photosynthetic organism.

The period of actinic light is followed by a period of dark recovery, during which the relaxation kinetics of the processes previously induced by light exposure can be analyzed. Also in

this phase repetitive saturating pulses are applied. In the Figure 18 is shown a chlorophyll fluorescence induction curve of *P. tricornutum*.

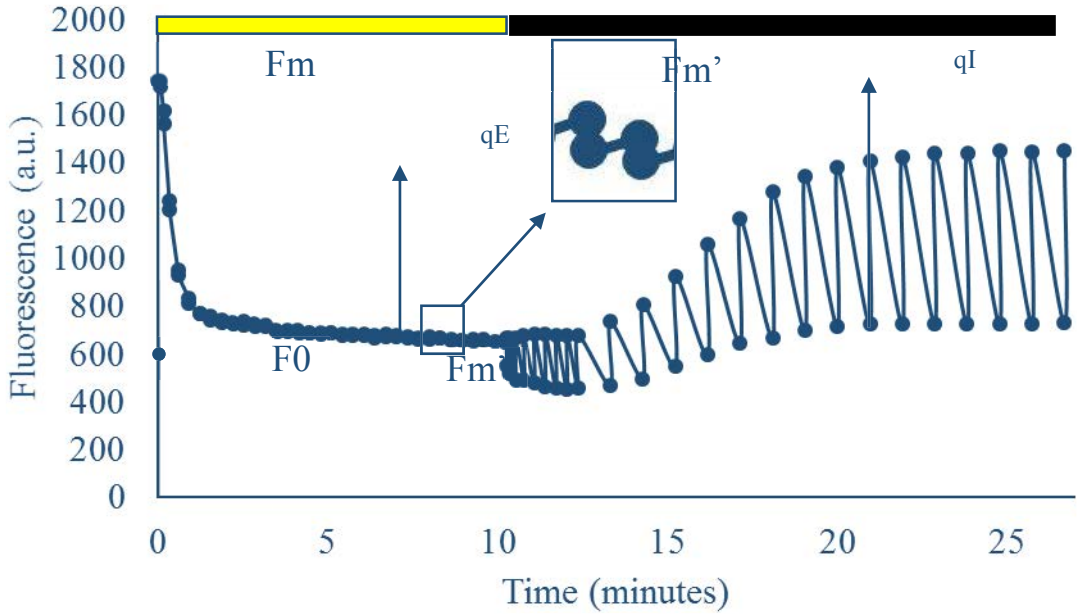

Figure 18: Chlorophyll fluorescence measurements in *P. tricornutum*. Cells were grown in non stressfull low light conditions. F0: minimal fluorescence level; Fm: maximal fluorescence level in the fully relaxed state following an absence of light; Fm': maximal fluorescence level during the exposure to actinic light. In the onset is visible the Fm'.

5. Time-resolved emission spectra measurements using the streak-camera set up

For the study of the quenching sites locations, ultrafast spectroscopic methods are necessary because femto to pico seconds is the time range in which the photochemical reactions and competing reactions take place. Therefore, time-resolved optical spectroscopy, as applied in this thesis work, enables the observation of ultrafast dynamic events in photosynthetic systems *in vivo* on a picosecond time scale, that are typical of energy transfer and photoprotection processes. To investigate time-resolved fluorescence dynamics a synchroscan streak-camera setup was used.

The streak-camera system, used in this thesis in collaboration with Dr. Olga Chukhutsina and Prof. Van Amerongen, operates by dispersing photoelectrons across an imaging screen in wavelength and time, allowing to monitor the evolution of whole spectra on a picosecond to nanosecond time scale instead of measuring fluorescence decay curves at individual wavelengths

(Schiller 1984). This method is extremely valuable when studying photosynthetic organisms in vivo, which usually contain fluorophores emitting at different wavelengths. Emitted fluorescence photons induced by the laser excitation are focused by an objective on the input slit of a spectrograph, where they are wavelength dispersed in the horizontal direction by a grating. Then the photons strike the photocathode, where they lead to the emission of electrons. The photo-electrons pass between a pair of sweep electrodes; a high sweeping voltage is applied to the electrodes and the sweep frequency is synchronized to the frequency of excitation light pulses. During the high-speed sweep, the electrons that arrive at slightly different times, are deflected at different angles in the vertical direction, and enter in the micro-channel plate (MCP) at different positions. As the photo-electrons strike the MCP, they are multiplied several thousands of times, after which they reach a phosphor screen, where they are converted again into light. The photoelectrons generated at different times experience different deflection fields and therefore hit the phosphor screen at different vertical positions. The light of the phosphor screen is focused on a CCD detector and these data are stored for further processing (Figure 19).

In a time-resolved fluorescence experiment, the fluorescence kinetics reflect the decay of the excited-sate population of contributing fluorophores as well as the excitation energy transfer between them. Through exponential functions and global analysis of the decay traces measured at different detection wavelengths it is possible to obtained the decay associated spectra (DAS).

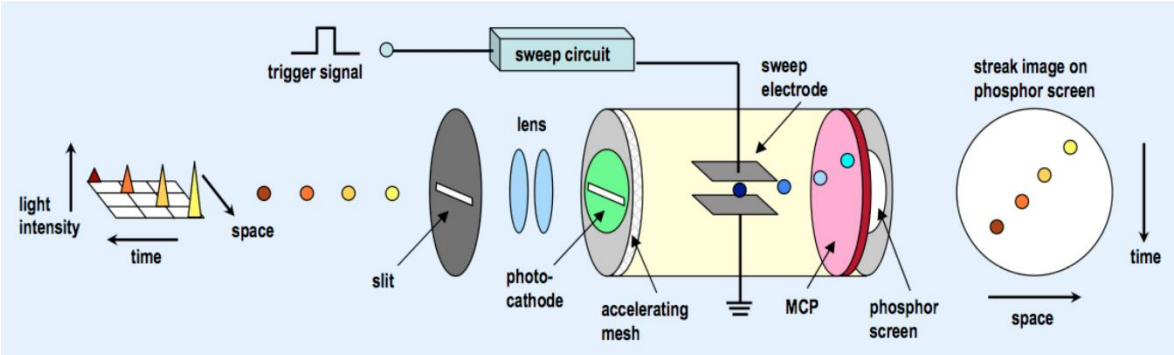

Figure 19 Operating principle of a streak camera set up, consisting of a photocatode, accelerating mesh, fast sweeping electrodes and imaging part.

Aim of this thesis

In diatoms, the NPQ depends on a light-driven proton gradient, a xanthophyll cycle and a light-stress-associated member of the antenna gene family, the LHCX1 protein. However, the mechanistic aspects of diatom NPQ as well as the role of the multiple LHCX family members are not completely understood.

When I started my PhD, very limited information was available on the expression and possible function of the different LHCXs. It was still not clear if there is a functional redundancy among the LHCX proteins or if the different LHCXs play specific functions in the regulation of chloroplast physiology under particular environmental conditions. In addition, the sites of dissipation of the excessive light absorbed (quenching sites) in short and high light acclimation were not characterized and the LHCX role in the formation of these quenching sites, as well as their localization, were not known. Therefore, the overall aim of this thesis was to explore the activity of the different LHCX family members in the regulation of *P. tricornutum* photoprotection through integrated approaches of genetics, molecular biology, biochemistry, and biophysics of photosynthesis.

Here I present an overview of the research questions that I addressed with my work and of the results that I obtained and that are described in the different chapters of this thesis:

Is the LHCX family expansion a common and adaptive trait in diatoms? Do the multiple LHCX proteins contribute to the impressive capacity of diatoms to grow and successfully perform in different environmental conditions?

LHCX belong to an expanded gene family and they possibly implement the photoprotection capacity of diatoms by diversifying their role in response to different stimuli and stresses. To test this hypothesis, in the second chapter of this thesis I analyzed the regulation of the 4 *LHCX* genes in *P. tricornutum* cells grown under different light conditions (absence, low light, high light) and nutrient limiting regimes (iron, nitrate), which are known to alter the growth and the photosynthetic ability of the organism. I correlated the expression of the LHCXs with specific photophysiological responses, in order to distinguish the contribution of the different LHCXs.

Subsequently, I analyzed the NPQ responses in *P. tricornutum* wild-type and various LHCX overexpressing transgenic lines to test the effect of the deregulated expression on the photoprotective capacity. These analyses, published in Journal of Experimental Botany ('Multiple stress signaling pathways regulate the gene expression of the LHCX family', Taddei et al., 2016) provided novel information on the function of the extended LHCX family in *P. tricornutum* and on the complex regulatory pathways controlling their expression under different environments.

Due to the lack of information about the energy dissipation sites and the localization of the LHCX proteins in the chloroplast, in the Chapter III, I addressed the following questions:

Which are the quenching sites in short and long-term high light acclimation? Are the quenching sites the same in the different conditions?

In which photosynthetic complexes are localized the LHCX proteins? Do they have different roles in the light energy quenching?

If the quenching sites are impaired, which is the effect on the chloroplast and the cell physiology?

To investigate the role and mode of action of the LHCX proteins in *P. tricornutum* light acclimation responses, I performed a comparative analysis of the wild-type and a knock-down line with a reduced amount of the protein LHCX1, in cells acclimated to low and high light regimes.

To characterize the photoprotective responses in these two conditions, I analyzed the kinetics of chlorophyll fluorescence yields at room temperature, whereas to trace the sites of photoprotection the cells were analyzed with an ultrafast spectroscopy method.

In order to correlate the observed quenching sites with the LHCX proteins activity, I isolated the different photosynthetic complexes and I localized the different LHCX proteins in each chloroplast fraction.

Through this integrative analysis, I identified different energy dissipation sites that I correlated with the presence of specific isoforms, to finally propose a model of dynamic regulation of NPQ capacity in short-terms and sustained high light stress. The results are described in Chapter III and are reported as article in preparation with the title" Role of LHCX proteins in short- and long-term high light acclimation in the marine diatoms *Phaeodactylum tricornutum*", by Taddei et al.

While doing this, I have also tried to get additional information on the specific function of each LHCX protein by using reverse genetic approaches in *P. tricornutum,* to address the questions:

Are the different members of the LHCX family all involved in the NPQ process? Do they act with the LHCX1 NPQ regulator or do they play specific functions in the regulation of chloroplast activity?

During my PhD I put considerable efforts to produce different transgenic lines with a deregulated amount of the LHCX proteins either by gene over-expression or gene silencing. More than 130 transgenic lines were generated.

Initially, I set-up the conditions for large-scale screenings of the mutants based on the photosynthetic properties, and subsequently performed a detailed molecular characterization of the knock-down lines showing the strongest phenotype. Even if not conclusive, these analyses provided novel information on the possible function of the LHCX2 and LHCX4 proteins, but also highlighted the limits of the reverse genetic approach for the characterization of the multiple *LHCX* gene family.

In the chapter V, I report general conclusions that can be drawn from this thesis work.

CHAPTER II

Multisignal control of expression of the LHCX protein family in the marine diatom *Phaeodactylum tricornutum*

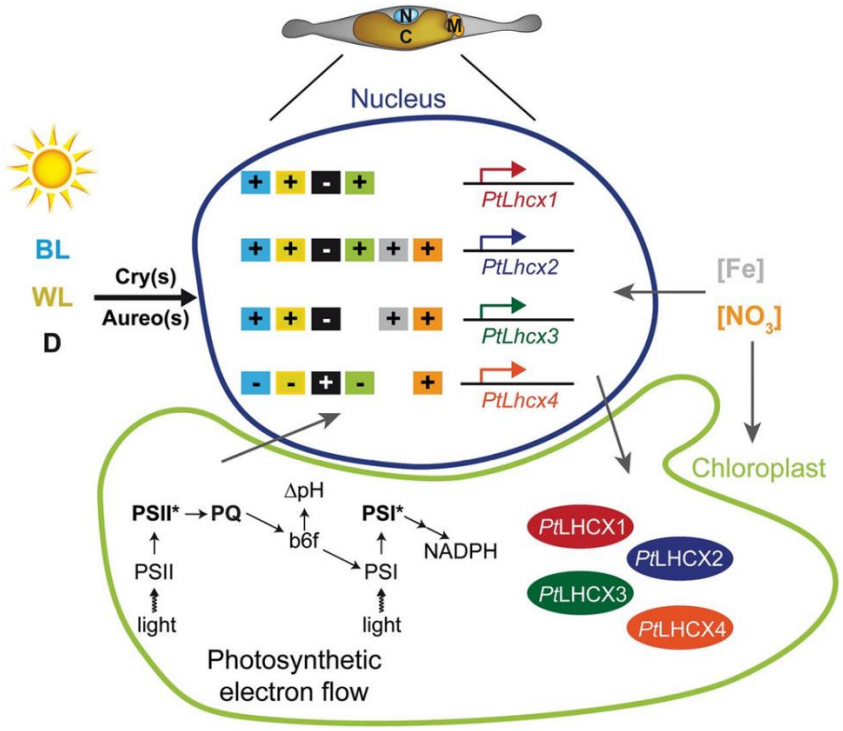

.

Multisignal control of expression of the LHCX protein family in the marine diatom *Phaeodactylum tricornutum*

1. Abstract

Diatoms dominate phytoplanktonic communities in contemporary oceans (Field et al. 1998), conserving an active photosynthetic activity in a wide range of environments, which is thought to be a key element of their ecological success. Still, the mechanisms used by diatoms to acclimate to light and nutrient changes are still largely obscure.

In the last years, studies of the light acclimation responses in the diatom *P. tricornutum* showed that LHCX1, a member of the light-harvesting protein family, contributes to dissipate as heat the light energy absorbed in excess through a process called Non Photochemical Quenching of chlorophyll fluorescence (NPQ).

Here, I have tried to get novel information on the possible function of the other members of the LHCX family, which is still mysterious. The starting point of this analysis was the observation that the LHCX proteins are particularly abundant in the genomes of different diatom species living in diverse ecological niches (we found up to 17 members in the polar species *Fragilariopsis cylindrus*!). This is an impressive gene family expansion compared to the limited number of the PsbS or LHCSR proteins found in the green lineage.

The assumption behind this work was that diatoms would use the diverse LHCXs to adjust their photoprotective capacity to changes with a final benefit their fitness. By duplicating these proteins and likely diversifying their function, diatoms could survive to sudden changes in light intensity or prolonged deprivations in nutrient and light.

To test this hypothesis, I conducted a comparative analysis of the expression of the LHCX family members in different light and nutrient conditions, known to affect the photobiology and the growth of diatoms. Then I correlated the presence of the LHCXs with specific photophysiological

responses to understand when the presence of each LHCX could be needed. At the same time I did this, I studied the photosynthetic and NPQ capacities in *P. tricornutum* wild type and several LHCX overexpressing mutants to assess the effect of the deregulated expression on the photoprotective process.

From the analysis performed in cells exposed to different light treatments, I concluded that three of the four *P. tricornutum* LHCX isoforms are expressed in the light, with the LHCX1 being constitutively expressed in both non stressful and stressful light conditions. The intensity of the light modulates the LHCX2 and LHCX3 isoforms which are induced with saturating light intenisities. Specifically, the LHCX3 is expressed transiently and the LHCX2 more steadily. *P. tricornutum* also possesses an isoform, the LHCX4 that is expressed only in light absence.

Differently from the high light stress, iron limitation mostly induces the LHCX2 isoform which correlates with an increased maximal NPQ capacity as compared to the replete condition. This suggests that LHCX2 could be the key regulator of the increased NPQ capacity observed in iron stress.

The nitrogen limitation induces the expression of the LHCX3 and LHCX4 mRNAs, but I observed a general increment in all the LHCX proteins. The LHCXs increase correlated with a higher maximal NPQ and a reduced photosynthetic capacity compared to the repleted conditions.

To get additional information on the function of the different LHCX, I analyzed different transgenic lines over-expressing the LHCX proteins in the Pt4 ecotype, a strain showing an intrinsically lower NPQ capacity compared to the Pt1 ecotype. Remarkably, we found that the increased expression of all the tested isoforms generates a small but still consistent increase in the NPQ levels, regardless of which isoform was overexpressed and the different overexpression levels. Altough these results are not obvious to interpretate, they suggest a potential involvement of the diverse proteins in NPQ modulation, as previously shown for LHCX1 (Bailleul et al. 2010).

Working on the transcriptional responses of LHCX genes to various light and nutrient conditions, I started to think that it could be interesting to identify the specific regulatory motifs in these genes. In this study we searched these motifs in the 5'-flanking regions of the four isoforms, by using *in silico* analysis and transcriptomic data. These analyses revealed the presence of novel cis-regulatory

elements that may contribute to the transcriptional regulation of the different isoforms in stress conditions.

The analyses described in this chapter suggest that diatoms such as *P. tricornutum* benefit of the expanded LHCX family to modulate the fast and efficient NPQ mechanism and successfully perform in variable environments. Altough not conclusive regarding the function of the different LHCX members, these results provide novel information on the actors potentially implicated in the NPQ regulations. The novel gene expression information provided in this work may also represent the starting point for the identification of unknown regulators, in the chloroplast and in the nucleus, controlling the differential expression of the LHCX protein family.

The results of this work, done in collaboration with Dr. Giovanni Finazzi at CEA Grenoble, Dr. Benjamin Bailleul at IBPC in Paris, Dr. Bernard Lepetit at the University of Kostanz and Dr. Johan Lavaud at La Rochelle University, has been recently published in the Journal of Experimental Botany: "Multisignal control of expression of the LHCX protein family in the marine diatom *Phaeodactylum tricornutum*", by Taddei et al.

The exact location of the LHCX proteins and the possible correlated formation of the quenching sites in the photosynthetic complexes are still unknow. These important questions represent the subject of the other investigations performed during my thesis and that will be presented in the next chapter.

Journal of Experimental Botany Advance Access published May 25, 2016

Journal of Experimental Botany
doi:10.1093/jxb/erw198
This paper is available online free of all access charges (see http://jxb.oxfordjournals.org/open_access.html for further details)

RESEARCH PAPER

Multisignal control of expression of the LHCX protein family in the marine diatom *Phaeodactylum tricornutum*

Lucilla Taddei[1,*], Giulio Rocco Stella[1,2,*], Alessandra Rogato[1,3,4,*], Benjamin Bailleul[5], Antonio Emidio Fortunato[1], Rossella Annunziata[1], Remo Sanges[4], Michael Thaler[1], Bernard Lepetit[6], Johann Lavaud[7], Marianne Jaubert[1], Giovanni Finazzi[8], Jean-Pierre Bouly[1] and Angela Falciatore[1,†]

[1] Sorbonne Universités, UPMC, Institut de Biologie Paris-Seine, CNRS, Laboratoire de Biologie Computationnelle et Quantitative, 15 rue de l'Ecole de Médecine, 75006 Paris, France
[2] Department of Biotechnology, University of Verona, Strada Le Grazie, I-37134 Verona, Italy
[3] Institute of Biosciences and BioResources, CNR, Via P. Castellino 111, 80131 Naples, Italy
[4] Biology and Evolution of Marine Organisms, Stazione Zoologica Anton Dohrn, Villa Comunale, 80121 Naples, Italy
[5] Institut de Biologie Physico-Chimique, UMR 7141 CNRS-UPMC, 13 rue Pierre et Marie Curie, 75005 Paris, France
[6] Zukunftskolleg, Department of Plant Ecophysiology, University of Konstanz, D-78457 Konstanz, Germany
[7] UMI 3376 TAKUVIK, CNRS/Université Laval, Département de Biologie, Pavillon Alexandre-Vachon, 1045 avenue de la Médecine, Québec (Québec) G1V 0A6, Canada
[8] Laboratoire de Physiologie Cellulaire et Végétale, UMR 5168, Centre National de la Recherche Scientifique (CNRS), Institut National Recherche Agronomique (INRA), Université Grenoble Alpes, Commissariat à l'Energie Atomique et aux Energies Alternatives (CEA), Institut de Biosciences et Biotechnologies de Grenoble, (BIG), CEA Grenoble, F-38054 Grenoble cedex 9, France

* These authors contributed equally to this work.
† Correspondence: angela.falciatore@upmc.fr

Received 26 February 2016; Accepted 26 April 2016

Editor: Markus Teige, University of Vienna

Abstract

Diatoms are phytoplanktonic organisms that grow successfully in the ocean where light conditions are highly variable. Studies of the molecular mechanisms of light acclimation in the marine diatom *Phaeodactylum tricornutum* show that carotenoid de-epoxidation enzymes and LHCX1, a member of the light-harvesting protein family, both contribute to dissipate excess light energy through non-photochemical quenching (NPQ). In this study, we investigate the role of the other members of the LHCX family in diatom stress responses. Our analysis of available genomic data shows that the presence of multiple *LHCX* genes is a conserved feature of diatom species living in different ecological niches. Moreover, an analysis of the levels of four *P. tricornutum* LHCX transcripts in relation to protein expression and photosynthetic activity indicates that LHCXs are differentially regulated under different light intensities and nutrient starvation, mostly modulating NPQ capacity. We conclude that multiple abiotic stress signals converge to regulate the LHCX content of cells, providing a way to fine-tune light harvesting and photoprotection. Moreover, our data indicate that the expansion of the *LHCX* gene family reflects functional diversification of its members which could benefit cells responding to highly variable ocean environments.

Key words: Dark, gene expression, iron starvation, LHCX, light, marine diatom, nitrogen starvation, non-photochemical quenching.

Introduction

The perception of environmental signals and the activation of appropriate responses to external stimuli are of major importance in the growth and survival of all organisms. At the cellular level, this requires the presence of complex signal perception and transduction networks, triggering changes in nuclear gene expression (Lee and Yaffe, 2014). External cues such as light, temperature, and nutrient availability strongly affect the physiology and metabolism of photosynthetic organisms, so acclimation mechanisms are needed to cope efficiently with short- and long-term environmental changes to maintain photosynthetic performances (Walters, 2005; Eberhard *et al.*, 2008). In eukaryotic phototrophs, chloroplast biogenesis and activity are integrated in broader regulatory programmes, requiring coordination between the nucleus and chloroplast genomic systems (Rochaix, 2011; Jarvis and Lopez-Juez, 2013). The nucleus responds to stimuli inducing the synthesis of regulatory proteins that modulate chloroplast responses. In turn, molecules originating from the chloroplast activity (e.g. redox state of the photosynthetic electron carriers, reactive oxygen species, plastid gene transcription, tetrapyrroles, and other metabolites) provide a retrograde signal feeding back to the nucleus (Woodson and Chory, 2008).

Marine photosynthesis is dominated by unicellular phytoplanktonic organisms, which are passive drifters in the water column and often experience drastic changes in their surrounding environment (Falkowski *et al.*, 2004; Depauw *et al.*, 2012). Diatoms are among the most abundant and diversified groups of photosynthetic organisms. They are particularly adapted to growing in very dynamic environments such as turbulent coastal waters and upwelling areas, as well as in polar oceans (Margalef, 1978; Field *et al.*, 1998; Kooistra *et al.*, 2007; Arrigo *et al.*, 2012). Several species can survive for long periods at depths where light is limiting for growth, and quickly reactivate their metabolism after returning to the photic zone (Sicko-Goad *et al.*, 1989; Reeves *et al.*, 2011). The adaptive capacity of such algae suggests that they have sophisticated mechanisms to perceive and rapidly respond to environmental variations. Consistent with this notion, genome sequence information of representative diatom model species such as *Thalassiosira pseudonana* and *Phaeodactylum tricornutum* (Armbrust *et al.*, 2004; Montsant *et al.*, 2007; Bowler *et al.*, 2008; Rayko *et al.*, 2010), and the availability of transcriptomic and proteomic data in various species exposed to different stimuli and stresses (Nymark *et al.*, 2009; Dyhrman *et al.*, 2012; Thamatrakoln *et al.*, 2012; Ashworth *et al.*, 2013; Nymark *et al.*, 2013; Keeling *et al.*, 2014; Valle *et al.*, 2014; Alipanah *et al.*, 2015; Muhseen *et al.*, 2015) have highlighted the existence of some diatom-specific adaptive strategies, pinpointing molecular regulators of environmental change responses. Several photoreceptors for efficient light colour sensing (Huysman *et al.*, 2013; Schellenberger Costa *et al.*, 2013; Fortunato et al., 2015, 2016) have been identified in diatoms. Peculiar iron acquisition and concentration mechanisms are also known (Allen *et al.*, 2008; Marchetti *et al.*, 2012; Morrissey *et al.*, 2015), which contribute to their survival in iron-limited waters and to their rapid proliferation when iron becomes available (de Baar *et al.*, 2005). Diatoms have peculiar gene sets implicated in nitrogen metabolism, such as a complete urea cycle, that could be used as temporary energy storage or as a sink for photorespiration (Allen *et al.*, 2011). Eventually, diatoms optimize their photosynthesis via extensive energetic exchanges between plastids and mitochondria (Bailleul *et al.*, 2015).

The ecological dominance of diatoms also relies on their capacity to cope with light stresses, thanks to very efficient photoprotective mechanisms. Diatoms possess a high capacity to dissipate excess light energy as heat through high energy quenching (qE) that, together with the photoinhibitory quenching (qI), can be visualized via the non-photochemical quenching (NPQ) of Chl *a* fluorescence (Lavaud and Goss, 2014; Goss and Lepetit, 2015). The xanthophyll diatoxanthin (Dt) pigment, synthesized from the de-epoxidation of diadinoxanthin (Dd) during illumination (Goss and Jakob, 2010; Lavaud *et al.*, 2012), and the LHCX1 protein, a member of the light-harvesting protein family (Bailleul *et al.*, 2010), have been identified as key components of the qE process in diatoms. *P. tricornutum* cells with deregulated LHCX1 expression display a significantly reduced NPQ capacity and a decreased fitness, demonstrating a key role for this protein in light acclimation (Bailleul *et al.*, 2010), similarly to the light harvesting complex stress-related (LHCSR) proteins of green algae and mosses (Alboresi *et al.*, 2010; Ballottari *et al.*, 2016).

Multiple nuclear-encoded and plastid-localized LHCX family members have been identified in the genomes of the diatoms *P. tricornutum* and *T. pseudonana*. Scattered information derived from independent gene expression analyses indicated that some *LHCX* isoforms are constitutively expressed while others are expressed in response to stress (Becker and Rhiel, 2006; Allen *et al.*, 2008; Nymark *et al.*, 2009; Zhu and Green, 2010; Bailleul *et al.*, 2010; Beer *et al.*, 2011; Lepetit *et al.*, 2013), similarly to what is observed for the two LHCSR proteins in *Physcomitrella patens* (Gerotto *et al.*, 2011). In this study, we have extended the characterization of the four *P. tricornutum* LHCXs, by combining detailed gene expression analysis in cells exposed to different conditions with *in vivo* analysis of photosynthetic parameters. The result of this analysis revealed a complex regulatory landscape, suggesting that the expansion of the LHCXs reflects a functional diversification of these proteins and may contribute to the regulation of the chloroplast physiology in response to diverse extracellular and intracellular signals.

Materials and methods

Analysis of the LHCXs *in the diatom genomes*

Phaeodactylum tricornutum and *T. pseudonana LHCX* gene model identifiers were retrieved from the diatom genomes, respectively, on *P. tricornutum* Phatr2 and *T. pseudonana* Thaps3 in the JGI database (http://genome.jgi.doe.gov/). *Phaeodactylum tricornutum* LHCX proteins were used as query to perform BlastP searches on the *Pseudo-nitzschia multiseries* (http://genome.jgi.doe.gov/Psemu1/Psemu1.home.html) and *Thalassiora oceanica* (http://protists.

ensembl.org/Thalassiosira_oceanica/Info/Index) genome portals. Best hit sequences were tested on Pfam (http://pfam.xfam.org/) to assess the presence of the Chloroa_b-bind domain (PF00504), characteristic of light-harvesting proteins. Protein alignments were performed with MUSCLE (http://www.ebi.ac.uk/Tools/msa/muscle/).

Diatom growth conditions

The *P. tricornutum* (Pt1 8.6, CCMP2561) cultures, obtained from the Provasoli-Guillard National Center for Culture of Marine Phytoplankton, were used for the gene expression and photophysiology analyses. Cells were grown in ventilated flasks in f/2 medium (Guillard, 1975) at 18 °C, in a 12 h light/12 h dark photoperiod using white fluorescence neon lamps (Philips TL-D 90), at 30 µmol m^{-2} s^{-1} (low light). High light treatments were performed by irradiating the cells with 500 µmol m^{-2} s^{-1} for 5 h, 2 h after the onset of light, with the same light sources. Dark adaptation treatments were performed for 60 h. Blue light (450 nm, 1 µmol m^{-2} s^{-1}) was applied for 10 min, 30 min, and 1 h on dark-adapted cells in the absence and presence of 2 µM DCMU [3-(3,4-dichlorophenyl)-1,1-dimethylurea]. In the iron starvation experiments, *P. tricornutum* cells at an initial concentration of 2×10^5 cells ml^{-1} were grown in f/2 artificial sea water medium (Allen *et al.*, 2008) modified to contain either 11 µM iron (iron-replete) or 5 nM iron with the addition of 100 µM of the Fe^{2+} chelator FerroZine™ (iron-limited) (Stookey, 1970). Cells were harvested after 3 d to perform the analyses. Nitrogen starvation was achieved by diluting *P. tricornutum* cells to 2×10^5 cells ml^{-1} in f/2 medium containing 1 mM nitrate (NO_3-replete) or 50 µM nitrate (NO_3-limited). When cells attained a concentration of 1×10^6 cells ml^{-1}, they were re-diluted to 2×10^5 cells ml^{-1} in their respective media and harvested after 3d, 2 h after the onset of light, and then used for experiments.

Generation of transgenic lines overexpressing the LHCX proteins

Vectors for LHCX overexpression were generated by cloning the full-length cDNA sequences of the four *LHCX* genes in the pKS-FcpBpAt-C-3HA vector (Siaut *et al.*, 2007), using the *Eco*RI and *Not*I restriction sites. The *LHCX* cDNAs were amplified by PCR using the primers described in Supplementary Table S1 at *JXB* online. Each vector was co-transformed with the pFCPFp-Shble vector for antibiotic selection into *P. tricornutum* Pt4 cells (DQ085804; De Martino *et al.*, 2007) by microparticle bombardment (Falciatore *et al.*, 1999). Transgenic lines were selected on 100 µg ml^{-1} phleomycin (Invitrogen) and screened by PCR using primers specific for the four LHCXs (Supplementary Table S1). Transgenic lines overexpressing the LHCX4 isoform in the Pt1 ecotype were also generated, as for the Pt4 ecotype.

RNA extraction and qRT-PCR analysis

Total RNA was isolated from 10^8 cells with TriPure isolation reagent (Roche Applied Science, IN, USA) according to the manufacturer's instructions. Quantitative real-time PCR (qRT-PCR) was performed on wild-type cells and on the LHCX-overexpressing clones as described in De Riso *et al.* (2009). The relative quantification of the different *LHCX* transcripts was obtained using *RPS* (ribosomal protein small subunit 30S; ID10847) and *H4* (histone H4; ID34971) as reference genes, and by averaging of two reference genes using the geometric mean and the fold changes calculated with the $2^{-\Delta\Delta Ct}$ Livak method (Livak and Schmittgen, 2001). Primer sequences used in qRT-PCR analysis are reported in Supplementary Table S1.

Protein extraction and western blot analysis

Western blot analyses were performed on total cell protein extracts prepared as in Bailleul *et al.* (2010), and resolved on 14% LDS–PAGE gels. Proteins were detected with different antibodies: anti-LHCSR (gift of G. Peers, University of California, Berkeley, CA, USA) (1:5000); anti-D2 (gift of J.-D. Rochaix, University of Geneva, Switzerland) (1:10 000); anti-PsaF (1:1000) and anti-βCF1 (1:10 000) (gift of F.-A. Wollman, Institut de Biologie Physico-Chimique, Paris, France); and anti-HA primary antibody (Roche) (1:2000). Proteins were revealed with Clarity reagents (Bio-Rad) and an Image Quant LAS4000 camera (GE Healthcare, USA).

Chlorophyll fluorescence measurements

Light-induced fluorescence kinetics were measured using a fluorescence CCD camera recorder (JTS-10, BeamBio, France) as described (Johnson *et al.*, 2009) on cells at 1–2 × 10^6 cells ml^{-1}. F_v/F_m was calculated as $(F_m–F_0)/F_m$. NPQ was calculated as $(F_m–F_m')/F_m'$ (Bilger and Bjorkman, 1990), where F_m and F_m' are the maximum fluorescence emission levels in the dark and light-acclimated cells, measured with a saturating pulse of light. All samples, except the 60 h dark-adapted cells, were adapted to dim light (10 µmol m^{-2} s^{-1}) for 15 min at 18 °C before measurements. The maximal NPQ response was measured upon exposure for 10 min to saturating green light of 950 µmol m^{-2} s^{-1}. The relative electron transfer rate ($rETR_{PSII}$) was measured with a JTS-10 spectrophotometer at different light intensities (20, 170, 260, 320, 520, and 950 µmol m^{-2} s^{-1}), by changing light every 4 min to minimize the photodamage. $rETR_{PSII}$ was calculated as: Y2×light intensity, where Y2 is the efficiency of PSII.

In silico analysis of the LHCX non-coding sequences

Determination of motif occurrence and *de novo* search of over-represented motifs in the 5'-flanking regions (1000 bp or the entire intergenic sequence between the coding gene of interest and the upstream gene) and the introns of the Pt*LHCX* genes were performed by the use of the FIMO (v4.11.1) and MEME Suite (v4.9.1) tools (Bailey *et al.*, 2009), with a *p*-value cut-off of 0.0001. The Tomtom tool (v4.11.1) on the MEME Suite was used to compare motifs with known transcription binding sites. Microarray data from Alipanah *et al.* (2015) (accession GSE58946) were downloaded from the GEO database (http://www.ncbi.nlm.nih.gov/pubmed/23193258) using the GEO query package (http://www.ncbi.nlm.nih.gov/pubmed/17496320). Data were loaded and analysed in the R environment using the Limma package (http://www.ncbi.nlm.nih.gov/pubmed/25605792). Selection of transcripts categories: (i) up-regulated, log2 fold change (Fc) >3, adjusted *p*-value <0.01 (122 genes); (ii) down-regulated, Fc <–3, adjusted *p*-value <0.01 (200 genes). The *P. tricornutum* genome sequences and gff mapping of filtered gene models were downloaded from the JGI website and refer to Phatr2 (http://genome.jgi.doe.gov/Phatr2/Phatr2.home.html). The significance of motif enrichment was evaluated using the binomial test with a *p*-value cut-off of 0.05. All analyses were performed using custom scripts in Perl and R.

Results

LHCX family expansion in the diatom genomes

Several genes belonging to the LHCX family have already been identified in the genome of the pennate diatom *P. tricornutum* (Bailleul *et al.*, 2010) and the centric diatom *T. pseudonana* (Zhu and Green, 2010), the most established model species due to the availability of molecular toolkits for genetic manipulations (Apt *et al.*, 1996; Poulsen and Kroger, 2005; De Riso *et al.*, 2009; Trentacoste *et al.*, 2013; Daboussi *et al.*, 2014; Karas *et al.*, 2015). The recently available genome sequences of the pennate diatom *P. multiseries*, belonging to a widely distributed genus also comprising toxic species (Trainer *et al.*, 2012), and the centric diatom

T. oceanica, a species adapted to oligotrophic conditions (Lommer *et al.*, 2012), opened up the possibility to extend this investigation to other ecologically relevant species. As summarized in Table 1, comparative analysis indicates an expansion of the *LHCX* family in diatoms, compared with the green algae: four members are present in *P. tricornutum*, five in *P. multiseries*, *T. pseudonana*, and *T. oceanica*, and up to 17 members have been found in the genome of the polar species *Fragilariopsis cylindrus* (B. Green and T. Mock, personal communication). Analysis of the intron–exon structure of all the available diatom *LHCX* genes revealed a variable number of introns (from zero to three) as well as variable intron and exon lengths (Table 1).

Light versus dark regulation of expression of the LHCX *genes*

Independent gene expression studies performed in *P. tricornutum* cells suggest that the *LHCX* gene family is regulated by light via multiple regulatory pathways. To explore the mechanisms controlling the light responses of the *LHCX* genes further, we analysed mRNA and protein contents in cells exposed to different light conditions. We first monitored the expression of the *LHCX* genes in cells grown in low light (LL) and then exposed to high light (HL). In line with previous studies (Bailleul *et al.*, 2010; Lepetit *et al.*, 2013), qRT-PCR and western blot analyses (Fig. 1A and B, respectively) showed that LHCX1 is expressed at very high levels in LL-adapted cells, and that HL treatment slightly increases the LHCX1 content. Conversely, the isoforms 2 and 3 showed different responses to the LL to HL shift. The *LHCX2* transcripts, which are significantly less abundant than that of *LHCX1* in LL, rapidly increased following HL stress, reaching levels comparable with those of *LHCX1* after 1 h HL exposure (Fig. 1A). This translated into an increase of the LHCX2 protein observed by western blot (Fig. 1B). However, the increase in the protein content was lower than that of the transcript, possibly because of a low affinity of the LHCSR antibody (Peers *et al.*, 2009) for the LHCX2 isoform. The *LHCX3* transcripts that were expressed at very low levels in LL quickly rose upon HL treatment, peaking after 30 min and starting to decrease after 1 h of light stress. Conversely, a different mRNA expression profile was found in the case of *LHCX4*, which, unlike the other isoforms, was barely detectable in both LL and HL conditions (Fig. 1A). The LHCX3 and LHCX4 proteins, having very similar molecular weights (22.8 kDa and 22.2 kDa, respectively), cannot be discriminated by western blot analysis. Based on the different transcriptional regulation of *LHCX3* and *LHCX4* by light, it is tempting to propose that the light-induced protein of ~22.8 kDa reflects the accumulation of the LHCX3 isoform (Fig. 1B). However, in contrast to the transient induction of the *LHCX3* mRNAs, this protein is gradually accumulated during the LL to HL shift and it remains stable over the treatment. This discrepancy between transcript and protein expression profiles could be explained assuming that: (i) some post-transcriptional modifications regulate the accumulation of LHCX3 in the light; or (ii) the light-induced protein isoform at 22.8 kDa also comprises the LHCX4 protein, which could be present in HL-exposed cells, along with LHCX3.

Table 1. *List of the* LHCXs *identified in the diatom genomes*

Species	Name	ID	Chromosomal localization	Length (no. of amino acids)	No. of introns
Thalassiosira pseudonana	LHCX1	264921	chr_23:365603–366232 (–)	209	0
	LHCX2	38879	chr_23:368273–368902 (+)	209	0
	LHCX4	270228	chr_5:1446306–1447125 (–)	231	0
	LHCX5	31128	chr_1:2849139–2850176 (–)	236	3
	LHCX6	12097	chr_23:366611–367378 (+)	255	0
Phaeodactylum	LHCX1	27278	chr_7:996379–997300 (+)	206	1
tricornutum	LHCX2	56312	chr_1:2471232–2472170 (+)	238	2
	LHCX3	44733	chr_5:76676–77606 (+)	206	1
	LHCX4	38720	chr_17:53010–53733 (+)	207	1
Pseudo-nitzschia	–	66239	scaffold_189:181982–182948 (+)	201	1
multiseries	–	238335	scaffold_95:121459–122306 (–)	202	1
	–	257821	scaffold_246:124909–125745 (+)	197	1
	–	264022	scaffold_1353:8720–9877 (+)	206	1
	–	283956	scaffold_38:284133–284828 (–)	231	0
Thalassiosira oceanica	–	Thaoc_09937	SuperContig To_g10869: 4.331–5.040 (–)	210	1
	–	Thaoc_12733	SuperContig To_g15184: 10.800–11.435 (–)	172	1
	–	Thaoc_28991	SuperContig To_g41561: 2.777–3.105 (+)	81	1
	–	Thaoc_31987	SuperContig To_g45669: 1–1.025 (–)	205	2
	–	Thaoc_32497	SuperContig To_g46152: 5.664–6.285 (–)	180	1

For *T. pseudonana* (Thaps3), *P. tricornutum* (Phatr2), and *P. multiseries* (Psemu1), ID numbers refer to the genome annotation in the JGI database (http://genome.jgi.doe.gov/). For *T. oceanica* (ThaOc_1.0), ID refers to the Ensembl Protist database (http://protists.ensembl.org/Thalassiosira_oceanica/Info/Index?db=core). (+) and (–) indicate the forward and reverse chromosomal or scaffolds, respectively. The protein length and intron numbers are also indicated.

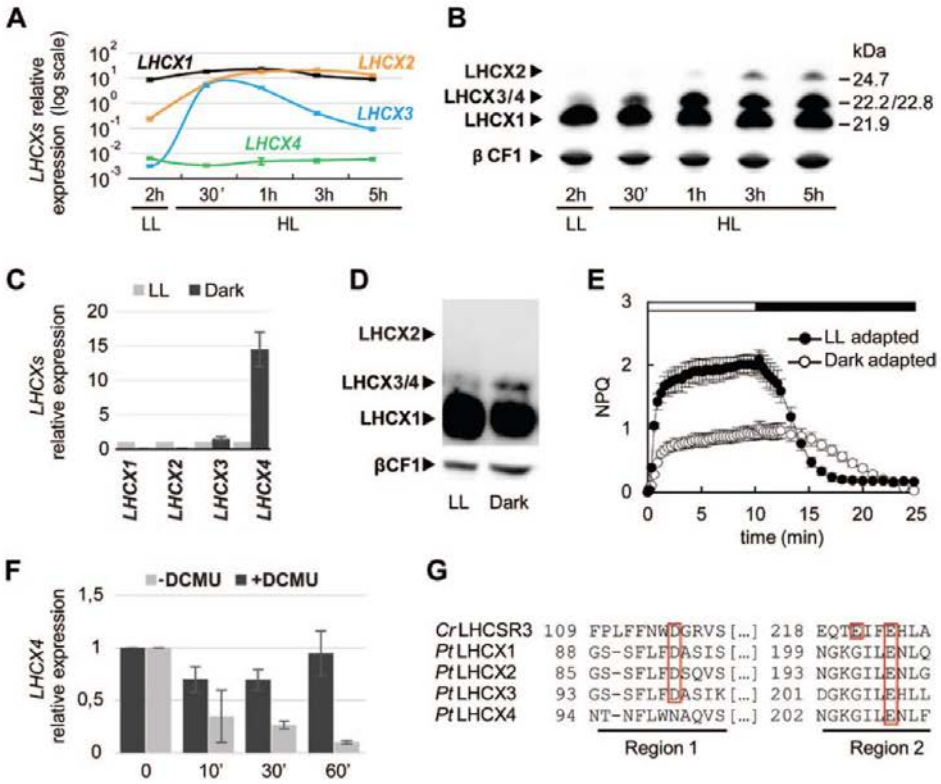

Fig. 1. Light and dark regulation of *P. tricornutum* LHCXs. Analysis of the four *LHCX* transcripts by qRT-PCR (A) and of LHCX proteins (B) by western blotting in cells adapted to low light (LL) (12L/12D cycles), after exposure to LL for 2 h then to high light (HL) for 30 min, 1 h, 3 h, or 5 h. mRNA levels were quantified by using *RPS* as the reference gene (A). Proteins were detected using the anti-LHCSR antibody which recognizes all the *Pt*LHCXs (arrowheads) and the anti-βCF1 antibody as loading control (B). Cells adapted to darkness for 60 h were compared with those grown in LL for the analysis of LHCX transcripts (C), proteins (D), and NPQ (E). Relative transcript levels were determined using *RPS* as a reference, and values were normalized to gene expression levels in LL. LHCX proteins were detected as in (B). The horizontal bar in (E) indicates when the actinic light was on (white) or off (black). (F) *LHCX4* mRNAs in 60 h dark-adapted cells (Time 0) and in response to 10 min, 30 min, or 1 h of blue light (1 μmol m^{-2} s^{-1}), in the presence (black) or absence (grey) of the inhibitor DCMU. Transcript levels were quantified by using *RPS* as the reference, and normalized to gene expression levels in the dark. Error bars represent ±SD of three technical replicates from one representative experiment in (A), and ±SD of three biological replicates in (C), (E), and (F). (G) Alignment of regions 1 and 2 of the *Chlamydomonas reinhardtii* LHCSR3 and *P. tricornutum* LHCX1, 2, 3, and 4 protein sequences. The boxes indicate the pH-sensing residues conserved between the LHCXs and LHCSR3. (This figure is available in colour at *JXB* online).

Previous reports (Lepetit *et al.*, 2013; Nymark *et al.*, 2013) indicate that the *LHCX4* transcript is induced in dark-adapted cells. Therefore, we extended the analysis of the expression of the four *LHCX* genes to cells adapted to prolonged darkness (60 h). In these conditions, we observed a significant increase only of the *LHCX4* mRNAs (Fig. 1C). For the same reason as described above, we attributed the band of ~22 kDa observed in the dark-adapted cells to the LHCX4 protein, although LHCX3 (Fig. 1D) could also be present. In the dark, cells were also showing a decreased NPQ capacity (Fig. 1E) and a slightly reduced PSII maximal quantum yield and overall photosynthetic electron flow capacity (Table 2). Other studies have revealed that blue light photoreceptors (Coesel *et al.*, 2009; Juhas *et al.*, 2014) and the redox state of the chloroplast (Lepetit *et al.*, 2013) could both contribute to the light regulation of *LHCX1*, *2*, and *3* gene expression. Thus, we tested the possible role of these processes in the inhibition of *LHCX4* expression upon light exposure. We irradiated dark-adapted cells with low intensity blue light (1 μmol m^{-2} s^{-1}) during 1 h, in the presence or absence of the PSII inhibitor DCMU (Fig. 1F). The analysis revealed that the *LHCX4* expression is repressed even at such low light irradiance. Moreover, this repression is lost by poisoning photosynthesis with DCMU, suggesting that this process plays an active role in the light-induced repression of *LHCX4*.

A recent study in *Chlamydomonas reinhardtii* showed that the activity of the protein LHCSR3 is regulated by the reversible protonation of three specific amino acidic residues following luminal pH acidification in the light (Ballottari *et al.*, 2016). In order to assess if this mechanism is conserved in diatoms, we analysed the *P. tricornutum* LHCX protein sequences. We found that LHCX1, 2, and 3 possess two of the three amino acids identified in LHCSR3 in conserved positions (Fig. 1G; Supplementary Fig. S2), suggesting that the pH-triggered activation of qE could be conserved in diatoms. On the other hand, only one of these protonatable residues was found in LHCX4.

LHCX expression in iron starvation

Besides light, nutrient availability also affects chloroplast activity (Wilhelm *et al.*, 2006; Gross, 2012). In many oceanic regions, iron is a major limiting factor for diatom distribution. A general down-regulation of photosynthesis has been reported in iron starvation in several diatom species (Laroche *et al.*, 1995; Allen *et al.*, 2008; Hohner *et al.*, 2013), with a consequent decrease of the carbon fixation reactions, growth rate, and cell size. Since increased NPQ was previously observed in iron-starved *P. tricornutum* cells (Allen *et al.*, 2008), we compared the expression of the different LHCX isoforms in cells grown under Fe-replete and Fe-limited conditions. We found that while a slight induction of the other LHCX proteins was seen, the *LHCX2* transcript was greatly induced in iron-limited cells (Fig. 2A), leading to a significant accumulation of the LHCX2 protein (Fig. 2B). Fe limitation also enhanced NPQ, while slowing down its kinetics (Fig. 2C), possibly because of a slower diadinoxanthin de-epoxidation rate. We also observed a severe impairment of the photosynthetic capacity in iron limitation as indicated by the decrease in F_v/F_m (Table 2) and in the PSII maximal electron transport rate ($rETR_{PSII}$) (Fig. 2D; see also Allen *et al.*, 2008). The decreased maximal $rETR_{PSII}$ was probably caused by a diminished capacity for carbon fixation. Moreover, in agreement with previous studies (Allen *et al.*, 2008; Thamatrakoln *et al.*, 2013), we observed a decrease in the amount of PSI (PsaF), which is the complex with the highest Fe content. This complex has been already shown to represent the first target of Fe limitation (Moseley *et al.*, 2002). We also found a significant decrease in PSII (D2 protein), which was probably degraded because of sustained photoinhibition (see also Allen *et al.*, 2008) (Fig. 2B).

Table 2. *Photosynthetic parameters of the* P. tricornutum *wild type and transgenic lines*

Strain	Conditions	F_v/F_m	$rETR_{PSII}$	NPQ max
Pt1	LL	0.66±0.03	74.4±1.2	2.1±0.1
Pt1	Dark	0.60±0.02	67.2±4.0	1.0±0.1
Pt1	+Fe	0.65±0.003	72.6±4.8	2.2±0.3
Pt1	–Fe	0.20±0.004	25.7±1.8	4.4±0.3
Pt1	+N	0.65±0.006	74.4±2.4	2.1±0.1
Pt1	–N	0.40±0.008	27.5±3.2	3.2±0.4
Pt4	WT	0.68±0.01	79.3±2.6	0.83±0.04
Pt4	EVL	0.66±0.01	72.5±3.5	0.82±0.03
Pt4	OE1	0.67±0.01	70.7±2.6	1.00±0.1
Pt4	OE2.5	0.67±0.01	70.0±1.6	1.06±0.05
Pt4	OE2.20	0.66±0.01	69.3±1.6	1.02±0.08
Pt4	OE3.12	0.66±0.01	75.8±4.9	1.04±0.07
Pt4	OE3.33	0.68±0.03	71.0±3.1	1.00±0.1
Pt4	OE4.11	**0.59±0.01**	68.7±1.9	1.03±0.01
Pt4	OE4.13	**0.58±0.02**	69.4±1.3	1.07±0.04

PSII efficiency (F_v/F_m) and relative electron transport rate ($rETR_{PSII}$) in different growth conditions are reported. $rETR_{PSII}$ was measured at 260 µmol photons m^{-2} s^{-1} light intensity and calculated as: $rETR_{PSII}$=ϕPSII×actinic light intensity. Non-photochemical quenching (NPQ) was measured with an actinic light intensity of 950 µmol photons m^{-2} s^{-1} and calculated as in Maxwell and Johnson (2000). Data are the average of three biological replicates ±SD.

LHCX expression in nitrogen starvation

Besides iron, nitrogen (N) is also a limiting resource for diatoms (Mills *et al.*, 2008; Moore *et al.*, 2013; Rogato *et al.*, 2015). Recent transcriptomic and proteomic analysis highlighted important metabolic modifications under N starvation, such as the up-regulation of nitrogen assimilation enzymes, the recycling of intracellular nitrogen-containing compounds from the photosynthetic apparatus and other sources, and the increase in lipid content as a consequence of remodelling of intermediate metabolism (Allen *et al.*, 2011; Palmucci *et al.*, 2011; Hockin *et al.*, 2012; Alipanah *et al.*, 2015; Levitan *et al.*, 2015; Matthijs *et al.*, 2016). We found that N limitation also has a significant effect on the expression of the LHCXs. In particular, N limitation triggered the induction of *LHCX3* and *LHCX4* mRNAs (Fig. 3A) and of LHCX3/4 proteins (Fig. 3B). The increase of the LHCX1 and 2 isoforms was only visible at the protein level (Fig. 3B). Up-regulation of the LHCX proteins in N limitation correlated with an increase of the NPQ capacity

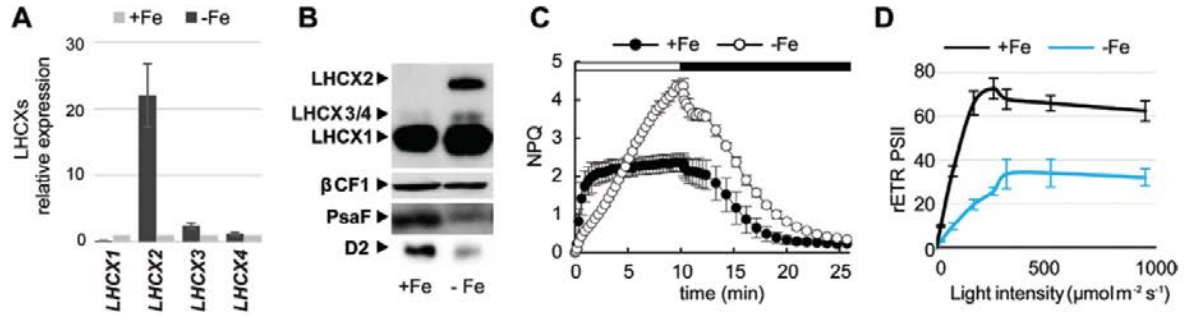

Fig. 2. Effect of iron starvation on *P. tricornutum* LHCX expression and photophysiology. Experiments were performed on cells grown in iron-replete (11 µM, +Fe) or iron-limited (5 nM iron+100 µM FerroZine™, –Fe) conditions: (A) qRT-PCR analysis of *LHCX* transcripts in –Fe, normalized against the +Fe condition and using *RPS* and *H4* as reference genes. (B) Immunoblot analysis of the LHCX, D2, and PsaF proteins, using βCF1 as loading control. NPQ capacity (C) and relative electron transfer rates ($rETR_{PSII}$) (D) of cells grown in +Fe or –Fe. The horizontal bar in (C) indicates when the actinic light was on (white) or off (black). $rETR_{PSII}$ was measured at different light intensities (20, 170, 260, 320, 520, and 950 µmol m^{-2} s^{-1}). In (A), (C), and (D), error bars represent ±SD of three biological replicates. (This figure is available in colour at *JXB* online).

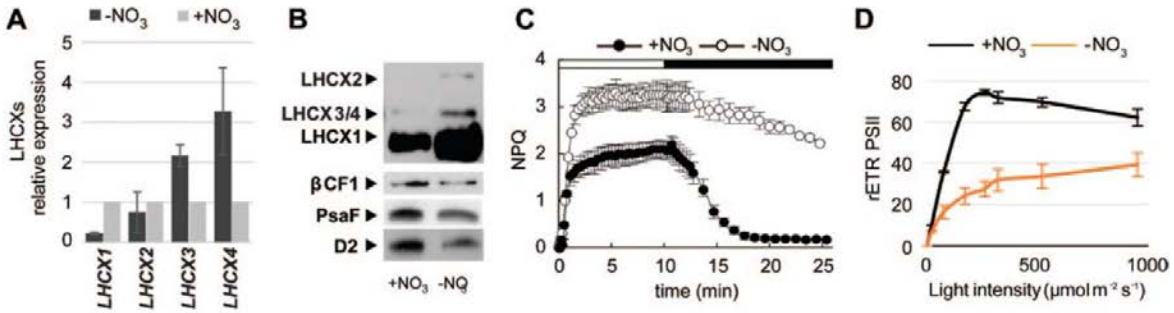

Fig. 3. Effect of nitrogen starvation on *P. tricornutum* LHCX expression and photophysiology. Experiments were performed on cells grown in nitrogen-replete (1 mM, $+NO_3^-$) or nitrogen starvation (50 μM, $-NO_3^-$) conditions: (A) qRT-PCR analysis of *LHCX* transcripts in $-NO_3^-$, normalized against the values in the $+NO_3^-$ condition, and using *RPS* and *H4* as reference genes. (B) Immunoblot analysis of the LHCX, D2, and PsaF proteins, using βCF1 as loading control. NPQ capacity (C) and relative electron transfer rates ($rETR_{PSII}$) (D) of cells grown in $+NO_3^-$ and $-NO_3^-$ conditions. The horizontal bar in (C) indicates when the actinic light was on (white) or off (black). $rETR_{PSII}$ was measured at different light intensities (20, 170, 260, 320, 520, and 950 μmol m^{-2} s^{-1}). In (A), (C), and (D), error bars represent ±SD of three biological replicates. (This figure is available in colour at *JXB* online).

(Fig. 3C). We note that NPQ was slowly relaxing upon dark exposure of N-limited cells, possibly reflecting the repression of the genes encoding the xanthophyll cycle enzymes including the zeaxanthin epoxidase (see Supplementary Fig. S3), when analysing available microarray data from N-depleted cells (Alipanah *et al.*, 2015). The N limitation also led to a drastically reduced F_v/F_m (Table 2) and a lower maximal $rETR_{PSII}$ (Fig. 3D). We also detected a reduced content of PSII and PSI proteins (Fig. 3B), in line with previous omic studies pointing to a general decrease of the photosynthetic capacity.

Analysis of the LHCX *non-coding regions*

Due to the observed transcriptional responses of *LHCX* genes in different light and nutrient conditions, we searched for known and potentially novel regulatory motifs in the 5'-flanking regions and the intronic sequences of the four isoforms (see Table 3; Supplementary Fig. S1). Because of their involvement in integrating light signals with CO_2/cAMP-induced transcriptional responses, we searched for the three CO_2/cAMP-responsive *cis*-regulatory elements (CCREs) identified in Ohno *et al.* (2012) and further characterized in Tanaka *et al.* (2016). Interestingly, we found CCRE-1 in the 5'-flanking sequences of *LHCX1* and *4*, CCRE-2 in *1*, *2*, and *4*, and CCRE-3 in *LHCX4*. These *cis*-regulatory elements may participate in the light-mediated regulation of the four *LHCX* genes.

In contrast, the two *P. tricornutum* iron-responsive elements identified in Yoshinaga *et al.* (2014) are not present in the analysed non-coding regions, suggesting that a different transcription factor should be involved in modulating the *LHCX2* transcriptional response to iron availability. Similarly, we could not find the two *P. tricornutum* motifs identified as responsive to short-term nitrogen deprivation (from 4 h to 20 h) in Matthijs *et al.* (2016), suggesting that distinct regulatory circuits may act in the short- and long-term acclimation to nitrogen deprivation.

To pinpoint possible novel regulatory motifs, we also scanned the non-coding sequences of the four isoforms using the MEME Suite program (Bailey *et al.*, 2009). The analysis revealed six motifs repeated at least twice in each isoform and/or shared by more than one isoform (Table 3; Supplementary Fig. S1). None of the identified motifs corresponds to a known transcription factor-binding site. This suggests that these motifs could represent novel diatom-specific *cis*-regulatory elements. In order to examine the potential involvement of the identified motifs in the long-term nitrate deprivation transcriptional responses of *LHCX* genes, we analysed a published microarray data set performed on 48 h and 72 h nitrogen-deprived *P. tricornutum* cells (Alipanah *et al.*, 2015). We compared the frequency of the six identified motifs in the 5'-flanking sequences of responsive and unresponsive transcripts. Interestingly, motif 6 ([T-A]TGACTG) was significantly enriched (p=0.035) in the 5'-flanking sequences of genes up-regulated in response to nitrogen starvation compared with down-regulated genes. The result suggests that motif 6 may be involved in gene transcriptional regulation in cells exposed to prolonged nitrogen starvation.

Table 3. *The identified regulatory motifs and their occurrence in the* P. tricornutum LHCX *non-coding sequences*

	Sequence	*LHCX1*	*LHCX2*	*LHCX3*	*LHCX4*
MOTIF 1	TCA[CT][AT]GTCA	2	2	1	–
MOTIF 2	CGAACCTTGG	–	–	2	–
MOTIF 3	CCT[GC]TCCGTA	–	–	2	–
MOTIF 4	GAGTCCATCG	–	–	–	2
MOTIF 5	CGATCACGGC	–	–	–	2
MOTIF 6	[TA]TGACTG	–	1	1	1
CCRE-1	TGACGT	1	–	–	1
CCRE-2	ACGTCA	1	1	–	1
CCRE-3	TGACGC	–	–	–	1

Modulation of LHCX *gene expression in* P. tricornutum *transgenic lines*

A role in the regulation of the NPQ in *P. tricornutum* has been proven for the LHCX1 protein by characterizing transgenic

lines with a modulated content of LHCX1 by either gene silencing or gene overexpression (Bailleul *et al.*, 2010). Unfortunately, all the attempts to down-regulate the expression of *LHCX2*, *3*, or *4* have been unsuccessful. Therefore, to explore their function, we opted for the strategy used in Bailleul *et al.* (2010), and tried to rescue the intrinsically lower NPQ capacity of the Pt4 ecotype. To this end, independent transgenic Pt4 lines were generated, bearing a vector in which the *LHCX2*, *3*, or *4* genes were expressed under the control of the *P. tricornutum FCPB (LHCF2)* promoter. A HA-tag was fused to the C-terminal end of the *LHCX* transgenes to allow the specific detection of the transgenic proteins. qRT-PCR and western blot analyses (Fig. 4A, C, E) on independent transgenic lines confirmed the expression of the transgenic LHCX isoforms. NPQ analyses (Fig. 4B, D, F) showed that the overexpression of each LHCX isoform generated a modest, but statistically significant, increase in the NPQ capacity compared with the Pt4 wild type as well as compared with a transgenic line transformed only with the antibiotic resistance gene and used as control. Strikingly, we found that all the transgenic lines showed a similar NPQ increase, regardless of which isoform was overexpressed and the different overexpression levels.

We also checked the possible effect of LHCX overexpression on growth and photosynthetic capacity. For the lines overexpressing the LHCX2 and LHCX3 proteins, we did not observe any altered phenotype (Table 2). In contrast, the Pt4 lines overexpressing LHCX4 showed a reduced PSII efficiency (Table 2). By performing a growth curve analysis, we also observed that these overexpressing lines showed a lag phase lasting 2–3 d (Fig. 4G), which was not the case in wild-type cells. A similar effect on growth was also observed in transgenic lines in which the *LHCX4* gene was overexpressed in the Pt1 ecotype (Fig. 4G).

Discussion

The presence of multiple *LHCX* genes in all the diatom genomes analysed to date strongly suggests that the expansion of this gene family is a common feature of these algae and may represent an adaptive trait to cope with highly variable environmental conditions. To investigate this scenario, in

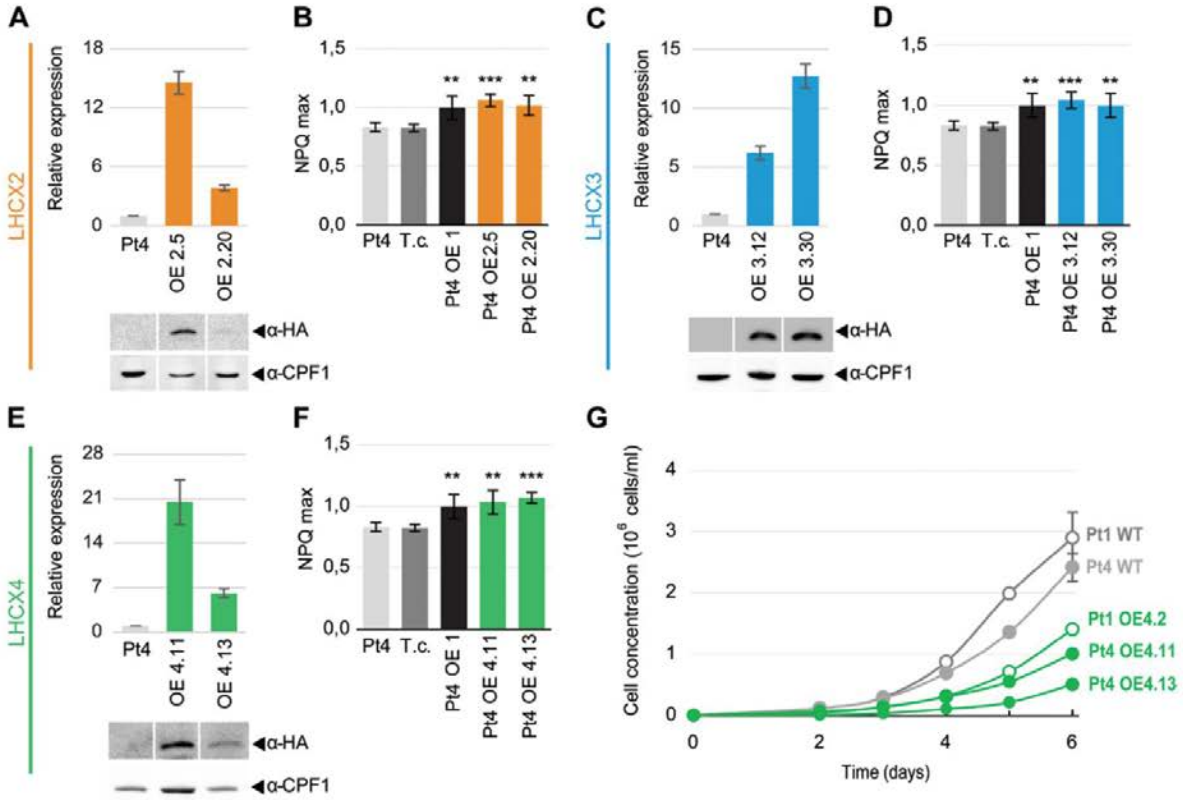

Fig. 4. *Phaeodactylum tricornutum* Pt4 ecotype lines overexpressing the *LHCX* genes. (A), (C), (E) LHCX transcript (upper panels) and protein (lower panels) analyses in the Pt4 wild type and transgenic strains overexpressing HA-tagged *LHCX2* (A), *LHCX3* (C), or *LHCX4* (E). Transcript abundance was measured by qRT-PCR using *RPS* as the reference gene and normalized to the wild type expression value. Tagged proteins were detected by immunoblot using an anti-HA antibody, and an anti-CPF1 antibody as loading control. Bands are taken from the same blots but from non-adjacent lanes. (B), (D), (F) NPQ max capacity in the Pt4 wild type, in a transgenic strain expressing the vector for antibiotic resistance (transformation control, T.c.), and in independent transgenic lines overexpressing *LHCX1* (OE1), *LHCX2* (OE2), *LHCX3* (OE3), and *LHCX4* (OE4) genes. Asterisks indicate the results of two-tailed Student *t*-tests: $^{**}p<0.01$; $^{***}p<0.001$. (G) Growth curves of Pt4 and Pt1 wild-type strains and Pt4 and Pt1 transgenic lines overexpressing the *LHCX4* (OE4) gene, grown in 12L/12D cycles (50 µmol m^{-2} s^{-1}). In all the experiments, $n \geq 3$, and bars represent ±SD. (This figure is available in colour at *JXB* online).

this work we correlated LHCX expression profiles with the photosynthetic and photoprotective performances in variable experimental conditions, including changes in light irradiance and nutrient availability. These analyses revealed that the four *P. tricornutum LHCX* genes respond differently to various environmental cues, as summarized in Fig. 5.

The analyses of the mRNA and protein responses indicate that amounts of the different LHCXs are tightly regulated at the transcriptional, and probably also the post-translational level. As LHCX3 and LHCX4 have a similar size, it was not possible to quantify the amount of these two proteins under the different stresses using one-dimensional electrophoresis. However, considering the transcript and biochemical analyses together (in the case of LHCX2 and LHCX1), it seems that LHCX1 is always expressed at high levels even in non-stress conditions, which is consistent with it having a pivotal role in NPQ regulation and light acclimation as proposed previously (Bailleul *et al.*, 2010).

LHCX2 and 3 are induced following high light stress, where they may contribute to increase the diatom photoprotection capacity. Their induction, as well as the accumulation of LHCX1, may result from the integration of different signals. Two members of the blue light-sensing cryptochrome photolyase family, CPF1 (Coesel *et al.*, 2009) and CRYP (Juhas *et al.*, 2014), modulate the light-dependent expression of LHCX1, LHCX2, and LHCX3. Also, the recently identified Aureochrome 1a blue light photoreceptor, which regulates *P. tricornutum* photoacclimation (Schellenberger Costa *et al.*, 2013), may affect how much of each LHCX there is in a cell. Moreover, chloroplast activity, through the redox state of the plastoquinone pool, may also regulate *LHCX1* and *LHCX2* gene expression in HL (Lepetit *et al.*, 2013).

A different regulation pattern is seen in the case of LHCX4, the only isoform which is induced in the absence of light. The amount of *LHCX4* mRNA rapidly decreases following a dark to light transition, and this repression is lost when photosynthesis is halted with the PSII inhibitor DCMU. This suggests that chloroplast-derived signals could participate in inhibiting gene expression, even at very low light irradiance, by an as yet unknown process. The peculiar trend observed in the LHCX4 light response suggests a possible role for this protein in *P. tricornutum* photoacclimation. The increased LHCX4 transcript and possibly protein content is mirrored by a decrease in NPQ capacity and a slightly reduced F_v/F_m in the dark-adapted cells, compared with cells grown in the light (Fig. 1E; Table 2). Moreover, reduced PSII efficiency and slightly altered growth were observed in cells overexpressing LHCX4 in the light (Fig. 4G), suggesting that LHCX4 could have a negative impact on chloroplast physiology. Indeed, a comparative analysis of the *P. tricornutum* LHCX protein sequences indicates that LHCX4 lacks key protonatable residues that in *Chlamydomonas* are involved in NPQ onset when the lumen acidifies (Ballottari *et al.*, 2016). These residues are, however, conserved in the LHCX1, 2, and 3 isoforms. According to the model established in green algae for the protein LHCSR3, these residues diminish their electrostatic repulsion upon protonation, allowing a rearrangement of the protein structure and pigment orientation and enhancement of the quenching capacity (Ballottari *et al.*, 2016). The substitution in LHCX4 of the acidic residues (aspartate and

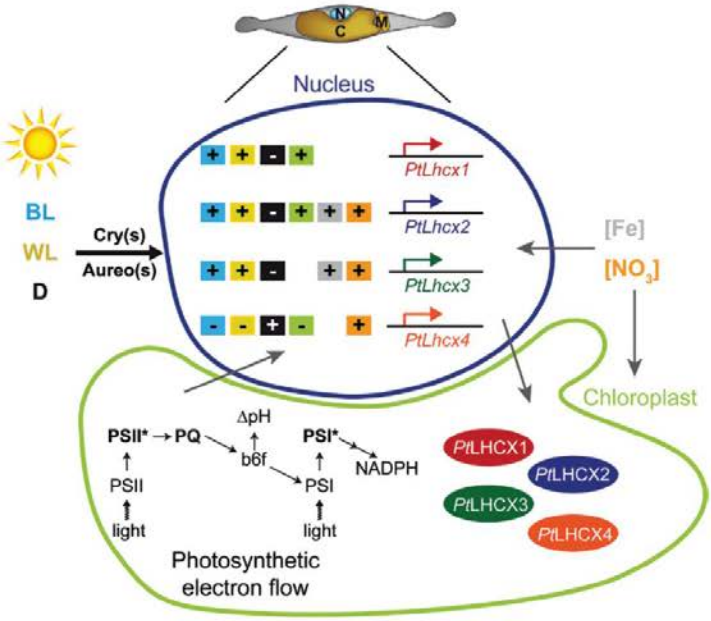

Fig. 5. Model of the *P. tricornutum* LHCX regulation. Scheme summarizing the multiple external signals and stresses that differentially regulate the expression of the four LHCXs. The *LHCX* genes are shown in the nucleus and the LHCX proteins in the chloroplast. + and – boxes indicate positive and negative transcriptional regulation, respectively, in response to white light (yellow), blue light (blue, through the cryptochromes, Cry, and aureochromes, Aureo, photoreceptors), darkness (black), chloroplast signals (green), iron starvation (grey), and nitrogen starvation (orange). In the *P. tricornutum* cell: N, nucleus; C, chloroplast; M, mitochondrion. In the chloroplast: PSI and PSII, photosystem I and II, respectively; PSI* and PSII*, excited photosystems; PQ, plastoquinone pool; b_6f, cytochrome b_6f complex; ΔpH, proton gradient; NADPH, redox potential.

glutamate) with non-protonatable residues (asparagine and glycine) would prevent such regulation. Instead, LHCX4 could contribute to the observed capacity of *P. tricornutum* to survive long periods in the dark and its repression could be needed for a rapid acclimation following re-illumination (Nymark at al., 2013). Consistent with this, high *LHCX* gene expression has also been observed in sea-ice algal communities dominated by diatoms that have adapted to the polar night (Pearson *et al.*, 2015).

Besides the light and redox signals discussed above, our study also shows that differences in the availability of iron and nitrogen strongly affect the expression of the different LHCXs. The signalling cascades controlling these responses are still largely unknown, but they probably involve multiple regulatory pathways into the nucleus and chloroplast, considering that these nutrients are essential for diatom photosynthesis and growth (Table 2; Fig. 5). Nitrogen starvation induces a general increase of all the LHCX isoforms, including LHCX4 that is normally repressed in light-grown cells (Fig. 3). We can hypothesize that the general increase of the LHCX content is needed to protect the photosynthetic apparatus, which is strongly affected by nitrogen deprivation, as shown by the drastically reduced F_v/F_m (Table 2), the lower maximal $rETR_{PSII}$ (Fig. 3D), and the reduction of PSI and PSII protein content. Interestingly, an opposite trend is observed for the main enzymes of the xanthophyll cycle, which are either not induced or are repressed in cells grown in similar nitrogen stress conditions (Supplementary Fig. S3). Thus, in nitrogen starvation, the LHCXs could represent the major contributors to the observed NPQ increase (Fig. 3C).

At variance with nitrogen starvation, iron starvation has a more specific effect on LHCX expression. A strong induction of the LHCX2 mRNA and protein levels (Fig. 2) compared with the other isoforms was observed, pinpointing this isoform as the most likely regulator of the increased NPQ capacity observed in iron stress (Fig. 2C). NPQ in iron-limiting conditions is characterized by a slow induction and a complete relaxation in the dark. These slow induction kinetics might reflect either lower concentrations of the pH-activated de-epoxidase enzyme or its cofactor ascorbate (Grouneva *et al.*, 2006) or slower acidification of the thylakoid lumen due to a reduced photosynthetic activity. Indeed, the photosynthetic capacity is severely impaired when iron is limiting, as demonstrated by the reduction in PSI and PSII subunits (Fig. 2B), but also the lower F_v/F_m (Table 2) and $rETR_{PSII}$ (Fig. 2D). The decreased electron flow per PSII could also reflect a decrease in the iron-containing cytochrome b_6f complex, as previously shown for other iron-limited diatoms (Strzepek and Harrison, 2004; Thamatrakoln *et al.*, 2013).

The observations made in this and in previous studies about the complex LHCX regulation in response to different signals prompted us to explore their possible functions in *P. tricornutum*, by modulating their expression in a natural Pt4 strain characterized by constitutive lower NPQ levels (Fig. 4). We observed that the increased expression of all the tested isoforms generates a small but still consistent increase in the NPQ levels, suggesting a potential involvement of the diverse proteins in NPQ modulation, as previously shown for LHCX1 (Bailleul *et al.*, 2010). However, we also noticed that different overexpressing lines with different transcript and protein levels showed a similar NPQ increase. It is difficult to interpret these first results, especially in the case of lines overexpressing LHCX4, whose endogenous expression is inhibited by light (Fig. 1F). They probably reflect the complexity of NPQ regulation in diatoms, where the presence of multiple players (e.g. several LHCXs and enzymes of the xanthophyll cycle) possibly tend to reduce the consequences on NPQ of genetic modifications of the qE machinery.

Finally, the exploration of the 5'-flanking regions and intronic sequences of the *LHCX* genes revealed the presence of known and potentially novel *cis*-regulatory elements that may contribute to the transcriptional regulation of the different isoforms in stress conditions. We revealed an uneven distribution of the CCREs (Ohno *et al.*, 2012; Tanaka *et al.*, 2016) in the four *LHCX* genes that may be linked to their different light-mediated transcriptional responses. In addition, we identified a 7 bp motif in the non-coding sequences of *LHCX2*, *3*, and *4*. Using genome-wide transcriptomic data, we found this motif specifically enriched in long-term nitrogen starvation-induced genes, suggesting a possible involvement in the regulation of gene expression in response to nitrogen fluctuations. Although additional studies are required to demonstrate the functionality of these motifs, their discovery may represent a starting point for the identification of the *LHCX* regulators in the diatom acclimation mechanisms to stress.

Outlook

Here we discovered that the four *P. tricornutum* LHCXs are regulated in a sophisticated way (Fig. 5). Different and probably interconnected regulatory pathways activated by different signals and stresses tightly control the amount of each LHCX isoform in the cell. By narrowing down the specific growth conditions in which the different LHCXs are required, our results set the basis for future work to define the function of each isoform in the regulation of chloroplast physiology. The generation of new transgenic lines in which the content of each LHCX isoform is specifically modulated will be instrumental in assessing whether they act with the NPQ regulator LHCX1, or play other specific roles. Considering the robustness of LHCX1 expression in all the conditions tested, future studies will probably require the use of new LHCX1 loss-of-function diatom strains. Additional information about the association of LHCXs with photosynthetic complexes and pigments will also be necessary to understand the role played by the expanded *LHCX* gene family in the efficient acclimation of diatoms to environmental changes.

Supplementary data

Supplementary data are available at *JXB* online.

Figure S1. Localization of the enriched motifs in non-coding regions of *P. tricornutum LHCX* genes.

Figure S2. Alignment of the LHCX proteins and three-dimensional model of LHCX1.

Figure S3. Expression of the *P. tricornutum* xanthophyll cycle genes in nitrogen starvation.

Table S1. List of the oligonucleotides used in this work.

Acknowledgements

This work was supported by Marie-Curie ITNs CALIPSO (ITN 2013 GA 607607) and AccliPhot (ITN 2012 GA 316427) grants and a Gordon and Betty Moore Foundation grant (GBMF 4966) to AF, the French ANR 'DiaDomOil' PROGRAMME BIO-MATIERES & ENERGIES to AF and GF, and the Marie Curie Zukunftskolleg Incoming Fellowship and a Zukunftskolleg Interim Grant to BL.

References

Alboresi A, Gerotto C, Giacometti GM, Bassi R, Morosinotto T. 2010. Physcomitrella patens mutants affected on heat dissipation clarify the evolution of photoprotection mechanisms upon land colonization. Proceedings of the National Academy of Sciences, USA **107,** 11128–11133.

Alipanah L, Rohloff J, Winge P, Bones AM, Brembu T. 2015. Whole-cell response to nitrogen deprivation in the diatom *Phaeodactylum tricornutum*. Journal of Experimental Botany **66,** 6281–6296.

Allen AE, Dupont CL, Obornik M, *et al.* 2011. Evolution and metabolic significance of the urea cycle in photosynthetic diatoms. Nature **473,** 203–207.

Allen AE, Laroche J, Maheswari U, Lommer M, Schauer N, Lopez PJ, Finazzi G, Fernie AR, Bowler C. 2008. Whole-cell response of the pennate diatom *Phaeodactylum tricornutum* to iron starvation. Proceedings of the National Academy of Sciences, USA **105,** 10438–10443.

Apt KE, Kroth-Pancic PG, Grossman AR. 1996. Stable nuclear transformation of the diatom *Phaeodactylum tricornutum*. Molecular and General Genetics **252,** 572–579.

Armbrust EV, Berges JA, Bowler C, *et al.* 2004. The genome of the diatom *Thalassiosira pseudonana*: ecology, evolution, and metabolism. Science **306,** 79–86.

Arrigo KR, Perovich DK, Pickart RS, *et al.* 2012. Massive phytoplankton blooms under arctic sea ice. Science **336,** 1408–1408.

Ashworth J, Coesel S, Lee A, Armbrust EV, Orellana MV, Baliga NS. 2013. Genome-wide diel growth state transitions in the diatom *Thalassiosira pseudonana*. Proceedings of the National Academy of Sciences, USA **110,** 7518–7523.

Bailey TL, Boden M, Buske FA, Frith M, Grant CE, Clementi L, Ren JY, Li WW, Noble WS. 2009. MEME SUITE: tools for motif discovery and searching. Nucleic Acids Research **37,** W202–W208.

Bailleul B, Berne N, Murik O, *et al.* 2015. Energetic coupling between plastids and mitochondria drives CO_2 assimilation in diatoms. Nature **524,** 366–369.

Bailleul B, Rogato A, de Martino A, Coesel S, Cardol P, Bowler C, Falciatore A, Finazzi G. 2010. An atypical member of the light-harvesting complex stress-related protein family modulates diatom responses to light. Proceedings of the National Academy of Sciences, USA **107,** 18214–18219.

Ballottari M, Truong TB, De Re E, Erickson E, Stella GR, Fleming GR, Bassi R, Niyogi KK. 2016. Identification of pH-sensing sites in the Light Harvesting Complex Stress-Related 3 protein essential for triggering non-photochemical quenching in *Chlamydomonas reinhardtii*. Journal of Biological Chemistry **291,** 7334–7346.

Becker F, Rhiel E. 2006. Immuno-electron microscopic quantification of the fucoxanthin chlorophyll a/c binding polypeptides Fcp2, Fcp4, and Fcp6 of *Cyclotella cryptica* grown under low- and high-light intensities. International Microbiology **9,** 29–36.

Beer A, Juhas M, Buchel C. 2011. Influence of different light intensities and different iron nutrition on the photosynthetic apparatus in the diatom *Cyclotella meneghiniana* (Bacillariophyceae). Journal of Phycology **47,** 1266–1273.

Bilger W, Björkman O. 1990. Role of the xanthophyll cycle in photoprotection elucidated by measurements of light-induced absorbance changes, fluorescence and photosynthesis in leaves of *Hedera canariensis*. Photosynthesis Research **25,** 173–185.

Bowler C, Allen AE, Badger JH, *et al.* 2008. The Phaeodactylum genome reveals the evolutionary history of diatom genomes. Nature **456,** 239–244.

Coesel S, Mangogna M, Ishikawa T, Heijde M, Rogato A, Finazzi G, Todo T, Bowler C, Falciatore A. 2009. Diatom PtCPF1 is a new cryptochrome/photolyase family member with DNA repair and transcription regulation activity. EMBO Reports **10,** 655–661.

Daboussi F, Leduc S, Maréchal A, *et al.* 2014. Genome engineering empowers the diatom *Phaeodactylum tricornutum* for biotechnology. Nature Communications **5,** 3831.

de Baar HJW, Boyd PW, Coale KH, *et al.* 2005. Synthesis of iron fertilization experiments: from the iron age in the age of enlightenment. Journal of Geophysical Research-Oceans **110,** C09S16.

De Martino A, Meichenin A, Shi J, Pan K, Bowler C. 2007. Genetic and phenotypic characterization of *Phaeodactylum tricornutum* (Bacillariophyceae) accessions. Journal of Phycology **43,** 992–1009.

Depauw FA, Rogato A, Ribera d'Alcala M, Falciatore A. 2012. Exploring the molecular basis of responses to light in marine diatoms. Journal of Experimental Botany **63,** 1575–1591.

De Riso V, Raniello R, Maumus F, Rogato A, Bowler C, Falciatore A. 2009. Gene silencing in the marine diatom *Phaeodactylum tricornutum*. Nucleic Acids Research **37,** e96.

Dyhrman ST, Jenkins BD, Rynearson TA, *et al.* 2012. The transcriptome and proteome of the diatom *Thalassiosira pseudonana* reveal a diverse phosphorus stress response. PLoS One **7,** e33768.

Eberhard S, Finazzi G, Wollman FA. 2008. The dynamics of photosynthesis. Annual Review of Genetics **42,** 463–515.

Falciatore A, Casotti R, Leblanc C, Abrescia C, Bowler C. 1999. Transformation of nonselectable reporter genes in marine diatoms. Marine Biotechnology **1,** 239–251.

Falkowski PG, Katz ME, Knoll AH, Quigg A, Raven JA, Schofield O, Taylor FJR. 2004. The evolution of modern eukaryotic phytoplankton. Science **305,** 354–360.

Field CB, Behrenfeld MJ, Randerson JT, Falkowski P. 1998. Primary production of the biosphere: integrating terrestrial and oceanic components. Science **281,** 237–240.

Fortunato AE, Annunziata R, Jaubert M, Bouly JP, Falciatore A. 2015. Dealing with light: the widespread and multitasking cryptochrome/photolyase family in photosynthetic organisms. Journal of Plant Physiology **172,** 42–54.

Fortunato AE, Jaubert M, Enomoto G, *et al.* 2016. Diatom phytochromes reveal the existence of far-red light based sensing in the ocean. The Plant Cell **28,** 616–628.

Gerotto C, Alboresi A, Giacometti GM, Bassi R, Morosinotto T. 2011. Role of PSBS and LHCSR in *Physcomitrella patens* acclimation to high light and low temperature. Plant, Cell and Environment **34,** 922–932.

Goss R, Jakob T. 2010. Regulation and function of xanthophyll cycle-dependent photoprotection in algae. Photosynthesis Research **106,** 103–122.

Goss R, Lepetit B. 2015. Biodiversity of NPQ. Journal of Plant Physiology **172,** 13–32.

Gross M. 2012. The mysteries of the diatoms. Current Biology **22,** R581–R585.

Grouneva I, Jakob T, Wilhelm C, Goss R. 2006. Influence of ascorbate and pH on the activity of the diatom xanthophyll cycle-enzyme diadinoxanthin de-epoxidase. Physiologia Plantarum **126,** 205–211.

Guillard RRL. 1975. Culture of phytoplankton for feeding marine invertebrates. In: Smith WL, Chanley MH, eds. Culture of marine invertebrate animals. New York: Plenum Press, 26–60.

Hockin NL, Mock T, Mulholland F, Kopriva S, Malin G. 2012. The response of diatom central carbon metabolism to nitrogen starvation is different from that of green algae and higher plants. Plant Physiology **158,** 299–312.

Hohner R, Barth J, Magneschi L, Jaeger D, Niehues A, Bald T, Grossman A, Fufezan C, Hippler M. 2013. The metabolic status drives

acclimation of iron deficiency responses in *Chlamydomonas reinhardtii* as revealed by proteomics based hierarchical clustering and reverse genetics. Molecular and Cellular Proteomics **12,** 2774–2790.

Huysman MJ, Fortunato AE, Matthijs M, *et al.* 2013. AUREOCHROME1a-mediated induction of the diatom-specific cyclin dsCYC2 controls the onset of cell division in diatoms (*Phaeodactylum tricornutum*). The Plant Cell **25,** 215–228.

Jarvis P, Lopez-Juez E. 2013. Biogenesis and homeostasis of chloroplasts and other plastids. Nature Reviews Molecular Cell Biology **14,** 787–802.

Johnson X, Vandystadt G, Bujaldon S, Wollman FA, Dubois R, Roussel P, Alric J, Beal D. 2009. A new setup for in vivo fluorescence imaging of photosynthetic activity. Photosynthesis Research **102,** 85–93.

Juhas M, von Zadow A, Spexard M, Schmidt M, Kottke T, Buchel C. 2014. A novel cryptochrome in the diatom *Phaeodactylum tricornutum* influences the regulation of light-harvesting protein levels. FEBS Journal **281,** 2299–2311.

Karas BJ, Diner RE, Lefebvre SC, *et al.* 2015. Designer diatom episomes delivered by bacterial conjugation. Nature Commununications **6,** 6925.

Keeling PJ, Burki F, Wilcox HM, *et al.* 2014. The Marine Microbial Eukaryote Transcriptome Sequencing Project (MMETSP): illuminating the functional diversity of eukaryotic life in the oceans through transcriptome sequencing. PLoS Biology **12,** e1001889.

Kooistra WHCF, Gersonde R, Medlin LK, Mann DG. 2007. The origin and evolution of the diatoms: their adaptation to a planktonic existence. In: Falkowski PG, Knoll AH, eds. Evolution of planktonic photoautotrophs. Burlington, MA: Academic Press, 207–249.

Laroche J, Murray H, Orellana M, Newton J. 1995. Flavodoxin expression as an indicator of iron limitation in marine diatoms. Journal of Phycology **31,** 520–530.

Lavaud J, Goss R. 2014. The peculiar features of non-photochemical fluorescence quenching in diatoms and brown algae. In: Demmig-Adams B, Garab G, Adams WW III, Govindjee, eds. Non-photochemical quenching and energy dissipation in plants, algae and cyanobacteria, Dordretch, The Netherlands: Springer, 421–443.

Lavaud J, Materna AC, Sturm S, Vugrinec S, Kroth PG. 2012. Silencing of the violaxanthin de-epoxidase gene in the diatom *Phaeodactylum tricornutum* reduces diatoxanthin synthesis and non-photochemical quenching. PLoS One **7,** e36806.

Lee MJ, Yaffe MB. 2014. Protein regulation in signal transduction. In: Cantley LC, Hunter T, Sever R, Thorner J, eds. Signal transduction: principles, pathways, and processes. Cold Spring Harbor, NY: Cold Sprring Harbor Laboratory Press, 31–50.

Lepetit B, Sturm S, Rogato A, Gruber A, Sachse M, Falciatore A, Kroth PG, Lavaud J. 2013. High light acclimation in the secondary plastids containing diatom *Phaeodactylum tricornutum* is triggered by the redox state of the plastoquinone pool. Plant Physiology **161,** 853–865.

Levitan O, Dinamarca J, Zelzion E, *et al.* 2015. Remodeling of intermediate metabolism in the diatom *Phaeodactylum tricornutum* under nitrogen stress. Proceedings of the National Academy of Sciences, USA **112,** 412–417.

Livak KJ, Schmittgen TD. 2001. Analysis of relative gene expression data using real-time quantitative PCR and the $2^{-\Delta\Delta Ct}$ method. Methods **25,** 402–408.

Lommer M, Specht M, Roy AS, *et al.* 2012. Genome and low-iron response of an oceanic diatom adapted to chronic iron limitation. Genome Biology **13,** R66.

Marchetti A, Schruth DM, Durkin CA, Parker MS, Kodner RB, Berthiaume CT, Morales R, Allen AE, Armbrust EV. 2012. Comparative metatranscriptomics identifies molecular bases for the physiological responses of phytoplankton to varying iron availability. Proceedings of the National Academy of Sciences, USA **109,** E317–E325.

Margalef R. 1978. Life-forms of phytoplankton as survival alternatives in an unstable environment. Oceanologica Acta **1,** 493–509.

Matthijs M, Fabris M, Broos S, Vyverman W, Goossens A. 2016. Profiling of the early nitrogen stress response in the diatom *Phaeodactylum tricornutum* reveals a novel family of RING-domain transcription factors. Plant Physiology **170,** 489–498.

Maxwell K, Johnson GN. 2000. Chlorophyll fluorescence: a practical guide. Journal of Experimental Botany **51,** 659–668.

Mills MM, Moore CM, Langlois R, Milne A, Achterberg E, Nachtigall K, Lochte K, Geider RJ, La Roche J. 2008. Nitrogen and phosphorus co-limitation of bacterial productivity and growth in the oligotrophic subtropical North Atlantic. Limnology and Oceanography **53,** 824–834.

Montsant A, Andrew EA, Coesel S, *et al.* 2007. Identification and comparative genomic analysis of signaling and regulatory components in the diatom *Thalassiosira pseudonana*. Journal of Phycology **43,** 585–604.

Moore CM, Mills MM, Arrigo KR, *et al.* 2013. Processes and patterns of oceanic nutrient limitation. Nature Geoscience **6,** 701–710.

Morrissey J, Sutak R, Paz-Yepes J, *et al.* 2015. A novel protein, ubiquitous in marine phytoplankton, concentrates iron at the cell surface and facilitates uptake. Current Biology **25,** 364–371.

Moseley JL, Allinger T, Herzog S, Hoerth P, Wehinger E, Merchant S, Hippler M. 2002. Adaptation to Fe-deficiency requires remodeling of the photosynthetic apparatus. EMBO Journal **21,** 6709–6720.

Muhseen ZT, Xiong Q, Chen Z, Ge F. 2015. Proteomics studies on stress responses in diatoms. Proteomics **15,** 3943–3953.

Nymark M, Valle KC, Brembu T, Hancke K, Winge P, Andresen K, Johnsen G, Bones AM. 2009. An integrated analysis of molecular acclimation to high light in the marine diatom *Phaeodactylum tricornutum*. PLoS One **4,** e7743.

Nymark M, Valle KC, Hancke K, Winge P, Andresen K, Johnsen G, Bones AM, Brembu T. 2013. Molecular and photosynthetic responses to prolonged darkness and subsequent acclimation to re-illumination in the diatom *Phaeodactylum tricornutum*. PLoS One **8,** e58722.

Ohno N, Inoue T, Yamashiki R, Nakajima K, Kitahara Y, Ishibashi M, Matsuda Y. 2012. CO(2)-cAMP-responsive cis-elements targeted by a transcription factor with CREB/ATF-like basic zipper domain in the marine diatom *Phaeodactylum tricornutum*. Plant Physiology **158,** 499–513.

Palmucci M, Ratti S, Giordano M. 2011. Ecological and evolutionary implications of carbon allocation in marine phytoplankton as a function of nitrogen availability: a Fourier transform infrared spectroscopy approach. Journal of Phycology **47,** 313–323.

Pearson GA, Lago-Leston A, Cánovas F, Cox CJ, Verret F, Lasternas S, Duarte CM, Agusti S, Serrão EA. 2015. Metatranscriptomes reveal functional variation in diatom communities from the Antartic Peninsula. ISME Journal **9,** 2275–2289.

Peers G, Truong TB, Ostendorf E, Busch A, Elrad D, Grossman AR, Hippler M, Niyogi KK. 2009. An ancient light-harvesting protein is critical for the regulation of algal photosynthesis. Nature **462,** 518–521.

Poulsen N, Kroger N. 2005. A new molecular tool for transgenic diatoms—control of mRNA and protein biosynthesis by an inducible promoter–terminator cassette. FEBS Journal **272,** 3413–3423.

Rayko E, Maumus F, Maheswari U, Jabbari K, Bowler C. 2010. Transcription factor families inferred from genome sequences of photosynthetic stramenopiles. New Phytologist **188,** 52–66.

Reeves S, McMinn A, Martin A. 2011. The effect of prolonged darkness on the growth, recovery and survival of Antarctic sea ice diatoms. Polar Biology **34,** 1019–1032.

Rochaix JD. 2011. Assembly of the photosynthetic apparatus. Plant Physiology **155,** 1493–1500.

Rogato A, Amato A, Iudicone D, Chiurazzi M, Ferrante MI, d'Alcala MR. 2015. The diatom molecular toolkit to handle nitrogen uptake. Marine Genomics **24,** 95–108.

Schellenberger Costa B, Sachse M, Jungandreas A, Bartulos CR, Gruber A, Jakob T, Kroth PG, Wilhelm C. 2013. Aureochrome 1a is involved in the photoacclimation of the diatom *Phaeodactylum tricornutum*. PLoS One **8,** e74451.

Siaut M, Heijde M, Mangogna M, Montsant A, Coesel S, Allen A, Manfredonia A, Falciatore A, Bowler C. 2007. Molecular toolbox for studying diatom biology in *Phaeodactylum tricornutum*. Gene **406,** 23–35.

Sicko-Goad L, Stoermer EF, Kociolek JP. 1989. Diatom resting cell rejuvenation and formation—time course, species records and distribution. Journal of Plankton Research **11,** 375–389.

Stookey LL. 1970. Ferrozine—a new spectrophotometric reagent for iron. Analytical Chemistry **42,** 779–781.

Strzepek RF, Harrison PJ. 2004. Photosynthetic architecture differs in coastal and oceanic diatoms. Nature **431,** 689–692.

Tanaka A, Ohno N, Nakajima K, Matsuda Y. 2016. Light and CO2/cAMP signal cross talk on the promoter elements of chloroplastic

β-carbonic anhydrase genes in the marine diatom *Phaeodactylum tricornutum*. Plant Physiology **170,** 1105–1116.

Thamatrakoln K, Bailleul B, Brown CM, Gorbunov MY, Kustka AB, Frada M, Joliot PA, Falkowski PG, Bidle KD. 2013. Death-specific protein in a marine diatom regulates photosynthetic responses to iron and light availability. Proceedings of the National Academy of Sciences, USA **110,** 20123–20128.

Thamatrakoln K, Korenovska O, Niheu AK, Bidle KD. 2012. Whole-genome expression analysis reveals a role for death-related genes in stress acclimation of the diatom *Thalassiosira pseudonana*. Environmental Microbiology **14,** 67–81.

Trainer VL, Bates SS, Lundholm N, Thessen AE, Cochlan WP, Adams NG, Trick CG. 2012. Pseudo-nitzschia physiological ecology, phylogeny, toxicity, monitoring and impacts on ecosystem health. Harmful Algae **14,** 271–300.

Trentacoste EM, Shrestha RP, Smith SR, Glé C, Hartmann AC, Hildebrand M, Gerwick WH. 2013. Metabolic engineering of lipid catabolism increases microalgal lipid accumulation without compromising growth. Proceedings of the National Academy of Sciences, USA **110,** 19748–19753.

Valle KC, Nymark M, Aamot I, Hancke K, Winge P, Andresen K, Johnsen G, Brembu T, Bones AM. 2014. System responses to equal doses of photosynthetically usable radiation of blue, green, and red light in the marine diatom *Phaeodactylum tricornutum*. PLoS One **9,** e114211.

Walters RG. 2005. Towards an understanding of photosynthetic acclimation. Journal of Experimental Botany **56,** 435–447.

Wilhelm C, Buchel C, Fisahn J, *et al.* 2006. The regulation of carbon and nutrient assimilation in diatoms is significantly different from green algae. Protist **157,** 91–124.

Woodson JD, Chory J. 2008. Coordination of gene expression between organellar and nuclear genomes. Nature Reviews Genetics **9,** 383–395.

Yoshinaga R, Niwa-Kubota M, Matsui H, Matsuda Y. 2014. Characterization of iron-responsive promoters in the marine diatom *Phaeodactylum tricornutum*. Marine Genomics **16,** 55–62.

Zhu SH, Green BR. 2010. Photoprotection in the diatom *Thalassiosira pseudonana*: role of LI818-like proteins in response to high light stress. Biochimica et Biophysica Acta **1797,** 1449–1457.

Supplementary Data

Multi-signal control of the expression of the LHCX protein family in the marine diatom *Phaeodactylum tricornutum*

Lucilla Taddei[,#], Giulio Rocco Stella[#], Alessandra Rogato[#], Benjamin Bailleul, Antonio Emidio Fortunato, Rossella Annunziata, Remo Sanges, Michael Thaler, Bernard Lepetit, Johann Lavaud, Marianne Jaubert, Giovanni Finazzi, Jean-Pierre Bouly, Angela Falciatore

PtLhcx1

5'-flanking sequence

TCAAAGGAAGGAATGTAGAGTAAGCAAACCATCATTTCGCCGCTTCCATTACCAAGAGAACCGACCAAGAGCCCTACCTTGTATGTCATTCGTATAAAC
GTGCACTGAATCGCCCCAGCATGTGAACGCACCATCTCGAATGGCCATCGACAATTCCTTCCGACCGAAAACGCAAACACCACAAGCTTTCTGAGAGGG
CTTATTCTCACATCCGTACATGACATCTTCGTTGAAGTCTACTAGGACAAGAAGCCACCGAGTCTTGTGCCGAACCATCGTGTAGCAAATCGGCGAGGC
GAAGCTATTACAACCTTAACTGGGTCAGTACAGCGTGTTGATTGTGAACAAAACCAATGGCCAGACGGATTCGCAAGTTCACGACAGCTTTCGACGGTG
AGAATGATGGTATCGCTTCGGGTCGGGTCGGTACTTTGCGGGACTGGCAACGTCGGCAGAGGGACTCACGGTCACTTCACTGTCTGTATCGACTGACGA
CTGACTCGTCTGATTCACTGTCAGGTTTCTGATCTAAGTTTATCAAATGCTACTACTTGAGGTAGTCGTATCATTTGAAACTGCAACTTACAAAATCGA
AGGTCCTTGCAACATTTCTGACATGGGTAATTTCATAGGATGTTACAATGTCGAGCTTGTATCACTCGGATACAACAGACCACTTTAGGAAAGGGATTT
TTTTTTGTCGAAAATAGGATGACATCAACAGGAAGTACGTTCATAGCCCTTTATTTATAATTGGATGGGTCAATCCGACGTACGCATGTGTCTTTTGAC
CTTGTCATCCATAACCAGATTGACCCGTCACTGTGCAATACGTCACGCCAATGAAAGACCCCCGGATAAAGGGCCTAAAATTCAGTCTCGTGCAAAACA
CGCAGGATGATGCACCTGAACAGGTGACGTGTTCGCGCAGTCGAATGAGTTCCGAAGCCATCAGAGGCGAATTTATTTTGCAACTGTTTGACCCCATAA
AACCATTCCT

PtLhcx2

5'-flanking sequence

ATCACGTGAGATATCACTGATATCTCACGTCAATAGACAAGCTGCTTTACAATGGGTGAAAACAACCACCACACGAAACAAGTTCCTGTAACTCTAAAT
ATTGATTGTAATTGGTGAAGAAAGCATTTTCCTGACTGTGGGTACATGGAATACATCCTTTTTTGATAAATGTACAAACAAAGACTCATTTACTGTTAG
TCATAGTCAAGCGCAGTGCGTACTTGACTGTGAAAAAATCGAGCTCTGAAAGGGTTAAAGTTCAAGAGGTACAAGGTAGCTGGTTTGCGTGTGTCAGGG
CATGGCCTACCTGACTCATGCATTCCGCGTGCCACAAAAACTCACAGTCAGAGAGCCACTCCGAGAATCCTCCAGAATTTCGTGGAAGATTTTTTCGTC
ATCTTTTTCCAGTTCTCCGCATAGCTCTCATAGTTTCGTTTGCGTTCTTCGTCAACACACCGCAAAAAGATATACGTCCAATTCCAGCCCACTACGTAC
ACC

PtLhcx3

5'-flanking sequence

AGAAATGTCAAGATCATGGATTGGTTTCAAGGACACATGACATTGTAATCCTTACGGCTATTTCGATCCGAACCCAGAGTATGGTAGGTAGGTAGTGAC
ACGAGCGAGTCATAGAATTGTTGTTTGATCAGACAATCTGTACACTTATTCGACCATGTCTATTTATTACCACACGTGTTTGTACGCGCCAAACAGATT
CTTTCGCTAGAATCCGACTGATCGACGACCACACAGAGAGAGGGACTGACGAAGTACAACCACGCGACGAAACCACCACGGCAACACAACATAGCGTTA
ATTTTACAATTAGTGCTGACTAACAGCGTATACTGTCAACAGAGTCCGATGACTGGCTGACAATGACTTGGAACGCCAATTTGCATTGATAGTGACTAT
GAGTTCCAAGCTTCGATCGGGCCGAACCAAGTAGAAAGATACATGTAAACGACTACCTATATACTGGCTGATTCAATCCGACCAGCAGAGTAACCCCAT
CTGGTGTCGATTCCTCTGCGAATACTCTAGAGGTATCACGGTATGTATATAGTATATAGTACTCGTCGCCCACGGTTGTCTTCGATTCCCATCCATCCT
GTTACGGACAGGAACCAGACACGACACGGCCCTACCTCTCCGTATCCGATCCTTGCCATCACTTTTGGGGTACTTTCGAAAAAGACTGATTCATAGTCA
AATGCCTTCTGACGGATCCAGAGGGTACGCAGAGTTCTGCTGACGAACTGTCTCGTACACTCATTCTTGGTTGTGGAAATCATCTCCCTACACACTACG
CTCCAAAATGATAACTCTGCACAATTCACACAATATCCTAAACAGTACACTTGCGATCGCACTTGCAACCCACGTACCACCACCAGTACCAAACACAAT
CATTACACC

intron1

GTACGTCTACGCGAACCTTGGCATTTTCCAGGTACCGCAGTGTCGGTGTGTTACAGTTAGTGTCGTCCGCGATTGCATTCCTCACGAACCACACTCGTT
CCGCTTTGTCCCGGCAG

PtLhcx4

5'-flanking sequence

GAAAACTCTAGCCCGGCACGGCAGGCCGTCCTCTGCACCTGTAGTGAAGCGAATGTCGAATGTCCATGTCGAAGTCGTAGGAGACGCCGACAGAGAAAC
CACGGCTATCATGTAAACAATATGCAAGAGTACCTTACTTATCGAACATGCTGGAGTTATTTGCTGTTGATTTAAGTATAATTTAATTGACGCAGTATA
TATAAATCAGTGCACATAAAGTTTGACGAAACCTCATAGTTCGAGTTTTGTTATGCATCACTGAATTTCCAGAACATGGCAAATCCTGTAACACCTATT
TTTACACTTACATCGATAATTGGTTACAATCAAGCCTTGGCCCACAAGCACCAGCTAACATAAGTGGTCACAGCAATTTTAGTGGTTCGTGTCATACTC
AAGCGACGAATCACCCAATTCTCGGAAGTAAACCGAACTCGATCACGGCGATGCAAGTCCTTTAATTCTCACGAGTCCATCGAACTCGATCACGGCGAT
GCAAGTCCTTTTCTCAGGAGTCCATCGAGCTCGATAACAACGAAGCAGGTCGACGCCACGTGTTCCAGAAATTGGTTGCCTTCTGTCGACTAATCGTTC
TTTCGATCTCGAATGAATTCCTTTTGCTTTCCATACTTGTTGACGTCGTCGAGGGGAGTCTGTGAGAGCAGGCAGCGAGTCGTTACTCCTCGGATTTGT
TCATTCCCAGTCATCGAAGCAGTGGTCGTTTGACTCTCACCTTACAATTTGAGATCCTTGCGGTTTTCGAGAGAGTGAGACACGTCAAACGCACTCAGC
CAGT

```
Motif 1:  TCA[CT][AT]GTCA
Motif 2:  CGAACCTTGG
Motif 3:  CCT[GC]TCCGTA
Motif 4:  GAGTCCATCG
Motif 5:  CGATCACGGC
Motif 6:  [TA]TGACTG
CCRE  1:  TGACGT
CCRE  2:  ACGTCA
CCRE  3:  TGACGC
```

Fig. S1: Localization of the enriched motifs in *LHCXs* non-coding regions.

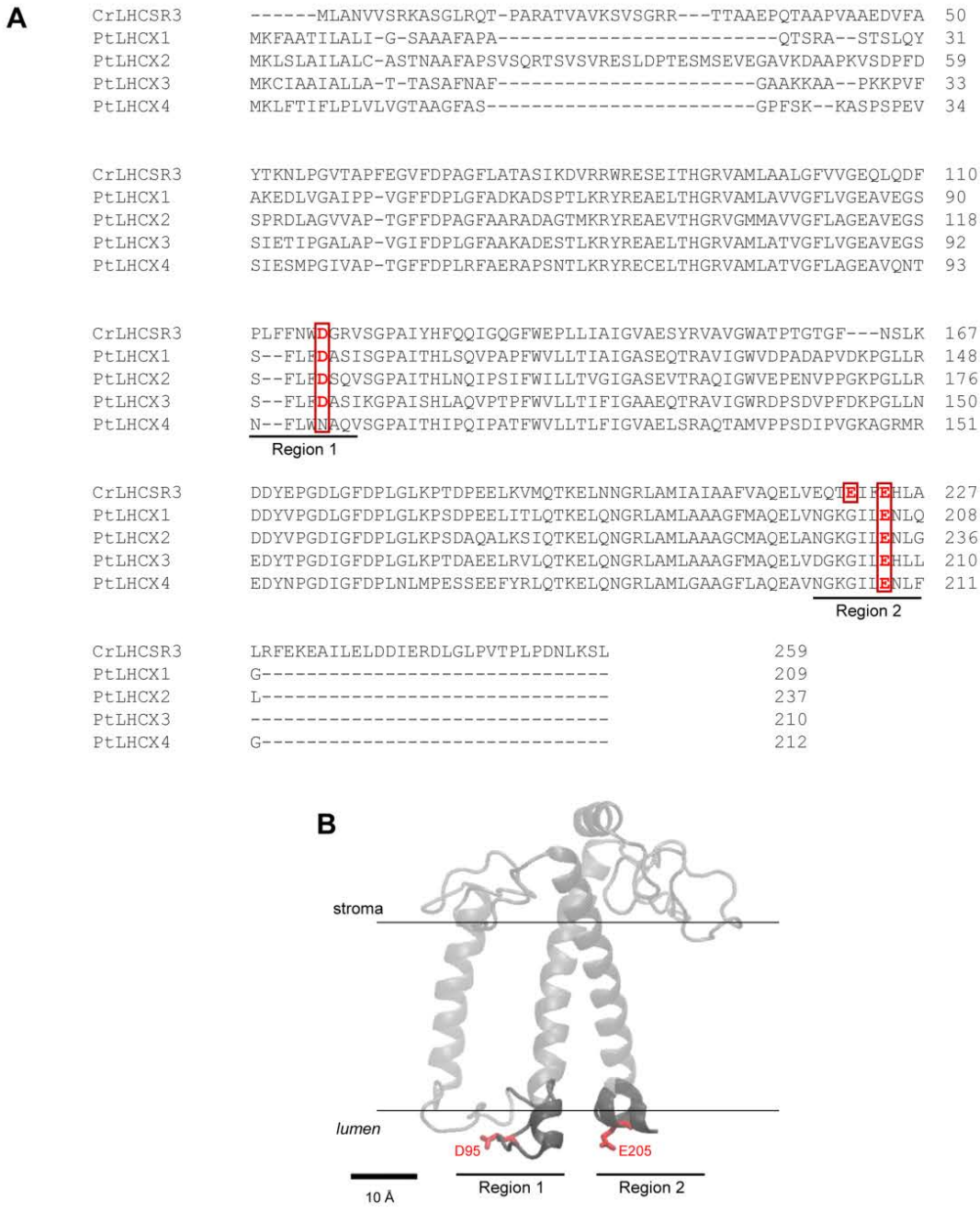

Fig. S2: Alignment of the LHCX proteins and three-dimensional model of the LHCX1. (A) Multiple sequence alignment of *Chlamydomonas reinhardtii* LHCSR3 and the four *Phaeodactylum tricornutum* LHCX proteins. Putative protonatable aminoacids in LHCX proteins conserved with respect to *C. reinhardtii* LHCSR3 (Ballottari et al. 2016) are indicated in red. (B) LHCX1 homology-based model from LHCII and CP29 crystallographic structures. Putative protonatable aminoacids conserved with respect to *C. reinhardtii* LHCSR3 are indicated in red (D95 and E205). Region 1 and 2 refers to part of LHCSR3 putatively exposed to thylakoydal lumen, where pH sensitive residues are located.

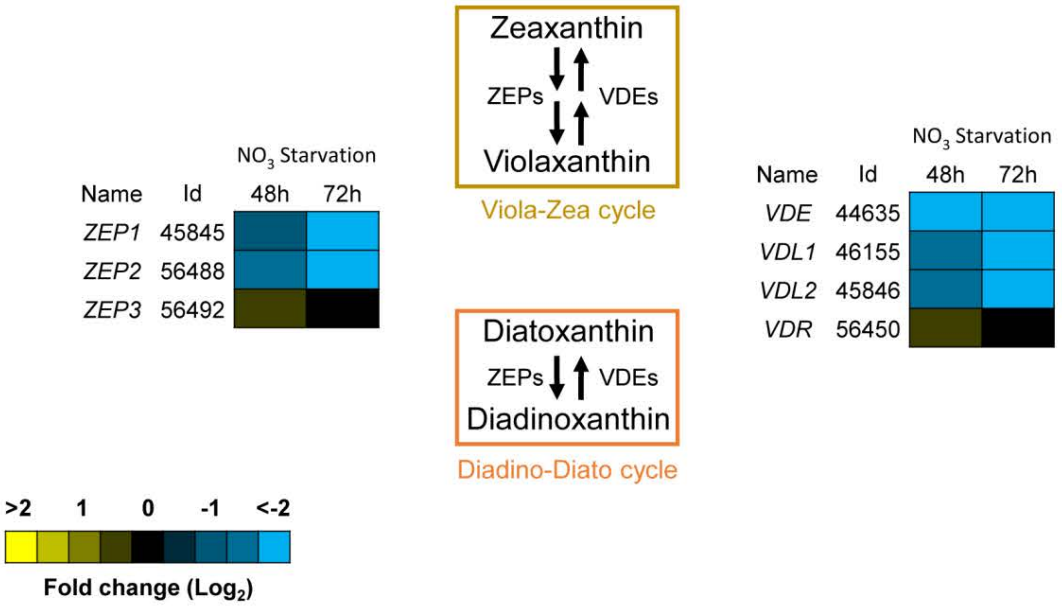

Fig. S3: Expression of *P. triconutum* xanthophyll cycles genes in nitrogen starvation. VDE (violaxanthin de-epoxidase), VDL1-2 (violaxanthin de-epoxidase like 1-2) and VDR (violaxanthin de-epoxidase related) are the enzymes putatively catalyzing the de-epoxidation reactions active in high light to form Zeaxanthin and Diatoxanthin from Violaxanthin and Diadinoxanthin, respectively. ZEP1, 2 and 3 (zeaxanthin epoxidase 1-2 and 3) enzymes putatively catalyse the epoxidation reaction, active in low light, to form Violaxanthin and Diadinoxanthin from Zeaxanthin and Diatoxanthin. Microarray data of cells after 48h and 72h of nitrogen starvation were taken from Alipanah *et al.,* 2015.

qPCR/PCR Oligos

Gene Id (Phatr2)	Oligo Name	Sequence (5' – 3')	Lenght
27278	Lhcx1Fw	CCTTGCTCTTATCGGCTCTG	20
	Lhcx1_Rv	ACGGTATCGCTTCAAAGTGG	20
56312	Lhcx2Fw	CAGCACTAATGCCGCTTTCG	20
	Lhcx2_Rv	CGTGAGTAACTTCCGCTTCC	20
44733	Lhcx3Fw	TCCCGTTGGTATCTTTGATCC	21
	Lhcx3_Rv	GAAGATCCTTCCACGGCTTC	20
38720	Lhcx4Fw	TCTTTGATCCACTCCGCTTC	20
	Lhcx4_Rv	GGCGTTCCATAGAAAGTTCG	20
10847	Rps F	CGAAGTCAACCAGGAAACCAA	21
	Rps R	GTGCAAGAGACCGGACATACC	21
34971	H4 Fw	AGGTCCTTCGCGACAATATC	20
	H4 Rv	ACGGAATCACGAATGACGTT	20

Cloning Oligos

Construct	Oligo Name	Sequence (5' – 3')	Lenght	Restriction Site
27278	L1OE_Fw	acgtGCGGCCGCATGAAGTTCGCTGCCACCATC	33	NotI
	L1OE_Rv	acgtGAATTCttaACCCTGAAGATTCTCAAGGA	33	EcoRI
56312	L2OE_Fw	acgtGCGGCCGCATGAAATTATCCTTGGCTATCC	34	NotI
	L2OE_Rv	acgtGAATTCttaGAGCCCAAGGTTTTCGAGGAT	34	EcoRI
44733	L3OE_Fw	acgtGCGGCCGCATGAAGTGCATCGCCGCTATC	33	NotI
	L3OE_Rv	acgtGAATTCttaGAGGAGGTGTTCCAAGATTCC	34	EcoRI
38720	L4OE_Fw	acgtGCGGCCGCATGAAATTGTTCACCATCTTC	33	NotI
	L4OE_Rv	acgtGAATTCttaGCCAAACAAATTCTCCAAAAT	34	EcoRI

Table S1: List of the oligonucleotides used in this work.

CHAPTER III

Role of LHCX proteins in short- and long-term high light acclimation in *Phaeodactylum tricornutum*

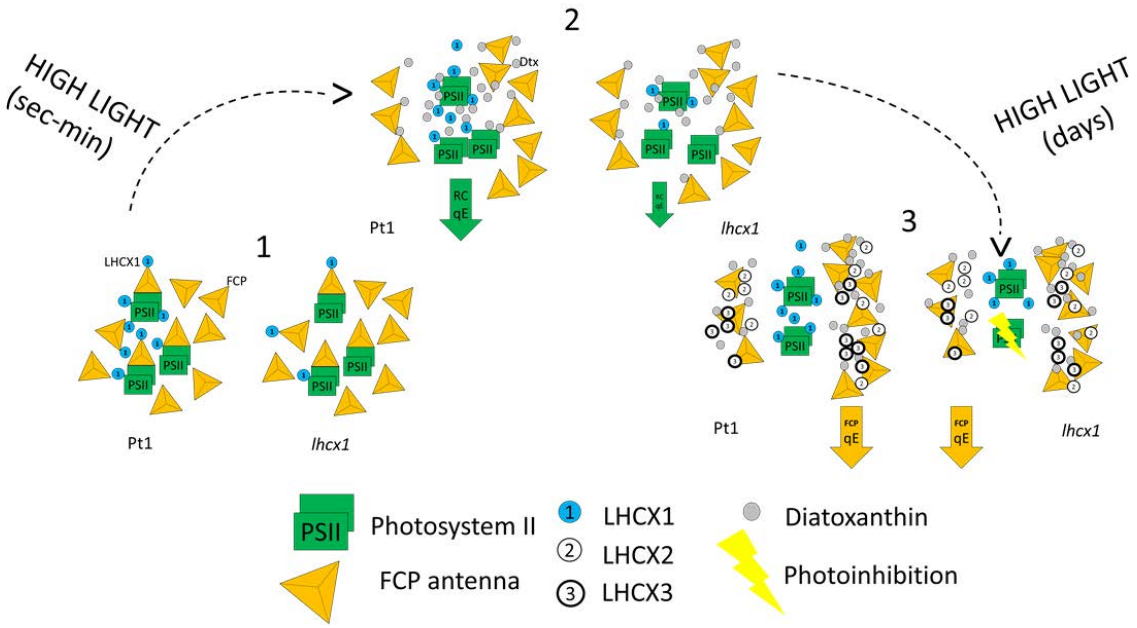

Role of LHCX proteins in short- and long-term high light acclimation in *Phaeodactylum tricornutum*

1. Abstract

The analyses described in the chapter II allowed to identify the environmental factors activating the expression of the four LHCX proteins in the diatom *P. tricornutum*. I also established a correlation between the presence of the four LHCX isoforms and the *P. tricornutum* responses to different signals and stresses.

To date, a role in the NPQ regulation has been proven only for the LHCX1 isoform, by characterizing *lhcx1* knock-down lines that displayed a lower NPQ compared to wild-type cells grown in low light (Beilleul et al. 2010). Initial functional characterizations on the other isoforms indicated that they might also be involved in the chloroplast regulation (Taddei et al. 2016), altough their specific function remained unknown.

Since then, I decided to further extend the characterization of this protein family by performing novel biochemical and biophysical investigations on the *lhcx1* mutant. In particular, I wanted to address the following questions:

- Which is the NPQ phenotype of a mutant with a modulated content of LHCX1 protein under sustained high light stress?
- Which are the quenching sites in short and long-term high light acclimation? Are the quenching sites the same in the different conditions?
- Do the LHCX proteins have a role in these quenching sites formation?
- In which photosynthetic complexes are localized the LHCX proteins?
- If these quenching sites are impaired, which is the effect on the chloroplast and in the cell physiology?

In *P. tricornutum,* LHCX1 is constitutively expressed also when cells are grown in light conditions that do not saturate the photosynthetic capacity and it is essential for NPQ activation after a short high light stress (Bailleul et al. 2010). However, since its functional ortholog in green algae is induced after a sustained high light treatment and so far the role of LHCX1 under constitutive high light (HL) stress conditions was not explored, I decided to challenge the wild-type and the mutant characterized in the previous work, with a sustained high light stress for two days.

To analyse the number and locations of the quenching sites in the photosynthetic complexes, we took advance of a collaboration with Prof. Van Amerongen and Dr. Chukhutsina at Wageningen University who have expertise in localizing the quenching sites of diatoms *in vivo* using a well established ultrafast spectroscopic technique (Chukhutsina et al. 2014). Thanks to these analyses, we could trace differential quenching sites in the low light and high light acclimated cells when are exposed to saturating light intensities.

To correlate the observed quenching sites with the possible activities of the LHCXs, it was important to get additional information on the localization of these proteins in the photosynthetic complexes. To do this, I visited the laboratory of Dr Peter Kroth and the Kostanz University and I performed biochemical characterization of the diatom photosynthetic complexes separated by sucrose-density-gradients centrifugation, under the supervision of Dr. Bernard Lepetit. Western blot analysis on the fractions obtained by the sucrose gradient allowed to localize the LHCXs in different fractions.

The results in the localization were in accordance with the ultrafast spectroscopic analysis and to characterize the macroscopic effect of this mutation, I visited the laboratory of Dr. Giovanni Finazzi at the CEA of Grenoble to performe a detailed analysis of chloroplast physiology.

Finally, these results allowed me to propose a new model for the NPQ regulation in *P. tricornutum* and to associate the discovered quenching sites to the possible activity of different LHCX proteins. This analysis is described in the article "Role of LHCX proteins in short- and long-term high light acclimation in the marine diatom *Phaeodactylum tricornutum",* by Taddei et al., in preparation.

Role of LHCX proteins in short- and long-term high light acclimation in the marine diatom *Phaeodactylum tricornutum*

Lucilla Taddei[1], Volha Chukutsina[2,3], Bernard Lepetit[5], Giulio Rocco Stella[1,4], Herbert Van Amerongen[2], Jean-Pierre Bouly[1], Marianne Jaubert[1], Giovanni Finazzi[6], Angela Falciatore[1]

Affiliations:

[1] Sorbonne Universités, UPMC, Institut de Biologie Paris-Seine, CNRS, Laboratoire de Biologie Computationnelle et Quantitative, 15 rue de l'Ecole de Médecine, 75006 Paris, France.

[2] Laboratory of Biophysics, Wageningen University, 6703HA Wageningen, The Netherlands

[3] Department of Physics and Astronomy, Vrije Universiteit Amsterdam, Amsterdam 1081, The Netherlands

[4] Department of Biotechnology, University of Verona, Strada Le Grazie, I-37134 Verona, Italy

[5] Zukunftskolleg, Department of Plant Ecophysiology, University of Konstanz, 78457 Konstanz, Germany

[6] Laboratoire de Physiologie Cellulaire et Végétale, UMR 5168, Centre National de la Recherche Scientifique (CNRS), Institut National Recherche Agronomique (INRA), Université Grenoble Alpes, Commissariat à l'Energie Atomique et aux Energies Alternatives (CEA), Institut de Biosciences et Biotechnologies de Grenoble, (BIG), CEA Grenoble, F-38054 Grenoble cedex 9, France

To whom correspondence may be addressed: Giovanni Finazzi: giovanni.finazzi@cea.fr; Angela Falciatore: angela.falciatore@upmc.fr

Keywords: Marine diatom; LHCX protein family; Non-Photochemical Quenching of chlorophyll fluorescence; quenching sites; time-resolved spectroscopy.

Abstract

Marine diatoms are prominent phytoplanktonic organisms, optimally performing in a wide range of environments. They show an extraordinary capacity to deal with light stress thanks to an impressive dissipation of the excessive light harvested as heat through the Non Photochemical Quenching (NPQ) process. In diatoms NPQ relies on a light driven proton gradient, the cycling of the xanthophyll pigments and on the LHCX1, a protein of the LHC family involved in photoprotection rather than light harvesting. By combining genetic and biochemical approaches with time-resolved spectroscopy and physiological studies, here we show that the pennate diatom *Phaoedactylum tricornutum* can use two kinds of quenching mechanisms, depending on the light stress conditions. Cells acclimated to low light conditions and suddenly exposed to high light treatments, quench the excessive energy in the Reaction Centre in a LHCX1 dependent-manner. Whereas in cells acclimated to high light, the quenching site is mostly localized in the antenna and it could rely also on the LHCX3 protein. Overall, our data provide a solid molecular interpretation for the extreme flexibility of diatoms with respect to light changes in the marine environments.

2. Introduction

Marine diatoms form a highly diverse group of unicellular algae, that dominates the eukaryotic photosynthetic community in different ocean environments (Depauw et al. 2012; Finazzi et al. 2010; Taddei et al. 2016). They successfully acclimate to a wide range of environmental changes, including nutrient and light. While extensive information is available on the metabolic bases of their nutrient responses (Alipanah et al. 2015; Allen et al. 2008), less is known about the mechanisms used by diatoms to acclimate to changing light environments.

Diatoms respond to light stress via a complex set of xanthophyll cycles, including the conventional plant cycle plus one that is specific for diatoms, catalyzing the de-epoxidation of diadinoxanthin (DD) to diatoxanthin (DT) and the epoxidation from DT to DD (Lohr & Wilhelm 1999; Coesel et al. 2008). Moreover, the LHCX1 gene product plays a major role in light acclimation in the diatom *P. tricornutum* (Bailleul et al. 2010).

This protein belongs to the family of the light-harvesting complex stress-related (LHCSR) proteins. First discovered in *Chlamydomonas reinhardtii* (Peers et al. 2009), these proteins behave as molecular switches for light-acclimation responses, triggering high-energy quenching (qE). The term qE describes the capacity of photosynthetic organisms to increase thermal dissipation of absorbed light when exposed to excess light, to diminish over-excitation of the photosystems and to reduce photodamage. qE is activated when the light-driven electron flux exceeds the capacity of the photosynthetic machinery to assimilate CO_2. The consequent lumenal acidification activates the xanthophyll cycle enzymes (which catalyse carotenoid deepoxidation), and qE protein effectors (the small PSII subunit PSBS in plants and members of the LHCSR family in microalgae and mosses, (Li et al. 2009). LHCSR proteins are also present in diatoms (where they are named LHCX) as evidenced by genomic and functional studies (Bailleul et al. 2010; Zhu & Green 2010; Taddei et al. 2016; Finazzi & Minagawa 2015). In diatoms, LHCX1 belong to an expanded gene family including several members (Zhu & Green 2010; Taddei et al. 2016). While LHCSR3, the qE effector in *Chlamydomonas reinhardtii*, is induced only upon exposure to high light (HL) for several hours (Allorent et al. 2013), LHCX1 is constitutively expressed, similarly to PsbS. Thus, at variance with LHCSR3, both LHCX1

and PSBS provide a constant photoprotection capacity to the photosynthetic cells (Bailleul et al. 2010; Demmig-Adams et al. 2006). Besides LHCX1, other LHCX isoforms exist in diatoms, which are induced under specific environmental conditions known to affect diatom photosynthesis and growth capacities (Taddei et al. 2016), but their role and their localization among photosynthetic pigment-protein complexes is still unclear. Using genetic and biochemical approaches, *in vivo* ultrafast spectroscopy and physiological studies, we demonstrate that, depending on environmental conditions, diatoms develop different types of qE quenching by inducing different LHCX isoforms. In particular, LHCX1 mediates a constitutive quenching process in low-light acclimated cells, occurring in the reactions center of photosystem (PS) II. Conversely, exposure to high light induces a new type of quenching process, which mostly takes place in the antenna complexes, and it is possibly triggered by LHCX3, one of the high light induced LHCX isoforms. Comparison of the physiological responses of *P. tricornutum* wild-type, Pt1, and knock-down lines with reduced LHCX1 content (*lhcx1a*), suggests that the antenna quenching is less effective in photoprotection than the reaction center one. Overall, by revealing the existence of different NPQ sites with different targets and molecular actors, our data provide a new molecular interpretation for the extreme flexibility of diatoms with respect to changes in the light environments in the oceans.

3. Material and Methods

3.1 Diatom growth conditions

Axenic *P. tricornutum* (*P. tricornutum*) cells (Pt1 8.6, CCMP2561), obtained from the Provasoli-Guillard National Center for Culture of Marine Phytoplankton and the *lhcx1a* strain (Bailleul et al. 2010) were grown in f/2 medium at 19 °C in a 12h: 12h light: dark photoperiod. For the following analysis cells were first acclimated to 30 µmol photons $m^{-2} \cdot s^{-1}$ (LL) and then shifted to 500 µmol photons $m^{-2} \cdot s^{-1}$ (HL) white light up to two days: the steady state fluorescence and ultrafast decay associated spectra measurements, the pigment quantification, the photosynthetic complexes purifications, the photosynthetic and respiratory capacities analysis. Cells were collected during the exponential phase of growth. For the analysis of cell growth, cells in their exponential growth phase and

acclimated to LL for several generations were either maintained in LL or exposed to HL conditions. Cell growth was monitored over a period of nine days.

3.2 Room temperature chlorophyll fluorescence measurements

The kinetics of chlorophyll fluorescence yields at room temperature were measured using a fluorescence CCD camera recorder (JTS-10, BeamBio, France (Johnson et al. 2009)) on cells at 1 to $2x10^6$ cells/ml. Before measurements all samples were adapted to dim light (10 μmol $m^{-2} \cdot s^{-1}$) for 15 min at 18 °C to open the reaction centres (RC) to photosynthesis. Fv/Fm was calculated as (Fm-F0)/Fm, where Fm and F0 are the maximum and the minimum fluorescence emission level during a saturating pulse and in the dark, respectively. NPQ was calculated as (Fm-Fm′)/Fm′ (Bilger & Björkman 1990), where Fm′ is the maximum fluorescence emission level in cells exposed to actinic light, measured with the saturating pulse of light. The maximal NPQ response was measured upon exposure for 10 minutes to saturating 950 μmol $m^{-2} \cdot s^{-1}$ green light.

3.3 Isolation of pigment-protein complexes

Thylakoid membranes from *P. tricornutum* were isolated according to (Lepetit et al. 2007) with some modifications. All the isolation steps were performed in dim light and at 4 °C. Cell pellets harvested by centrifugation (3800 rpm, 10 min) were suspended in isolation medium A (10 mM MES at pH 6.5, 2 mM KCl, 5 mM EDTA, and 1M Sorbitol) and disrupted in a French press cell at 12,500 psi. Unbroken cells were separated from broken cells by a centrifugation step at 3,000 rpm for 10 min, then suspended in isolation medium A, and passed through the French press for a second time. After centrifugation, the supernatants of both centrifugation steps were merged and centrifuged at 18,500 rpm for 20 min. Finally, the pelleted thylakoids were suspended in a small amount of isolation medium B (10 mM MES at pH 6.5, 2 mM KCl, and 5 mM EDTA), and Chlorophyll concentration was determined. Equal amounts of isolated thylakoids, corresponding to 0.5-1 mg of total Chlorophyll, were centrifuged for 20 min at 3,000 rpm. The pelleted thylakoids were suspended in n-dodecyl β-D-maltoside (DM) to yield the final detergent/Chlorophyll ratios of 30 corresponding to 3% DM (w/v). The thylakoids were solubilized on ice for 20 min under continuous stirring. After solubilization, the membranes were centrifuged at 300 rpm for 20 min. The supernatant, containing the solubilized pigment-protein

complexes, was collected and immediately applied to the sucrose gradients used for sucrose density gradient centrifugation (SDC). A linear sucrose gradient from 0 to 0.6 M sucrose (w/v, in isolation medium B, complemented with 0.03% DM) was used. The samples were centrifuged for 17 h at 29,000 rpm using a swing-out rotor. After the separation, sucrose gradient bands were harvested with a syringe and stored for further characterization at -80°C.

3.4 Protein analysis by Western Blot

Western blot analysis on total cell protein extracts were performed as previously described (Bailleul et al. 2010) and resolved in 14% LDS-PAGE gels. Proteins were detected by using specific antibodies: anti-LHCSR for the LHCX proteins (dilution 1: 5000, gift of Prof. G. Peers, University of California, Berkeley, CA, USA), anti-D2 for the PSII (dilution 1:10 000; gift of Prof. J.-D. Rochaix, University of Geneva, Switzerland), anti-PsaF for the PSI and anti-ßCF1 for the chloroplastic ATPase (dilution 1: 1000 and 1: 10 000 respectively, gifts of F.-A. Wolllman, Institut de Biologue Physico-Chimique, Paris, France), anti-LHCF1-11 for the LHCF antenna (dilution 1: 2000, gift of Prof. C. Büchel, Institut für Molekulare Biowissenschaften Universität Frankfurt, Frankfurt, Germany). Isolated photosynthetic pigment-protein complexes were extracted as previously described and analyzed by charging 1 µg of Chlorophyll, quantified according to Lohr and Wilhelm (Lohr & Wilhelm 2001), in a 14% LDS-PAGE following the method described in Bailleul et al. (Bailleul et al. 2010). To obtain total cell protein extracts 50–100 µL 1× lysis buffer (Protease Cocktail Inhibitor solution (SIGMA Aldrich) 1x, Tris· HCl pH 6.8 50 mM and 2% lithium dodecyl sulfate (LDS)) were added to pellets, and samples were solubilized by vortexing at room temperature for 30 minutes. After, samples were centrifuged at 15,000 × rpm at 4 °C for 30 min. Protein concentrations were determined using a Pierce BCA Protein Assay Kit (Thermo Fisher Scientific). Equal protein amounts (30 µg total protein) or chlorophyll a concentration (a volume containing 1 µg of chlorophyll photosynthetic extracts) were denaturated at 37°C for one hour in the sample buffer (Tris pH 6.8 0.03 M, LDS 1%, 2-Mercapthoethanol 0.13%, Bromphenolblue a spoon tip, Glycerol 20%) were loaded onto 14% LDS gels (Acrylamide/Bis Solution 37.5:1 BIO-RAD: 14%, Tris-HCl pH 8.45 1 M, LDS 0.3 %, Ammonium Persulfate 0.1%, TEMED 0,6%), with a stacking gel 4% (Acrylamide/Bis Solution 37.5:1 BIO-RAD: 4%, Tris-HCl pH 8.45 0.75

M, LDS 0.3 %, Ammonium Persulfate 0.1%, TEMED 1%). The migration buffer was composed as follow: Tricine 0.1 M, Tris 0.1 M, LDS 0.1%). Proteins were transferred to Nitrocellulose membranes using a Transfer Buffer (Sodium dodecyl sulfate 0.003 M, Tris 0.2 M, Glycine 0.15 M, Ethanol 20%). Membranes were blocked in milk 5% diluted in Phosphate-Buffered Saline (PBS) for one hour at room temperature, before applying the primary antibodies overnight at 4°C. Blots were washed after each incubation with one quick rinse in 1x PBS followed by three washes for 10 minutes each. A HRP-conjugated secondary antibody (1:10,000 dilution; Agrisera) was applied for one hour at room temperature and the membranes were developed using ECL Advance (GE Healthcare). Images of immunoblots were obtained using a CCD imager (ImageQuant LAS 4000; GE Healthcare, Life Sciences).

3.5 Time-resolved emission spectra measurements using the streak-camera set up

Time-resolved emission spectra were recorded using a synchroscan streak-camera system as described in Van Stokkum et al. (Van Stokkum et al., 2008; Van Oort et al. 2010). An excitation wavelength of 540 nm was used to excite preferentially Fucoxanthin (Fx) in the antenna, while 400 nm was used to preferentially excite Chlorophyll a (Chl a). All samples were measured in two different states: original ("unq") state (10 min of dark adaptation); "quenched" state (~10 min of white light preillumination at ~ 400 μmol photons m− 2 s− 1). The laser power was 40-60 μW, the time-window 2 ns, the spot size 100 μm, and the repetition rate 250 kHz. An average of 100 images, all measured for 10 s, was used to achieve a high signal/noise ratio. Before analysis, the images were corrected for background signal and detector sensitivity and sliced up into traces of 5 nm. The streak-camera images were analyzed as described previously (Chukhutsina et al. 2013). In short, a number of parallel, non-interacting kinetic components was used as a kinetic model, so the total dataset was fitted with function f (t, λ):

$$f(t,\lambda) = \sum_{1,2\ldots}^{N} DAS_i(\lambda)\,\exp(-\frac{t}{\tau_i}) \oplus i(t)$$

where DAS (Decay Associated Spectra) is the amplitude factor associated with a decay component i having a decay lifetime τi. A Gaussian-shaped instrument response function (i(t)) was used

as input for the analysis with the width as a free fitting parameter. FWHM values obtained from the fitting procedure were in the range of 28±2 ps. The slowest component was always fixed to 4 ns. This lifetime was obtained independently for many datasets, but due to the limited time window of our setup, it was not possible to resolve it in a reliable way. When we add all 5 DAS for a specific sample and excitation wavelength then we obtain the fluorescence spectrum immediately after excitation (t=0) before any energy transfer has taken place (unless some processes are too fast to be detected). The resulting spectra do not depend on the state of the cells (unquenched/quenched). For comparison, the total fluorescence spectra at t = 0 are normalized to their maximum (as shown in the Supplemental Figure S2), while the DAS are scaled accordingly.

3.6 Pigment preparation and quantification

Pigments from Pt1 wild type and *lhcx1a* mutant cells were extracted using 96% ethanol, buffered with Na_2CO_3. Cells were collected during the NPQ measurement and immediately frozen in liquid nitrogen. Pigment extraction was performed in ice, at the dark, for 30 minutes and centrifuged. The supernatant was loaded in a HPLC Thermo with a detector Diode array for analyze the visible region with a C18 spherisorb column (7.3 x 30mm) and ran using an aqueous mixture of acetonitrile/methanol/0.1 M Tris- HCI buffer (pH 8.0) (72:8:3, buffer A) and a methanol hexane mixture (4:1, buffer B). The runs were done at a flux of 1.5 mL, starting with 100% buffer A: 0-5 min 97% A, 5-17 min a gradient to 80% A, 17-18 min to 100% of buffer B, 18-23 min 100% B. Pigments are distinguishable by the retention time and by the absorption spectrum.

3.7 Oxygen evolution and consumption analysis

Rates of oxygen evolution and consumption were measured with a Clark electrode (Hansatech) at different light intensities (0, 90, 200, 450, 750, and 2300 μmol photons $m^{-2} \cdot s^{-1}$) and the measurement was taken when the signal was stable. To minimize the photodamage, light was changed every two minutes and cells were left to relax in the dark between measurements.

4. Results

4.1 LHCX1 knock-down line shows a comparable NPQ capacity to Pt1 under high-light stress

P. tricornutum possesses four LHCX proteins. Among them, the LHCX1 is constitutive, while the other three isoforms (LHCX 2-4) are differently expressed under various light and dark treatments and nutrient limitation conditions (Taddei et al. 2016). LHCX1 is the most abundant isoform in cells grown in non-stressful light conditions, where it modulates the NPQ capacity in low-light (LL) grown cells. This is revealed by the phenotype of the *P. tricornutum lhcx1a* line, which shows reduced NPQ capacity as compared to the wild-type Pt1 ecotype in LL, i.e. the light regime usually employed to grow this diatom in the laboratory (Figure 1 A, Bailleul et al. 2010). So far, the role of LHCX1 under high light (HL) stress conditions was not explored. To address this point, we compared the NPQ responses in Pt1 and *lhcx1a* cell lines adapted to LL (30 µmol photons $m^{-2} \cdot s^{-1}$, 12:12 h L:D cycle) or to HL (500 µmol photons $m^{-2} \cdot s^{-1}$, 12:12 h L:D cycle) for two days (Figure 1 A- B). We found that NPQ increased upon high light exposure (Fig. 1 A-B) in both Pt1 and mutant cells, but the relative NPQ increase was larger in the latter, even though the LHCX1 was still silenced (Figure 1.C). As a consequence, the NPQ capacity is no longer different for the two strains in HL (Figure 1 A-B).

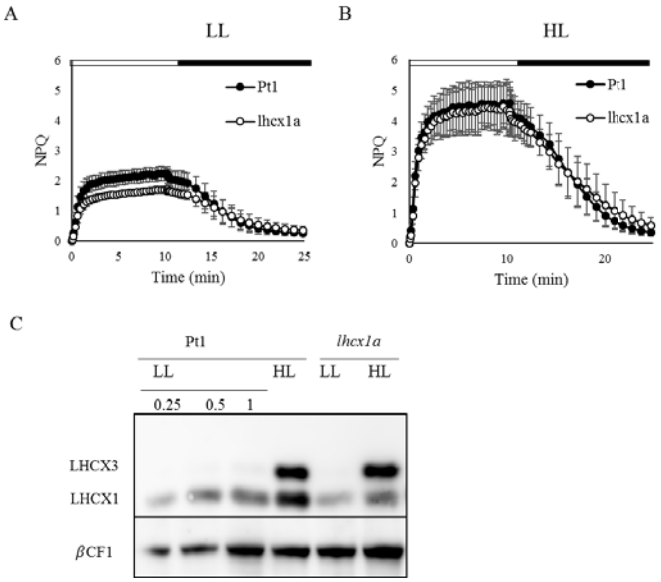

Figure 1. *lhcx1a* line loses its reduced NPQ phenotype during prolonged HL exposure. NPQ capacity in *P. tricornutum* (black) and *lhcx1a* (white) cells grown under low light, LL (30 µmol photons m^{-2} s^{-1}

(panel A), or under high light (HL) (500 µmol photons m^{-2} s^{-1}) for 2 days (2dHL, panel B). (C) Western blotting showing LHCX protein accumulation. Proteins were detected with antibodies against the LHCSR/LHCX and the βCF1 protein has been used as loading control.

In plants, changes in the NPQ capacity are related to changes of the pigment composition, and of the content of NPQ protein effectors (Li et al. 2002). This prompted us to investigate these parameters in wild-type Pt1 and *lhcx1a* cells in LL and HL. Analysis of pigments extracted from Pt1 and *lhcx1a* (Table 1) revealed that HL exposure triggered a similar increase of both the diadino/diatoxanthin and viola/antera/zeaxanthin (VAZ) pools. Thus, while changes in the xanthophyll cycle pigments could account for the higher NPQ observed in HL cells, these changes are likely not responsible for the recovery of Pt1 NPQ in *lhcx1a* cells upon exposure to HL. Immunoblot analysis showed that although LHCX1 was induced in HL, *lhcx1a* cells maintained a lower LHCX1 content than Pt1 even upon HL exposure. Other isoforms were also induced in this condition. In particular, the LHCX3 isoform (Figure 1C) and to a less extent also the LHCX2 (Taddei et al., 2016) accumulated in the thylakoid membranes of both genotypes upon shifting from LL to HL. Based on these findings, we conclude that LHCX1 and the xanthophyll cycle pigments are not responsible for the NPQ recovery in mutant cells, while other LHCX isoforms could be involved in this phenomenon. Their induction in HL could provide an "extra" qE capacity in the *lhcx1a* mutant, thereby increasing its NPQ to Pt1 levels.

Strain	DES diadino/diato	DES viola/zea	total xanthophylls	diadinoxanthin	diatoxanthin	violaxanthin	zeaxanthin
Pt1 LL	0.55±0.05	0.17±0.03	0,14±0,02	0,054±0,0148	0,063±0,0086	0,0031±0,0005	0,0001±0,0001
Pt1 HL	0.75±0.07	0.57±0.03	0,55±0,02	0,118±0,0086	0,343±0,0158	0,0099±0,0037	0,0161±0,0073
lhcx1a LL	0.49±0.04	0.29±0.05	0,16±0,03	0,072±0,0249	0,065±0,0142	0,0014±0,0003	0,0001±0,0001
lhcx1a HL	0.72±0.03	0.57±0.08	0,61±0,04	**0,160±0,0114**	0,407±0,0455	0,0015±0,0005	0,0037±0,0027

Table 1. Pigment composition of *P. tricornutum* wild-type and *lhcx1a* knock-down lines grown either in low (LL (30 µmol photons m^{-2} s^{-1}) or high light (500 µmol photons m^{-2} s^{-1}) for two days. Cells were collected by quick filtration and pigments were extracted in Ethanol 96% buffered with Na_2CO_3. Pigment composition was measured as described in Material and Methods. Pigment concentration normalized to chl a content (mol/mol). Diadino, diadinoxanthin; diato, diatoxanthin; viola, violaxanthin; zea, zeaxanthin. SD is relative to three independent biological replicas. In bold are indicated the values which are statistically different compared to WT cells in the same condition (p-value < 0.05).

4.2 High-light exposure induces a change in the NPQ mechanism and site in *P. tricornutum* cells

A previous work has shown that different types of quenching can occur in the diatoms *Cyclotella meneghiniana* and *P. tricornutum* (Miloslavina et al. 2009; Chukhutsina et al. 2014). One is mostly localized in the antenna complexes, while the second one is mainly located near the PSII reaction centers, and it is longer-lived upon going back to the dark (Chukhutsina et al. 2014). To gain further information about the molecular nature of the NPQ observed for LL and HL cells, we used the same well-established time-resolved fluorescence approach (Miloslavina et al. 2009; Chukhutsina et al. 2014) and compared the *lhcx1* and wild-type Pt1 cells in the two conditions, using a streak-camera setup at 77 K. In order to test the possible involvement of the Reaction Centers (RCs) and the antenna, also called Fucoxanthin Complex Binding Proteins (FCP), in NPQ in LL and HL, different pigment pools were selectively excited. We used 540 nm (monochromatic) laser pulses to preferentially excite the antenna complexes via Fucoxanthin (Fx) (Lepetit et al. 2010), while employing 400 nm to excite mainly chlorophyll a (Chl) (Chukhutsina et al. 2013; Szabó et al. 2008), and thus both reaction centers and FCPs. Time-resolved fluorescence emission data were fitted globally to evaluate the decay lifetimes and the associated decay-associated spectra (DAS) (Van Stokkum et al. 2004).

We found that five DAS corresponding to decay lifetimes of 14 ps, 64 ps, 242 ps, 0.8 ns and 4 ns were required to reproduce the fluorescence decay spectra in Pt1 LL upon 400 nm excitation (Figure 2A). The amplitudes of the three fastest DAS reflect excitation energy transfer (EET) processes. For example, the shortest component has a DAS with a positive peak at 685 nm and two negative bands at 700 nm and 720 nm, respectively. Therefore, excitation energy transfer (EET) from Chlorophylls with fluorescence peaking around 685 nm (Chl685) to Chl700 and Chl720 takes place. The 0.8-ns and 4-ns DAS represent decay processes as witnessed by their positive amplitudes: the 0.8-ns component, assigned to Photosystem II (PSII) and Photosystem I (PSI) according to the spectral shape (see Supplementary Material for details). The spectral shape and lifetime of the 4-ns is characteristic for red antennas in diatoms (Chukhutsina et al. 2014; Herbstová et al. 2015). In HL cells, four components were required to obtain a good fit: 13 ps, 104 ps, 467 ps and 4 ns, respectively (Figure 2 B). The 13-ps DAS

largely represents EET within/between FCPs and from FCP towards PSII cores (see also (Chukhutsina et al., 2014; Ikeda et al., 2008)). FCP as well as PSII emission contributes to the 104-ps component. The 467-ps component peaks at 690 nm and represents mainly Chl685 of PSII and some smaller contribution of PSI. In the wild-type Pt1 cells in HL, the red antenna does not contribute to the 4-ns component, in contrast to the LL-grown cells: the 4-ns DAS peaks at 700 nm, pointing to the PSII-related origin of the fluorescence. Such a long-lived PSII-related component was not observed in Pt1 cells grown in LL, therefore it might originate from deactivated/photoinhibited PSII. The lifetimes are rather similar for different excitation wavelengths and strains regardless of the measured state (unquenched/quenched) (Table S2). On the other hand, significant differences were seen in the relative contribution and in the shape of the DAS in the different cells (Figure S1, S2, Supplementary Material). To discrimate between the NPQ sites (antenna- or RCs–related), we analyzed the difference between time-resolved fluorescence measured for unquenched and quenched states upon Chl a and Fx excitations. We found that in Pt1 LL-grown cells, the average lifetime calculated in the region of PSII emission maxima (685 nm) decreases by 100 ps in the quenched state, while it only decreases by 8 ps upon Fx excitation. In contrast, the average lifetime increases for the quenched state in the region of PSII emission in lhcx1 LL- grown cells for both excitation wavelengths (Table 2). This suggests that, in Pt1 LL grown cells, quenching takes place in the “red antenna”, and in RCs. On the other hand, fluorescence quenching mostly occurs in the “red antenna” in *lhcx1a* LL grown cells, while quenching in RC is almost undetectable (at variance with Pt1). Indeed, a decrease of lifetime upon quenching in this sample is only observed at 720 nm, which is the “red antenna” emission maximum.

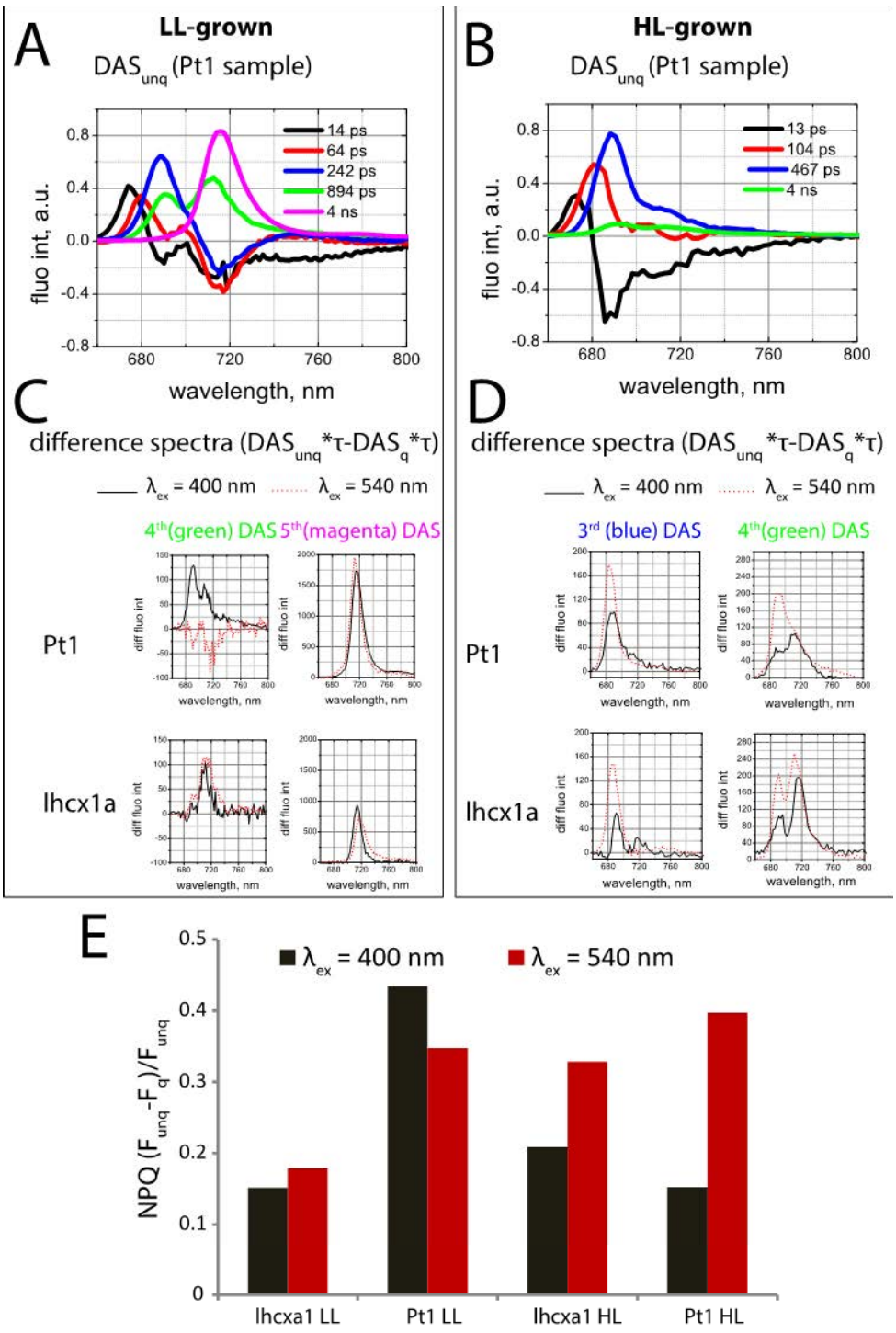

Figure 2. Time-resolved fluorescence and revealed quenching sites. A, B: DAS for Pt1 low-light- (A) and high-light- (B) grown cells measured in unquenched state upon 400 nm excitation at 77 K. C, D: Difference between DASunq and DASq of Pt1 and *lhcx1a* cells grown in low light (C) and high light (D). Black solid lines: difference spectra obtained upon 400 nm excitation; red dotted lines: difference spectra obtained upon 540 nm excitation. To make a direct comparison of the changes in the DAS, we had to correct for the small differences in the lifetimes of the components. Spectra were multiplied by corresponding lifetimes before subtraction (DASunq*τunq-DASq*τq). (E) Amount of total fluorescence decrease upon NPQ, calculated as (Funq-Fq)/Funq, where F (reconstructed total fluorescence yield) was calculated as:

$$F = \sum_{\lambda} \sum_{i} DAS_i(\lambda) * \tau_i$$

where λ is detection wavelength.

To further discriminate the NPQ sites, we also calculated difference spectra between the corresponding DAS in unquenched and quenched states for LL grown samples. Negative difference spectra represent decrease of fluorescence in the quenched state, while positive spectra indicate a fluorescence increase. In Pt1 LL grown cells we mainly observed a decrease of the PSII-related emission (685-700 nm region) in the 4th difference DAS (lifetime 0.8 – 1 ns) upon quenching (Figure 2C). This decrease of PSII-related emission was only observed upon excitation of Chl a at 400 nm, but not upon excitation of the FCPs. We also observed a decrease of the 4-ns DAS upon quenching at both excitation wavelengths for Pt1 LL-grown cells. In the *lhcx1a* strain Chl a –specific quenching previously assigned to PSII cores (4th DAS) is not observed as opposed to the quenching of red antenna in the 5th DAS. Consistent with this observation, around 45% of the total fluorescence is quenched upon excitation in the Chl a absorption region as compared to only 35% upon antenna excitation via fucoxanthin (Figure 2E) in Pt1. In Pt1 HL cells, we observed that quenching is predominantly localized in FCP. First of all, fluorescence quenching of the 3rd DAS at 685 nm (corresponding to the lifetimes of 450-590 ps) was more pronounced upon excitation of FCPs than upon Chl a excitation (Figure 2D). Furthermore, upon antenna excitation the amplitude of the 4-ns component also decreased to a higher extent as compared to Chl excitation. This suggests that both quenching processes are mostly antenna-related. Unlike in LL grown strains, the total amount of fluorescence quenching is similar in the HL exposed *lhcx1a* line and the HL Pt1 cells (Figure 2 E), in accordance with steady-state room temperature fluorescence measurements (Figure 1 B).

	λ_{ex} = 400nm			λ_{ex} = 540 nm		
Pt1 LL						
λ_{det}	685 nm	700 nm	720 nm	685 nm	700 nm	720 nm
τ_{unq} , ps	512	1301	3683	485	1540	4705
τ_{q} , ps	418	1014	2712	477	1122	3413
diff, ps	*94*	*286*	*971*	*8*	*418*	*1292*
Pt1 HL						
λ_{det}	685 nm	700 nm	720 nm	685 nm	700 nm	720 nm
τ_{unq} , ps	530	952	1545	808	1861	2264
τ_{q} , ps	532	865	1263	523	1164	1460
diff, ps	*-3*	*87*	*282*	*285*	*696*	*805*
***lhcx1a* LL**						
λ_{det}	685 nm	700 nm	720 nm	685 nm	700 nm	720 nm
τ_{unq} , ps	500	1279	3574	575	1506	4946
T_{q} , ps	591	1227	3238	593	1610	4685
diff, ps	*-91*	*52*	*336*	*-19*	*-103*	*262*
***lhcx1a* HL**						
λ_{det}	685 nm	700 nm	720 nm	685 nm	700 nm	720 nm
τ_{unq} , ps	492	815	2465	627	1228	4321
τ_{q} , ps	353	627	1780	409	815	2673
diff, ps	*139*	*188*	*685*	*219*	*413*	*1649*

Table 2. Calculated averaged lifetimes at characteristic wavelengths in *P. tricornutum* (Pt1) and *lhcx1a* knock-down line grown in low light (LL) or high light (HL). τunq, average lifetime of the cells in unquenched state; τq , average lifetime of the cells in quenched state; diff, difference τunq -τq.

Overall, the ultrafast fluorescence results indicate that a substantial fraction of quenching stems from a reaction-center based phenomenon in LL grown cells, while quenching is mostly localized in the antenna proteins in HL treated cells. We made the hypothesis that the different quenching sites in HL and LL cells could reflect a heterogeneous distribution of the differentially expressed LHCX isoforms in the chloroplast fractions. Previously published proteomic studies indicated that LHCX1 is localized

either in the FCP complexes (Szabó et al. 2010; Schaller-Laudel et al. 2015) or in PSI (Grouneva et al. 2011). LHCX2 has also been detected in FCP complexes (Szabó et al. 2010) and in a fraction containing all loose proteins of different origins designated as free protein fraction (Grouneva et al. 2011). On the other hand, no clear information was provided on LHCX3, which, according to our gene expression analysis, could be a major player of NPQ in HL. Therefore, to establish a possible involvement of the different LHCXs in the observed quenching sites, we investigated their localization in the thylakoid membranes of *P. tricornutum* using a biochemical approach.

Starting from detergent treated thylakoids, we purified the photosynthetic complexes by sucrose density gradient centrifugation (Figure 3A), and tested the different fractions for their content of LHCX proteins by western blot analysis. Five distinct fractions were isolated from LL and HL wild-type Pt1 and *lhcx1a* strains (Figure 3 A): Free Pigments, FCPs, PSII monomers, PSI fraction and PSII dimers. Immunoblot analyses confirmed that LHCX1 is the only isoform to be expressed in LL. This protein was found in all the purified fractions (thylakoidal membranes, FCP, PSI and PSII dimers, Figure 3 B), although in a lower amount in samples isolated from *lhcx1a* cells. On the other hand, LHCX3, which was only present in HL cells, turned to have a more specific localization, being only found in the FCP and PSI fractions (Figure 3 B).

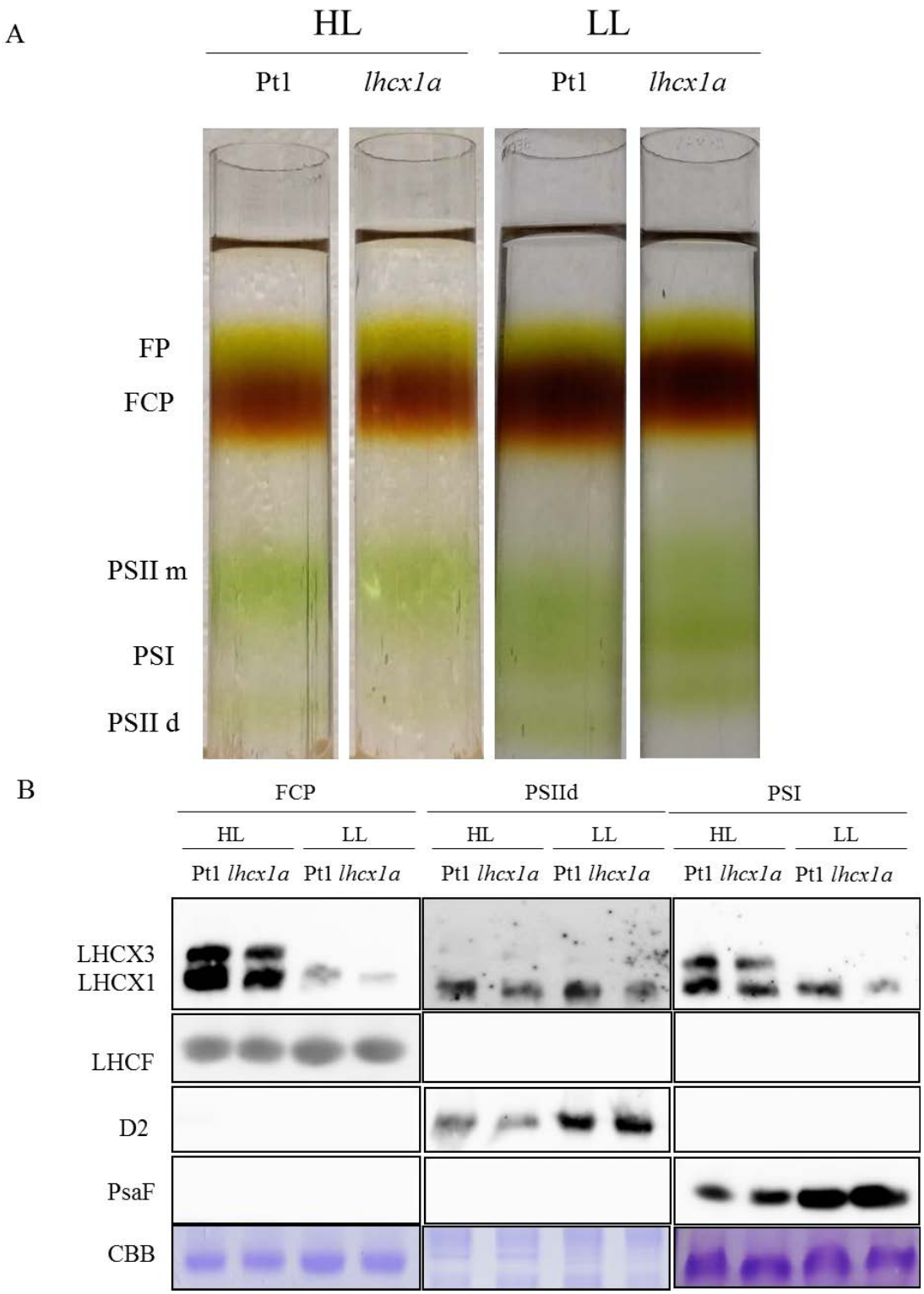

Figure 3. Localization of the LHCX isoforms in different chloroplast fractions. (A) Sucrose density gradient fractionation of solubilized thylakoids from Pt1 and *lhcx1a* strains grown in LL and in HL for two days. The abbreviations used for the fractions are: FP, free pigments; FCP, fucoxanthin chlorophyll binding protein complex; PSI, photosystem I; PSII m is photosystem II monomers; PSII d is PSII dimers. (B) Western blot analysis of the proteins extracted from the Thylakoids and the FCP, PSII and PSI fractions. Samples at equal total Chl concentration (1 µg) were applied to the gels. Proteins were detected with antibodies against the LHCSR/LHCX. The Coomassie blue staining of the protein gel is also indicated.

Overall, the comparison between the fluorescence lifetime analysis and the biochemical analysis of *P. tricornutum* wild-type and mutant cells acclimated to LL and HL suggests that the Reaction Centre quenching is linked to LHCX1. Indeed, this is the only isoform found in the Reaction centers, where quenching is mostly induced in LL. Moreover, decreasing this isoform in the *lhcx1a* strains strongly diminished the Reaction Centre quenching. On the other hand, quenching in the antenna could be related to the inducible LHCX proteins, and possibly to LHCX3. Indeed, HL triggers the induction of this isoform, which is localized in the antenna, i.e. the major site of quenching in HL.

4.3 Consequences of "antenna" and "reaction center" localized quenching on light acclimation in *P. tricornutum* cells.

In plants, qE is mostly localized in the antenna complexes. Although the existence of reaction center quenching has been proposed (Weis & Berry 1987), its occurrence *in vivo* is likely limited only to the first seconds of illumination of dark-adapted plants (Finazzi et al. 2004), while antenna quenching dominates in steady-state conditions. In diatoms, our findings indicate that reaction center qE largely dominates NPQ in low light grown cells, while antenna quenching becomes prominent upon prolonged exposure to HL. These data open therefore the possibility to compare the relative efficiency of the two types of quenching (the "reaction center" and the "antenna" localized one) in protecting *P. tricornutum* cells from photodamage. Indeed, while *lhcx1a* cells display a significantly reduced NPQ capacity in LL, because of their reduced reaction center quenching, these cells show a similar response as Pt1 in HL, owing to compensation by the "antenna" quenching. We reasoned therefore that if both quenching phenomena were equally efficient in protecting cells, *lhcx1a* cells should be more prone to photodamage than the WT in LL, while being equally resistant to light upon transfer to HL conditions.

To test this, we compared photosynthetic activity in the wild-type Pt1 and *lhcx1a* cells in both LL and HL conditions. We found that Pt1 cells reached a higher photosynthetic activity upon exposure to HL for two days, indicating that the cells had properly acclimated to the higher photon flux (Figure 4 B). A similar effect was also found at the level of respiration (Table S1). Consistent with a higher photosynthetic capacity, Pt1 reached a higher cell concentration in HL than in LL (Figure 4 C-D). On the contrary, HL exposure for 2 days led to a reduced photosynthetic and respiration capacity in *lhcx1a*

cells, (Figure 4B and Table S1) thereby limiting the growth capacity (Figure 4 D). This suggests that despite its increased NPQ capacity, *lhcx1a* cells are prone to photoinhibition also in HL. This conclusion was directly supported by biochemical assessment of the PSII level by western blot analysis, using specific antibodies for the LHCX proteins, the PSII (D2) and PSI (PsaF) photosynthetic subunits (Fig 4 E), and the ATPase complex (β-CF1). These analyses indicated a reduction of PSII subunits in Pt1 cells acclimated to HL for 2 days, as compared to the LL irradiated cells, which is also faintly visible in the photosynthetic complexes protein analysis.

This suggests that *P. tricornutum* responds to increasing light intensities by reducing the number of reaction centres, a known strategy in diatoms and other microalgae named the n-type photoacclimation by Falkowski and Owens (Falkowski & Owens 1980). The mutant, showed a similar photoacclimation profile to the wild type Pt1, but the reduction of the PSII subunits after the HL stress was more important as compared to the Pt1. Altogether, the data suggest that despite compensation of the reaction center quenching by the enhanced antenna quenching, mutant cells are more sensitive to HL stress than the Pt1 ones.

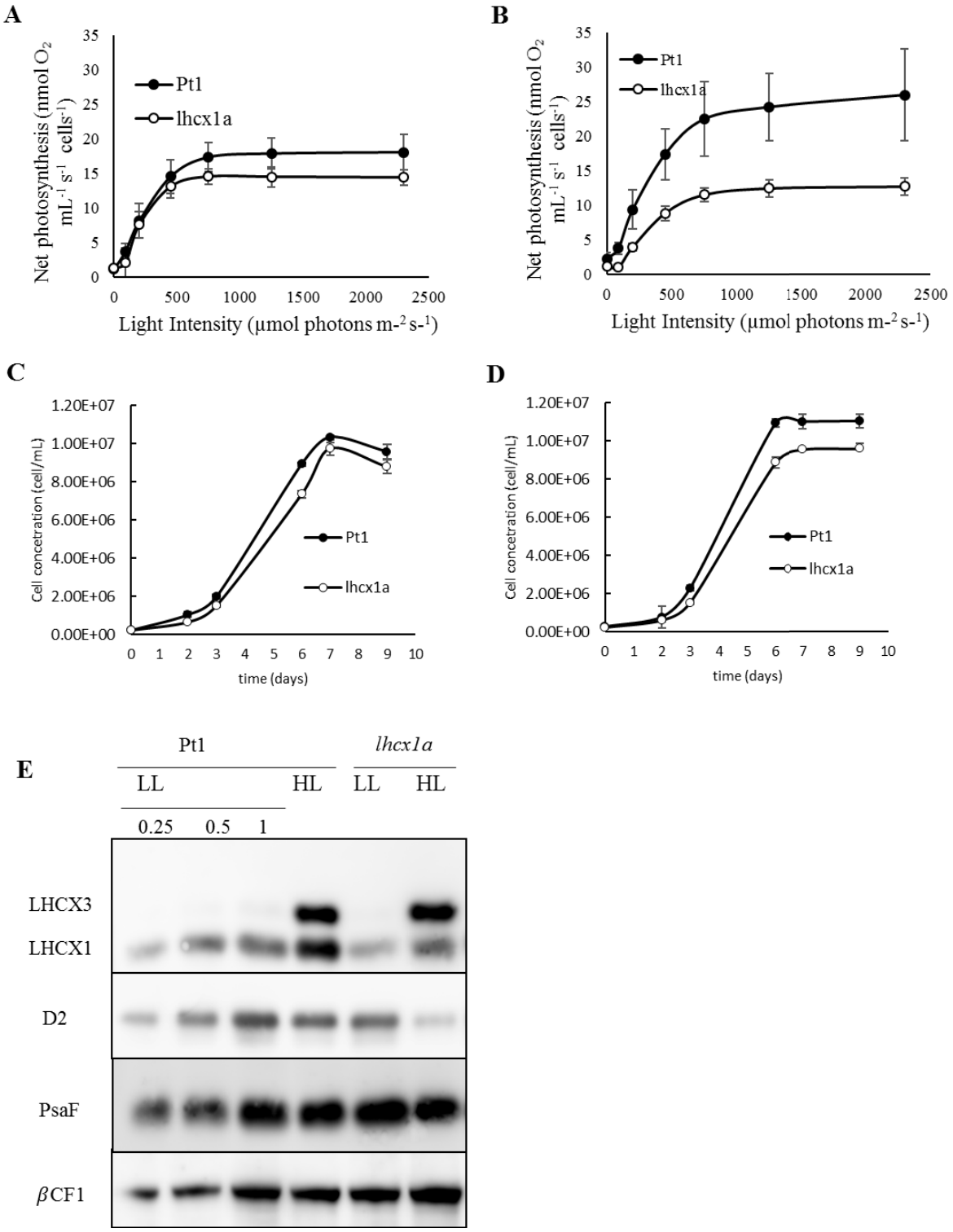

Figure 4. Physiological analysis of Pt1 and *lhcx1a* cells grown in low light and in high light conditions. (A-B) Net photosynthesis derived from the oxygen evolution rates, measured with a Clark electrode (Hansatech) at different light intensities (0, 90, 200, 450, 750, and 2300 µmol photons m^{-2} s^{-1}) from cells grown in LL (A, 30 µmol photons m^{-2} s^{-1}) and in high light (B, 500 µmol photons m^{-2} s^{-1}) for two days, 2dHL. (C-D) Growth curve obtained by counting the number of wild-type and *lhcx-1a* cells in LL (C) or following a LL to HL shift (D) during ten days. (E) Western blot analysis of total protein extracts (30 µg) from the same cells used in the analysis in A and B.

5. Discussion

Taken together our results are consistent with the recent idea that two different sites of quenching exist in diatoms: the reaction center and the antenna ones (Chukhutsina et al. 2014). Reaction-center quenching is the dominant form of quenching in low-light grown cells, while the antenna one becomes predominant upon exposure to high light. This notion is recapitulated in Figure 5, where we propose that after a brief exposure to HL in the wild-type Pt1 low light grown cells the major quenching site is triggered by LHCX1 and occurs in the Reaction Center (2 in the Figure 5). This explains why cells with a lower LHCX1 content display reduced NPQ capacity. Prolonged high-light treatment (days) leads to the accumulation of other inducible LHCX proteins, thereby shifting the quenching site to the FCPs, where these proteins preferentially localize (3 in the Figure 5). While previous analysis has suggested that the two quenchings have different dynamics of onset and relaxation, our data also show that they have a different capacity of protecting the photosynthetic apparatus against stress. Reaction Centre quenching seems to be particularly efficient in protecting cells from light stress, as shown by the fact that despite the increased NPQ capacity in HL, mutants with a reduced content of LHCX1 are more prone to photoinhibition than the WT (3 in the Figure).

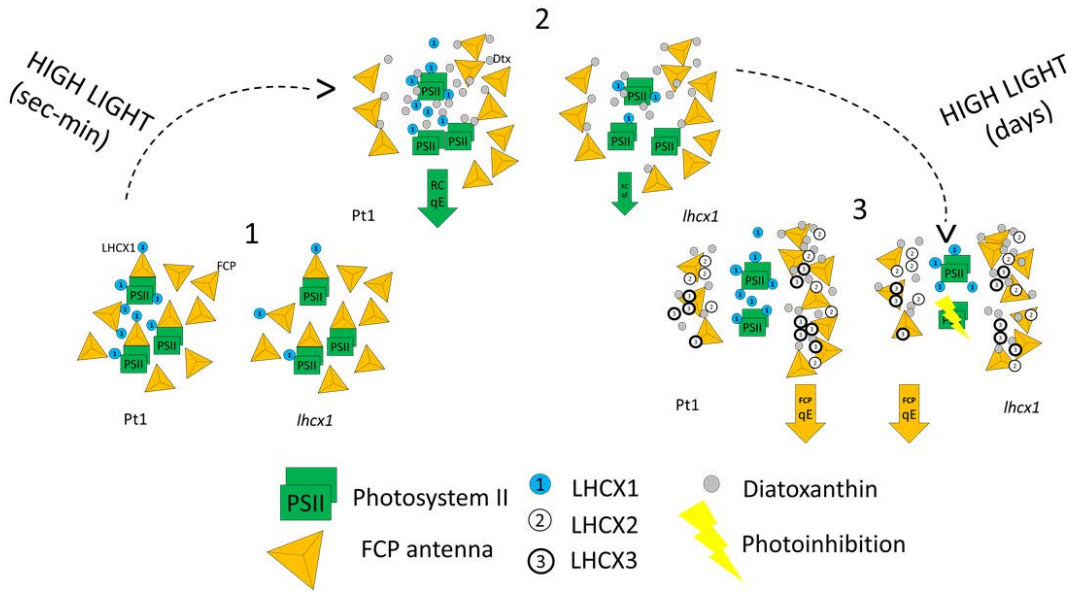

Figure 5. Model for NPQ in *P. tricornutum* wild type and *lhcx1a* knock down cells (1) after short (2) and long-term (3) high light exposure. In wild-type low light grown cells experiencing a short high light treatment (from seconds to minutes) the major quenching site is in Reaction Centre (2). *LHCX1* knock-down line show a reduced quenching capacity because of the reduced content of the LHCX1, which is the only isoform to be expressed in low light and to be located in PSII Reaction Centre. After a prolonged high light treatment (days), the quenching sites of excessive energy is mainly in FCP antenna in wild-

type cells (3). *lhcx1a* recovers its NPQ capacity (3). Since there is no substantial difference in the quenching capacity between wild type and *lhcx1a*, the observed NPQ could be related to the LHCX3, the most abountant isoform dected in HL in our analysis and also found in the FCP fraction. The diminished photosynthetic activity and growth in *lhcx1a* in HL could be dependent on the degradation of the D2 protein. The possible directy link between the deregulation of the D2 and LHCX1 proteins need to be established.

Our analyses allowed to establish for the first time, the presence on the PSI and the FCP of both LHCX1 and LHCX3 and the only LHCX1 on PSII. Our data also suggests that the switch between the different quenching sites could rely on the induction of specific LHCX proteins accumulating either in the reaction center or in the FCP proteins, besides the occurrence of the xanthophyll cycle. However, they also indicate that the antenna localized NPQ mechanism is less efficient in counteracting photodamage to PSII.

In plants, where the two types of quenching have also been observed (Bergantino et al. 2003), Bergantino and colleagues have proposed that PSBS, the plant qE effector, could modulate NPQ via its association with the RC or the antenna complexes. This would occur via a hypothesized protein dimerization, which has recently been experimentally confirmed (Fan et al. 2015). In green algae, differential binding of LHCSR3 with the two reaction centres has been reported and also related to changes in NPQ (Allorent et al. 2013). More recently, Pinnola and colleagues showed that LHCSR3 is able to induce NPQ in PSI (Pinnola et al. 2015) in the moss *Physcomitrella patens*. Therefore, it seems that the NPQ in the diatom *P. tricornutum* has a combined action of a fast and a long term quenching mechanisms which could allow to respond to both fluctuating and prolonged stressful conditions respectively. The fast responding NPQ is LHCX1 related and RC located, while the slow and long-term HL related quenching is antenna located. The active control of the commutation between the two forms of quenching would provide a rationale for the existence of several isoforms of LHCSR/LHCX. By inducing different LHCX isoforms, diatoms could successfully acclimate to multiple types of stress, as required for successful acclimation to the continuous changes of the ocean environment.

6. Supplementary Data

Role of LHCX proteins in short- and long-term high light acclimation in *Phaeodactylum tricornutum*

Lucilla Taddei, Volha Chukutsina, Bernard Lepetit, Giulio Rocco Stella, Herbert Van Amerongen, Jean-Pierre Bouly, Marianne Jaubert, Giovanni Finazzi, Angela Falciatore

Strain	PSII efficiency (Fv/Fm)	Respiration capacity (-nmol O_2 mL^{-1} s^{-1} $cells^{-1}$)
Pt1 LL	0.69±0.01	1.67±0.58
Pt1 HL	0.55±0.08	2.33±0.29
lhcx1a LL	0.66±0.02	1.67±0.58
lhcx1a HL	0.50±0.04	1.83±0.28

Table S1. Photosystem II efficiency in wild type and transgenic lines with reduced LHCX1 content. PSII efficiency (Fv/Fm = (Fm-Fo)/Fm) was calculated from minimum (Fo) and maximum fluorescence emission (Fm) measured in dark and high light light exposed cells respectively (Genty B, Harbinson J, Briantais J-M, Baker NR (1990) Photosynth Res 25:249–257.). Respiration capacity in LL and HL derived from the oxygen consumption rates measured in the dark.

Strain	state	λ_{ex}	τ_1 (black DAS), ps	τ_2 (red DAS), ps	τ_3 (blue DAS), ps	τ_4 (green DAS), ps	τ_5 (magenta DAS), ns
Pt1 LL	unq	400	14	64	242	894	4
	q	400	14	61	219	816	4
	unq	540	14	54	230	818	4
	q	540	14	62	266	1053	4
Pt1 HL	unq	400	13	104	467	4	
	q	400	13	105	446	4	
	unq	540	13	119	595	4	
	q	540	13	100	479	4	
lhcx1a LL	unq	400	14	68	245	909	4
	q	400	14	66	262	942	4
	unq	540	14	56	234	787	4
	q	540	14	66	250	821	4
lhcx1a HL	unq	400	12	147	485	4	
	q	400	12	140	395	4	
	unq	540	13	120	451	4	
	q	540	13	132	430	4	

Table S2. Results of global fitting of the streak-camera data upon 400 nm and 540 nm excitation in unquenched (unq) and quenched (q) states. Lifetimes estimated from global analysis of the fluorescence data obtained for Pt1 and *lhcx1a* strains *(LL and HL)* measured in two states: unquenched (10 min of dark adaptation) and quenched (10 min of actinic light). The DAS colors specified in the lifetimes rows correspond to the colors of the DAS in Figures S2 and S3. The slowest component is at the limit of the setup resolution and was always fixed to 4 ns.

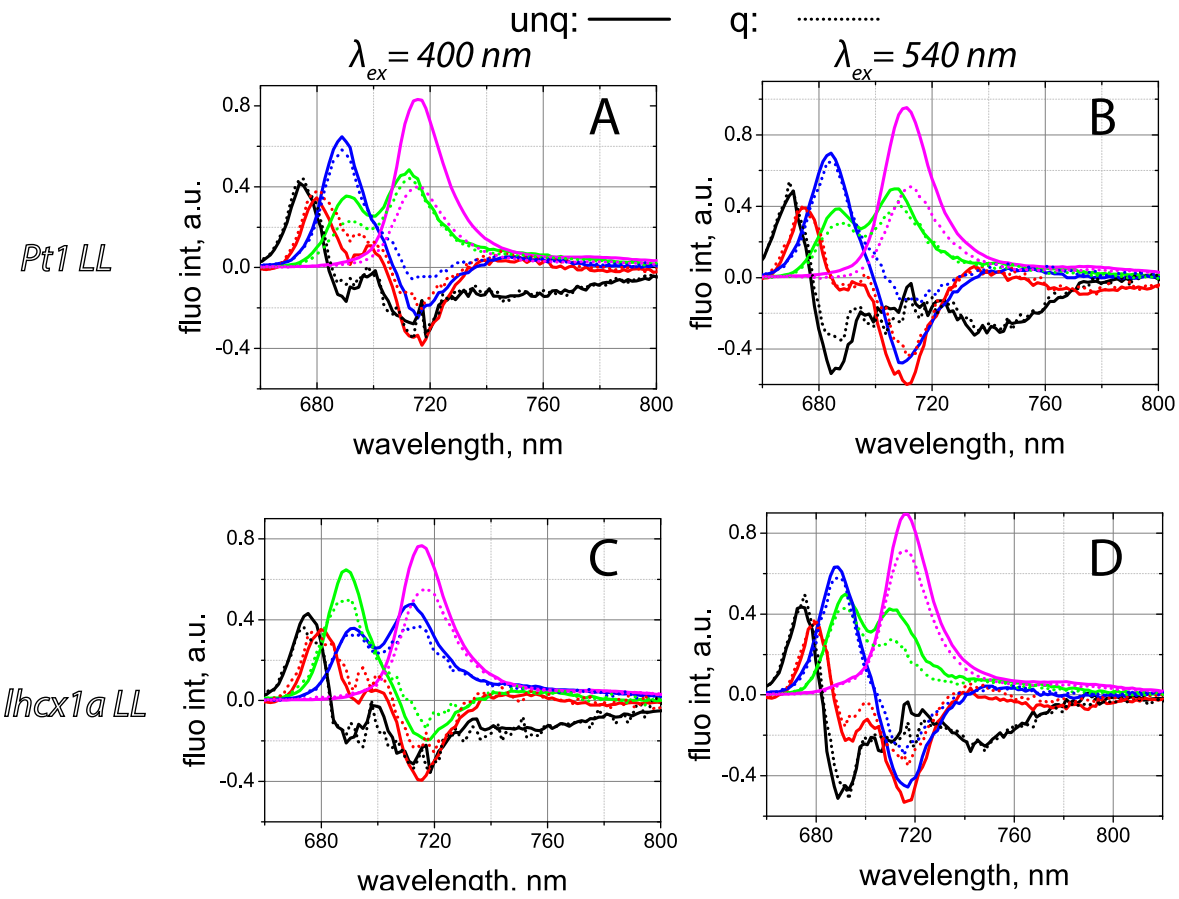

Figures S1. Results of global fitting of the streak-camera data upon 400 nm and 540 nm excitation in unquenched (unq) and quenched (q) states. Lifetimes estimated from global analysis of the fluorescence data obtained for Pt1 LL and *lhcx1a LL* strains measured in two states: unquenched (10 min of dark adaptation) and quenched (30 min of actinic light). The DAS colors specified in the lifetimes rows Table S1) correspond to the colors of the DAS in Figures S2 and S3. The slowest component is at the limit of the setup resolution and was always fixed to 4 ns.

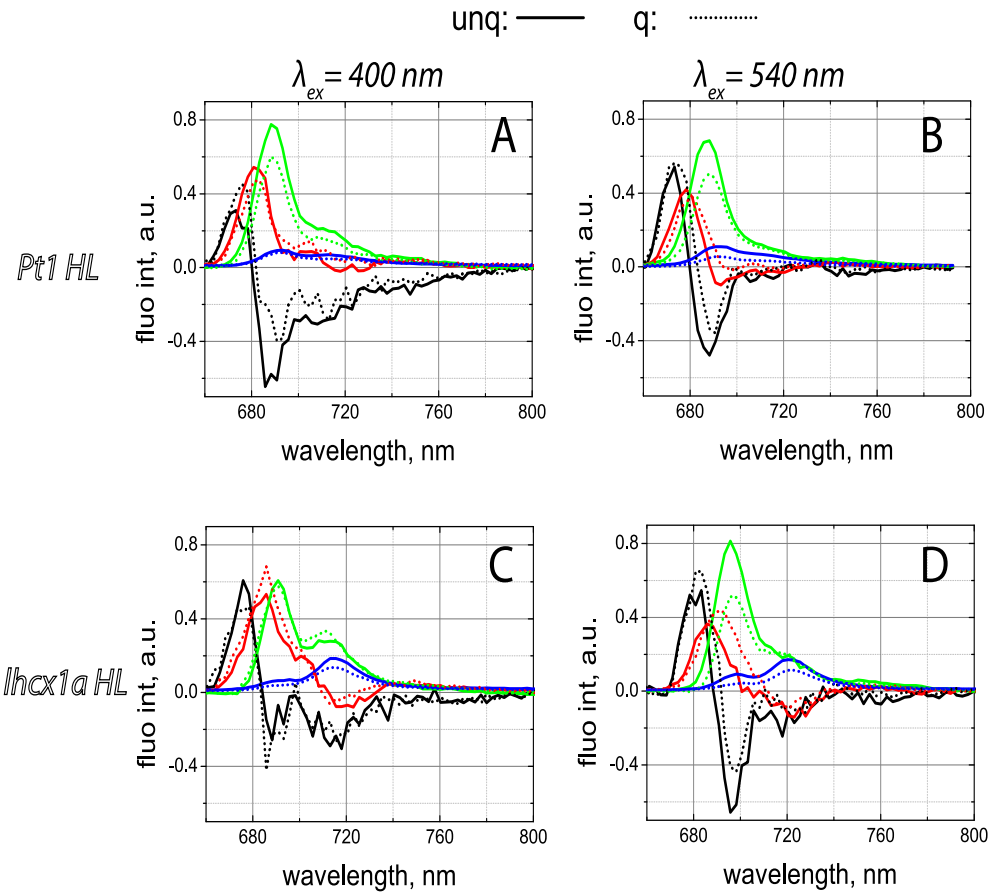

Figures S2. Results of global fitting of the streak-camera data upon 400 nm and 540 nm excitation in unquenched (unq) and quenched (q) states. Lifetimes estimated from global analysis of the fluorescence data obtained for Pt1 HL and *lhcx1a HL* strains measured in two states: unquenched (10 min of dark adaptation) and quenched (30 min of actinic light). The DAS colors specified in the lifetimes rows Table S1) correspond to the colors of the DAS in Figures S2 and S3. The slowest component is at the limit of the setup resolution and was always fixed to 4 ns.

CHAPTER IV

Modulation of the expression of the *LHCX* gene family in the marine diatom *Phaeodactylum tricornutum*

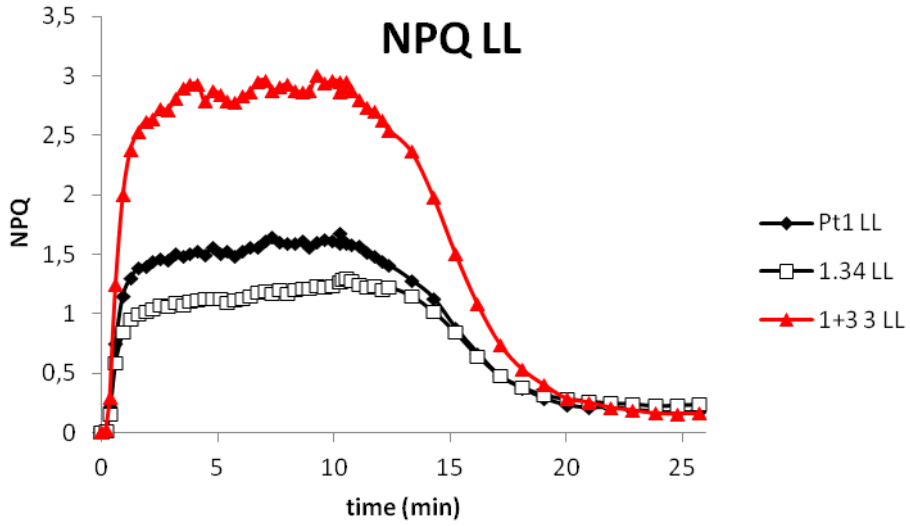

Modulation of the expression of the *LHCX* gene family in the marine diatom *Phaeodactylum tricornutum*

1. Introduction

Diatoms are of great interest in a wide variety of areas ranging from oceanography to materials science. Despite the global importance of diatoms and their extraordinary metabolic and cellular capabilities, they have received little attention from molecular biologists. This has drastically changed during the last decade with the emerging insights from diatom genome projects and substantial progress in genetic manipulation of selected model species (Bowler & Falciatore, 2014; Paragraph1.2 of this thesis).

In particular, the team where I have performed my doctoral training has put considerable efforts to establish *P. tricornutum* as the model system for the diatom molecular and cellular research. The setup of a genetic transformation system by the biolistic particle delivery technique (Falciatore *et al*., 1999) opened the possibility to characterize gene function by reverse genetic approaches in this species. Subsequently, a series of diatom-specific expression vectors has been generated for a variety of purposes including protein localization (by fusion to cyan fluorescent protein (CFP) or yellow fluorescent protein (YFP)), and immunodetection and affinity purification (by fusion to haemagglutinin (HA) epitope tag) (Siaut *et al*., 2007). Vectors has been designed to allow gene over-expression, by using the strong light-inducible *FCPB* (Fucoxanthin Chlorophyll Binding Protein B, *FCPBp*) or the weaker but more constitutive *H4* (*Histone 4*) promoters (Siaut *et al*., 2007; De Riso *et al*., 2009). These vectors have been already used in different studies to generate transgenic lines (over-)expressing an endogenous protein in the native or mutated form in *P. tricornutum*. It has been clearly shown that gene over-expression can induce the appearance of a novel phenotype, this allowing studies of its function (Vardi *et al*., 2008; Coesel *et al*., 2009; Bailleul *et al*., 2010).

More recently, it has also been demonstrated the feasibility of establishing gene silencing in *P. tricornutum* via the RNA interference (De Riso *et al*., 2009), a double-stranded RNA (dsRNA) triggered

post-transcriptional gene silencing process that efficiently works in many organisms (Baulcombe, 2005; Filipowicz *et al*., 2005; Brodersen and Voinnet, 2006). Constructs containing either antisense or inverted repeat sequences of selected target genes have been generated and successfully used to silence a GUS reporter gene expressed in transgenic lines, as well as numerous *P. tricornutum* endogenous genes (De Riso *et al*., 2009; Bailleul *et al*., 2010; Allen *et al*., 2011; Lavaud *et al*., 2012; Huysman *et al*., 2013).

In the context of my research project, I have exploited these tools to get novel insight on the function of the *LHCX* gene family. As described in the Chapter II, *LHCX* over-expressing lines have been generated in the *P. tricornutum* Pt4 ecotype. This strain possesses an intrinsically lower NPQ capacity of the commonly used Pt1 ecotype (Bailleul *et al*., 2010) and the over-expression of the *LHCX* genes generated a small but still consistent increase in the NPQ levels, suggesting a potential involvement of the diverse proteins in NPQ modulation (Taddei *et al*., 2016). To further characterize their specific function, here I have generated new transgenic lines over-expressing the four *LHCX* genes also in the Pt1 ecotype. Moreover, I have also tried to specifically down-regulate the expression of each *LHCX2*, *LHCX3* and *LHCX4* gene by RNA interference, like previously done for the *LHCX1* (Bailleul *et al*., 2010). During my PhD, more than 143 independent transgenic lines putatively deregulated in its LHCX protein content have been generated, with the aim of identifying novel strains showing altered chloroplast physiology and growth. The initial idea was to characterize these strains based on their photosynthetic activity using fluorescence-based non-invasive approach and with the flow cytometer, to get additional information on their growth and physiology. Strains showing altered physiology would have been further characterized at the molecular level, to establish correlation between the phenotype and the content of each LHCX isoform. Unfortunately, this large scale screening approach did not provide reproducible results. Therefore, in a second moment, I focused my efforts on the characterization of putative knock-down lines for the four *LHCX* genes. The gene expression analyses described in Chapter 2 have been instrumental to narrow down the specific growth conditions in which the different LHCXs could be required.

2. Material and Methods

2.1 *P. tricornutum* strain and growth conditions

P. tricornutum Pt1 cells (Pt1 8.6, CCMP2561, obtained from the Provasoli-Guillard National Center for Culture of Marine Phytoplankton) and *P. tricornutum* Pt4 cells (DQ085804, De Martino et al., 2007) were grown in ventilated flasks in f/2 medium (Guillard, 1975) at 18°C, in a 12h light/12h dark photoperiod using white fluorescence neon lamps (Philips TL-D 90), at 50 µmol $m^{-2} \cdot s^{-1}$.

2.2 Growth conditions used for the analysis of the LHCX function

Low light growth for wild-type and transgenic cells corresponds to 30 µmol $m^{-2} \cdot s^{-1}$ of irradiance. Cells were exposed to 500 µmol $m^{-2} \cdot s^{-1}$ for 5 hours, 2 hours after the light onset, with the same light sources as above. Dark prolonged treatment lasted for 60 h. In iron starvation experiments, cells were grown at 30 µmol $m^{-2} \cdot s^{-1}$ in f/2 artificial sea water medium modified to contain either 11 µM iron (iron-repleted) or 5 nM iron with the addition of 100 µM of the Fe2+ chelator FerroZine™ (iron-limited) (Stookey, 1970), at an initial concentration of $2x10^5$ cells/ml and harvested three days after to perform analysis. Nitrogen starvation was achieved diluting cells to $2x10^5$ cells/ml in f/2 medium containing 1mM nitrate (NO_3-repleted) or 50 µM nitrate (NO_3-limited). When cells reached a concentration of $1x10^6$ cells/ml, a second round of dilution was performed in their respective media, before harvesting and analyzing three days after, 2h after the light onset. Growth was monitored by daily cellular counting on Malassez cell.

2.3 Plasmids for LHCX gene expression modulation

To generate LHCX silencing vectors, an antisense fragment from the different LHCXs was amplified by PCR from the Pt1 wild type cDNA using the following primers:

ASL1fw: 5′-ccgGAATTCGACCAAGGAACTCCAGAACG-3′ and
ASL1rv: 5′-ctagTCTAGAGGTCGGTGAACAAGAGCTTC-3′, product size: 242 bp;
ASL2fw: 5′-ccgGAATTCTTGAACACTAGGCGCGATG-3′ and
ASL2rv: 5′-ctagTCTAGAGGGCAATAACTCGGAATACG-3′, product size: 210 bp ;
ASL3fw: 5′-ccgGAATTCCTTCTGACCCGGAAGAACTG-3′ and
ASL3rv: 5′-ctagTCTAGAGTGCATGTGACCAGCCATAC-3′, product size: 182 bp ;
ASL4fw: 5′-ccgGAATTCACTACAGAATGGGCGTTTGG-3′ and
ASL4rv: 5′-ctagTCTAGACCATTGCAACTCTTGGTTGA-3′, product size: 182 bp).

To avoid aspecific silencing of the gene family, the 3′-UTR region of each LHCX gene was used as targeted regions. The resulting amplification products were digested with EcoRI and XbaI and subsequently introduced in the antisense orientation, between the Phleomycin resistance gene, *Shble*, and the *FcpA* terminator, into the EcoRI–XbaI linearized pKS–hsa PtGUS (for *H4* promoter constructs) or pKS-fas PtGus (for *FcpB* promoter constructs) vectors, replacing the GUS gene fragment (De Riso *et al*., 2009).

Vectors for the LHCX overexpression were generated by amplifying the full-length cDNA sequences of the four LHCXs with the following primers:

L1OE_Fw : 5′-acgtGCGGCCGCATGAAGTTCGCTGCCACCATC-3′ and
L1OE_Rv: 5′-acgtGAATTCTTAACCCTGAAGATTCTCAAGGATT-3′ for the LHCX1;
L2OE_Fw: 5′-acgtGCGGCCGCATGAAATTATCCTTGGCTATCC-3′ and
L2OE_Rv: 5′-acgtGAATTCttaGAGCCCAAGGTTTTCGAGGAT-3′ for the LHCX2;
L3OE_Fw: 5′-acgtGCGGCCGCATGAAGTGCATCGCCGCTATC-3′ and
L3OE_Rv: 5′-acgtGAATTCttaGAGGAGGTGTTCCAAGATTCC-3′, for the LHCX3;
L4OE_Fw: 5′-acgtGCGGCCGCATGAAATTGTTCACCATCTTC-3′ and
L4OE_Rv: 5′-acgtGAATTCttaGCCAAACAAATTCTCCAAAAT-3′, for the LHCX4.

The PCR products were inserted in the pKS-FcpBp-At-C-3'HA vector (Siaut *et al*., 2007), using the EcoRI and NotI restriction sites. A schematic representation of the different generated constructs is provided in Figure 1.

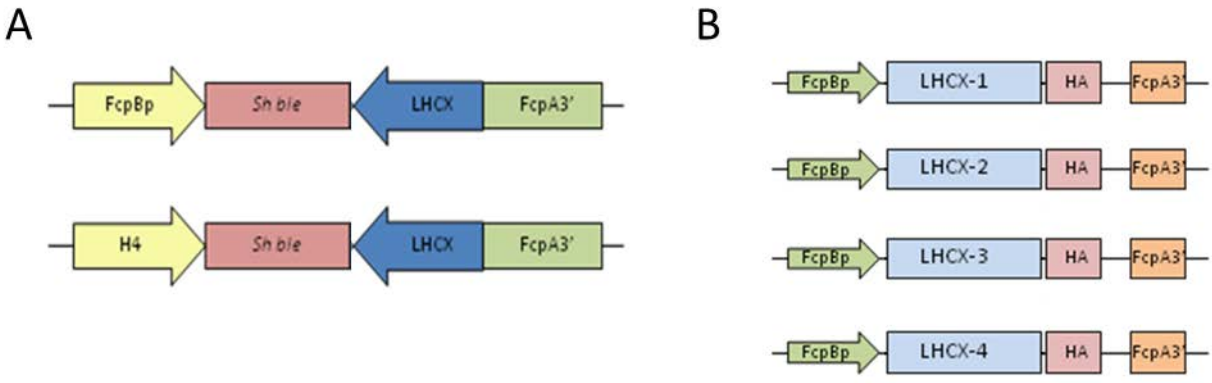

Figure 1. Schematic representation of the constructs generated to modulate the level of expression of the *LHCX* genes. A) *LHCX*-silencing vectors. 182 to 242-bp fragments of *LHCX* 3'end and 3' untranslated transcribed region were transcriptionally fused in antisense orientation to the phleomycin resistance gene (*Sh ble*). *FcpB* (Fucoxanthin Chlorophyll a/c-binding Protein B) or *H4* (Histone 4) promoters were used to drive the *Sh ble* and antisense expression, and the *FcpA* (Fucoxanthin Chlorophyll a/c-binding Protein A) terminator (*FcpA3'*) to terminate the transcription. B) *LHCX*-overexpressing vectors. The different *LHCX* full length cDNA were inserted in frame upstream the HA epitope tag sequence, under the control of *FcpB* promoter and *FcpA* terminating region.

2.4 Transformation with the biolistic approach

The vectors previously described were introduced into Pt1 and Pt4 *P. tricornutum* strains by microparticle bombardment using a Biolistic PDS-1000/He Particle Delivery System equipped with hepta-adaptor (BioRad). Single transformation was performed with the antisense vectors because they contained the antisense fragment as part of a transcriptional fusion downstream of the selectable *Sh ble* gene, which confers resistance to the antibiotic phleomycin. Plasmids for the LHCX over-expression were co-transformed with the *FCPFp-Sh ble* vector (Falciatore *et al.,* 1999), containing the *Sh ble* gene. Approximately 1.10^8 cells were spread on f/2 agar plates containing 50% seawater and allowed to dry in a sterile hood. Plasmid DNA (5µg in total) was coated onto M17 tungsten particles (1,1 µm diameter, BioRad), as described in the PDS/1000 He instruction manual. Agar plates containing the diatom cells were positioned at level 3 of the Biolistic chamber, and burst pressures of 1550 psi were used for the transformation. For the selection of positive transformants, bombarded cells were plated onto fresh plates supplemented with 50 µg/mL phleomycin (InvivoGen). After three weeks of incubation in white light (80 µmol m^{-2} s^{-1}; 12h light-12h dark photoperiod at 18 °C), individual resistant colonies were checked for co-transformation of the construct of interest by colony PCR according to the following protocol: a diatom cell pellet, corresponding to approximately 1.10^8 cells, was resuspended in 20 µL lysis buffer (1% Triton X100; 20 mM Tris-HCl pH 8, 2 mM EDTA pH8), placed on ice for 15 min and then at 95°C for 10 min to induce cell lysis, and then diluted 1/5 with distilled water. Five µL was used for each PCR reaction performed with the FcpAt_Rv1 primer (5'-aaatctagatgaagacgagctagtgttattcc-3') and the ASL1, 2, 3 or 4 reverse primer. Positive clones were re-streaked on 50% f/2 agar plates supplemented with 50 µg/mL zeocin (InvivoGen).

2.5 Protein extraction and western blot analysis

Western blot analyses were performed on total cell protein extracts prepared as in Bailleul *et al.*, 2010, and resolved on 14% LDS-PAGE gels. Proteins were detected with the anti-LHCSR (gift of G. Peers, University of California, Berkeley, CA) (1:5000) and anti-βCF1 (1:10000) (gift of F-A.

Wollman, Institut de Biologie Physico-Chimique, Paris, France) antibodies, and revealed with Clarity reagents (Bio-Rad) and Image Quant LAS4000 camera (GE Healthcare, USA).

2.6 Chlorophyll fluorescence measurements

Light-induced fluorescence kinetics were measured using a fluorescence CCD camera recorder (JTS-10, BeamBio, France) as described (Johnson *et al*., 2009) on cells at 1 to 2x10^6 cells/ml. Fv/Fm was calculated as (Fm-F0)/Fm. NPQ was calculated as (Fm-Fm′)/Fm′ (Bilger and Bjorkman, 1990), where Fm and Fm′ are the maximum fluorescence emission level in the dark and light acclimated cells, measured with the saturating pulse of light. All samples, except the 60 hour dark-adapted cells, were adapted to dim light (10 µmol m^{-2} s^{-1}) for 15 min at 18 °C before measurements. The maximal NPQ response was measured upon exposure for 10 minutes to saturating of 950 µmol m^{-2} s^{-1} green light.

3. Results

3.1 Construction of LHCX modulated content mutant library

In diatoms, LHCX is an expanded gene family (Taddei *et al*., 2016). Four isoforms have been described in *P. tricornutum*. The expression of the different LHCX proteins is tightly regulated in responses to different signals and stresses, strongly suggesting that the different isoforms could contribute to the regulation of NPQ in cells grown in different conditions. The LHCX2, 3 and 4 proteins could work with the NPQ-regulator LHCX1. However, a specific and different function of the other isoforms cannot be excluded. Therefore, to test these possibilities, we generated independent transgenic lines containing different vectors for the over-expression or down-regulation of each isoform. The overexpression was driven by the *FCPB* promoter while the expression of the antisense fragments was either driven by the *FCPB* or *H4* promoter, providing a strong light-inducible expression, or a weaker but more constitutive expression, respectively (Siaut *et al*., 2007). More than one hundred transgenic lines have been produced during the past 5 years in the laboratory (Table 1) and I have contributed to the generation of these lines.

			Ecotypes	
Promoter	**Mutant**	**LHCX**	**Pt1**	**Pt4**
FCPB	OE	1	1,3,4,5	1,2
		2	25,27	5,20
		3	1,2,3,5,7	12,30
		4	1,2	9,13,11
FCPB	AS	1		
		2	10,40,46,53,60	
		3	3	
		4	12,19	
H4	AS	1	1-59	
		2	1-27	
		3	1-7,9	
		4	1,2,3,16,20,21	
		1+3	3,6,7,9	
		1+2	1-9	

Table 1. List of the different mutants generated to modulate the LHCX cellular content. FCPB*: Fucoxanthin Chlorophyll Binding Protein B* promoter; *H4: Histon 4* promoter; OE: overexpressor; AS: antisense. Numbers in the Ecotypes columns represent the clone names.

When I started my PhD, the initial idea was to set up a large scale screening of these putative *LHCX* mutants for altered chloroplast physiology, on transgenic lines grown either on plates or in liquid media (96-well microplates) (Figure 2). Initial analyses were performed by growing the cells under normal light conditions and after exposing them to different light stresses, known to induce NPQ responses.

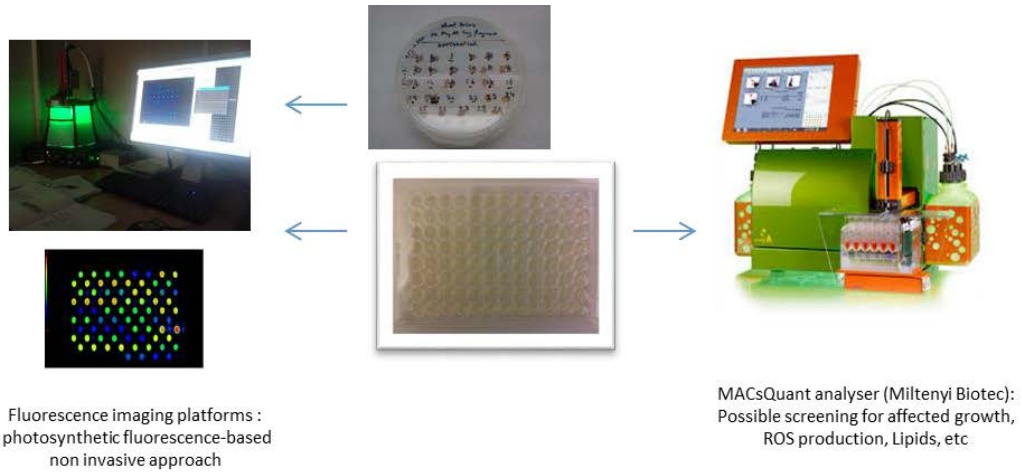

Figure 2. Strategy for the high-throughput screening of the *LHCX* mutants. Independent transgenic lines grown on solid media or in liquid media in 96-well microplates were analyzed for the photosynthetic

parameters by using a fluorescence CCD camera recorder (JTS-10, BeamBio, France). Cell growth and fluorescence were also measured for the liquid cultures by fluorescence flow cytometer analysis. Strains that showed altered phenotype compared to wild-type strains, were analyzed by western blot analyses to assess the level of deregulation of the different LHCX proteins.

Unfortunately, even if different attempts have been performed to optimize the experimental set up (e.g., different cell density for the analysis and different acclimation time and growth conditions before the analysis), the results that I obtained were not reproducible. Already the wild-type Pt1 and Pt4 lines and the knock-down lines for the *LHCX1* gene, that have been extensively characterized in the lab, showed variable photosynthetic and NPQ parameters. Moreover, the obtained data were not always as expected based on the light treatments experienced by the cells. As consequence, also the results obtained on the transgenic lines were of not obvious interpretation. Therefore, in a second phase, I have preferred to focus my efforts on the characterization of a restricted number of putative knock-down lines grown in ventilated flask in liquid media, as normally done. The analysis started with the characterization of the LHCX proteins content by western blot. On the clones that showed a deregulated LHCX expression, phenotypic analyses were performed in cells exposed to different conditions. Because in parallel with this work, I was obtaining novel data on the differential expression of the different LHCX genes, I also integrated this information for the phenotypic characterization of these mutants.

3.2 Analysis of the transgenic lines containing the LHCX2 silencing vector

As previously mentioned, high light and iron limitation are two conditions triggering the expression of the *LHCX2*. The level of LHCX2 was therefore assessed by western blot on protein extracts from high light (and iron replete) and iron-limited (and low light) grown cells.

Upon high light stress, LHCX2 was present in the WT cells and showed a lower content in the 3 tested transgenic lines containing the *LHCX2* silencing vector, indicating an effective silencing, although the protein is still detectable on the immunoblot (Figure 3 A). We then measured the NPQ capacity and photosynthetic efficiency of these silenced strains. Upon high light exposure, Pt1 shows an enhancement of the NPQ capacity and slightly reduced photosynthetic activity, indicating that some photoinhibition occurred during the high light treatment (Figure 3 B and C). In spite of the silencing,

LHCX2 knock-down lines displayed similar photosynthetic efficiency than Pt1, and no significant difference in NPQ capacity was observed in high light treated cells (Figure 3 B and C).

In cells undergoing iron starvation, a reduction in the LHCX2 protein content was also observed in the transgenic lines with respect to the WT, indicating that the silencing is also working in these conditions (Figure 3 D). As already described in the previous chapter, Pt1 exhibited an enhancement of the NPQ capacity upon iron starvation, and a strongly affected photosynthetic capacity (Figure 3 E and F). However, this enhancement is also seen for the different silenced lines (Figure 3 E), indicating that these lines with a reduced LHCX2 protein content are not affected in their NPQ capacity.

To address possible other effects of a reduced amount of LHCX2 on cell physiology, growth was also monitored following exposure to high light or during iron starvation. However, no difference appeared in the growth rate of the different silenced lines and the wild-type (Figure 3 G).

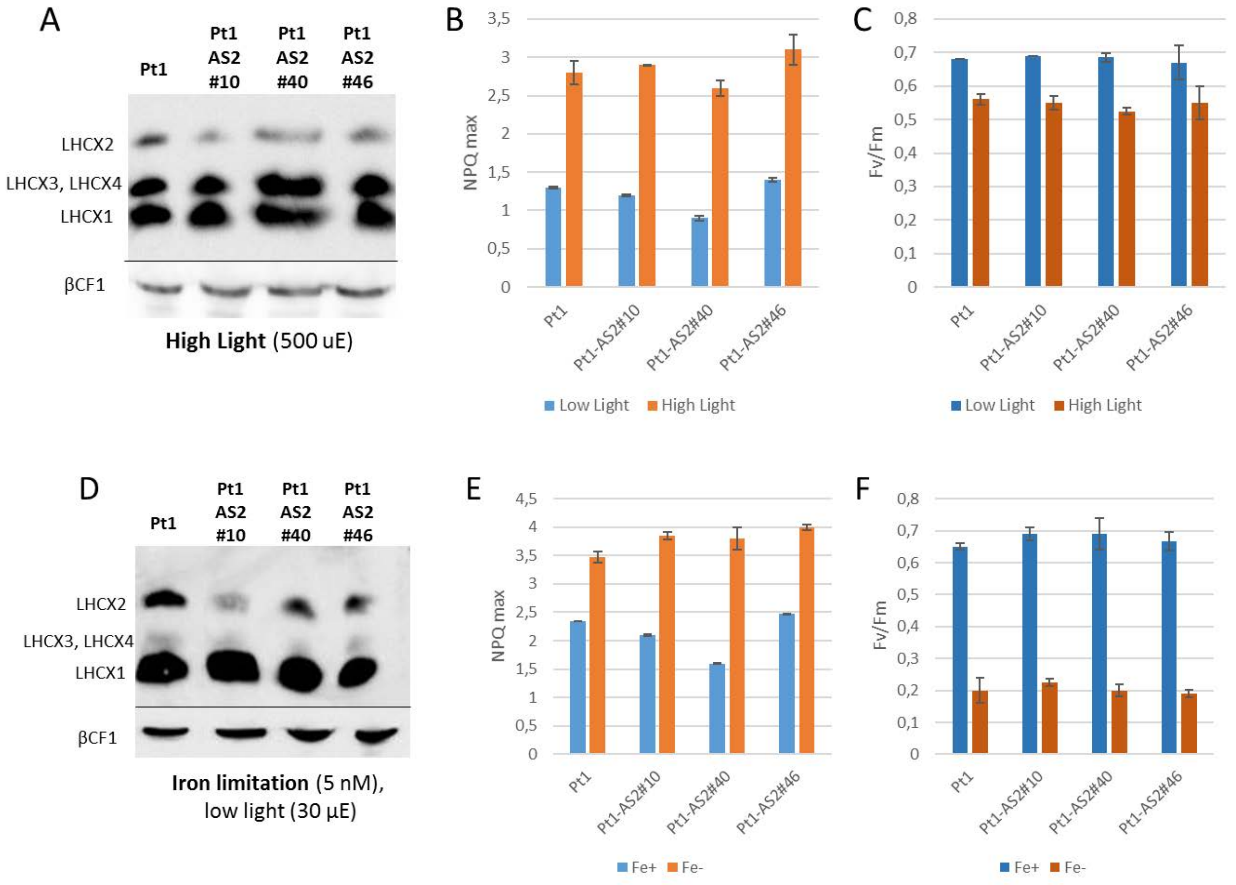

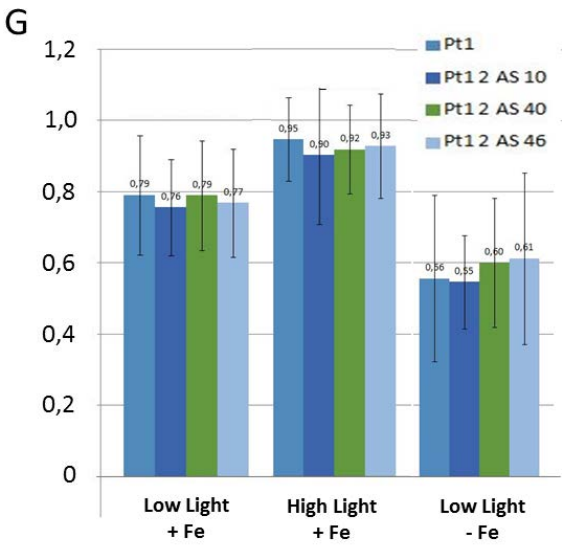

Figure 3. Characterization of transgenic lines containing the *LHCX2* antisense vector. A) Immunoblot analysis of the LHCX content in *wild-type* and independent transgenic lines upon high light treatment. Total proteins were extracted from cells grown in light-dark cycle (30 µmol of photons m^{-2} s^{-1} of light), and then exposed for 5 hours to high light (500 µmol of photons m^{-2} s^{-1}). Blots were hybridized with anti-LHCSR antibodies, recognising the different isoforms, and anti-bCF1 as loading control. B) and C) Maximal NPQ and photosynthetic efficiency (Fv/Fm), respectively, measured for cells grown in the conditions described in A. D) Immunoblot analysis of the LHCX content in wild-type and independent transgenic lines, upon iron starvation. Total proteins were extracted from cells grown in light-dark cycle (30 µmol of photons m^{-2} $s^{-1}$of light) and iron replete (Fe+) or iron depleted (Fe-) conditions. Blots were hybridized as described above. E) and F) Maximal NPQ and photosynthetic efficiency (Fv/Fm), respectively, measured for cells grown as described in D. The values in B, C, E and F correspond to the mean of 3 technical replicates, and bars to +/- SD. G) Growth rate of the different lines cultivated under different light and iron conditions. The values correspond to the mean of 3 replicates, and bars to +/- SD

3.3 Analysis of the transgenic lines containing the LHCX3 silencing vector

As *LHCX3* is induced upon high light stress and nitrogen limitation, I assessed the photosynthetic parameters of the putative knock-down lines in these two conditions. During high light exposure, LHCX3 is present along with LHCX1 and LHCX2 in Pt1 (Figure 4 A). However, in the two transgenic lines analysed, the level of the protein did not show any reduction (Figure 4 A). In line with this result, no difference in photosynthetic efficiency and NPQ capacity was observed in these lines transformed with the *LHCX3* antisense vector, both upon high light exposure and nitrate starvation (Figure 4 B, C, D, E). Seven additional antisense lines have also been screened, but I did not find a strain showing a significant reduction of the LHCX3 protein so far.

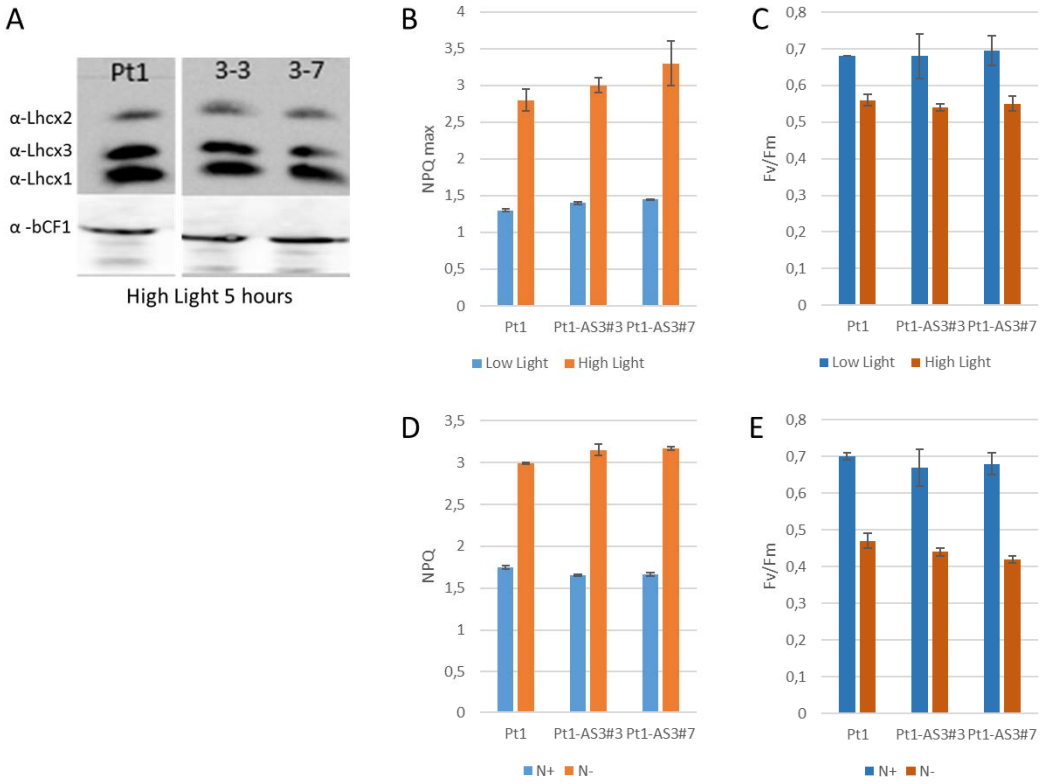

Figure 4. Characterization of transgenic lines containing the *LHCX3* antisense vector. A) Immunoblot analysis of the LHCX content in *wild-type* and independent transgenic lines. Total proteins were extracted from cells grown in light-dark cycle (30 µE of light), and then exposed for 5 hours to high light (500 µE). Blots were hybridized with anti-LHCSR antibodies, recognising the different isoforms, and anti-bCF1 for loading control. B) and C) Maximal NPQ and photosynthetic efficiency (Fv/Fm), respectively, measured for cells grown in the same conditions as described above. D) and E) Maximal NPQ and photosynthetic efficiency (Fv/Fm), respectively, measured for cells grown in low light and nitrogen replete (N+) or nitrogen limited (N-) conditions. The values in B, C, D and E correspond to the mean of 3 technical replicates, and bars to +/- SD.

3.4 Analysis of the transgenic lines containing both the LHCX1 and LHCX3 silencing vectors

As *LHCX1* is constitutively and highly expressed, I started to generate double mutants in which both the content in LHCX1 and another LHCX isoform would be reduced. I have first co-transformed *LHCX1*-silencing vector along with *LHCX3*-silencing vector. The transformants were selected on phleomycin and then tested for the presence of both constructs by PCR (Figure 5 A).

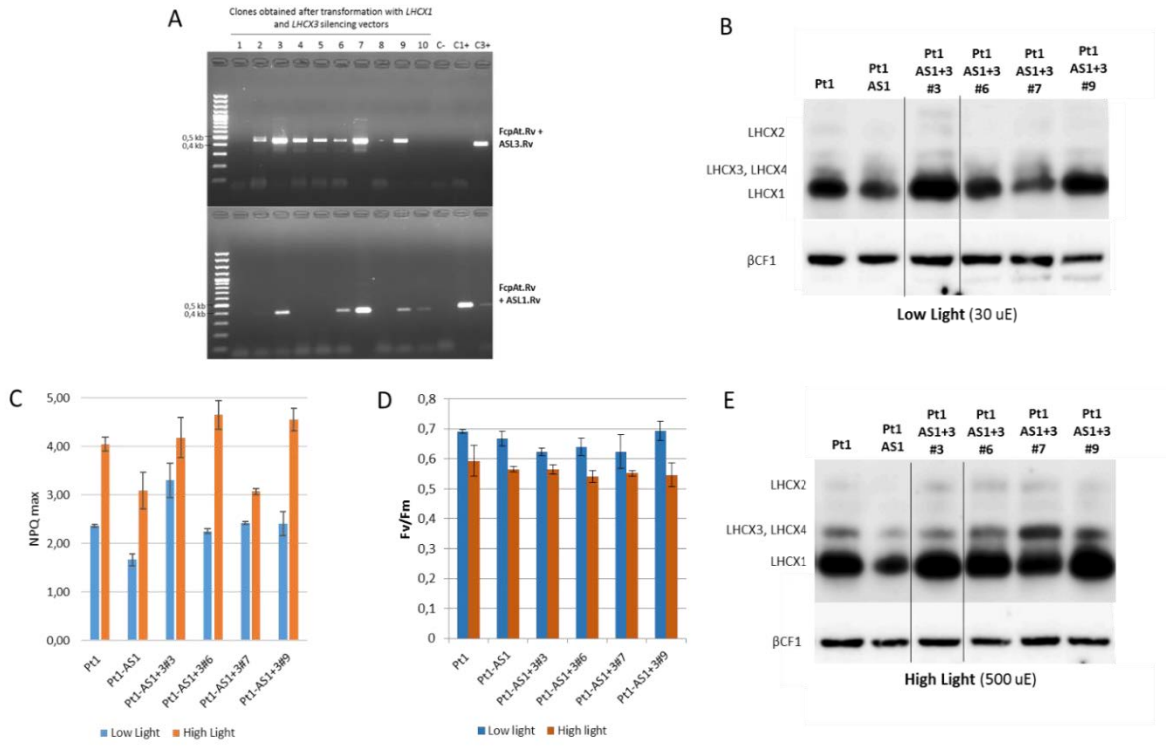

Figure 5. Characterization of clones obtained after co-transformation with *LHCX1* and *LHCX3* silencing vectors. A) PCR screening of the transformants obtained. In the upper panel, PCR was performed using a primer pair hybridizing in the terminating region of the constructs (*FcpAt*) and the *LHCX3* antisense sequence. In the lower panel, PCR was performed using a primer pair hybridizing in the terminating region of the constructs (*FcpAt*) and the *LHCX1* antisense sequence. C- : negative control of PCR using distilled water instead of genomic DNA; C1+ : positive control using gDNA from the previously characterized Pt1-AS1 mutant (Bailleul *et al*., 2010); C3+ : positive control using gDNA from the previously obtained lines containing *LHCX3* silencing vector. The lane on the left corresponds to molecular weight marker. B) Immunoblot analysis of the LHCX content in wild-type, *LHCX1* mutant (AS1) and double transformed lines. Total proteins were extracted from cells grown in light-dark cycle (30 µE of light). Blots were hybridized with anti-LHCSR antibodies, recognising the different isoforms, and anti-bCF1 for loading control. C) Maximal NPQ, measured for cells grown in low light, and then exposed for 5 hours to high light (500 µmol of photons m^{-2} s^{-1}). The values correspond to the mean of 3 independent experiments, and bars to +/- SD. D). Immunoblot analysis of the LHCX content in cells analysed in C. Blots were hybridized as in B. Vertical lines on the immunoblots indicate non adjacent lanes from the same membrane.

I succeeded to obtain 4 lines containing both vectors (#3; #6; #7; #9) (Fig. 4.5 A). At the level of the protein content, in low light conditions, one of them (line #7) displayed a reduction of

LHCX1, whereas, unexpectedly, a higher amount of LHCX1 is observed in lines #3 and #9 (Figure 5 B). Interestingly, whereas no difference in the NPQ capacity is observed for lines #7 and #9 compared to the wild-type, a higher NPQ capacity was found for the line #3 (Figure 5 C). Upon high light exposure, the LHCX content is similar between the wild-type and the transformed lines, except for the line #7, which presents a lower LHCX1 and a higher LHCX3 amount (Figure 5 D). In parallel, all lines enhance their NPQ capacity as does the wild-type, except clone #7, possibly due to the reduction of the LHCX1 content (Figure 5 C).

3.5 Analysis of the transgenic lines containing the LHCX4 silencing vector

LHCX4 has the intriguing feature to accumulate upon prolonged darkness (Taddei *et al*., 2016). Therefore, I analysed the protein content of the putative LHCX4 antisense lines after 60h of darkness. Compared to Pt1, all the transgenic lines tested, except line #16, displayed a lower amount of LHCX4 after prolonged darkness, although, as for *LHCX2* mutants, the protein is still detectable on immunoblot (Figure 6 A). Regarding the NPQ, silenced lines #12 and #19 display the same capacity that Pt1 in low light, as well as in darkness (Figure 6 B). The line #16 which does not show reduction in LHCX4 content presents a reduction of the NPQ capacity both upon prolonged darkness and low light. However, in the silenced lines #1 and #2, a reduction of the NPQ capacity compare to Pt1 is observed for dark treated cells, but not in low light, condition where LHCX4 is not expressed. The result of these two latter lines suggests that NPQ capacity following a prolonged period of darkness would be influenced by the presence of the LHCX4.

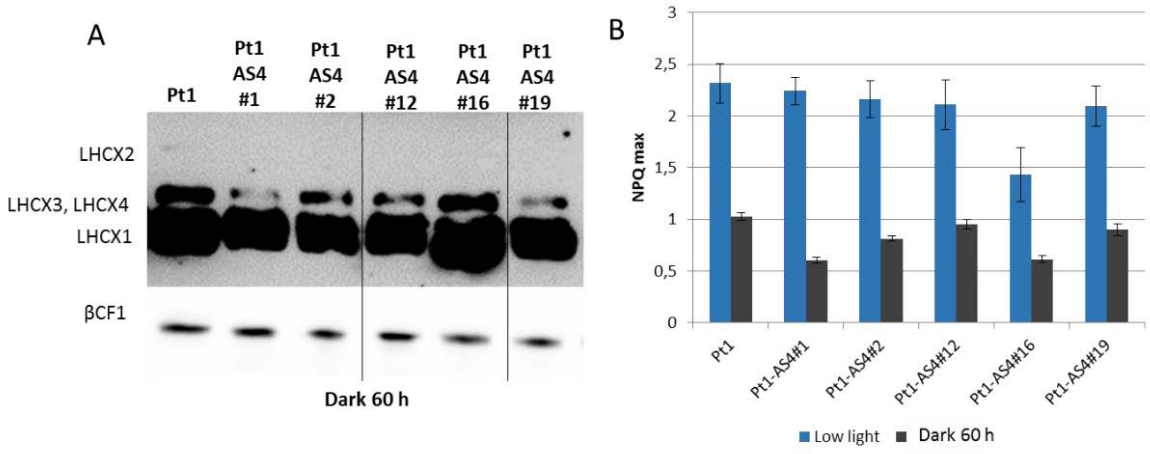

Figure 6. Characterization of transgenic lines containing the *LHCX4* silencing vector. A) Immunoblot analysis of the LHCX content in wild-type and transgenic lines following prolonged darkness treatment. Total proteins were extracted from cells grown in light-dark cycle (30µE of light) , and

then maintained for 60h in the dark. Blots were hybridized with anti-LHCSR antibodies, recognising the different isoforms, and anti-bCF1, as loading control. B) Maximal NPQ measured for cells grown in the conditions described in A. The values correspond to the mean of 3 independent experiments, and bars to +/- SD

4. Discussion

With the analyses provided in this chapter, I wanted to extend the functional characterization of the *P. tricornutum* LHCX2, 3 and 4 genes. In order to assess whether they act with NPQ-regulator LHCX1, or play other specific functions, I contribute to generate new transgenic lines in which the content of each LHCX isoform has been modulated either by gene over-expression or gene-silencing. Unfortunately, all the initial attempts to identify and characterize putative new mutants by performing a large-scale analysis of strains showing altered chloroplast physiology were not successful. This could be due to the difficulties that we are encountering to control the physiology of diatom populations under laboratory conditions, especially on cells grown on plates or small volumes such as in multi-well plates. As fact, characterization of various physiological parameters, such as photosynthesis, growth and gene expression, performed on independent diatom cultures grown under very controlled growth conditions, also shows a certain level of variability. Before getting conclusive information on a specific process, we often need to perform several independent experiments. Moreover, we are also accumulating more and more evidences that multiple factors (agitation of the cultures, nutrients, light, temperature, etc.) affect chloroplast physiology and activity. Differences in the cell concentration, the growth phase and synchronization of the cell cycle in a population also determine variations in physiological cell responses. Therefore, additional efforts are still needed to standardize the conditions for a large scale screening of *P. tricornutum* photosynthetic mutants by fluorescence-based non-invasive approaches.

However, because many interesting lines were available, I decided to use more classical approaches to characterize the function of the different *LHCX* genes. In particular, I focused on the characterization of putative knock-down lines grown under standard liquid conditions and exposed to different stresses. This approach allowed me to get additional and also unexpected new information on the *LHCX* gene family.

I succeeded to identify new lines with a reduced LHCX2 content by western blot analyses. Several lines showed a clear protein deregulation in cells exposed to high light stress or iron starvation, the two conditions showing high LHCX2 protein expression (Taddei *et al*., 2016). These lines did not show any clear alteration of photosynthetic parameters in cells grown under normal low light conditions, as expected considering that the protein is not expressed. However, cells showed normal NPQ and photosynthesis also when exposed to high light stress or if grown in iron starvation. The result suggests that: i) either the LHCX2 protein is not implicated in these processes; ii) or that the level of LHCX2 reduction is not sufficient to cause an alteration of the phenotype; iii) or that LHCX1 protein, strongly expressed in the LHCX2 knock-down lines, is able to compensate the LHCX2 deregulation. Recent data obtained by Dr. B. Lepetit (University of Kostanz, Germany) show that the LHCX2 isoform is also strongly expressed in cells exposed to dynamic light changes (Lepetit *et al*., under review). Therefore, in the future, it will be very interesting to further characterize the NPQ capacity of *LHCX2* knock-down lines also in cells exposed to dynamic light changes (sine or fluctuating lights).

In this study, I also searched for putative *LHCX3* knock-down lines by western blotting analysis in cells grown in low light and then exposed to high light for 5 hours, because these were the conditions showing high LHCX3 expression (Taddei *et al*., 2016). Even if many independent transgenic lines were characterized, I did not find any clone with a reduced content of this isoform. This was surprising because in *P. tricornutum* the silencing efficiency by RNAi is more than 20% (De Riso *et al*., 2009). Puzzling results also derived by the characterization of transgenic lines containing antisense vectors for both the *LHCX1* and *LHCX3* genes. One line showed increased NPQ levels in cells grown under non-stressful light, that were comparable to that obtained in cells grown in high light. Protein analysis indicated that the NPQ increase correlated with a higher accumulation of LHCX1, that acts as a molecular modulator of the NPQ levels in *P. tricornutum* (Bailleul *et al*., 2010). This result is of difficult interpretation at a molecular level, as the sole expression of the *LHCX1* silencing vector has always led to a reduction in the LHCX1 content. Therefore, we could hypothesize that, in this line, the presence of the *LHCX3* silencing vector is for a still unknown reason problematic, and that the cells try to compensate this deregulation by increasing the LHCX1 isoform. Independent on the still obscure processes behind the observed phenotype, this line showing a strong

NPQ increase and a normal photosynthetic activity in cells acclimated to non-stressful light conditions are interesting. Many scientists are trying to manipulate photoprotective pathways to enhance both stress resistance, and photosynthetic productivity in photosynthetic organisms. It has been proposed that increasing qE capacity might improve photoprotection and crop production in adverse environments (Horton 2000; Murchie & Niyogi 2011). Therefore, the comparative analyses of wild-type strain, *LHCX1* knock-down strain and *LHCX1* over-expressing lines possessing different NPQ levels could represent a starting point to investigate the effect of NPQ manipulation on diatom cell physiology and metabolism in cells grown under stressful and not stressful conditions. At the moment, analyses of pigment and lipid content on these lines are in progress in the laboratory.

Another very interesting result derived by the characterization of the knock-down lines for the *LHCX4* gene. As described in the chapter 2, this isoform is a very atypical LHCX protein because its content accumulates in the dark and is inhibited by light. The chloroplast actively participates to the light-dependent inhibition of the *LHCX4* expression (Taddei *et al*., 2016). The characterization of different transgenic lines by western blotting allowed identifying several clones showing a reduced LHCX4 protein content in dark-adapted cells. Some of these clones showed also reduced NPQ levels compared to the wild-type cells. The function of the LHCX4 protein in the regulation of chloroplast physiology is still enigmatic, but also very intriguing. The different regulation of its expression in dark and light compared to the other isoforms let us hypothesize that it plays a distinct role in chloroplast regulation. Recent transcriptomic studies in *P. tricornutum* cells adapted to dark also indicated that diatoms possess peculiar mechanisms to survive for long period in darkness and to quickly adapt to light when returned to photic zone. In particular, it seems that *P. tricornutum* maintains a functional photosynthetic apparatus during dark periods that enables prompt recovery upon re-illumination (Nymark et al. 2013). We can hypothesize that LHCX4 contributes to the high NPQ capacity observed in diatom cells in the dark and that it could play an essential role during dark to light acclimation. In the future, it will be very interesting to test if the deregulation of the LHCX4 protein also affects the growth and photoprotective capacity of diatom cells exposed to different light and nutrient stresses. Moreover, the possible interaction of the LHCX4 with the other LHCX isoforms by genetic and biochemical approaches will be also very informative. Because diatoms are the most abundant phytoplankton organisms in the Polar Regions, where they are exposed to

prolonged darkness for several months, these analyses could also help to decipher the mechanisms controlling the extraordinary ecological success of diatoms in these environments.

Finally, the analyses described in this chapter confirm that complex processes contribute to the regulation of the LHCX protein expression and function in diatoms. The deregulation of the *LHCX2*, *3*, and *4* genes by RNA interference have started to provide some indications on their possible role in chloroplast physiology. However, the possible redundant function of the LHCX1 protein and its strong expression in the *LHCX2, 3* and *4* knock-down lines, clearly represents a major limitation for the characterization of the other isoforms. Recently, it has been shown that is possible to perform gene knock-out in *P. tricornutum* by the TALEN and CRISPRs technologies (Daboussi *et al*., 2014; Nymark *et al*., 2016). The complete inactivation of the LHCX1 protein as well as of the other isoforms will certainly allow getting a more complete picture of the role played by the expanded *LHCX* gene family in chloroplast regulations.

CHAPTER V

Conclusions and future perspectives

Conclusions and future perspectives

The recent availability of genome sequence information from several diatom species opened up the possibility to extend the investigation of the *LHCX* genes to other ecologically relevant species. The comparative analysis described in the second chapter of this thesis indicates an expansion of the LHCX family in diatoms compared with the green algae. That strongly suggests that this expansion is a common feature of these algae and may represent an adaptive trait to cope with highly variable environmental conditions, likely through a diversification of the LHCX proteins role. To prove this assumption, I further analyzed the regulation of the 4 *P. tricornutum LHCX* gene expression in cells grown in conditions known to alter the growth and the photosynthetic ability of the organism.

Previous works suggested a complex regulation of this family, without clearly correlating the presence of the different proteins with the diatom NPQ capacity and other photophysiological parameters. Therefore, I characterized the expression of the LHCX proteins and specific photophysiological responses to understand when the presence of each LHCX could be necessary. I discovered that the four *P. tricornutum* LHCX proteins are regulated in a sophisticated way. Different and probably interconnected regulatory pathways activated by various signals and stresses tightly control the amount of each LHCX isoform in the cell.

Differently from the NPQ regulator LHCX1, that is strongly and constitutively expressed, the content of the other LHCX isoforms is tightly dependent on the dark and light availability: high light induces the expression of the *LHCX2* and *LHCX3*, while a sustained exposure to dark conditions induces the expression of the sole *LHCX4* isoform. The amount of *LHCX4* mRNA rapidly decreases following a dark to light transition, and this repression is lost when photosynthesis is halted with the PSII inhibitor DCMU. This suggests that chloroplast-derived signals could participate in inhibiting gene expression, even at very low light irradiance, by a yet unknown process. Based on these data, we hypothesized that LHCX2 and LHCX3 proteins may work with the LHCX1 and increase the NPQ capacity in high light. On the contrary, the LHCX4 could contribute to the observed capacity

of *P. tricornutum* to survive long periods in the dark and its repression could be needed for a rapid acclimation following re-illumination (Nymark et al. 2013)**.**

Besides the light and redox signals discussed above, my analysis also shows that differences in the availability of iron and nitrogen strongly affect the expression of the LHCX proteins. During the iron starvation, there is the exclusive induction of the LHCX2 protein, pinpointing this isoform as the most likely regulator of the increased NPQ capacity observed in iron stress. On the contrary, the increase in NPQ level observed in nitrogen starvation is associated to a general increase of all the LHCX isoforms.

All together, these initial analyses unveiled that multiple external as well as internal signals deriving by the chloroplast activity, contribute to the tight regulation of the different LHCX members. Therefore, these data represent an important support to further analyses aimed to dissect the signalling cascades linking the external and internal signals to the LHCX expression.

Initial bioinformatics analyses of the LHCX promoters allowed identifying known and also potentially novel *cis*-regulatory elements that may contribute to the transcriptional regulation of the different isoforms in stress conditions. Ideally, these motifs could be further characterized by cloning them down-stream a reporter gene (GFP or GUS), and by testing their capacity to modulate the reporter expression under different conditions, as recently done for the identification of the CO_2/cAMP-responsive *cis*-regulatory elements (CCREs) (Ohno et al. 2012; Tanaka et al. 2015). Moreover, specific Transcription Factors involved in the *LHCXs* expression could be identified through a genome-wide yeast one-hybrid (Y1H) cDNA library screening (Huysman et al. 2013).

Ca^{2+} and the chloroplast calcium sensor (CAS) are essential for *LHCSR3* expression in *C. reinhardtii* (Petroutsos et al. 2011), however such information is missing in diatoms. I think that it might be intriguing to study diatom *LHCX* expression in cells grown in a Ca2+ deprived media: first, because this could be one hint to trace the molecular messenger active in the pathway that connects the chloroplast to the nucleus; and second, because it could sleuths out a conserved feature between green algae and diatoms.

By narrowing down the specific growth conditions in which the different LHCX are required, I had the possibility to perform additional studies aimed to define the function of each isoform in the regulation of chloroplast physiology. In particular, I tried to understand if all the members of the LHCX family were involved in the NPQ process and if they have a similar role to LHCX1 or another specific function. For this purpose, during my PhD, I also tried to specifically modulate the content of each LHCX either by gene silencing or gene over-expression. I tried to deregulate their expression in the reference strain *P. tricornutum* Pt1, but also in the Pt4 ecotype that showed an intrinsically lower NPQ capacity of the Pt4 ecotype. The analysis in the Pt4 ecotype, described in the Chapter 2 and in Taddei et al. (2016) showed that the overexpression of each LHCX isoform generated a modest, but statistically significant, increase in the NPQ capacity compared with the Pt4 wild type. Strikingly, we found that all the transgenic lines showed a similar NPQ increase, regardless of which isoform was overexpressed and the different overexpression levels. These first results were difficult to interpret, especially in the case of lines overexpressing LHCX4, whose endogenous expression is inhibited by light.

Thus, I decided to focus my efforts on the characterization of transgenic lines, with a putatively reduced LHCX2, LHCX3 or LHCX4 protein content in the Pt1 ecotype, as previously done for the characterization of the LHCX1 (Bailleul et al., 2010).

As described in Chapter 4, I performed a molecular characterization of these lines to establish the effectiveness of the *LHCX* gene silencing, by exposing the cells to stresses known to regulate their expression. As a result of this analysis, I got silenced lines only for the *LHCX2* and *LHCX4* genes. Contrary to our expectation, the silencing of the *LHCX2* did not affect NPQ responses in cells exposed in high light or in iron-starvation conditions. This result showed that a partial reduction in the LHCX2 content is not sufficient to discriminate its function, also considering the robustness of LHCX1 in all the conditions.

Interesting but still puzzling results have been obtained by the characterization of the knock-down lines for the *LHCX4*, the sole isoform induced in darkness and whose expression is repressed by light via plastid-derived signals. These analyses indicated that reduction of LHCX4 content determined a decrease of the NPQ levels observed in dark-adapted diatom cells. Clearly, the LHCX4

has very "atypical" features for a member of the LHCX family. As described in Chapter 2 and Taddei et al. 2016, the protein has a lower number of putative pH sensing residues in its sequence compared to the other LHCX isoforms and the *Chlamydomonas* LHCSR3 (Ballottari et al. 2015). This might pinpoint a decreased sensitivity to pH compared to the other LHCXs and possibly a lower activity to quench the excessive energy. In addition, it is known that during a prolonged dark treatment, the intrathylakoidal pH decreases (Jakob et al. 1999) and the presence of an isoform with a reduced sensitivity to the pH might be useful to maintain a reduced photoprotective capacity while giving the opportunity to harvest light in the first hours of the morning light. Therefore, the reduced NPQ capacity after a prolonged dark period might be lower compared to the low light conditions because of the low proton gradient sensitivity of this isoform.

Based on all these results, we concluded that the LHCX4 might have a different role in the diatom photoacclimation from that of the other isoforms. We think that it can contribute to the capacity of diatoms to survive for long period in the dark and to re-adjust the photosynthetic activity following dark to light transition. To date, we do not know if and how the LHCX4 interacts with the other LHCX isoforms and if it participates to the LHCX1-mediated regulation of the NPQ. As fact, lines over-expressing the LHCX4 isoform in both the Pt1 and the Pt4 ecotypes showed a reduced PSII efficiency and also a slower growth (longer lag phase, which was not the case in wild-type cells (Taddei et al. 2016), strongly suggesting that the presence of this protein in normal light condition can disturb cell physiology.

This could also explain why active signals from chloroplast to the nucleus contribute to quickly repress its content, even at very low light irradiance. In future study, it will be very interesting to further characterize the physiology of the generated *LHCX4* knock-down lines, by analysing their growth and photosynthetic capacity in cells adapted to dark for different periods and then exposed to different light regimes. Also, it will be very interesting to analyze the effect of the *LHCX4* deregulation under different nutrient deficiency conditions.

While figuring out the specific growth conditions in which each LHCX was required, I was astonished by the diversity of the NPQ shapes in each condition that I studied and how they correlate with the presence or absence of the different LHCXs. Beside the different signatures of NPQ and the

LHCX combinations, I matured an interest in understanding what in my mind could have been the common property of the member of this family: the mechanism of action for dissipating the excitation energy.

At that time some theories on the diatoms quenching sites located in the antenna and in the reaction centers started to appear. It became appealing to use one of the mutant present in the lab with a modulated content of the LHCX protein and to study it with an ultrafast spectroscopy technique to trace the defective quenching site and thus the site of action of the LHCX. In this purpose, the LHCX1 protein was chosen as paradigm for the family, because its role in the low light condition was already characterized, and also because it is constitutively expressed, pinpointing to such an important site to protect that it is constitutively protected by the LHCX1.

At the same time, I had in mind that in *C. reinhardtii,* the major contributor to the NPQ process, LHCSR3, was expressed only after sustained high light exposure, and the effect of the LHCX1 mutation had never been studied before in *P. tricornutum* upon this stress. This condition, after the first comparative study that I conducted, revealed to be particularly interesting because also the LHCX2 and the LHCX3 were induced and I hoped to gain some knowledge also on their activity.

Surprisingly, while studying the kinetics of chlorophyll fluorescence at room temperature, I discovered that the mutant with a reduced content of the LHCX1 protein showed an NPQ capacity comparable to that of the wild type after a sustained high light treatment, while the LHCX1 content was still strongly down-regulated and the xanthophyll pigment contents were comparable to the wild-type.

This recovered NPQ capacity could be due to several mechanisms. The first simple case is that all the quenching sites of *LHCX1* mutant and the wild type are active and both have overwhelmed a saturating threshold of quenching occupancy and thus of possible NPQ capacity. This situation might be due to a temporal disengagement of the NPQ from the LHCX1 necessity because the LHCX2 and the LHCX3 provide the additional quenching sites in the mutant to reach the wild type NPQ level. This saturation of the quenching sites in the mutant and in the wild-type might be induced by a sufficiently high proton gradient and xanthophyll cycle activity. Indeed, this resemble to the phenotype of an *A. thaliana* mutant deprived of PsbS whose NPQ capacity becomes close to the wild

type if the proton gradient is high enough (Johnson & Ruban 2011). The same effect on the NPQ in the PsbS mutant is also obtained under sustained illumination (Johnson & Ruban 2010). In both these cases, the *A. thaliana* mutant needs some time to reach the wild type NPQ, but in the case of *P. tricornutum* the presence of the LHCX2 and LHCX3 could explain the quick recovery of the NPQ.

Another possible explanation is the occurrence of a slow photoinhibitory quenching, which decreases the maximal fluorescence level during the actinic light and that distorts the NPQ value. This is mathematically evident looking at the Bilger and Bjorgman equation (Eq. 1) in the section 1.14. Traditionally, in plants, the presence of a photoinhibitory component can be pinpointed looking at the relaxation kinetics of the NPQ traces because when the qE component relaxes with the proton gradient dissipation, the photoinhibitory component is still active. Unfortunately, this is not the case for diatoms, whose qE has a slow relaxation kinetic because the epoxidation reaction, which marks the extinction of the qE amplitude, not only has a slow activity but it is also strictly inhibited by the proton gradient. The merged effect is that the qE and the qI might co-exist in diatoms.

To test these hypotheses, we analyzed the samples with the ultrafast spectroscopic techniques to pinpoint and localize *in vivo* the events of energy dissipation among the photosynthetic complexes. We confirmed that two different sites of quenching exist in diatoms, the reaction centers and the antenna ones (Chukhutsina et al. 2014). From these analyses, the reaction center quenching appears to become predominant in low light acclimated cells after a short high light stress, while the antenna quenching is mostly active in the sustained high light conditions. This result provided a rationale for the existence of two diverse quenching sites in diatoms.

LHCX1 turned out to have a role in the reaction center quenching formation: indeed, the *lhcx1a,* at difference with the wild type, had an impaired quenching capacity in the reaction center (RC), allowing to assign the formation of this quenching site to the presence of LHCX1 protein. However, the antenna quenching capacity was unaltered in the mutant when grown in high light. The understanding of the molecular actors present at each quenching site become of primary interest.

It is possible to determine the molecular components in the photosynthetic complexes first by extracting the thylakoidal membranes, then by separating the photocomplexes and finally probing the presence of the molecules in each fraction by western blot analysis. To perform these

experiments, I visited Dr. Lepetit in Kostanz University because he is an expert in the biochemistry and biophysics of diatom photosynthesis and set up the method necessary to this case.

This analysis revealed the presence of the sole LHCX1 in all the photosynthetic complexes in low light grown cells. However, after sustained high light conditions also the LHCX3 was detected in the antenna and in PSI, but in the PSII dimers only the LHCX1 was found. The presence of the LHCX3 in the antenna, where the quenching capacity was unaffected in the mutant, let us thinking that this protein might could be the molecular actor potentiating the NPQ capacity in the mutant at this site, and possibly the total NPQ.

At this point I aimed at understanding the efficacy of the two quenching sites in photoprotecting the reaction center impoverished of the LHCX1 protein. For this purpose, I measured the net photosynthesis in the samples in the laboratory of Dr. Giovanni Finazzi at CEA of Grenoble, as proxy for the photosynthetic capacity. The mutant showed a decrease in the photosynthetic capacity in sustained high light condition and as a consequence also a decrease growth capacity. The PSII complexes were decreased in the mutant meaning that the reaction center quenching is essential for photoprotection of the PSII but not for NPQ.

How is it possible that the overall NPQ is recovered and the PSII is degradated in the *lhcx1a* mutant? Are the two quenching sites differently efficient in the photoprotection? Lambrev et al. calculated the contribution of the two different quenching sites in *A. thaliana* and correlated their contributions to total NPQ (Lambrev et al. 2012). They unveiled that there is not a direct relationship between total NPQ and protection against photoinhibition. Even though the antenna quenching site contributes largely to the overall NPQ, the reaction center quenching is more efficient in protecting photosystems from ROS. This is in line with the phenotype of *lhcx1a* mutant in high light, where the reduction of the reaction center quenching site decreases the protection of PSII from degradation although the antenna quenching is active and possibly generates an NPQ value comparable to the wild-type in the mutant.

Therefore, the reaction center quenching sites LHCX1-mediated, could play a more important role in the total NPQ capacity in *P. tricornutum* in cells adapted to low light and exposed to short high light treatments, when the antenna quenching is less important. This observation meets

the results from *A. thaliana*: when grown in continuous versus short high light exposure, the lack of PsbS had a bigger effect on the total NPQ only in the short high light exposure (Külheim et al. 2002). In addition, as in PsbS KO mutant there is greater ROS production than in wild type (Frenkel et al. 2009), the side effect of the reduced quenching capacity in *lhcx1a* seems to be a greater production of ROS. This hypothesis can explain the higher PSII degradation observed in the mutant compared to the wild type in HL, however, a precise ROS quantification in the *lhcx1* should be performed.

This study has allowed to associate, for the first time, LHCX to the quenching site formation and to measure the weight of the impairement of one of this quenching on the chloroplast physiology in cells acclimated to low light and high light for different time (short and long high light acclimation).

Interestingly, the LHCX3 protein has not the same distribution as LHCX1 and I made the hypothesis that it can be the isoform responsible of the NPQ recovery observed in sustained high light. At the same time when I was doing these analyses, I produced several putative mutants with a modulated content of the LHCX3 protein as described in the Chapter 4. The LHCX3 is the only isoform that I did not succeed to down-regulate by RNA interference, although many transgenic lines containing the LHCX3 antisense fragments have been analyzed. Because our transgenic lines have been isolated in cells grown in low light cells and normally the LHCX3 is expressed at a very low level in this condition, it is unlikely that the mutants have not been obtained because of its essential function. However, we cannot exclude that the LHCX3 is required for the LHCX1 activity. Some indications of a possible co-action of these proteins derive by preliminary analyses of lines co-expressing the LHCX1 and LHCX3 antisenses, and showing an increase in the LHCX1 protein. Therefore, in the future it will be important to get additional information about the association between the different LHCXs and their partners in the different photosynthetic complexes. Such a kind of study could be performed by using a co-immunoprecipitation technique, as recently used to uncover the PsbS interacting molecules (Correa-Galvis et al. 2016). Remarkably, during my PhD I already generated independent transgenic lines over-expressing an HA-tag version of the LHCX proteins that can be used for future studies.

Finally, this work has given us a new understanding of how LHCX proteins work in the *P. tricornutum* quenching sites. From what I have learned, upon short or sustained high light treatment different quenching sites appear. The constitutively expressed LHCX1 protein operates in a reaction center quenching site without the presence of other isoforms, whereas the LHCX3 is induced after a sustained high light stress and it is possibly responsible for the recovery of the NPQ capacity in the *lhcx1* mutant, suggesting an important flexibility in the regulation of this process in diatoms.

Many new questions arise from this study, such as which is the enigmatic function of the dark-induced LHCX4? Which is the functional and biochemical interaction between the different LHCXs? Considering that tools for gene editing have been now set up in *P. tricornutum* (Daboussi et al. 2014; Nymark et al. 2016), future studies will certainly benefit of the the generation of new LHCXs loss-of-function mutants. Integrated approaches of biochemistry, cell physiology, and biophysics such as those used in this thesis, will certainly help to further characterize the function of the LHCX protein family, that appears today as key regulator of the diatom chloroplast.

References

Adams, W.W. et al., 2014. Photosystem II Effi ciency and Non-Photochemical Fluorescence Quenching in the Context of Source-Sink Balance. In Springer, ed. *Non-Photochemical Quenching and Energy Dissipation in Plants, Algae and Cyanobacteria*. pp. 503–529.

Ahn, T.K. et al., 2008. Architecture of a charge-transfer state regulating light harvesting in a plant antenna protein. *Science (New York, N.Y.)*, 320(5877), pp.794–7. Available at: http://www.ncbi.nlm.nih.gov/pubmed/18467588 [Accessed March 28, 2013].

Alboresi, A. et al., 2008. In silico and biochemical analysis of Physcomitrella patens photosynthetic antenna: identification of subunits which evolved upon land adaptation. *PloS one*, 3(4), p.e2033. Available at: http://www.pubmedcentral.nih.gov/articlerender.fcgi?artid=2323573&tool=pmcentrez&rendertype=abstract [Accessed February 19, 2013].

Alboresi, A. et al., 2010. Physcomitrella patens mutants affected on heat dissipation clarify the evolution of photoprotection mechanisms upon land colonization.

Alipanah, L. et al., 2015. Whole-cell response to nitrogen deprivation in the diatom Phaeodactylum tricornutum. *Journal of Experimental Botany*, 66(20), pp.6281–6296.

Allen, A.E. et al., 2011. Evolution and metabolic significance of the urea cycle in photosynthetic diatoms. *Nature*, 473(7346), pp.203–7. Available at: http://www.ncbi.nlm.nih.gov/pubmed/21562560 [Accessed July 16, 2012].

Allen, A.E. et al., 2008. Whole-cell response of the pennate diatom Phaeodactylum tricornutum to iron starvation. *Proceedings of the National Academy of Sciences of the United States of America*, 105(30), pp.10438–43. Available at: http://www.pubmedcentral.nih.gov/articlerender.fcgi?artid=2492447&tool=pmcentrez&rendertype=abstract.

Allen, J., 2002. Photosynthesis of ATP-electrons, proton pumps, rotors, and poise. *Cell*, 110(3), pp.273–6. Available at: http://www.ncbi.nlm.nih.gov/pubmed/12176312.

Allen, J.F. et al., 2011. A structural phylogenetic map for chloroplast photosynthesis. *Trends in Plant Science*, 16(12), pp.645–655. Available at: http://linkinghub.elsevier.com/retrieve/pii/S1360138511002263 [Accessed September 24, 2013].

Allorent, G. et al., 2013. A Dual Strategy to Cope with High Light in Chlamydomonas reinhardtii. *The Plant cell*, (3). Available at: http://www.ncbi.nlm.nih.gov/pubmed/23424243 [Accessed March 1, 2013].

Amunts, A. et al., 2010. Structure determination and improved model of plant photosystem I. *Journal of Biological Chemistry*, 285(5), pp.3478–3486.

Anderson, J.M. & Andersson, B., 1988. The dynamic photosynthetic membrane and regulation of solar energy conversion. *Trends in Biochemical Sciences*, 13, pp.351–355.

Apt, K.E., Grossman, A.R. & Kroth-Pancic, P.G., 1996. Stable nuclear transformation of the diatomPhaeodactylum tricornutum. *MGG Molecular & General Genetics*, 252(5), pp.572–579. Available at: http://link.springer.com/article/10.1007/BF02172403 [Accessed November 16, 2012].

Archibald, J.M. & Keeling, P.J., 2002. Recycled plastids: a “green movement” in eukaryotic evolution. *Trends in Genetics*, 18(11), pp.577–584.

Armbrust, E.V., 2009. The life of diatoms in the world’s oceans. *Nature*, 459(7244), pp.185–92. Available at: http://www.ncbi.nlm.nih.gov/pubmed/19444204 [Accessed October 28, 2012].

Armbrust, E.V. & et al., 2004. The genome of the diatom Thalassiosira pseudonana: ecology, evolution, and metabolism. *Science*, 306, pp.79–86.

Armstrong, G. a & Hearst, J.E., 1996. Carotenoids 2: Genetics and molecular biology of carotenoid pigment biosynthesis. *The FASEB journal : official publication of the Federation of American Societies for Experimental Biology*, 10(2), pp.228–237. Available at: http://www.ncbi.nlm.nih.gov/pubmed/8641556.

Arnoux, P. et al., 2009. A structural basis for the pH-dependent xanthophyll cycle in Arabidopsis thaliana. *The Plant cell*, 21(7), pp.2036–2044.

Aro, E., Virgin, I. & Andersson, B., 1993. Photoinhibition of Photosystem II. Inactivation, protein damage and turnover. *Biochimica et Biophysica Acta (BBA) - Bioenergetics*, 1143(2), pp.113–134. Available at: http://linkinghub.elsevier.com/retrieve/pii/0005272893901342.

Avenson, T.J. et al., 2008. Zeaxanthin radical cation formation in minor light-harvesting complexes of higher plant antenna. *The Journal of biological chemistry*, 283(6), pp.3550–8. Available at: http://www.ncbi.nlm.nih.gov/pubmed/17991753 [Accessed January 2, 2015].

Bailleul, B. et al., 2010. An atypical member of the light-harvesting complex stress-related protein family modulates diatom responses to light. *Proceedings of the National Academy of Sciences of the United States of America*, 107(42), pp.18214–9. Available at: http://www.pubmedcentral.nih.gov/articlerender.fcgi?artid=2964204&tool=pmcentrez&rendertype=abstract.

Bailleul, B. et al., 2015. Energetic coupling between plastids and mitochondria drives CO2 assimilation in diatoms. *Nature*.

Baker, N.R., 2008. Chlorophyll fluorescence: a probe of photosynthesis in vivo. *Annual review of plant biology*, 59, pp.89–113. Available at: http://www.ncbi.nlm.nih.gov/pubmed/18444897 [Accessed February 28, 2013].

Ballottari, M. et al., 2013. Chlorophyll triplet quenching and photoprotection in the higher plant monomeric antenna protein Lhcb5. *Journal of Physical Chemistry B*, 117(38), pp.11337–11348.

Ballottari, M. et al., 2015. Identification of pH-sensing sites in the Light Harvesting Complex Stress-Related 3 protein essential for triggering non-photochemical quenching in Chlamydomonas reinhardtii. , Submitted.

Bassi, R. et al., 1992. Characterization of chlorophyll a/b proteins of photosystem I from Chlamydomonas reinhardtii. *Journal of Biological Chemistry*, 267(36), pp.25714–25721.

Beer, A. et al., 2006. Subunit composition and pigmentation of fucoxanthin-chlorophyll proteins in diatoms: evidence for a subunit involved in diadinoxanthin and diatoxanthin binding. *Biochemistry*, 45(43), pp.13046–53. Available at: http://www.ncbi.nlm.nih.gov/pubmed/17059221.

Bellafiore, S. et al., 2005. State transitions and light adaptation require chloroplast thylakoid protein kinase STN7. *Nature*, 433(7028), pp.892–895. Available at: http://www.nature.com/doifinder/10.1038/nature03286.

Ben-Shem, A., Frolow, F. & Nelson, N., 2003. Crystal structure of plant photosystem I. , 426(6967), pp.630–635. Available at: file://localhost/Users/jmb/Documents/Papers/Ben-Shem/Ben-Shem2003Nature.pdf\nhttp://www.ncbi.nlm.nih.gov/entrez/query.fcgi?db=pubmed&cmd=Retrieve&dopt=AbstractPlus&list_uids=14668855.

Bergantino, E. et al., 2003. Light- and pH-dependent structural changes in the PsbS subunit of photosystem II. *Proceedings of the National Academy of Sciences of the United States of America*, 100(25), pp.15265–15270.

Berkaloff, C., Caron, L. & Rousseau, B., 1990. Subunit organization of PSI particles from brown algae and diatoms: polypeptide and pigment analysis. *Photosynthesis Research*, 23(2), pp.181–193.

Betterle, N. et al., 2009. Light-induced dissociation of an antenna hetero-oligomer is needed for non-photochemical quenching induction. *The Journal of biological chemistry*, 284(22), pp.15255–66. Available at: http://www.pubmedcentral.nih.gov/articlerender.fcgi?artid=2685706&tool=pmcentrez&rendertype=abstract [Accessed February 13, 2013].

Bhaya, D. & Grossman, a R., 1993. Characterization of gene clusters encoding the fucoxanthin chlorophyll proteins of the diatom Phaeodactylum tricornutum. *Nucleic acids research*, 21(19), pp.4458–66. Available at: http://www.pubmedcentral.nih.gov/articlerender.fcgi?artid=311176&tool=pmcentrez&rendertype=abstract.

Bilger, W. & Björkman, O., 1990. Role of the xanthophyll cycle in photoprotection elucidated by measurements of light-induced absorbance changes, fluorescence and photosynthesis in leaves of Hedera canariensis. *Photosynthesis Research*, 25(3), pp.173–185. Available at: http://www.springerlink.com/index/10.1007/BF00033159.

Bonente, G. et al., 2011. Analysis of LhcSR3, a protein essential for feedback de-excitation in the green alga Chlamydomonas reinhardtii. *PLoS biology*, 9(1), p.e1000577. Available at:

http://www.pubmedcentral.nih.gov/articlerender.fcgi?artid=3022525&tool=pmcentrez&rendertype=abstract [Accessed January 31, 2013].
Bonente, G., Howes, B.D., et al., 2008. Interactions between the photosystem II subunit PsbS and xanthophylls studied in vivo and in vitro. *The Journal of biological chemistry*, 283(13), pp.8434–45. Available at: http://www.pubmedcentral.nih.gov/articlerender.fcgi?artid=2417184&tool=pmcentrez&rendertype=abstract [Accessed April 27, 2014].
Bonente, G., Passarini, F., et al., 2008. The occurrence of the psbs gene product in chlamydomonas reinhardtii and in other photosynthetic organisms and its correlation with energy quenching. *Photochemistry and Photobiology*, 84(6), pp.1359–1370.
Borowitzka, M. a & Volcani, B.E., 1978. Polymorphic diatom Phaeodactylum Tricornutum: Ultrastructure of its morphotypes. *Journal of Phycology*, (14), pp.10–21.
Borowitzka, M.A. & Siva, C.J., 2007. The taxonomy of the genus Dunaliella (Chlorophyta, Dunaliellales) with emphasis on the marine and halophilic species. *Journal of Applied Phycology*, 19, pp.567–590.
Bowler, C. et al., 2008. The Phaeodactylum genome reveals the evolutionary history of diatom genomes. *Nature*, 456(7219), pp.239–44. Available at: http://www.ncbi.nlm.nih.gov/pubmed/18923393 [Accessed July 20, 2012].
Bowler, C., De Martino, A. & Falciatore, A., 2010. Diatom cell division in an environmental context. *Current opinion in plant biology*, 13(6), pp.623–30. Available at: http://www.ncbi.nlm.nih.gov/pubmed/20970371 [Accessed July 16, 2012].
Brzezinski, M.A., Olson, R.J. & Chisholm, S.W., 1990. Silicon avail- ability and cell-cycle progression in marine diatoms. *Marine Ecology Progress Series*, 67, pp.83–96.
Büch, K., Stransky, H. & Hager, A., 1995. FAD is a further essential cofactor of the NAD (P) H and O 2-dependent zeaxanthin-epoxidase. *FEBS letters*, 376(1), pp.45–48.
Buchel, C., 2003. Fucoxanthin-Chlorophyll Proteins in Diatoms : 18 and 19 kDa Subunits Assemble into Different Oligomeric States †. , (19), pp.13027–13034.
Büchel, C. & Kühlbrandt, W., 2005. Structural differences in the inner part of Photosystem II between higher plants and cyanobacteria. *Photosynthesis Research*, 85(1), pp.3–13.
Bugos, R.C., Hieber, A.D. & Yamamoto, H.Y., 1998. Xanthophyll cycle enzymes are members of the lipocalin family, the first identified from plants. *Journal of Biological Chemistry*, 273(25), pp.15321–15324.
Carpenter, E.J. & Janson, S., 2000. INTRACELLULAR CYANOBACTERIAL SYMBIONTS IN THE MARINE DIATOM CLIMACODIUM FRAUENFELDIANUM (BACILLARIOPHYCEAE) 1. , 544(August 1999), pp.540–544.
Chepurnov, V.A. et al., 2004. Experimental studies on sexual reproduction in diatoms. *International Review of Cytology*, 237, pp.91–154.
Chepurnov, V.A. et al., 2002. Sexual reproduction, mating system, and protoplast dynamics of Seminavis (Bacillariophyceae). *Journal of Phycology*, 38(5), pp.1004–1019.
Chukhutsina, V.U., Büchel, C. & van Amerongen, H., 2014. Disentangling two non-photochemical quenching processes in Cyclotella meneghiniana by spectrally-resolved picosecond fluorescence at 77K. *Biochimica et biophysica acta*, pp.1–10. Available at: http://www.ncbi.nlm.nih.gov/pubmed/24582663 [Accessed March 5, 2014].
Chukhutsina, V.U., Büchel, C. & van Amerongen, H., 2013. Variations in the first steps of photosynthesis for the diatom Cyclotella meneghiniana grown under different light conditions. *Biochimica et biophysica acta*, 1827(1), pp.10–8. Available at: http://www.ncbi.nlm.nih.gov/pubmed/23036902 [Accessed October 16, 2014].
Coesel, S. et al., 2008. Evolutionary origins and functions of the carotenoid biosynthetic pathway in marine diatoms. *PloS one*, 3(8), p.e2896. Available at: http://www.pubmedcentral.nih.gov/articlerender.fcgi?artid=2483416&tool=pmcentrez&rendertype=abstract [Accessed July 20, 2012].
Correa-Galvis, V. et al., 2016. PsbS interactions involved in the activation of energy dissipation in Arabidopsis. *Nature Plants*, 2(2), p.15225. Available at: http://www.nature.com/articles/nplants2015225.
Croce, R. et al., 2003. Energy transfer pathways in the minor antenna complex CP29 of photosystem II: a femtosecond study of carotenoid to chlorophyll transfer on mutant and WT complexes. *Biophysical journal*, 84(4), pp.2517–32. Available at: http://www.sciencedirect.com/science/article/pii/S0006349503750577.

D'Alelio, D. et al., 2009. Sexual and vegetative phases in the planktonic diatom Pseudo-nitzschia multistriata. *Harmful Algae*, 8(2), pp.225–232. Available at: http://linkinghub.elsevier.com/retrieve/pii/S1568988308000632 [Accessed July 25, 2012].

Daboussi, F. et al., 2014. Genome engineering empowers the diatom Phaeodactylum tricornutum for biotechnology. *Nature Communications*, 5(May), pp.1–7. Available at: http://www.nature.com/doifinder/10.1038/ncomms4831.

Dall'Osto, L.C., 2005. A Mechanism of Nonphotochemical Energy Dissipation , Independent from PsbS , Revealed by a Conformational Change in the Antenna Protein CP26. , 17(April), pp.1217–1232.

Dekker, J.P. & Boekema, E.J., 2005. Supramolecular organization of thylakoid membrane proteins in green plants. *Biochimica et biophysica acta*, 1706(1-2), pp.12–39. Available at: http://www.ncbi.nlm.nih.gov/pubmed/15620363 [Accessed April 1, 2014].

Delwiche, C.F., 1999. Tracing the Thread of Plastid-Diversity through the Tapestry of Life. *American Naturalist*, 154(october). Available at: http://www.jstor.org/stable/10.2307/2463984.

Demmig, B. et al., 1987. Photoinhibition and Zeaxanthin Formation in Intact Leaves. A possible role of the xanthophyll cycle in the dissipation of excess light energy. *Plant physiology*, 84, pp.218–224.

Demmig-Adams, B., 1990. Carotenoids and photoprotection in plants: a role for the xanthophyll zeaxanthin. *Biochimica et Biophysica Acta (BBA)*, 1020, pp.1–24.

Demmig-Adams, B. et al., 2012. Modulation of photosynthetic energy conversion efficiency in nature: From seconds to seasons. *Photosynthesis Research*, 113(1-3), pp.75–88.

Demmig-Adams, B. et al., 2006. Modulation of PsbS and flexible vs sustained energy dissipation by light environment in different species. *Physiologia Plantarum*, 127, pp.670–680.

Demmig-Adams, B. & Adams, W.W., 2006. Photoprotection in an ecological context: The remarkable complexity of thermal energy dissipation. *New Phytologist*, 172, pp.11–21.

Demmig-Adams, B. & Adams, W.W., 1996. The role of xanthophyll cycle carotenoids in the protection of photosynthesis. *Trends in Plant Science*, 1, pp.21–26.

Depauw, F.A. et al., 2012. Exploring the molecular basis of responses to light in marine diatoms. *Journal of experimental botany*, 63(4), pp.1575–91. Available at: http://www.ncbi.nlm.nih.gov/pubmed/22328904 [Accessed July 27, 2012].

Douglas, E.S., 1998. Plastid evolution: origins, diversity, trends. *Current Opinion in Genetics & Development*, 8(6), pp.655–661.

Dunahay, T.G. & Jarvis, E.E., 1995. Genetic transformation of the diatoms Cyclotella Cryptica and Navicula Saprophila. *Journal of Phycology*, 31, pp.1004–1012.

Duysens, L.N.M., Amesz, J. & Kamp, B.M., 1961. Two Photochemical Systems in Photosynthesis. *Nature*, 190, pp.510–511.

Eberhard, S., Finazzi, G. & Wollman, F.-A., 2008. The dynamics of photosynthesis. *Annual review of genetics*, 42, pp.463–515. Available at: http://www.ncbi.nlm.nih.gov/pubmed/18983262 [Accessed February 28, 2013].

Elrad, D., Niyogi, K.K. & Grossman, A.R., 2002. A Major Light-Harvesting Polypeptide of Photosystem II Functions in Thermal Dissipation. , 14(August), pp.1801–1816.

Esteban-Pretel, G. et al., 2010. Vitamin A deficiency increases protein catabolism and induces urea cycle enzymes in rats. *The Journal of nutrition*, 140(4), pp.792–8. Available at: http://jn.nutrition.org/content/140/4/792.short [Accessed November 27, 2012].

Falciatore, A. et al., 2000. Perception of environmental signals by a marine diatom. *Science (New York, N.Y.)*, 288(5475), pp.2363–2366. Available at: http://www.ncbi.nlm.nih.gov/pubmed/10875921.

Falciatore, A. et al., 1999. Transformation of Nonselectable Reporter Genes in Marine Diatoms. *Marine biotechnology (New York, N.Y.)*, 1(3), pp.239–251. Available at: http://www.ncbi.nlm.nih.gov/pubmed/10383998.

Falciatore, A. & Bowler, C., 2002. Revealing the molecular secrets of marine diatoms. *Annual review of plant biology*, 53(29), pp.109–30. Available at: http://www.ncbi.nlm.nih.gov/pubmed/12221969 [Accessed December 16, 2013].

Falkowski, P. & Raven, J.A., 2007. *Aquatic photosynthesis*,

Falkowski, P.G. et al., 2004. The evolution of modern eukaryotic phytoplankton. *Science (New York, N.Y.)*, 305(5682), pp.354–60. Available at: http://www.sciencemag.org/content/305/5682/354.abstract [Accessed February 28, 2013].

Falkowski, P.G. & Owens, T.G., 1980. Light- Shade Adaptation ’. , pp.592–595.
Fan, M. et al., 2015. Crystal structures of the PsbS protein essential for photoprotection in plants. *Nature Publishing Group*, 22(9), pp.729–735. Available at: http://dx.doi.org/10.1038/nsmb.3068.
Ferreira, K.N. et al., 2004. Architecture of the Photosynthetic Oxygen-Evolving Center. , 43(March), pp.1831–1839.
Field, C.B. et al., 1998. Primary Production of the Biosphere: Integrating Terrestrial and Oceanic Components. *Science*, 281(5374), pp.237–240.
Finazzi, G. et al., 2004. A zeaxanthin-independent nonphotochemical quenching mechanism localized in the photosystem II core complex. *Proceedings of the National Academy of Sciences of the United States of America*, 101(33), pp.12375–12380.
Finazzi, G., 2005. The central role of the green alga Chlamydomonas reinhardtii in revealing the mechanism of state transitions. *Journal of Experimental Botany*, 56(411), pp.383–388.
Finazzi, G. & Minagawa, J., 2015. High light acclimation in green microalgae in non-photochemical quenching and thermal energy dissipation in plants, algae and cyanobacteria. *Advances in Photosynthesis and Respiration 40*, 40, pp.445–469.
Finazzi, G., Moreau, H. & Bowler, C., 2010. Genomic insights into photosynthesis in eukaryotic phytoplankton. *Trends in plant science*, 15(10), pp.565–72. Available at: http://dx.doi.org/10.1016/j.tplants.2010.07.004 [Accessed November 15, 2012].
Fischer, H. et al., 1999. Targeting and covalent modification of cell wall and membrane proteins heterologously expressed in the diatom Cylindrotheca fusiformis (Bacillariophyceae). *Journal of Phycology*, 35, pp.113–120.
Fisher, A.E., Berges, J.A. & Harrison, P.J., 1996. DOES LIGHT QUALITY AFFECT THE SINKING RATES OF MARINE DIATOMS?1. *Journal of Phycology*, 32(3), pp.353–360. Available at: http://doi.wiley.com/10.1111/j.0022-3646.1996.00353.x [Accessed November 29, 2012].
Frank, H.A. et al., 1994. Photophysics of the carotenoids associated with the xanthophyll cycle in photosynthesis. *Photosynthesis research*, (3), pp.389–395.
Frank, H.A. et al., 1996. The lifetimes and energies of the first excited singlet states of diadinoxanthin and diatoxanthin. *Biochimica et Biophysica Acta*, 1277, pp.243–252.
Frenkel, M. et al., 2009. Improper excess light energy dissipation in Arabidopsis results in a metabolic reprogramming. *BMC plant biology*, 9, p.12. Available at: http://www.pubmedcentral.nih.gov/articlerender.fcgi?artid=2656510&tool=pmcentrez&rendertype=abstract.
Fromme, P., Jordan, P. & Krauss, N., 2001. Structure of photosystem I. *Biochimica et Biophysica Acta - Bioenergetics*, 1507(1-3), pp.5–31.
Gerotto, C. et al., 2011. Role of PSBS and LHCSR in Physcomitrella patens acclimation to high light and low temperature. *Plant, Cell and Environment*, 34(6), pp.922–932.
Ghazaryan, A. et al., 2016. Involvement of the Lhcx protein Fcp6 of the diatom Cyclotella meneghiniana in the macro-organization and structural flexibility of thylakoid membranes. *Biochimica et Biophysica Acta (BBA) - Bioenergetics*. Available at: http://linkinghub.elsevier.com/retrieve/pii/S0005272816303875.
Goss, R. et al., 2007. Lipid dependence of diadinoxanthin solubilization and de-epoxidation in artificial membrane systems resembling the lipid composition of the natural thylakoid membrane. *Biochimica et biophysica acta*, 1768(1), pp.67–75. Available at: http://www.sciencedirect.com/science/article/pii/S0005273606002161 [Accessed February 24, 2015].
Goss, R. et al., 2005. Role of Hexagonal Structure-Forming Lipids in Diadinoxanthin and Violaxanthin. , (Ps Ii), pp.4028–4036.
Goss, R. et al., 2006. The importance of a highly active and DeltapH-regulated diatoxanthin epoxidase for the regulation of the PS II antenna function in diadinoxanthin cycle containing algae. *Journal of plant physiology*, 163(10), pp.1008–21. Available at: http://www.ncbi.nlm.nih.gov/pubmed/16971213 [Accessed January 8, 2014].
Goss, R. & Lepetit, B., 2014. Biodiversity of NPQ. *Journal of plant physiology*, 172, pp.13–32. Available at: http://www.ncbi.nlm.nih.gov/pubmed/24854581.
Goss, R., Richter, M. & Wild, A., 1995. Role of ΔpH in the mechanism of zeaxanthin-dependent amplification of qE. *Journal of Photochemistry and Photobiology, B: Biology*, 27(2), pp.147–152.

Green, B.R., 2011. Chloroplast genomes of photosynthetic eukaryotes. *The Plant Journal*, 66, pp.34–44.
Green, B.R., Anderson, J.M. & Parson, W.W., 2003. Photosynthetic Membranes and Their Light-Harvesting Antennas. In *Advances in Photosynthesis and Respiration*. pp. 1–28.
Green, B.R. & Durnford, D.G., 1996. the Chlorophyll-Carotenoid Proteins of Oxygenic Photosynthesis. *Annual Review of Plant Physiology and Plant Molecular Biology*, 47(1), pp.685–714.
Grossman, A.R. et al., 1995. Light-harvesting complexes in oxygenic photosynthesis: diversity, control, and evolution. *Annual review of genetics*, 29, pp.231–88. Available at: http://www.ncbi.nlm.nih.gov/pubmed/8825475.
Grossman, A.R., Bhaya, D. & He, Q., 2001. Tracking the Light Environment by Cyanobacteria and the Dynamic Nature of Light Harvesting. *The Journal of biological chemistry*, 276, pp.11449–11452.
Grotjohann, I. & Fromme, P., 2005. Structure of cyanobacterial Photosystem I. *Photosynthesis Research*, 85(1), pp.51–72.
Grouneva, I. et al., 2006. Influence of ascorbate and pH on the activity of the diatom xanthophyll cycle-enzyme diadinoxanthin de-epoxidase. , (Hager 1969), pp.205–211.
Grouneva, I., Rokka, A. & Aro, E.-M., 2011. The thylakoid membrane proteome of two marine diatoms outlines both diatom-specific and species-specific features of the photosynthetic machinery. *Journal of proteome research*, 10(12), pp.5338–53. Available at: http://www.ncbi.nlm.nih.gov/pubmed/22017178.
Gundermann, K. & Büchel, C., 2012. Factors determining the fluorescence yield of fucoxanthin-chlorophyll complexes (FCP) involved in non-photochemical quenching in diatoms. *Biochimica et biophysica acta*, 1817(7), pp.1044–52. Available at: http://www.ncbi.nlm.nih.gov/pubmed/22440329 [Accessed February 13, 2013].
Gundermann, K. & Büchel, C., 2008. The fluorescence yield of the trimeric fucoxanthin-chlorophyll-protein FCPa in the diatom Cyclotella meneghiniana is dependent on the amount of bound diatoxanthin. *Photosynthesis research*, 95(2-3), pp.229–35. Available at: http://www.ncbi.nlm.nih.gov/pubmed/17912602 [Accessed April 21, 2014].
Hager, A., 1969. Light dependent decrease of the pH-value in a chloroplast compartment causing the enzymatic interconversion of violaxanthin to zeaxanthin; relations to photophosphorylation. *Planta (Berlin)*, 89, pp.224–243.
Hager, A., 1975. The reversible, light-induced conversions of xanthophyll in the chloroplast. *Berichte der Deutschen Botanischen Gesellschaft*, 88, pp.27–44.
Hager, A. & Holocher, K., 1994. Localization of the xanthophyll-cycle enzyme violaxanthin de-epoxidase within the thylakoid lumen and abolition of its mobility by a (light-dependent) pH decrease. *Planta*, 192(4), pp.581–589.
Haimovich-Dayan, M. et al., 2012. The role of C(4) metabolism in the marine diatom Phaeodactylum tricornutum. *The New phytologist*. Available at: http://www.ncbi.nlm.nih.gov/pubmed/23078356 [Accessed October 22, 2012].
Havaux, M. & Niyogi, K.K., 1999. The violaxanthin cycle protects plants from photooxidative damage by more than one mechanism. *Proceedings of the National Academy of Sciences of the United States of America*, 96(15), pp.8762–8767.
Herbstová, M. et al., 2015. Molecular basis of chromatic adaptation in pennate diatom Phaeodactylum tricornutum. *Biochimica et Biophysica Acta (BBA) - Bioenergetics*. Available at: http://linkinghub.elsevier.com/retrieve/pii/S000527281500047X.
Hill, R. & Bendall, F., 1960. Function of the two cytochrome components in chloroplasts: a working hypothesis. *Nature (London, United Kingdom)*, 186, pp.136–137.
Holzwarth, A.R. et al., 2009. Identification of two quenching sites active in the regulation of photosynthetic light-harvesting studied by time-resolved fluorescence. *Chemical Physics Letters*, 483(4-6), pp.262–267. Available at: http://dx.doi.org/10.1016/j.cplett.2009.10.085.
Horton, P. et al., 1991. Control of the light-harvesting function of chloroplast membranes by aggregation of the LHCII chlorophyll-protein complex. *FEBS Letters*, 292(1-2), pp.1–4.
Horton, P., 2000. Prospects for crop improvement through the genetic manipulation of photosynthesis: morphological and biochemical aspects of light capture. *Journal of experimental botany*, 51 Spec No(February), pp.475–485.
Huysman, M.J.J. et al., 2013. AUREOCHROME1a-mediated induction of the diatom-specific cyclin dsCYC2 controls the onset of cell division in diatoms (Phaeodactylum tricornutum).

The Plant cell, 25(1), pp.215–28. Available at: http://www.pubmedcentral.nih.gov/articlerender.fcgi?artid=3584536&tool=pmcentrez&rendertype=abstract [Accessed December 3, 2014].
Ikeda, Y. et al., 2008. Photosystem I complexes associated with fucoxanthin-chlorophyll-binding proteins from a marine centric diatom, Chaetoceros gracilis. *Biochimica et Biophysica Acta - Bioenergetics*, 1777(4), pp.351–361.
Jahns, P. & Heyde, S., 1999. Dicyclohexylcarbodiimide alters the pH dependence of violaxanthin de-epoxidation. *Planta*, 207(3), pp.393–400.
Jahns, P., Latowski, D. & Strzalka, K., 2009. Mechanism and regulation of the violaxanthin cycle: The role of antenna proteins and membrane lipids. *Biochimica et Biophysica Acta - Bioenergetics*, 1787(1), pp.3–14. Available at: http://dx.doi.org/10.1016/j.bbabio.2008.09.013.
Jakob, T., Goss, R. & Wilhelm, C., 1999. Activation of Diadinoxanthin De-Epoxidase Due to a Chiororespiratory Proton Gradient in the Dark in the Diatom Phaeodactylum tricornutum. *Plant Biology*, 1(1), pp.76–82. Available at: http://doi.wiley.com/10.1111/j.1438-8677.1999.tb00711.x.
Johnson, M.P. & Ruban, A. V., 2010. Arabidopsis plants lacking PsbS protein possess photoprotective energy dissipation. *Plant Journal*, 61(2), pp.283–289.
Johnson, M.P. & Ruban, A. V., 2011. Restoration of rapidly reversible photoprotective energy dissipation in the absence of PsbS protein by enhanced ??pH. *Journal of Biological Chemistry*, 286(22), pp.19973–19981.
Johnson, X. et al., 2009. A new setup for in vivo fluorescence imaging of photosynthetic activity. *Photosynthesis research*, 102(1), pp.85–93. Available at: http://www.ncbi.nlm.nih.gov/pubmed/19697150 [Accessed November 7, 2012].
Jordan, P. et al., 2001. Three-dimensional structure of cyanobacterial photosystem I at 2.5 A resolution. *Nature*, 411(6840), pp.909–917.
Kamiya, N. & Shen, J.-R., 2003. Crystal structure of oxygen-evolving photosystem II from Thermosynechococcus vulcanus at 3.7-A resolution. *Proceedings of the National Academy of Sciences of the United States of America*, 100(1), pp.98–103.
Karas, B.J. et al., 2015. Designer diatom episomes delivered by bacterial conjugation. *Nature Communications*, 6, p.6925. Available at: http://www.nature.com/doifinder/10.1038/ncomms7925.
Karp-Boss, L. & Jumars, P.A., 1998. Motion of diatom chains in steady shear flow. *LIMNOLOGY AND OCEANOGRAPHY*, 43, pp.1767–1773.
Keeling, P.J., 2010. The endosymbiotic origin, diversification and fate of plastids. *Philosophical Transactions of the Royal Society B: Biological Sciences*, 365(1541), pp.729–748. Available at: http://rstb.royalsocietypublishing.org/content/365/1541/729.short [Accessed October 25, 2012].
Keeling, P.J. et al., 2014. The Marine Microbial Eukaryote Transcriptome Sequencing Project (MMETSP): Illuminating the Functional Diversity of Eukaryotic Life in the Oceans through Transcriptome Sequencing. *PLoS Biology*, 12(6).
Kirk, J.T.O., 1994. *Light and Photosynthesis in Aquatic Ecosystems*. Cambridge .,
Kooistra, W.H.C.F. et al., 2007. The origin and evolution of the diatoms: their adaptation to a planktonic existence. In: Falkowski PG, Knoll AH, eds. Evolution of planktonic photoautotrophs. *Burlington, MA: Academic Press*, pp.207–249.
Kouřil, R. et al., 2013. High-light vs. low-light: effect of light acclimation on photosystem II composition and organization in Arabidopsis thaliana. *Biochimica et biophysica acta*, 1827(3), pp.411–9. Available at: http://www.ncbi.nlm.nih.gov/pubmed/23274453 [Accessed April 8, 2014].
Krause, G.H. & Weis, E., 1991. Chlorophyll Fluorescence and Photosynthesis: The Basics. *Annual review of plant physiology and plant molecular biology*, 42, pp.313–349.
Kroth, P.G. et al., 2008. A model for carbohydrate metabolism in the diatom Phaeodactylum tricornutum deduced from comparative whole genome analysis. *PloS one*, 3(1), p.e1426. Available at: http://www.pubmedcentral.nih.gov/articlerender.fcgi?artid=2173943&tool=pmcentrez&rendertype=abstract [Accessed July 25, 2012].
Külheim, C., Ågren, J. & Jansson, S., 2002. Rapid Regulation of Light Harvesting and Plant Fitness in the Field. *Science (New York, N.Y.)*, 297, pp.91–93.

Lambrev, P.H. et al., 2012. On the relationship between non-photochemical quenching and photoprotection of Photosystem II. *Biochimica et Biophysica Acta - Bioenergetics*, 1817(5), pp.760–769. Available at: http://dx.doi.org/10.1016/j.bbabio.2012.02.002.

Latowski, D., Gryzb, J. & StrzaAka, K., 2004. The xanthophyll cycle - molecular mechanism and physiological significance. *Acta Physiologiae Plantarum*, 26, pp.196–213.

Lavaud, J. & Kroth, P.G., 2006. In diatoms, the transthylakoid proton gradient regulates the photoprotective non-photochemical fluorescence quenching beyond its control on the xanthophyll cycle. *Plant & cell physiology*, 47(7), pp.1010–6. Available at: http://www.ncbi.nlm.nih.gov/pubmed/16699176 [Accessed April 18, 2014].

Lavaud, J., Rousseau, B. & Etienne, a-L., 2002. In diatoms, a transthylakoid proton gradient alone is not sufficient to induce a non-photochemical fluorescence quenching. *FEBS letters*, 523(1-3), pp.163–6. Available at: http://www.ncbi.nlm.nih.gov/pubmed/12123825.

Lavaud, J., Rousseau, B. & Etienne, A.L., 2003. Enrichment of the light-harvesting complex in diadinoxanthin and implications for the nonphotochemical fluorescence quenching in diatoms. *Biochemistry*, 42(19), pp.5802–5808.

Lepetit, B. et al., 2010. Evidence for the existence of one antenna-associated, lipid-dissolved and two protein-bound pools of diadinoxanthin cycle pigments in diatoms. *Plant physiology*, 154(4), pp.1905–20. Available at: http://www.plantphysiol.org/content/154/4/1905.full [Accessed November 27, 2012].

Lepetit, B. et al., 2013. High light acclimation in the secondary plastids containing diatom Phaeodactylum tricornutum is triggered by the redox state of the plastoquinone pool. *Plant physiology*, 161(2), pp.853–65. Available at: http://www.pubmedcentral.nih.gov/articlerender.fcgi?artid=3561024&tool=pmcentrez&rendertype=abstract [Accessed December 16, 2013].

Lepetit, B. et al., 2012. Molecular dynamics of the diatom thylakoid membrane under different light conditions. *Photosynthesis research*, 111(1-2), pp.245–57. Available at: http://www.ncbi.nlm.nih.gov/pubmed/21327535 [Accessed March 14, 2013].

Lepetit, B. et al., 2007. Spectroscopic and molecular characterization of the oligomeric antenna of the diatom Phaeodactylum tricornutum. *Biochemistry*, 46(34), pp.9813–22. Available at: http://www.ncbi.nlm.nih.gov/pubmed/17672483.

Li, X. et al., 2002. PsbS-dependent enhancement of feedback de-excitation protects photosystem II from photoinhibition. *Proceedings of the National Academy of Sciences of the United States of America*, 99(23), pp.15222–15227.

Li, X.P. et al., 2000. A pigment-binding protein essential for regulation of photosynthetic light harvesting. *Nature*, 403(6768), pp.391–5. Available at: http://www.ncbi.nlm.nih.gov/pubmed/10667783.

Li, X.P. et al., 2002. Structure-function analysis of photosystem II subunit S (PsbS) in vivo. *Functional Plant Biology*, 29(10), pp.1131–1139.

Li, X.-P. et al., 2004. Regulation of Photosynthetic Light Harvesting Involves Intrathylakoid Lumen pH Sensing by the PsbS Protein. *Journal of Biological Chemistry*, 279(22), pp.22866–22874. Available at: http://www.jbc.org/cgi/doi/10.1074/jbc.M402461200.

Li, Z. et al., 2009. Sensing and responding to excess light. *Annual review of plant biology*, 60, pp.239–60. Available at: http://www.ncbi.nlm.nih.gov/pubmed/19575582 [Accessed October 26, 2012].

Liu, Z. et al., 2004. Crystal structure of spinach major light-harvesting complex at 2.72 A resolution. *Nature*, 428(6980), pp.287–292. Available at: http://dx.doi.org/10.1038/nature02373.

Lohr, M. & Wilhelm, C., 1999. Algae displaying the diadinoxanthin cycle also possess the violaxanthin cycle. *Proceedings of the National Academy of Sciences of the United States of America*, 96(15), pp.8784–9. Available at: http://www.pubmedcentral.nih.gov/articlerender.fcgi?artid=17594&tool=pmcentrez&rendertype=abstract.

Lohr, M. & Wilhelm, C., 2001. Xanthophyll synthesis in diatoms: quantification of putative intermediates and comparison of pigment conversion kinetics with rate constants derived from a model. *Planta*, pp.382–391. Available at: http://link.springer.com/article/10.1007/s004250000403 [Accessed February 21, 2014].

MacIntyre, H.L., Kana, T.M. & Geider, R.J., 2000. The effect of water motion on short-term rates of photosynthesis by marine phytoplankto. *Trends in plant science*, 5, pp.12–17.

Maheswari, U. et al., 2005. The Diatom EST Database. *Nucleic acids research*, 33(Database issue), pp.D344–7. Available at: http://www.pubmedcentral.nih.gov/articlerender.fcgi?artid=540075&tool=pmcentrez&rendertype=abstract [Accessed August 1, 2012].

Maheswari, U. et al., 2009. Update of the Diatom EST Database: a new tool for digital transcriptomics. *Nucleic acids research*, 37(Database issue), pp.D1001–5. Available at: http://www.pubmedcentral.nih.gov/articlerender.fcgi?artid=2686495&tool=pmcentrez&rendertype=abstract [Accessed August 13, 2012].

Malviya, S. et al., 2015. Insights into global diatom distribution and diversity in the world's ocean. *Proceedings of the National Academy of Sciences*, 348(6237), p.in review.

Mann, D.G., 1993. Patterns of sexual reproduction in diatoms. *Hydrobiologia*, 269, pp.11–20.

Mann, K.H. & Lazier, J.R.N., 2006. *Dynamics of marine ecosystems: biological-physical interactions in the oceans* USA: Black.,

Marchetti, A. et al., 2009. Ferritin is used for iron storage in bloom-forming marine pennate diatoms. *Nature*, 457(7228), pp.467–70. Available at: http://www.ncbi.nlm.nih.gov/pubmed/19037243\nhttp://dx.doi.org/10.1038/nature07539.

Margalef, R., 1978. Life-Forms of Phytoplankton As Survival Alternatives in An Unstable Environment. *Oceanologia*, 1(4). Available at: https://www.researchgate.net/publication/246685934_Life-Forms_of_Phytoplankton_As_Survival_Alternatives_in_An_Unstable_Environment.

De Martino, A. et al., 2007. Genetic and phenotypic characterization of Phaeodactylum tricornutum (Bacillariophyceae) accessions 1. *Journal of Phycology*, 43(5), pp.992–1009. Available at: http://doi.wiley.com/10.1111/j.1529-8817.2007.00384.x [Accessed August 13, 2012].

De Martino, A., Amato, A. & Bowler, C., 2009. Mitosis in diatoms: Rediscovering an old model for cell division. *BioEssays*, 31(8), pp.874–884.

Materna, A.C. et al., 2009. First induced plastid genome mutations in alga with secondary plastids: psbA mutations in the diatom Phaeodactylum tricornutum (Bacillariophyceae) reveal consequences on the regulatioin of photosynthesis. *Journal of Phycology*, 45, pp.838–846.

Miloslavina, Y. et al., 2009. Ultrafast fluorescence study on the location and mechanism of non-photochemical quenching in diatoms. *Biochimica et biophysica acta*, 1787(10), pp.1189–97. Available at: http://www.ncbi.nlm.nih.gov/pubmed/19486881 [Accessed April 14, 2014].

Mock, T. et al., 2008. Whole-genome expression profiling of the marine diatom Thalassiosira pseudonana identifies genes involved in silicon bioprocesses. , 105(5).

Morel, F.M.M. & Price, N.M., 2003. The Biogeochemical Cycles of Trace Metals in the Oceans. *Science*, 300, pp.944–947.

Morosinotto, T., Baronio, R. & Bassi, R., 2002. Dynamics of chromophore binding to Lhc proteins in vivo and in vitro during operation of the xanthophyll cycle. *Journal of Biological Chemistry*, 277(40), pp.36913–36920.

Morrissey, J. et al., 2014. A Novel Protein, Ubiquitous in Marine Phytoplankton, Concentrates Iron at the Cell Surface and Facilitates Uptake. *Current Biology*, pp.1–8. Available at: http://linkinghub.elsevier.com/retrieve/pii/S0960982214015632 [Accessed January 5, 2015].

Mou, S. et al., 2012. Cloning and expression analysis of two different LhcSR genes involved in stress adaptation in an Antarctic microalga, Chlamydomonas sp. ICE-L. *Extremophiles*, 16(2), pp.193–203.

Moustafa, A. et al., 2009. Genomic footprints of a cryptic plastid endosymbiosis in diatoms. *Science (New York, N.Y.)*, 324(5935), pp.1724–6. Available at: http://www.sciencemag.org/content/324/5935/1724.abstract [Accessed October 29, 2012].

Muhseen, Z.T. et al., 2015. Proteomics studies on stress responses in diatoms. *Proteomics*, pp.1–11. Available at: http://www.ncbi.nlm.nih.gov/pubmed/26364674.

Muller, P., Li, X. & Niyogi, K.K., 2001. Non-Photochemical Quenching . A Response to Excess Light Energy 1. , 125(April), pp.1558–1566.

Munekage, Y. et al., 2001. Cytochrome b6f mutation specifically affects thermal dissipation of absorbed light energy in Arabidopsis. *Plant Journal*, 28(3), pp.351–359.

Murchie, E.H. & Niyogi, K.K., 2011. Manipulation of photoprotection to improve plant photosynthesis. *Plant physiology*, 155(1), pp.86–92.

Nagao, R. et al., 2013. Comparison of oligomeric states and polypeptide compositions of fucoxanthin chlorophyll a/c-binding protein complexes among various diatom species. *Photosynthesis research*. Available at: http://www.ncbi.nlm.nih.gov/pubmed/23925427

[Accessed August 16, 2013].
Nagao, R. et al., 2007. Isolation and characterization of oxygen-evolving thylakoid membranes and Photosystem II particles from a marine diatom Chaetoceros gracilis. *Biochimica et Biophysica Acta - Bioenergetics*, 1767(12), pp.1353–1362.
Nelson, D.L. & Cox, M.M., 2013. Lehninger Principles of Biochemistry, 6th Edn. *NewYork: W. H. Freeman*.
Nelson, D.M. et al., 1995. Production and dissolution of biogenic silica in the ocean: Revised global estimates, comparison with regional data and relationship to biogenic sedimentation. *Global Biogeochemical Cycles*, 9(3), pp.359–372. Available at: http://dx.doi.org/10.1029/95GB01070.
Nield, J. et al., 2000. Photosystem II complexes allows for comparison of their OEC organisation.
Nilkens, M. et al., 2010. Identification of a slowly inducible zeaxanthin-dependent component of non-photochemical quenching of chlorophyll fluorescence generated under steady-state conditions in Arabidopsis. *Biochimica et Biophysica Acta - Bioenergetics*, 1797(4), pp.466–475. Available at: http://dx.doi.org/10.1016/j.bbabio.2010.01.001.
Niyogi, K.K., Grossman, A.R. & Björkman, O., 1998. Arabidopsis Mutants Define a Central Role for the Xanthophyll Cycle in the Regulation of Photosynthetic Energy Conversion. , 10(July), pp.1121–1134.
Nymark, M. et al., 2016. A CRISPR/Cas9 system adapted for gene editing in marine algae. *Scientific Reports*, 6(April), p.24951. Available at: http://www.nature.com/articles/srep24951.
Nymark, M. et al., 2009. An Integrated Analysis of Molecular Acclimation to High Light in the Marine Diatom Phaeodactylum tricornutum M. Grebe, ed. *PLoS ONE*, 4(11), p.14. Available at: http://www.pubmedcentral.nih.gov/articlerender.fcgi?artid=2766053&tool=pmcentrez&rendertype=abstract.
Nymark, M. et al., 2013. Molecular and Photosynthetic Responses to Prolonged Darkness and Subsequent Acclimation to Re-Illumination in the Diatom Phaeodactylum tricornutum R. Subramanyam, ed. *PLoS ONE*, 8(3), p.e58722. Available at: http://dx.plos.org/10.1371/journal.pone.0058722 [Accessed March 15, 2013].
Ohno, N. et al., 2012. CO2-cAMP-Responsive cis-Elements Targeted by a Transcription Factor with CREB/ATF-Like Basic Zipper Domain in the Marine Diatom Phaeodactylum tricornutum. *Plant Physiology*, 158(January), pp.499–513.
Okegawa, Y. et al., 2007. A balanced PGR5 level is required for chloroplast development and optimum operation of cyclic electron transport around photosystem I. *Plant and Cell Physiology*, 48(10), pp.1462–1471.
Oudot-Le Secq, M.P. et al., 2007. Chloroplast genomes of the diatoms Phaeodactylum tricornutum and Thalassiosira pseudonana: Comparison with other plastid genomes of the red lineage. *Molecular Genetics and Genomics*, 277, pp.427–439.
Owens, T.G., 1986. Light-Harvesting Function in the Diatom Phaeodactylum tricornutum ’. , pp.739–746.
Peers, G. et al., 2009. An ancient light-harvesting protein is critical for the regulation of algal photosynthesis. *Nature*, 462(7272), pp.518–21. Available at: http://www.ncbi.nlm.nih.gov/pubmed/19940928 [Accessed December 16, 2013].
Peers, G. & Price, N.M., 2006. Copper-containing plastocyanin used for electron transport by an oceanic diatom. *Nature*, 441, pp.341–344.
Peterson, R.B. & Havir, E.A., 2000. A nonphotochemical-quenching-deficient mutant of Arabidopsis thaliana possessing normal pigment composition and xanthophyll- cycle activity. *Planta*, 210, pp.205–214.
Petroutsos, D. et al., 2011. The chloroplast calcium sensor CAS is required for photoacclimation in Chlamydomonas reinhardtii. *The Plant cell*, 23(8), pp.2950–63. Available at: http://www.pubmedcentral.nih.gov/articlerender.fcgi?artid=3180803&tool=pmcentrez&rendertype=abstract [Accessed March 4, 2013].
Pickett-Heaps, J., Schmid, J.A.-M. & Edgar, L.A., 1990. The cell biology of the diatom valve formation. *Round FE, Capman DJK, eds. Progress in phycology research. Bristol, UK: Biopress Ltd*, pp.1–168.
Pinnola, A. et al., 2015. LHCSR proteins catalyze Excess Energy Dissipation in both Photosystems of Physcomitrella patens. *Submitted*.
Pinnola, A. et al., 2013. Zeaxanthin binds to light-harvesting complex stress-related protein to

enhance nonphotochemical quenching in Physcomitrella patens. *The Plant cell*, 25(9), pp.3519–34. Available at: http://www.pubmedcentral.nih.gov/articlerender.fcgi?artid=3809547&tool=pmcentrez&rendertype=abstract [Accessed December 15, 2014].

Plumley, F.G. & Schmidt, G.W., 1987. Reconstitution of chlorophyll a/b light-harvesting complexes: Xanthophyll-dependent assembly and energy transfer. *Proceedings of the National Academy of Sciences of the United States of America*, 84(1), pp.146–150.

Pocock, T. et al., 2007. Excitation pressure regulates the activation energy for recombination events in the photosystem II reaction centres of Chlamydomonas reinhardtii. *Biochem Cell Biol*, 85(6), pp.721–729. Available at: http://www.ncbi.nlm.nih.gov/pubmed/18059530.

Polivka, T. & Sundström, V., 2004. Ultrafast dynamics of carotenoid excited states - From solution to natural and artificial systems. *Chemical Reviews*, 104, pp.20121–2071.

Poulsen, N., Chesley, P.M. & Kröger, N., 2006. MOLECULAR GENETIC MANIPULATION OF THE DIATOM THALASSIOSIRA PSEUDONANA (BACILLARIOPHYCEAE). *Journal of Phycology*, 42(5), pp.1059–1065. Available at: http://doi.wiley.com/10.1111/j.1529-8817.2006.00269.x [Accessed November 8, 2012].

Pyszniak, A.M. & Gibbs, S.P., 1992. Immunocytochemical localization of photosystem I and the fucoxanthin-chlorophylla/c light-harvesting complex in the diatomPhaeodactylum tricornutum. *Protoplasma*, 166(3-4), pp.208–217. Available at: http://link.springer.com/article/10.1007/BF01322783 [Accessed November 20, 2012].

Raven, J.A., Evans, M.C.W. & Korb, R.E., 1999. The role of trace metals in photosynthetic electron transport in O-2-evolving organisms. *Photosynthesis Research*, 60(2-3), pp.111–149. Available at: <Go to ISI>://WOS:000081949800002\nhttp://download.springer.com/static/pdf/451/art%3A10.1023%2FA%3A1006282714942.pdf?auth66=1414840657_00fbbf25310c5a2d2de3269f737c14ff&ext=.pdf.

Rensing, S.A., Lang, D. & Zimmer, A.D., 2008. The Physcomitrella Genome Reveals Evolutionary Insights into the Conquest of Land by Plants. *Science*, 319(January), pp.64–69.

De Riso, V. et al., 2009. Gene silencing in the marine diatom Phaeodactylum tricornutum. *Nucleic acids research*, 37(14), p.e96. Available at: http://www.pubmedcentral.nih.gov/articlerender.fcgi?artid=2724275&tool=pmcentrez&rendertype=abstract [Accessed July 16, 2012].

Roberts, K. et al., 2007. C3 and C4 pathways of photosynthetic carbon assimilation in marine diatoms are under genetic, not environmental, control. *Plant physiology*, 145(1), pp.230–235.

Rochaix, J.-D., 2002. Chlamydomonas, a model system for studying the assembly and dynamics of photosynthetic complexes. *FEBS letters*, 529, pp.34–38.

Rockholm, D.C. & Yamamoto, H.Y., 1996. Violaxanthin De-Epoxidase '. , pp.697–703.

Ruban, A. et al., 2004. The super-excess energy dissipation in diatom algae: comparative analysis with higher plants. *Photosynthesis research*, 82(2), pp.165–75. Available at: http://www.ncbi.nlm.nih.gov/pubmed/16151872.

Ruban, A. V et al., 2007. Identification of a mechanism of photoprotective energy dissipation in higher plants. *Nature*, 450(7169), pp.575–8. Available at: http://www.ncbi.nlm.nih.gov/pubmed/18033302 [Accessed April 22, 2013].

Sabatino, V. et al., 2015. Establishment of Genetic Transformation in the Sexually Reproducing Diatoms Pseudo-nitzschia multistriata and Pseudo-nitzschia arenysensis and Inheritance of the Transgene. *Marine Biotechnology*, 17, pp.452–462.

Scanlan, D.J. et al., 2009. Ecological genomics of marine picocyanobacteria. *Microbiology and molecular biology reviews : MMBR*, 73(2), pp.249–299.

Schaller-Laudel, S. et al., 2015. The diadinoxanthin diatoxanthin cycle induces structural rearrangements of the isolated FCP antenna complexes of the pennate diatom Phaeodactylum tricornutum. *Plant Physiology and Biochemistry*, 96, pp.364–376. Available at: http://www.sciencedirect.com/science/article/pii/S0981942815301042 [Accessed September 12, 2015].

Schiller, N., 1984. Picosecond streak camera photonics. In *Semiconductors probed by ultrafast laser spectroscopy*. pp. 441–458.

Shinopoulos, K.E. & Brudvig, G.W., 2012. Cytochrome b559 and cyclic electron transfer within photosystem II. *Biochimica et Biophysica Acta - Bioenergetics*, 1817(1), pp.66–75. Available at: http://dx.doi.org/10.1016/j.bbabio.2011.08.002.

Siaut, M. et al., 2007. Molecular toolbox for studying diatom biology in Phaeodactylum tricornutum. *Gene*, 406(1-2), pp.23–35. Available at: http://www.ncbi.nlm.nih.gov/pubmed/17658702 [Accessed August 8, 2012].

Sineshchekov, O.A., Jung, K.-H. & Spudich, J.L., 2002. Two rhodopsins mediate phototaxis to low- and high-intensity light in Chlamydomonas reinhardtii. *Proceedings of the National Academy of Sciences of the United States of America*, 99, pp.8689–8694.

Sonoike, K., 2011. Photoinhibition of photosystem I review 2011.pdf. *Physiologia plantarum*, 142(1), pp.56–64. Available at: http://www.springerlink.com/index/XW307617G7071272.pdf\nhttp://www.ncbi.nlm.nih.gov/pubmed/21128947.

Sonoike, K., 1996. Photoinhibition of Photosystem I: Its Physiological Significance in the Chilling Sensitivity of Plants. *Plant and Cell Physiology*, 37(3), pp.239–247. Available at: http://pcp.oxfordjournals.org/cgi/doi/10.1093/oxfordjournals.pcp.a028938.

Sonoike, K. & Terashima, I., 1994. Mechanism of Photosystem-I Photoinhibition in Leaves of Cucumis-Sativus L. *Planta*, 194(2), pp.287–293. Available at: <Go to ISI>://A1994NW25500018.

Van Stokkum, I.H.M., Larsen, D.S. & Van Grondelle, R., 2004. Global and target analysis of time-resolved spectra. *Biochimica et Biophysica Acta - Bioenergetics*, 1657(2-3), pp.82–104.

Stroebel, D. et al., 2003. An atypical haem in the cytochrome b6f complex. *Nature (London, United Kingdom)*, 426, pp.413–418.

Stryer, L., 1995. *Biochemistry* N. Y. W. H. F. and Company, ed.,

Strzepek, R.F. & Harrison, P.J., 2004. Photosynthetic architecture differs in coastal and oceanic diatoms. *Nature*, 431(October 2004), pp.689–692.

Sturm, S. et al., 2013. A novel type of light-harvesting antenna protein of red algal origin in algae with secondary plastids. *BMC evolutionary biology*, 13(1), p.159. Available at: http://www.pubmedcentral.nih.gov/articlerender.fcgi?artid=3750529&tool=pmcentrez&rendertype=abstract.

Szabó, M. et al., 2010. Functional heterogeneity of the fucoxanthins and fucoxanthin-chlorophyll proteins in diatom cells revealed by their electrochromic response and fluorescence and linear dichroism spectra. *Chemical Physics*, 373(1-2), pp.110–114.

Szabó, M. et al., 2008. Structurally flexible macro-organization of the pigment-protein complexes of the diatom Phaeodactylum tricornutum. *Photosynthesis research*, 95(2-3), pp.237–45. Available at: http://www.ncbi.nlm.nih.gov/pubmed/17891473 [Accessed January 14, 2015].

Taddei, L. et al., 2016. Multisignal control of expression of the LHCX protein family in the marine diatom Phaeodactylum tricornutum. *Journal of Experimental Botany*. Available at: http://jxb.oxfordjournals.org/lookup/doi/10.1093/jxb/erw198.

Tanaka, A. et al., 2015. Light and CO2/cAMP signal crosstalk on the promoter elements of chloroplastic β-carbonic anhydrase genes in the marine diatom Phaeodactylum tricornutum. *Plant Physiology 170,*, 170, pp.1105–1116.

Thamatrakoln, K. et al., 2013. Death-specific protein in a marine diatom regulates photosynthetic responses to iron and light availability. *Proceedings of the National Academy of Sciences of the United States of America*, 110(50), pp.20123–8. Available at: http://www.ncbi.nlm.nih.gov/pubmed/24277817 [Accessed December 16, 2013].

Thoms, S., Pahlow, M. & Gladrow, D.A.W., 2008. Model of the carbon concen- trating mechanism in chloroplasts of eukaryotic algae. *Journal of theoretical biology*, pp.295–313.

Tikkanen, M. & Aro, E.M., 2012. Thylakoid protein phosphorylation in dynamic regulation of photosystem II in higher plants. *Biochimica et Biophysica Acta - Bioenergetics*, 1817(1), pp.232–238. Available at: http://dx.doi.org/10.1016/j.bbabio.2011.05.005.

Tirichine, L. & Bowler, C., 2011. Decoding algal genomes: tracing back the history of photosynthetic life on Earth. *The Plant journal : for cell and molecular biology*, 66(1), pp.45–57. Available at: http://www.ncbi.nlm.nih.gov/pubmed/21443622 [Accessed October 29, 2012].

Tokutsu, R. & Minagawa, J., 2013. Energy-dissipative supercomplex of photosystem II associated with LHCSR3 in Chlamydomonas reinhardtii. *Proceedings of the National Academy of Sciences of the United States of America*, 110(24), pp.10016–21. Available at: http://www.pubmedcentral.nih.gov/articlerender.fcgi?artid=3683755&tool=pmcentrez&rendertype=abstract [Accessed December 16, 2013].

Truong, T.B., 2011. Investigating the Role(s) of LHCSRs in Chlamydomonas reinhardtii. *UC*

Berkeley Plant Biology. Retrieved from: http://escholarship.org/uc/item/2154v8x8.
Umena, Y. et al., 2011. Crystal structure of oxygen-evolving photosystem II at a resolution of 1.9 Å. *Nature*, 473(7345), pp.55–60. Available at: http://dx.doi.org/10.1038/nature09913.
Valle, K.C. et al., 2014. System Responses to Equal Doses of Photosynthetically Usable Radiation of Blue , Green , and Red Light in the Marine Diatom Phaeodactylum tricornutum. , pp.1–37.
Vanormelingen, P., Verleyen, E. & Vyverman, W., 2007. The diversity and distribution of diatoms: from cosmopolitanism to narrow endemism. *Biodiversity and Conservation*, 17, pp.393–405.
Vargas, C. De et al., 2015. Eukaryotic plankton diversity in the sunlit ocean. , 348(6237), pp.1–11.
Veith, T. & Büchel, C., 2007. The monomeric photosystem I-complex of the diatom Phaeodactylum tricornutum binds specific fucoxanthin chlorophyll proteins (FCPs) as light-harvesting complexes. *Biochimica et biophysica acta*, 1767(12), pp.1428–35. Available at: http://www.ncbi.nlm.nih.gov/pubmed/18028870 [Accessed December 9, 2012].
Villareal, T.A. & Carpenter, E.J., 2003. Buoyancy Regulation and the Potential for Vertical Migration in the Oceanic Cyanobacterium Trichodesmium. *Microbial ecology*, 45, pp.1–10.
Wada, M., Kagawa, T. & Sato, Y., 2003. CHLOROPLAST MOVEMENT. *Plant Biology*, 54, pp.455–468.
Wagner, H., Jakob, T. & Wilhelm, C., 2006. Balancing the energy flow from captured light to biomass under fluctuating light conditions. *The New phytologist*, 169(1), pp.95–108. Available at: http://www.ncbi.nlm.nih.gov/pubmed/16390422 [Accessed March 1, 2013].
Watt, I.N. et al., 2010. Bioenergetic cost of making an adenosine triphosphate molecule in animal mitochondria. , 107(39).
Weis, E. & Berry, J.A., 1987. Quantum efficiency of Photosystem II in relation to "energy"-dependent quenching of chlorophyll fluorescence. *BBA - Bioenergetics*, 894(2), pp.198–208.
Westermann, M. & Rhiel, E., 2005. Localisation of fucoxanthin chlorophyll a/c-binding polypeptides of the centric diatom Cyclotella cryptica by immuno-electron microscopy. *Protoplasma*, 225(3-4), pp.217–223.
Wientjes, E. & Croce, R., 2011. The light-harvesting complexes of higher-plant Photosystem I: Lhca1/4 and Lhca2/3 form two red-emitting heterodimers. *Biochemical Journal*, 433, pp.477–485.
Wilhelm, C. et al., 2006. The Regulation of Carbon and Nutrient Assimilation in Diatoms is Significantly Different from Green Algae. *Protist*, 157(2), pp.91–124.
Wu, H. et al., 2012. Photosystem II photoinactivation, repair, and protection in marine centric diatoms. *Plant physiology*, 160(1), pp.464–76. Available at: http://www.pubmedcentral.nih.gov/articlerender.fcgi?artid=3440219&tool=pmcentrez&rendertype=abstract [Accessed November 25, 2014].
Yamamoto, H.Y. & Kamite, L., 1972. The effects of dithiothreitol on violaxanthin de-epoxidation and absorbance changes in the 500-nm region. *BBA - Bioenergetics*, 267(3), pp.538–543.
Zhu, S.-H. & Green, B.R., 2010. Photoprotection in the diatom Thalassiosira pseudonana: role of LI818-like proteins in response to high light stress. *Biochimica et biophysica acta*, 1797(8), pp.1449–57. Available at: http://www.ncbi.nlm.nih.gov/pubmed/20388491 [Accessed February 19, 2013].

Rôle des protéines de la famille des antennes collectrices de lumière, LHCX, dans la photoprotection chez les diatomées

Résumé :

Les diatomées constituent le principal groupe du phytoplancton dans les océans, contribuant à près de 20% de la production primaire globale. Dans leur environnement très variable, les diatomées sont particulièrement efficaces dans leur capacité à ajuster leur activité photosynthétique en dissipant sous forme de chaleur l'énergie lumineuse absorbée en excès, par un processus appelé le « Non-Photochemical Quenching of chlorophyll fluorescence », (NPQ). Chez la diatomée modèle, *Phaeodactylum tricornutum*, il a été montré que LHCX1, une protéine proche des antennes photosynthétiques, est impliquée dans le NPQ. Par des approches intrégrées de génétique, biologie moléculaire, biochimie, imagerie des cinétiques de fluorescence et spectroscopie ultrarapide, j'ai étudié le rôle de la famille des LHCX chez *P. tricornutum*. J'ai tout d'abord pu corréler une expression différentielle des 4 gènes *LHCX* de *P. tricornutum* avec différentes dynamiques de NPQ et activités photosynthétiques, dans différentes conditions de lumiére et nutriments. En localisant les LHCX dans les differents complexes photosynthétiques et les différents sites de dissipation d'énergie, j'ai pu proposer un modèle de régulation dynamique du NPQ impliquant à court terme prinicipalement LHCX1 au niveau des centres réactionnels, et une autre isoforme, possiblement LHCX3, au niveau des antennes lors d'un stress lumineux prolongé. Enfin, par le criblage d'une série de mutants potentiellement dérégulés dans leur contenu en LHCXs, j'ai pu identifier des lignées avec un NPQ altéré qui pourront constituer des nouveaux outils de recherche. Dans l'ensemble ce travail de thèse a permis de mettre en évidence la diversification fonctionnelle et l'importance de la famille des LHCX dans la fine modulation des capacités de collecte de lumière et de photoprotection, expliquant sans doute en partie le succès des diatomées dans leur environnement très fluctuant.

Mots clés : Diatomées, photosynthèse, LHCX, *non-photochemical quenching of chlorophyll,* lumière.

The Role of the LHCX Light-Harvesting Complex Protein Family in Diatom Photoprotection

Abstract:

Diatoms dominate phytoplanktonic communities in contemporary oceans, contributing to 20% of global primary productivity. In their extremely variable environment, diatoms are especially efficient in adjusting their photosynthetic activity by dissipating as heat the light energy absorbed in excess, through a process called "Non-Photochemical Quenching of chlorophyll fluorescence", (NPQ). In the model diatom *Phaeodactylum tricornutum*, it has been shown that *LHCX1*, a photosynthetic antenna-related gene, is involved in the NPQ process. Through integrated approaches of genetics, molecular biology, biochemistry, study of the kinetics of chlorophyll fluorescence yields and ultrafast spectroscopy, I studied the role of the *LHCX* family in the photoprotection activity of *P. tricornutum.* I first correlated a differential regulation of the 4 *P. tricornutum* LHCX genes with different dynamics of NPQ and photosynthetic activity, in different light and nutrient conditions. By localizing the LHCXs in fractioned photosynthetic complexes and the different sites of energy dissipation, I was able to propose a model of dynamic regulation of NPQ capacity involving mainly the LHCX1 in the reaction centers, during short-term high light responses. During prolonged high light stress, the quenching occurs mainly in the antennas, potentially mediated by the LHCX3 isoform. Finally, using photosynthetic parameters, I screened a series of transgenic lines putatively deregulated in their LHCX amount, and I identified lines with altered NPQ, which could represent novel investigation tools. Altogether, this work highlighted the functional diversification and the importance of the LHCX protein family in the fine-tuning of light harvesting and photoprotection capacity, possibly contributing to explain diatoms success in their highly fluctuating environment.

Keywords: Diatoms, photosynthesis, LHCX, non-photochemical quenching of chlorophyll fluorescence, light.